# EURAD state-of-the-art report on the understanding of radionuclide retention and transport in clay and crystalline rocks

Norbert Maes, Sergey Churakov, Martin Glaus, Bart Baeyens, Rainer Dähn, Sylvain Grangeon, Laurent Charlet, Felix Brandt, Jenna Poonoosamy, Alwina Hoving, et al.

frontiers | Frontiers in Nuclear Engineering

TYPE Review
PUBLISHED 22 November 2024
DOI 10.3389/fnuen.2024.1417827



OPEN ACCESS

EDITED BY
Bernd Grambow,
UMR6457 Laboratoire de Physique Subatomique et des Technologies Associées (SUBATECH), France

REVIEWED BY
Lara Duro,
Amphos21, Spain
Mavrik Zavarin,
Lawrence Livermore National Laboratory (DOE), United States

*CORRESPONDENCE
Norbert Maes,
norbert.maes@sckcen.be
Sergey Churakov,
sergey.churakov@psi.ch;

RECEIVED 15 April 2024
ACCEPTED 18 July 2024
PUBLISHED 22 November 2024

CITATION
Maes N, Churakov S, Glaus M, Baeyens B, Dähn R, Grangeon S, Charlet L, Brandt F, Poonoosamy J, Hoving A, Havlova V, Fischer C, Noseck U, Britz S, Siitari-Kauppi M, Li X, Fabritius O and Missana T (2024) EURAD state-of-the-art report on the understanding of radionuclide retention and transport in clay and crystalline rocks.
*Front. Nucl. Eng.* 3:1417827.
doi: 10.3389/fnuen.2024.1417827



# EURAD state-of-the-art report on the understanding of radionuclide retention and transport in clay and crystalline rocks

Norbert Maes[1]*, Sergey Churakov[2,3]*, Martin Glaus[2], Bart Baeyens[2], Rainer Dähn[2], Sylvain Grangeon[4], Laurent Charlet[5], Felix Brandt[6], Jenna Poonoosamy[6], Alwina Hoving[7], Vaclava Havlova[8], Cornelius Fischer[9], Ulrich Noseck[10], Susan Britz[10], Marja Siitari-Kauppi[11], Xiaodong Li[10,11], Otto Fabritius[10,11] and Tiziana Missana[12]

[1]SCK CEN, Mol, Belgium, [2]Paul Scherrer Instute (PSI), Villigen, Switzerland, [3]Institute of Geological Sciences, University of Bern, Bern, Switzerland, [4]BRGM, Orléans, France, [5]Institut des Sciences de la Terre (ISTERRE), Grenoble, France, [6]Forschungszentrum Jülich GmbH (FZJ), Jülich, Germany, [7]Dutch Organization for Applied Scientific Research (TNO), Utrecht, Netherlands, [8]Nuclear Research Institute Rez plc (UJV), Prague, Czech, [9]Helmholtz-Zentrum Dresden-Rossendorf (HZDR), Rosendorf, Germany, [10]Gesellschaft für Anlagen- und Reaktorsicherheit (GRS), Braunschweig, Germany, [11]University of Helsinki (UH), Helsinki, Finland, [12]Centro de Investigaciones Energéticas, Medioambientales y Tecnológicas (CIEMAT), Madrid, Spain

After isolation of radioactive waste in deep geological formations, radionuclides can enter the biosphere via slow migration through engineered barriers and host rocks. The amount of radionuclides that migrate into the biosphere depends on the distance from a repository, dominant transport mechanism (diffusion vs. advection), and interaction of dissolved radionuclides with minerals present in the host rock and engineered barrier systems. Within the framework of the European Union's Horizon 2020 EURAD project (https://www.ejp-eurad.eu/), a series of state-of-the-art reports, which form the basis of a series of papers, have been drafted. This state-of-the-art paper aims to provide non-specialists with a comprehensive overview of the current understanding of the processes contributing to the radionuclide retention and migration in clay and crystalline host rocks, in a European context. For each process, a brief theoretical background is provided, together with current methodologies used to study these processes as well as references for key data. Owing to innovative research on retention and migration and the extensive knowledge obtained over decades (in the European context), process understanding and insights are continuously improving, prompting the adaptation and refinement of conceptual descriptions regarding safety assessments. Nevertheless, there remains important research questions to be investigated in the future.

KEYWORDS

**geological disposal, radionuclide migration, diffusion, retention, sorption, redox chemistry, clay host rock, crystalline host rock**

# 1 Introduction to transport controlling processes in clay and crystalline host rocks

After isolation of radioactive waste in deep geological formations and design-based repository closure, radionuclides are expected to enter the biosphere via slow migration. The amount of radionuclides that migrate into the biosphere depends on the distance of a repository from the biosphere, dominant transport mechanism (diffusion vs. advection), and interaction of dissolved radionuclides with minerals present in the host rock and engineered barrier systems (Churakov et al., 2020).

A geological disposal system (GDS) for radioactive waste has to fulfil three main "safety functions": Containment, Isolation, and Retention (ONDRAF/NIRAS, 2013).

The host rock, as major part of this system, is expected to contribute to these functions by:

- Providing favorable and stable chemical and mechanical conditions to ensure good containment on a geological time scale.
- Isolating waste packages from man and the biosphere.
- Limiting radionuclide release to the biosphere via slow transport and sufficient retention in the host rock.

As deep clay and granitic formations offer the perspective required to fulfil these three safety functions, they are intensively studied by several countries, both in Europe and worldwide. In this paper, however, we will mainly relate them to the European context.

Within the EC EURAD project, Work package 5 (FUTURE: fundamental understanding of radionuclide retention—https://www.ejp-eurad.eu/implementation/fundamental-understanding-radionuclide-retention-future) deals with the fundamental understanding of retention and transport processes in clay and crystalline host rocks, and this manuscript describes the current state of knowledge.

Retention processes, generally called "sorption or uptake," assure that potential radionuclide transport from a repository to the biosphere is much slower than the transport of groundwater. These processes depend on the pore water chemistry, which controls radionuclide speciation and influence the functional groups of reactive surfaces, present on the minerals. The most extensively studied "sorption" processes are surface complexation and ion exchange. Other processes, such as surface-induced reduction–oxidation (redox) uptake, incorporation, surface precipitation, and solid-solution formation, are less studied. However, they may be important retention mechanisms for a variety of radionuclides and are, therefore, gaining more attention. Section 2 describes these retention processes (clay surfaces will be taken as solid-phase examples to discuss the processes).

The two main transport mechanisms of radionuclides in host rock are diffusion and advection, driven by chemical concentration and hydraulic pressure gradients, respectively. Which mechanism predominates depends on the host rock matrix and the environmental conditions. This is described in detail in Section 3 for clay and crystalline host rocks.

In clay host rocks, diffusion is the dominant transport process. The negatively charged clay mineral surfaces not only result in a high retention capacity for cationic radionuclides but also in a distinct diffusion behavior of anionic, cationic, and neutral species. The most important retention processes, influencing the transport rate, are ion exchange and surface complexation. As clay materials may exhibit strong reducing properties (i.e., a negative redox potential), due to the presence of reducing elements, Fe(II), in their crystal structure, surface-induced reduction–adsorption and reduction–precipitation in clays has become a field of intensive research.

In crystalline rocks, solute transport is mainly controlled by advection in connected fractures forming a preferential flow path and by matrix diffusion. The latter may be enhanced in weathered/altered zones along the fractures. Moreover, the presence of fracture-filling materials, which are composed of clay minerals, Fe-oxy-hydroxides, and calcite, among others, may cause retention via different mechanisms such as ion exchange, surface complexation, surface-induced precipitation, and solid-solution formation.

This state-of-the-art report aims to provide a comprehensive overview of our current understanding of the processes that contribute to radionuclide retention and migration in clay and crystalline rocks within the European context. For each process, a brief theoretical background is provided, together with current methods used to study these processes as well as references to key publications.

Owing to decades of innovative research on the retention and migration of radionuclides, extensive knowledge and process understanding have been obtained, prompting the adaptation and refinement of conceptual descriptions regarding safety assessments. Uncertainties remain, and the key uncertainties that presently need to be resolved are listed in Section 4.

# 2 Retention processes

This chapter, on retention processes, is divided into three sections. In the first section, we briefly discuss aqueous speciation and the importance of thermodynamic data. This is a cornerstone for acquiring a good understanding and description of retention processes. In the two remaining sections, so-called "classical" retention processes, such as ion exchange and surface complexation, are discussed. These two processes are the dominant sorption phenomena and are the most extensively studied. These processes are described by taking clay minerals as an example but are also valid for other surfaces (e.g., oxides). In the second section, other relevant but less studied retention processes, such as surface-induced redox uptake, incorporation, surface precipitation, and solid-solution formation, are discussed.

## 2.1 Aqueous speciation, thermodynamic data, and thermodynamic databases

The study of RN aqueous speciation (i.e., its distribution among the different occurring chemical forms or species) determines the conditions under which contaminants can be mobile or can be retarded via (co) precipitation or sorption, making it fundamental

for understanding the environmental fate and transport of contaminants.

The most important factors controlling aqueous speciation are: pH, redox ($E_h$), salinity, and temperature; however, the presence of solid phases, colloids, and organic and inorganic ligands should also be accounted for. Many experimental methods can be used for determining radionuclide speciation. These include chemical analytical methods, such as potentiometry; calorimetry; spectroscopic techniques, including Ultraviolet-Visual-Near Infrared (UV-Vis-NIR); Raman; attenuated total reflectance Fourier-transform infrared (ATR-FT-IR); fluorescence or optical spectroscopy; time-resolved laser fluorescence spectroscopy (TRLFS); and nuclear magnetic resonance (NMR). Recent techniques, such as extended X-ray absorption spectroscopy (EXAFS), small-angle X-ray scattering (SAXS), and high-energy X-ray scattering (HEXS), have been successfully applied in this field, even in the case of actinides, and have benefited from recent developments on beamlines (Schacherl et al., 2022a; Schacherl et al., 2022b).

Some of the above-mentioned techniques provide indirect information on the formation of complexes in solution; others may give additional information on metal–ligand coordination modes, coordination numbers, and ion distances. Additional detailed information on the techniques used for actinide speciation can be found in a recent review (Batrice et al., 2016).

It is well accepted that speciation and solubility data should be obtained in well-defined solutions, with the knowledge of the nature (oxidation state and coordination environment) of the species involved in equilibrium reactions under consideration, and of the solid phases limiting the solubility. However, experimental studies cannot be performed under all the potential chemical conditions. Geochemical and thermodynamic modeling represents an important tool for the interpretation of empirical radionuclide speciation and solubility data and for predicting their behavior under different environments.

Thus, the main objective of experimental studies is to derive stability constants and all the thermodynamic parameters needed to feed geochemical models. Laboratory analyses provide a direct measure of different forms of an element, but chemical modeling is needed to apply all known thermodynamic relationships among chemical forms and to predict the overall equilibrium distribution. The model-based description of uptake, thus, includes several coupled physico-chemical processes that are described by thermodynamic and kinetic laws.

The mathematical approach to the analysis of aqueous speciation, above all in natural systems, is quite complex, and the development of dedicated software has been ongoing since the ’80s. Far from being exhaustive, among the most known speciation software packages (and their updates) are: MINEQL (Westall et al., 1976); PHREEQE (Parkhurst et al., 1980) and PHREEQC (Parkhurst and Appelo, 2013); MINTEQA2 (Allison et al., 1991) and MINEQL+ (Schecher and McAvoy, 1992); EQ3/6 (Wolery and Daveler, 1992); CHESS and JCHESS (Van der Lee and de Windt, 2002); Geochemists’ Workbench (Bethke and Yeakel, 2016); and GEMSs (http://gems.web.psi.ch/) (Kulik et al., 2013).

The quality of calculations strongly depends not only on the underlying assumptions, i.e., on the selection of chemical processes by a user, but also on the completeness and reliability of thermodynamic data used as an input, and kinetics may also be important. Knowledge of fundamental thermodynamic properties, such as solubility products and complexation constants, is required. In addition, depending on the geochemical code used, there are code-specific dependent limitations such as temperature (only 25°C), pressure (only at 1 bar), ionic strength, and correction models. The combination of thermodynamic data completeness and the capabilities inherent to a geochemical code limit the modeling outcome.

The development of sound thermodynamic databases (TDBs) for radionuclide aqueous speciation and solid formation is, therefore, a prerequisite for geochemical calculations. In the last years, extensive research on the chemical thermodynamics and speciation of radionuclides in dilute, low-temperature groundwater systems has been carried out within the OECD-NEA TDB Project (www.oecd-nea.org/dbtdb/guidelines/tdb2.pdf). The nuclear Energy Agency compiles and evaluates existing thermodynamic data “to make available a comprehensive, internally consistent, quality-assured and internationally recognized chemical thermodynamic database of selected chemical elements in order to meet the specialized modeling requirements for safety assessments of radioactive waste disposal systems” (https://www.oecd-nea.org/dbtdb/). The Chemical Thermodynamics Series comprises review reports with selected data for elements of interest in radioactive waste management (https://www.oecd-nea.org/dbtdb/info/publications/). This work reflects present quantitative knowledge based on available experimental information and intends to be self-consistent. Despite the high quality of the databases, they are limited and insufficient to use alone, as many species are missing because data have not been evaluated according to the high standards of data selection.

Following the principles of NEA TDBs, some European agencies for nuclear waste management and some research institutions develop and continuously update their own, more exhaustive (and more widely applicable) databases. This is the case for the “ThermoChimie” TDB (https://www.thermochimie-tdb.com/), initially created and developed by ANDRA (French National Radioactive Waste Management Agency (Giffaut et al., 2014)) and later joined by “Radioactive Waste Management Limited” (NDA, UK) and ONDRAF/NIRAS (National Agency for Radioactive Waste Management, Belgium). It should be mentioned that SCK CEN developed first the MOLDATA database for ONDRAF/NIRAS, complemented with a software called Geochemical Data Processor (GDP) enabling internal consistency checking of data for the compilation of the in-house MOLDATA database (Wang et al., 2020a; Wang et al., 2020b). In Switzerland, the PSI/Nagra TDB (Hummel and Thoenen, 2021) is constantly updated and is provided in various formats compatible with most common geochemical tools (https://nagra.ch/wp-content/uploads/2023/05/NTB-21-03.pdf; https://www.psi.ch/en/les/database). Other examples are THEREDA (thermodynamic reference database for nuclear waste disposal in Germany, https://www.thereda.de/de/) (Voigt et al., 2007), the WEIMAR.dat (https://www.grs.de/publikationen/grs-500) database, which includes relevant mineral phases of the Gorleben site (Noseck et al., 2012), and EQ3/6 from the Lawrence Livermore National Laboratory (https://seaborg.llnl.gov/resources/geochemical-databases-modeling-codes).

Despite these important efforts, some gaps in data still exist, as well as uncertainties associated with the use of the models under certain conditions. Work is ongoing internationally to further develop the TDB and to extend the ability to model chemical speciation. It must be mentioned that, when dealing with natural systems, some of the necessary thermodynamic data are missing or not completely reliable (many experimental data likely exist but have not been evaluated entirely). Revisions and updates of these databases are still required, considering up-to-date experimental and theoretical studies published in peer-reviewed journals. For example, the lack of information on the kinetics of environmental processes obliges calculations assuming equilibrium. New studies should focus on specific chemical conditions, such as higher pH or high ionic strengths, or on the influence of other agents, such as organics or colloids, that may affect solubility, speciation, and sorption reactions and must be further analyzed.

Laboratory experiments, chemical analysis, modeling, and database maintenance and improvement are all part of an important iterative work that must be continued and even reinforced.

## 2.2 Classical retention processes

To assess the suitability of geological formations as potential host rocks for the deep disposal of high-level radioactive waste worldwide, detailed long-term safety studies are carried out, such as ONDRAF/NIRAS (2001), NAGRA (2002), SKB (2011), and POSIVA (2012b). Classical retention processes (adsorption) of radionuclides on rock substrates (vs. colloids) in the near and far field of a repository are an important component in such safety studies. It is a common practice to treat adsorption in terms of a distribution ratio, $R_d$, or distribution coefficient, defined as

$$R_d = \frac{C_{sorbed}}{C_{eql}} \quad (1)$$

where $C_{sorbed}$ is the radionuclide concentration retained in the solid phase (mol/kg) and $C_{eql}$ is the equilibrium radionuclide concentration in the liquid phase [mol/L]. In the literature, most often, the term $K_d$ is used (same relationship), but this term entails that the sorption on a solid has linear dependency on the concentration in the solution and is reversible (when sorption is not linear, this term is often referred to as $R_d$). Sorption databases consisting of the selected $K_d$ values for safety relevant radionuclides are crucial for the performance assessments of a GDS but are important as well for surface disposal sites.

Clay minerals such as montmorillonite and illite (including illite–smectite mixed layers) play an important role in the capacity of engineered and geological barriers to retain radionuclides in many disposal concepts for radioactive waste, either as part of a host formation (argillaceous rocks), an engineered barrier system (bentonite), or natural fracture-filling materials in crystalline host rocks (see Section 3.3.2.3.1). In addition to clay minerals, other minerals exhibit sorption properties. For crystalline rocks, in particular, rock-forming minerals, such as feldspars, quartz, mica, and (hydr)oxides, are important contributors to radionuclide sorption. The two most important sorption mechanisms are ion exchange (especially for clays) and surface complexation.

In an ion-exchange process, the adsorption of cations occurs via Coulomb attractions at permanent, negatively charged surface sites. Ion-exchange sites are a typical feature of clay minerals (also see the next section where the process of ion exchange is explained based on the properties of clays). Moreover, 2:1 clay minerals, such as vermiculite, montmorillonite, illite, and illite–smectite mixed layers, exhibit large cation exchange capacities (CECs), whereas 1:1 clay minerals, such as kaolinite, have low CECs.

Interactions are dominated by electrostatic forces and mainly result in so-called "outer sphere" complexes. The maximum adsorption capacity of a mineral or rock by ion exchange is denoted as the CEC. Cation exchange is strongly dependent on the ionic strength through competitive adsorption of a background electrolyte.

Surface complexation takes place on amphoteric surface groups (>SOH) present in minerals and is strongly dependent on pH because of the protolysis behavior of amphoteric groups (Dzombak and Morel, 1990). In clays, for example, functional groups are either related to Si atoms in tetrahedral sheets or Al atoms in octahedral sheets (>SiOH, >AlOH, $>Al_2OH$, and >AlSiOH). These groups are common to the edge surfaces of clay minerals (broken bonds). Generally, surface complexation leads to the formation of "inner sphere" surface complexes. In contrast, in an "outer sphere" complex, an ion retains its hydration sphere and attaches to the surface only via electrostatic forces.

In the next section, ion exchange and surface complexation are discussed using clay minerals as an example substrate because clays are an essential part of European geological disposal concepts in clays and crystalline rocks (bentonite buffer, and fracture fillings). The sorption by other rock forming minerals is discussed in Section 3.3.2.3.1. Various sorption-modeling approaches are discussed, and information on the atomistic nature of these classical adsorption mechanisms is addressed mainly for clays.

### 2.2.1 Ion exchange

#### 2.2.1.1 Theory and current understanding

Mineral surfaces may carry a permanent charge, and charge neutrality is maintained by the presence of an excess of counterions in solution held electrostatically in close proximity of the charged surface. Electrostatically bound ions, which constitute an electrical double layer, can undergo stoichiometric exchange with the ions in solution. This process is called ion exchange.

The surfaces of clay mineral platelets (also see Section 3.2.1 for more background on clay structural properties) carry a permanent negative charge arising from isomorphous substitution of the main lattice cations by other cations of lower valency, such as Si(IV) by Al(III) in a tetrahedral layer, and Al(III) by Mg(II) or Fe(II) in an octahedral layer (Liu et al., 2012b; Liu et al., 2013; Liu et al., 2014; Liu et al., 2015b). This permanent negative charge of a clay mineral gives rise to the so-called CEC (e.g., Grimm, 1953; Van Olphen, 1963). The CEC of montmorillonites (smectitic or swelling clay, with full access to the interlayer) is approximately 1 equiv/kg, and that of illites (non-swelling clay with only access to the outer surface) is approximately 0.2 equiv/kg. Notably, in the latter case, a large part of the structural charge is neutralized by potassium entrapped in the collapsed interlayer and is, thus, not readily available for cation exchange. By expressing the CEC in equivalent per unit mass, the value is independent of the charge of the exchangeable cations

compensating for the negative surface charge arising from isomorphous substitution in a clay mineral matrix. On this convention, the Gaines and Thomas formalism (Gaines and Thomas, 1953) is based. The description of equations for the law of mass action is expressed by a selectivity coefficient ($K_c$). Another well-known expression for the description of the cation exchange processes is given by the Vanselow Vanselow (1932) selectivity coefficient ($K_v$). The main difference between these two approaches is that $K_c$ is based on the equivalent fraction scale, whereas $K_v$ uses the molar fraction scale for the cations on the exchange complex. The current understanding of ion exchange in clay minerals is advanced because this topic has been a subject of intensive research for more than 40 years.

#### 2.2.1.2 Ion-exchange models

*Law of mass-action models:* Cation exchange reactions are often expressed in terms of a selectivity coefficient obtained by the application of the mass action law. The cation exchange reaction of metal B, of valence $z_B$, exchanging with a metal A, of valence $z_A$, on a clay mineral in the A-form can be written as:

$$z_B A^{z_A} - clay + z_A B^{z_B} \Leftrightarrow z_A B^{z_B} - clay + z_B A^{z_A} \quad (2)$$

Following the convention given by Gaines and Thomas (1953), a selectivity coefficient, ${}^{B}_{A}K_c$ [-], for reactions Equation 2 can be defined as:

$${}^{B}_{A}K_c = \frac{(N_B)^{z_A}}{(N_A)^{z_B}} \cdot \frac{[A]^{z_B}}{[B]^{z_A}} \cdot \frac{(\gamma_A)^{z_B}}{(\gamma_B)^{z_A}} \quad (3)$$

where $N_A$ and $N_B$ are the equivalent fractional occupancies, defined as the equivalents of A (or B) sorbed per kg of clay, divided by the CEC [equiv/kg]. $[A]$ and $[B]$ are the aqueous concentrations [mol/L], and $\gamma_A$ and $\gamma_B$ represent the aqueous-phase-activity coefficients [-].

A selectivity coefficient can be derived from experimental data at trace $B$ concentrations ($N_A \sim 1$), using:

$${}^{B}_{A}K_c = ({}^{B}R_d)^{z_A} \frac{(z_B)^{z_A}}{(CEC)^{z_A}} \cdot [A]^{z_B} \cdot \frac{(\gamma_A)^{z_B}}{(\gamma_B)^{z_A}} \quad (4)$$

where ${}^{B}R_d$ [m$^3$/kg] represents the sorption of cation $B$ by cation exchange, defined as the number of moles of $B$ sorbed per unit mass of the solid phase, divided by the number of moles of $B$ in the aqueous solution per unit volume.

An extensive literature review of cation exchange on clay minerals has been compiled by Bruggenwert and Kamphorst (1982). In their survey, cation exchange constant $K_c$ (Gaines and Thomas, 1953), or $K_v$ (Vanselow, 1932), are listed and can be easily incorporated in geochemical software to model cation exchange. A tabulation and an evaluation of ion-exchange data on smectites have been carried out by Benson (1982). Data are presented as log($K$) values and reflect very well the ranges found for some common ion equilibria on smectite. More recent data on cation exchange are available from Charlet and Tournassat (2005), Tournassat et al. (2007), Tournassat et al. (2008), Tournassat et al. (2009), and Tournassat et al. (2011).

Illite possesses a very specific type of exchange site, often called frayed edge sites (FESs), which have a high affinity for (and are only accessible by) large alkali ions because of their specific ionic size matching the surface structure. Brouwer et al. (1983) have developed a three-site (FES, type II, and planar sites) cation exchange model for Cs and Rb sorption on illite. This model has been extended to a generalized Cs sorption model (Bradbury and Baeyens, 2000) to predict Cs sorption isotherms for argillaceous rocks. Recently, this three-site cation-exchange model could be implemented for $Tl^+$ adsorption on illite (Wick et al., 2018). Non-linear sorption of Cs has been also observed in some smectites, attributable to the presence of randomly interstratified illite–smectite mixed layers, providing highly selective sorption sites for alkaline metals. This behavior could be modeled considering a two-site exchange model accounting for sorption on planar and FES-like sites (Missana et al., 2014). An overview of cation-exchange systems relevant to geological disposal is given in Table 1, together with information on surface complexation (see Section 2.2.2).

#### 2.2.1.3 Atomistic cation exchange models

Atomistic simulations are widely used to elucidate the hydration and adsorption mechanisms of ions in the interlayer of clay particles and the structure of the electric double layer at the basal plane of clay minerals. Such simulations are performed using Molecular Dynamics (MD) and Monte–Carlo approaches. In the Monte–Carlo technique, the equilibrium distribution of ions is obtained by stochastic modification of atomic positions following the Markov Chain stochastic process. In MD, simulation trajectories of ions and molecules are obtained by solving Newton's equation of motion for all atoms in a system. Thermodynamic properties and structural parameters of the system are obtained by time and ensemble averaging of the corresponding physical quantities depending on the atomic position over the entire simulated trajectory. The most important factors controlling the accuracy of the simulations are the underlying model for interatomic interactions and surface structural models used in the simulations. Most of the simulations are performed using so-called empirical pair interaction potentials. Such an approach provides a compromise between accuracy and computational efficiency. Only a few studies are known to have used a quantum mechanical system description (see Churakov and Liu (2018) for an exhaustive review). The most popular and widely used force fields for the simulations of clay minerals are CLAYFF (Cygan et al., 2004), INTERFACE (Heinz et al., 2013), and OPLS (Jorgensen and Tirado-Rives, 1988). These empirical force fields can, in principle, be combined with a variety of models for water (Guillot, 2002) and ions (Aqvist, 1990). More recently, several efforts were undertaken to develop a so-called polarizable force field, which takes into account the electronic polarization of electron shells depending on the instantaneous atomic configuration (Tesson et al., 2016).

The investigation of cation exchange in molecular simulations is based on calculations of the equilibrium distributions of ions between an interlayer space and a bulk electrolyte, in direct simulations with interfaces (Lammers et al., 2017) or by thermodynamic integration without interfaces (Rotenberg et al., 2009).

### 2.2.2 Surface complexation

#### 2.2.2.1 Theory and current understanding

Different thermodynamic sorption models (TSM) have been introduced to describe the solid–solution interface during

TABLE 1 Overview of cation exchange and surface complexation models on 2:1 clay minerals.

| Clay | Model | Proto-lysis | SC | CE | Cations | Reference |
|---|---|---|---|---|---|---|
| bentonite, zeolites | CE | - | - | $K_v$ | $Na^+$, $K^+$, $NH_4^+$, $Ca^{2+}$, $Ba^{2+}$ | Vanselow (1932) |
| montmorillonite | CE | - | - | $K_c$ | $Cs^+$, $K^+$, $Sr^{2+}$ | Faucher and Thomas (1954); Gaines and Thomas (1955) |
| montmorillonite | CE | - | - | $K_c$ | $Na^+$, $Co^{2+}$, $Ni^{2+}$, $Cu^{2+}$, $Zn^{2+}$, $Cd^{2+}$ | Maes et al. (1975) |
| Illite | CE | - | - | $K_c$ | $Na^+$, $Rb^+$, $Cs^+$, $Tl^+$, $Ca^{2+}$, $Sr^{2+}$, $Ba^{2+}$ | Brouwer et al. (1983); Poinssot et al. (1999); Wick et al. (2018) |
| montmorillonite | CE | - | - | $K_c$ | $Na^+$, $Fe^{2+}$ | Singhal and Kumar (1975) |
| montmorillonite | CCM | | 1 site | - | $H^+$ | Wanner et al. (1994) |
| montmorillonite | DDLM | | 1 site | - | $H^+$ | Kraepiel et al. (1998) |
| montmorillonite | MUSIC | | 4 sites | - | $H^+$ | Tournassat et al. (2004b) |
| Illite | GEMS | | 2 sites | | $H^+$, Ln | Sinitsyn et al. (2000)<br>Kulik et al. (2000) |
| montmorillonite illite | 2SPNESC/ CE | 2 $pK_a$ | strong/weak | $K_c$ | Ni(II), Zn(II), Eu(III), Sn(IV), Am(III), Np(V), U(VI) | Baeyens and Bradbury (1997), Bradbury and Baeyens (1997b); Bradbury and Baeyens (2009a), Bradbury and Baeyens (2009b) |
| montmorillonite | EM/CE SC | 2 pKa | strong/weak | $K_{ex}$ | Ni(II), Zn(II) | Kraepiel et al. (1999) |
| montmorillonite | | 4 pKa | ≡AlOH ≡SiOH | $K_{ex}$ | $UO_2^{2+}$ | McKinley et al. (1995) |
| montmorillonite | spillover | | | | $UO_2^{2+}$ | Tournassat et al. (2018) |
| montmorillonite | EM/CE SC | 2 pKa | 1 site KSOM | $K_{ex}$ | Pb(II), Cd(II) | Barbier et al. (2000) |
| montmorillonite | DLM | 3 pKa (two ≡AlOH, ≡SiOH) | ≡AlOH ≡SiOH | neglected I = 0.1 | Np(V) | Turner et al. (1998) |
| montmorillonite silica alumina | EM CCM | 3 pKa (KA1, KSi1 and KSi2 | ≡AlOH ≡SiOH | $K_{ex}$ | $Eu^{3+}$; $UO_2^{2+}$ | Kowal-Fouchard et al. (2004b), Kowal-Fouchard et al. (2004a) |
| bentonite | DLM | 3 pKa | 1 site | n.i | U(VI), Se(IV) | Boult et al. (1998) |
| beidellite | TLM | | 2 sites ≡AlOH ≡SiOH | $K_{ex}$ | $UO_2^{2+}$ | Pabalan and Turner (1996) |

SC: surface complexation; CE: cation exchange; $K_v$: Vanselow constant; $K_c$: Gaines & Thomas selectivity constant; $K_{ex}$: cation exchange constant; CCM: constant capacitance modelling; EM: electrostatic modelling; DLM: Diffuse layer model (Dzombak and Morel, 1990); ECCM: (Extended) constant capacitance model (Nilsson et al., 1996); TLM: Triple-layer model (Hayes et al., 1991); MUSIC: Multi-site complexation model (Hiemstra et al., 1996); GEMS: Gibbs energy minimization selector (http://gems.web.psi.ch/).

sorption processes (Ochs et al., 2012). TSMs used to calculate defined surface complexation processes of metal cations (Me), for example, are called surface complexation models (SCMs). Each SCM is characterized by an individual set of surface complexation parameters (SCPs) defining the mechanistic approach to describe retardation processes at the solid–solution interface. These parameters comprise surface complexation constants ($\log K_{Me}$), specific surface area (SSA), surface site density (SSD), and protolysis constants ($\log K_{prot}$), which describe the acid–base characteristics of each mineral surface (Britz, 2018). TSMs extend the ion-association theory of aqueous species to surface species through thermodynamic equilibrium reactions using measurements of SSAs and estimated SSDs. In addition to the commonly applied diffuse double-layer model (DDLM) and non-electrostatic models (non-electrical double layers (EDL) models, noEDLM), more sophisticated model approaches exist, such as the basic Stern model (BSM), triple-layer models, and three-plane models (TPMs), which are widely used TSMs. All TSMs are based on mass law equations and mole balance equations (Davis and Kent, 1990b), but they involve different descriptions of the electric double layer, i.e., an electrostatic interaction term (Westall and Hohl, 1980; Davis and Kent, 1990a). In the noEDLM, electrostatic interaction is not considered; thus, the DDL is neglected. Each TSM (except noEDLMs) considers different electrostatic planes that contribute to sorption processes.

### 2.2.2.2 Surface complexation models

*Acid–base modeling of minerals*. The protolysis behavior of amphoteric surface hydroxyl sites is usually described by following protonation and deprotonation reactions, with their corresponding mass action relationship:

TABLE 2 $pK_a$'s of edge sites for individual surfaces of phyllosilicates. Modified and augmented after Churakov and Liu (2018), with permission from Elsevier.

| Surfaces | Sites | p*Ka*'s | Reference |
|---|---|---|---|
| Pyrophyllite/Montmorillonite | | | |
| (110) Neutral | ≡$Si(OH_2)$/≡Si(OH) | −6.8/8.3 | Liu et al. (2014) |
| | ≡AlSiOH | 1.7 | |
| | ≡$Al(OH_2)$ | 5.5 | |
| (110) Mg-sub | ≡$Si(OH_2)$/≡Si(OH) (connecting Mg *via* O) | −2.5/11.0 | |
| | ≡MgSiOH | 4.2 | |
| (110) Al-sub | ≡$Al(OH_2)_{Tetra}$/≡$Al(OH)_{Tetra}$ | −2.4/17.5 | |
| | ≡AlAlOH | 10.2 | |
| | ≡$Al(OH_2)_{Octa}$ | 12.7 | |
| (010) Neutral | ≡$Si(OH_2)$/≡Si(OH) | −14.3/7.0<br>6.8 | Liu et al. (2013), Tazi et al. (2012) |
| | ≡$Al(OH_2)(OH_2)_{Octa}$/≡$Al(OH_2)(OH)_{Octa}$ | 3.1/8.3<br>7.6/22.01 | Tazi et al. (2012), Liu et al. (2014) |
| (010) Mg-sub | ≡$Si(OH_2)$/≡Si(OH) (connecting Mg *via* O) | −10.9/10.8 | Liu et al. (2013) |
| | ≡$Mg(OH_2)_2$ | 13.2 | |
| (010) Al-sub | ≡$Al(OH_2)_{Tetra}$/≡$Al(OH)_{Tetra}$ | −2.4/15.1 | Liu et al. (2014) |
| | ≡$Al(OH_2)(OH_2)_{Octa}$/≡$Al(OH_2)(OH)_{Octa}$ | 4.9/8.5 | |
| (010) Fe(III) | ≡Si(OH) | 8.6 | Liu et al. (2015a) |
| | ≡$Fe(OH_2)(OH_2)$/≡$Fe(OH_2)(OH)$ | 1.2/5.1 | |
| (010) Fe(II) | ≡Si(OH) | 11.2 | |
| | ≡$Fe(OH_2)$ [5-fold]/≡$Fe(OH_2)(OH_2)$ [6-fold] | 6.6/10.2 | |
| Nontronite | | | |
| (010) Fe(III) | ≡Si(OH) | 8.7 | Liu et al. (2015a) |
| | ≡$Fe(OH_2)(OH_2)$/≡$Fe(OH_2)(OH)$ | 1.2/4.4 | |
| (010) Fe(II) | ≡Si(OH) | 9.9 | |
| | ≡$Fe(OH_2)$ [5-fold] | 8.4 | |

$$\equiv SOH + H^+ \Leftrightarrow \equiv SOH_2^+ \quad K^+ = \frac{[\equiv SOH_2^+]}{[\equiv SOH]\{H^+\}} \tag{5}$$

$$\equiv SOH \Leftrightarrow \equiv SOH^- + H^+ \quad K^- = \frac{[\equiv SOH^-]\{H^+\}}{[\equiv SOH]} \tag{6}$$

where [ ] represents molar concentration and { } denotes activities.

Of note, the above mass action equations are written without an electrostatic term. In electrostatic models (see Table 2), an additional electrostatic term is included in the equations, which accounts for the distribution of the ions in a double layer according to the Maxwell–Boltzmann equation (e.g., Dzombak and Morel, 1990).

We would like to refer to two comprehensive review papers on this subject, related to clay minerals. The first, by Duc et al. (2005), details the experimental difficulties/constraints regarding titration measurements and their influence on modeling. The second review is by Bourg et al. (2007), giving an overview of available protolysis models. This review contains data on *pK*, site densities, and specific edge surface areas from 12 different studies on acid–base titration models of Na-montmorillonite.

The site types, their densities, and the protolysis constants can vary in the various model approaches, from one single site to 27 sites (Tournassat et al., 2004b; Tournassat et al., 2004a). In general, two sites are considered and are associated with tetrahedral silanol sites and octahedral aluminol sites (Bradbury and Baeyens, 2000).

Table 1 lists a number of model approaches for the acid–base behavior of clay minerals, which are isolated from metal sorption data and can only be used for describing the proton buffer capacity of clay minerals.

*Sorption of anions*. The sorption of anionic species generally takes place via a ligand-exchange mechanism. For example, the sorption of boron on the edge sites of montmorillonite, illite, and kaolinite was modeled by Goldberg and Glaubig (1986) by means of the following reaction:

$$\equiv SOH + H_3BO_3 \Leftrightarrow \equiv SH_2BO_3 + H_2O \quad (7)$$

with the associated mass action equation:

$$K = \frac{[\equiv SH_2BO_3]}{[\equiv SOH][H_3BO_3]} \quad (8)$$

In this study, the boron sorption on the three clay minerals was modeled either by fitting protolysis constants to tetrahedral silanol sites and octahedral aluminol sites or by using protolysis constants from Al and Fe oxides (Goldberg and Sposito, 1984).

Modeled sorption data of anions on clay minerals are very sparse in the open literature. Most studies are limited to B(III), Mo(VI), Se(IV), and As(V) uptake on montmorillonite and illite (Goldberg and Glaubig, 1986; Goldberg and Glaubig, 1988a; Goldberg and Glaubig, 1988b; Motta and Miranda, 1989; Manning and Goldberg, 1996). More recently, Bruggeman (2006) investigated the uptake of Se(IV/VI) on illite and was capable of applying a non-electrostatic model (NEM) to quantitatively describe the pH-dependent adsorption of anionic species, using both wet chemistry and spectroscopic methods. Missana et al. (2009) investigated selenite sorption on smectite and illite and modeled the sorption behavior on smectite–illite mixtures, using a two-site NEM.

*Sorption of cations*. The general form of the surface complexation equations used for representing the surface binding of cations can be written as:

$$\equiv SOH + Me^{z+} + yH_2O \Leftrightarrow \equiv SOMe(OH)_y^{z-(y+1)} + (y+1)H^+ \quad (9)$$

where *Me* is a metal with valency *z*, *y* is an integer, and the corresponding surface stability constant is expressed as $K_y$. For $y = 0$ the surface complex is $\equiv SOMe^{(z-1)}$.

In a NEM, the corresponding surface complexation constant, $K_y$, can be expressed as:

$$K_y = \frac{\left[SOMe(OH)_y^{z-(y+1)}\right]}{[\equiv SOH]} \cdot \frac{f_{\equiv SOMe(OH)_y^{z-(y+1)}}}{f_{\equiv SOH}} \frac{\{H^+\}^{y+1}}{\{Me^{z+}\}} \quad (10)$$

where [ ] terms are surface concentrations, $f$ terms are surface activity coefficients, and { } terms are aqueous activities. Following discussions given in Dzombak and Morel (1990), an assumption concerning surface activity coefficients is made, i.e., the ratios of the surface activity coefficients in the mass action equations describing surface complexation reactions are taken to be unity.

A model developed for montmorillonite and illite, the two-site protolysis non-electrostatic surface complexation and cation exchange, and 2SPNE SC/CE (Bradbury and Baeyens, 1997b; Bradbury and Baeyens, 2009a), can be used to illustrate the modeling approach using the following three datasets:

- clay acid–base titration data,
- sorption edges (trace sorption as a function of pH at a fixed ionic strength),
- sorption isotherms (concentration-dependent sorption at a fixed pH and fixed ionic strength).

A consequent iterative process was applied to model all three datasets until all experimental measurements were satisfactorily described. The model results were described with site capacities (two weak protolysis sites ($\equiv S^{W1}OH$ and $\equiv S^{W2}OH$) and one strong site ($\equiv S^{S}OH$) for metal sorption at trace concentration), protolysis constants, cation-exchange capacities, cation-exchange selectivities, and surface complexation constants for strong and, in some cases, weak sites. Furthermore, there were enough elements investigated so that linear free energy relations could be derived for cation sorption (Bradbury and Baeyens, 2005b; Bradbury and Baeyens, 2005a).

An overview of the cation exchange and SCMs of anionic and cationic species for relevant geological disposal elements on 2:1 clay minerals is given in Table 1.

*Atomistic acid–base and surface complexation models*. The intrinsic acidity of surface OH groups is one of most important parameters controlling the development of surface charge on the edge sites of clay particles as a function of pH. Intrinsic acidity depends on the structural position of OH groups and the isomorphic substitutions in TOT sheets. Significant progress has been made recently in understanding the stability and structure of edge sites in clay minerals (Keri et al., 2020; Churakov, 2007; Churakov, 2006; Liu et al., 2012b; Okumura et al., 2017). The obtained data were used to investigate the acidity of surface groups using *ab initio* simulations (Liu et al., 2015b; Liu et al., 2014; Liu et al., 2013; Liu et al., 2011). The essence of the method is the calculation of free energy for the proton transfer reaction in the presence of explicit solvent molecules:

$$\equiv SOH_n^p + H_2O_{aq} \leftrightarrow \equiv SOH_{n-1}^{p-1} + H_3O_{aq}^+ \quad (11)$$

using thermodynamic integration techniques. The site acidities obtained in such a way represent so-called intrinsic *pK*'s, corresponding to the deprotonation reaction of an isolated > SiOH site in pure water on an "ideal" charge neutral surface. To describe experimental data, these constants have to be combined with an electrostatic "analytical" model or one based on molecular simulations, which accounts for interactions between the surface charge and the ions in an electrolyte solution, using thermodynamic integration techniques (Churakov et al., 2014b). Table 2 summarizes currently available data obtained by *ab initio* simulations for different clay minerals.

Recent work by Orucoglu et al. (2022), Liu et al. (2022) and Gao et al. (2023b) allowed for obtaining a multi-scale understanding of structures, the reactivity of pyrophyllite (Schliemann and Churakov, 2021b; Schliemann and Churakov, 2021a), the and sorption capacity of montmorillonite (Kunipia) edges. It was demonstrated that Kunipia clay has crystalline edges and a cis-vacant layer structure. This atomic-scale study allowed for building and predicting edge acid–base properties and sorption properties, including sorption reversibility.

Ab initio simulations have been applied to reveal energetically favorable configurations of surface complexation ions on the edge surfaces of phyllosilicate minerals (Table 3). Most of the relevant studies were performed for the simple structural prototype of pyrophyllite (pyrophyllite has no structural charge). The general conclusions about the sorption mechanism should be transferable to other clay minerals, however. The extent and the distribution of surface charge has a strong influence on the strength of the ion–surface interactions.

TSMs described in previous sections rely on the existence of at least two sorption sites (Bradbury and Baeyens, 1997b; Baeyens and Bradbury, 1997). These sites are referred to as strong and weak sites,

TABLE 3 Ab initio surface studies of sorption complexation mechanism of cation on edges of clay minerals.

| Mineral | Cation | References |
|---|---|---|
| Montmorillonite | $Zn^{2+}$ | Churakov and Daehn (2012) |
| Pyrophyllite | $Fe^{2+}/Fe^{3+}$ | Keri et al. (2020) |
| Pyrophyllite | $Fe^{2+}$ | Liu et al. (2012a), Liu et al. (2013), Liu et al. (2014) |
| Pyrophyllite | $Cd^{2+}/Ni^{2+}$ | Zhang et al. (2016), Zhang et al. (2017) |
| Kaolinite/pyrophyllite/illite | $UO_2^{2+}$ | Kremleva et al. (2015a), Kremleva et al. (2015b), Kremleva et al. (2012), Kremleva et al. (2011) |

which can be related to the higher and lower affinity constants of the surface complexation reaction. Ab initio simulations combined with X-ray absorption spectroscopy (XAS) studies specifically address the molecular structure of such sorption sites. It could be shown that, for divalent and trivalent transition metals, high-affinity sites are represented by, etch pits (single-atom defects) on the edge of clay minerals. The weak sites in the TSM are structurally related to the inner-sphere sorption complexes on the edge surfaces (Churakov and Daehn, 2012; Keri et al., 2020). The structure and site density of the cationic surface complexes obtained by *ab initio* simulations are consistent with spectroscopic data and thermodynamic simulations, respectively.

### 2.2.3 Reversibility

An analysis of radionuclide desorption behavior is essential for evaluating the (ir)reversibility of sorption processes in order to predict the long-term migration behavior of radionuclides.

Desorption tests are typically performed following sorption tests. In the sorption step, after the selected contact time, the solid-to-liquid distribution coefficient, $R_{d,sorb}$, is determined. The solid in which the adsorbate is retained and can be suspended again in a fresh solution to determine the distribution coefficient, $R_{d,desorb}$, for the desorption step. From a thermodynamic perspective of reaction chemistry, when $R_{d,sorb}$ and $R_{d,desorb}$ are equal for reaction times within the same time span of hours to a few days, this process is considered "reversible"; if not, it is considered "irreversible." For longer reaction times, other processes, such as recrystallisation, the restructuring of surface complexes, or the neoformation of clay minerals, might occur, changing an initial reversible surface complex to an irreversible one over years.

The reasons why retention is (or is not) reversible are numerous and must be evaluated in detail. In some of the cases, irreversibility is only apparent because the sorption and desorption processes were not at equilibrium. However, hysteretic behavior might indicate that reactions other than sorption are taking place, which contribute to the overall retention in a system.

The main mechanism leading to contaminant retention in a mineral surface is adsorption, which is generally rapid and reversible, when no other process such as the recrystallization restructuring of surface complexes or neoformation of clay minerals occur (Dähn et al., 2001; Dähn et al., 2002; Dähn et al., 2003; Dähn et al., 2011; Begg et al., 2017). However, several kinetically controlled processes contributing to slower uptake exist, such as diffusion processes inside a solid where the formation of stronger bonds and the crystallization of new phases can occur (Sparks, 2003). In addition, aging can have a significant effect on contaminant release. These processes are usually not included in surface complexation modeling.

The importance of the "reaction time" and kinetically controlled processes increases when dynamic phenomena (diffusion, advective–dispersive transport) must be described. An apparently "irreversible" process for short residence times can be completely reversible at the long-time scales considered in safety assessment for radioactive waste repositories.

Among the most important processes contributing to irreversible sorption on clays is the formation of surface precipitates incorporating and sequestrating a contaminant (also see Section 2.2, other uptake processes). The identification and characterization of surface precipitates is an important task that has to be accomplished using microscopic and spectroscopic techniques (Scheidegger et al., 1997; Ford et al., 2001).

Structural modifications within the layered structure of phyllosilicates (clays) can lead to irreversible retention of contaminants. Many recent studies have been devoted to the analysis of the irreversible sorption of Cs into illite, focusing on processes favoring its fixation caused by the collapse of the FESs, and their de-lamination favored in the presence of divalent ions (Benedicto et al., 2014c; Fuller et al., 2015; Durrant et al., 2018).

One of the key factors determining the degree of reversibility of the surface complexation on the edges of clay minerals at an atomistic scale is the structural evolution of the mineral surfaces as part of dissolution and precipitation processes. These processes determine the availability of high-affinity sorption sites and the structural (irreversible) incorporation of cations. Ab initio simulations can provide direct information on the dissolution process for individual surface sites (Schliemann and Churakov, 2021a). The macroscopic description of these data needs a global view of the temporal evolution of site density. Such information can be obtained using coarse-grained models for clay particle dissolution and growth as well as mineral–fluid interactions (Kurganskaya and Luttge, 2013; Delhorme et al., 2010; Yang et al., 2020).

### 2.2.4 Research methods

Different approaches exist to characterize mineral-specific and sorption-relevant processes, such as the acid–base behavior of surfaces and the retardation of cations (e.g., cation-exchange and surface complexation processes), in general. To examine sorption reactions at the solid–liquid interface, commonly applied methods include classical potentiometric titration experiments, so-called batch experiments to elucidate adsorption, and spectroscopic investigations.

#### 2.2.4.1 Wet chemistry

*Determination of CEC*. A large range of methods exists to determine the CEC. Those using the highly selective metal dyes (e.g., Cu(trien) (Meier and Kahr, 1999), $Ni(en)_3$ (Baeyens and Bradbury, 1991), or CoHex (Rémy and Orsini, 1976)) are the most popular because of their simplicity (single extraction, possibility of colorimetric measurements of selective metal-ion consumption, etc.).

Within the Mont Terri Project, an extensive intercomparison study was set up on different methods in order to find their advantages, disadvantages, and potential drawbacks (Hadi et al., 2019).

*Acid–base titrations*. Wet chemistry investigations on dispersed systems are aimed at elucidating the nature of the radionuclide retention at the solid–liquid interface, i.e., to characterize the different adsorption site types and capacities. Detailed knowledge of the protonation and deprotonation processes (acid–base behavior) of mineral surfaces are of great importance for realistically describing retardation processes at mineral–water interfaces, since they are—for most radionuclides/contaminants—pH dependent.

Potentiometric acid–base titration experiments of mineral surfaces have been widely applied (e.g., Arnold et al., 2001; Lützenkirchen et al., 2012a; Lützenkirchen et al., 2012b; Schwarz et al., 1984) to characterize mineral electrostatic behavior in terms of points of zero charge, surface charge densities, and net surface proton excess. A combination of discontinuous electrolyte and mass titration experiments with continuous potentiometric acid–base titrations offer even deeper insight into mineral surface protonation and deprotonation states as a function of, for example, pH, ionic strength, and solid–liquid ratio (e.g., Lützenkirchen et al., 2012a; Lützenkirchen et al., 2012b; Preocanin and Kallay, 1998; Noh and Schwarz, 1989). An alternative experimental approach (Baeyens and Bradbury, 1995; Baeyens and Bradbury, 1997; Bradbury and Baeyens, 2009a; Tournassat et al., 2004b) is a batch titration technique with back-titration on aluminum oxides, as originally proposed by Schulthess and Sparks (1986).

*Adsorption experiments*. The research methods for ion exchange and surface complexation mainly target the elucidation of the nature of the uptake mechanisms (inner sphere/outer sphere complexes) and the type and capacities of the adsorption sites of sorbents investigated. Wet-chemistry investigation on dispersed systems is the most common experimental method used.

Sorption experiments are carried out by equilibrating an adsorbate solution of known composition and volume with a known amount of adsorbent. The suspension is gently shaken/stirred for a certain period of time until sorption equilibrium is reached. After equilibrium, the solution is separated from the solid phase via centrifugation and/or filtration and analyzed. From these experiments, the distribution coefficient $R_d$ is calculated (see Equation 1). When a series of experiments is conducted at a well-defined ionic strength and similar initial concentrations but at varying pH values, so-called "sorption edges" are obtained. When a series of experiments is conducted at a well-defined ionic strength and constant pH but by varying the initial concentration, so-called "adsorption isotherms" are determined.

*Spectroscopic and atomistic techniques*. Surface complexation studies of ionic species are generally carried out using batch sorption techniques similar to those used in ion-exchange studies. These methods are frequently complemented by a number of alternative techniques such, as micro-calorimetry and infrared spectroscopy, to elaborate on the nature of the surface complexes. X-ray Adsorption spectroscopy (XAS) techniques (Extended X-ray Adsorption Fine Structures (EXAFS)/X-ray Adsorption Near Edge Structure (XANES), see Section 2.3.2.3.1 for more details) have been applied to demonstrate the outer-sphere character of ions in an interlayer.

EXAFS has proven successful in providing a molecular understanding of sorption on edge sites (Dähn et al., 2003; Schlegel et al., 2001b; Dähn et al., 2011), uptake on interlayer sites via cation exchange (Sposito, 1984; Muller et al., 1997; Chisholm-Brause et al., 1994), and uptake in newly formed lamellar phases such as layer silicates (Schlegel et al., 2001a; Dähn et al., 2002) and mixed layered double hydroxides (LDHs) (Scheidegger et al., 1998; Thompson et al., 1999a; Towle et al., 1997).

MD and Monte–Carlo simulations are used to reveal the equilibrium distribution of ions in the interlayers of smectites minerals, as well as cation-exchange processes and the structure of the electrical double layer at solid–liquid interfaces. Surface complexation processes involve protonation and deprotonation reactions at the edges of clay minerals. The surface complexation reactions result in the direct interaction of ions with deprotonated oxygen sites. These processes lead to a significant change in the electron density between the interacting atoms and, thus, require a quantum mechanical description of systems. Recent reviews of quantum mechanical studies of adsorption processes on clay minerals are available in Churakov and Liu (2018) and (Liu et al., 2022).

## 2.3 Other uptake processes

### 2.3.1 Neoformation/surface precipitation

#### 2.3.1.1 Theory and current understanding

Most of the studies on the uptake of contaminants in clay systems have been based on wet chemistry experiments and modeling at the macroscopic level. Batch studies (also see Section 2.2.4) provide an efficient tool for determining the distribution coefficients of metal ions and, under certain circumstances, allow for differentiation between ion exchange and surface complexation processes occurring at the solid–water interface (Sposito, 1984). However, the ability of a particular SCM to fit macroscopic data does not certify that the assumptions underlying a model are correct. For example, macroscopic data do not allow unambiguous discrimination between surface complexation and nucleation processes. A way to gain mechanistic information about metal interactions on solid surfaces is to combine batch studies with synchrotron-based spectroscopic investigations.

With increasing reaction time and metal concentrations, transition-metal surface precipitates (neo-formed phyllosilicate or LDHs) can form on clay minerals. This process can irreversibly bind contaminants to mineral surfaces, whereas (pure) sorption models assume that the adsorption of trace metals is reversible. Using EXAFS, it has been demonstrated that Ni-, Co- and Zn-containing precipitates can form when clay minerals and Al- and Si-(hydr)oxides are treated with Ni, Co, and Zn, and this occurs even when the initial metal concentration in solution is undersaturated

relative to that of the pure (oxyhydr)oxide forms of the metal (Towle et al., 1997; Scheidegger et al., 1998; Manceau et al., 1999; Thompson et al., 1999a; Thompson et al., 1999b; Morton et al., 2001; Schlegel et al., 2001a; Dähn et al., 2001; Dähn et al., 2002; Lee et al., 2004). For example Scheidegger et al. (1998) observed the formation of a LDH phase when pyrophyllite (a 2:1 clay that lacks isomorphic substitution) was treated with Ni. A Ni-Al LDH phase formed after a contact time of only a few minutes between pyrophyllite and Ni, suggesting that nucleation can occur rapidly in metal clay sorption systems. LDH formation has been further reported for Co(II) and Zn(II) sorption on kaolinite and Al-(hydr)oxides (Towle et al., 1997; Thompson et al., 1999a; Thompson et al., 1999b). Similarly, the uptake of Co on quartz was shown to result in the neoformation of a trioctahedral clay-like structure (Manceau et al., 1999).

Using polarized-EXAFS (P-EXAFS) Dähn et al. (2002) and Schlegel et al. (2001a) demonstrated the presence of neo-formed phyllosilicates after treating di- and tri-octahedral 2:1 clay minerals (montmorillonite and hectorite) with Ni and Zn solutions at elevated pH and metal concentrations. The neo-formed phases were oriented parallel to the octahedral smectite sheets. In a study by Schlegel et al. (2001a), a structural link of neo-formed phases to hectorite particles could be observed. A study of Dähn et al. (2002) indicated that neoformation processes of clay minerals had already started after 1 day of reacting and continued for as long as metal ions were present in solution.

#### 2.3.1.2 Research methods

As mentioned in Section 2.2.4.2, EXAFS has proven successful in gaining a molecular understanding of sorption on edge sites, uptake on interlayer sites via cation exchange, and uptake in newly formed lamellar phases. In the relevant studies, macroscopic wet chemistry investigations were combined with synchrotron-based spectroscopic analysis. Studies on the uptake of metals on mineral surfaces observed the formation of phyllosilicates upon the uptake of Co on quartz (Manceau et al., 1999), Zn on hectorite (Schlegel et al., 2001a), and Ni on montmorillonite (Dähn et al., 2001; Dähn et al., 2002), as well as the formation of LDH phases for Co uptake on Al-(hydr)oxides (Towle et al., 1997), Zn on kaolinite and Al-(hydr)oxides (Thompson et al., 1999b; Thompson et al., 1999a), and Ni on gibbsite, pyrophyllite, and montmorillonite (Scheidegger et al., 1997; Scheidegger et al., 1998). The sensitivity of EXAFS measurements on clay minerals can be significantly improved by performing P-EXAFS. In P-EXAFS, neighboring atoms along the polarization direction of an X-ray beam are preferentially probed, and atoms located perpendicular to this direction are attenuated. Applying P-EXAFS to self-supporting clay films has the advantage of minimizing the contributions from out-of-plane Si atoms from a tetrahedral sheet, when an X-ray polarization vector is in the *ab* plane of a montmorillonite self-supporting film (Manceau et al., 1998; Dähn et al., 2002; Dähn et al., 2003; Dähn et al., 2011). Conversely, when the polarization vector is aligned normal to the film plane, the contribution from octahedral-layer cations vanishes. This method allows for determining the speciation of chemical entities at the atomistic scale, even when the element of interest is present at low concentrations (concentrations of X-ray absorber down to approximately 100 ppm in clay matrixes).

#### 2.3.1.3 Remaining uncertainties

Research on the neoformation of minerals raises many questions, such as how can stable mineral clay phases generate sufficient soluble Al or Si to react with sorbed metals? None of the above-mentioned studies could provide deep insights into what triggers the precipitation of a phyllosilicate or a LDH phase. In both cases, it was observed that high pH, high metal concentrations, and prolonged reaction times favored the formation of phyllosilicates or LDH precipitates. In the past, most efforts in radioactive waste management studies focused on the understanding of sorption process at low metal concentrations in solution, as it was assumed that precipitation processes are not relevant for the safety analyses, considering a conservative approach, of future radioactive waste disposal sites. However, nowadays it has been accepted that, for example, high Fe concentrations arising from waste forms can occur, deeming the precipitation processes relevant (Soltermann et al., 2014b; Soltermann et al., 2013b; Soltermann et al., 2014c). In order to understand the neoformation of phyllosilicates or LDH phases from a thermodynamic perspective, solubility products need to be determined in the future (Dähn et al., 2003). Presently, such information is lacking in TDBs. The heterogeneous formation of phyllosilicates has important geochemical implications because layer silicates are stable minerals under mildly-acidic-to-basic pH conditions and can irreversibly bind metals in waste and soil matrices, as demonstrated in Zn-smelter impacted soils (Manceau et al., 2000; Vespa et al., 2010).

For long-duration sorption experiments, the development of microbial activity with time could interfere with sorption processes and neoformation/surface precipitation. There is, however, not much documentation on the effect of microbial perturbation on the results of batch sorption tests. It is suggested to thoroughly review the literature and to consider this in future studies.

### 2.3.2 Surface-induced redox uptake

#### 2.3.2.1 Theory and current understanding

**2.3.2.1.1 General definition of redox processes and selected examples.** Redox reactions require the transfer of electrons between aqueous species (homogenous) or between aqueous species and mineral surfaces (heterogeneous) (Ahmed and Hudson-Edwards, 2017). Redox processes are key geochemical processes because they strongly influence the mobility of redox-sensitive contaminants (e.g., Se, Tc, U, Np, and Pu), which are abiotically reduced to often less toxic or less mobile forms (Ma et al., 2019; Guillaumont et al., 2003; Olin et al., 2005; Winkel et al., 2012). These include the tetravalent oxides of U, Np, Pu, and Tc; Se(0); FeSe; and sulfide phases such as TcS, while notable exceptions to this rule include the aqueous $Pu^{3+}$ complexes and gaseous Se species (Kirsch et al., 2011; Winkel et al., 2012).

Minerals containing redox-active species such as Fe (II, III) or Mn (II, III, IV) can participate in a wide range of surface-induced electron-transfer reactions. For instance, Fe-bearing minerals cover a large range of redox potentials depending on the amount and location of Fe in a crystal lattice (Gorski et al., 2012a; Gorski et al., 2012b; Gorski et al., 2013; Gorski et al., 2016; Sander et al., 2015; Li et al., 2019a). The rates and extents of redox reactions are controlled by the physico-chemical properties (e.g., redox and sorption potential, or electron conductivity, depending on factors such as composition or particle size) of the minerals (Ilgen et al., 2019; Scheinost et al., 2008).

In the last two decades, many studies have addressed the influence of Fe-bearing minerals on the immobilization of redox-sensitive nuclides such Fe, Se, Tc, U, Np, and Pu. Studies on relevant minerals are summarized below:

- Clays: Alexandrov and Rosso, 2013, Boland et al., 2011, Chakraborty et al., 2010, Fox et al., 2013, Hoving et al., 2017, Ilton et al., 2010, Jaisi et al., 2009, Jeon et al., 2005, Jones et al., 2017, Latta et al., 2012, Latta et al., 2017, Liger et al., 1999, O'Loughlin et al., 2003, Pearce et al., 2017, Peretyazhko et al., 2008, Peretyazhko et al., 2012, Roberts et al., 2019, Schaefer et al., 2011, Soltermann et al., 2014a, Soltermann et al., 2013a, Stumm and Sulzberger, 1992, Tsarev et al., 2016, Yang et al., 2012, Zhu and Elzinga, 2014, Joe-Wong et al., 2017, Charlet et al., 2007, Frohlich et al., 2012, Brookshaw et al., 2015, Qian et al., 2023.
- Iron oxides (including oxyhydroxides and hydroxides): Bender and Becker, 2019, Dumas et al., 2019, Emmanuel and Ague, 2009, Emmanuel et al., 2010, Kirsch et al., 2011, Kobayashi et al., 2013, Um et al., 2011, Yalçıntaş et al., 2016, Scheinost and Charlet, 2008, Scheinost et al., 2008, Christiansen et al., 2011, Wylie et al., 2016, O'Loughlin et al., 2003, O'Loughlin et al., 2010, Huber et al., 2012, Pidchenko et al., 2017, Roberts et al., 2017, Börsig et al., 2018, Peretyazhko et al., 2008, Poulain et al., 2022.
- Fe(II) (hydroxo-) carbonates: Scheinost et al., 2016; Scheinost and Charlet, 2008; Kirsch et al., 2011; Ithurbide et al., 2009; Badaut et al., 2012; Llorens et al., 2007)
- Fe(II) sulfides: (Moyes et al., 2002, Scheinost and Charlet, 2008, Scheinost et al., 2008, Yalçıntaş et al., 2016, Finck et al., 2012, Han et al., 2011, Kirsch et al., 2011, Wharton et al., 2000, Rodriguez et al., 2020, Breynaert et al., 2008, Liu et al., 2008, Bruggeman et al., 2007, Pearce et al., 2018, Livens et al., 2004.

Element-specific reviews, for example those focusing on Tc (Meena and Arai, 2017; Pearce et al., 2020), can also be used as a state-of-the art introduction on the nature of the redox interactions between Fe minerals and redox-sensitive elements.

**2.3.2.1.2 Redox-relevant minerals in disposal systems.** The following section is based on the mineralogical data available for clay formations, namely Boom Clay, Opalinus Clay, and the clay-rich horizon of the Callovian-Oxfordian Formation in Bure and for the granitic formation of Aspö.

As discussed above, for a redox reaction to occur at the mineral–aqueous solution interface, the solid phase must contain a chemical element that can have different oxidation states in the considered chemical system, and it must be in a reduced state if the element with which it interacts is in the oxidized state, and *vice versa*. In the environment, two major metallic elements reported to be capable of participating in redox reactions are Fe and Mn. In the following section, Mn will not be discussed specifically. Although Mn oxyhydroxides are extremely reactive (Manceau et al., 1997; Means et al., 1978), the deep geological formations that are reviewed here contain little amounts of Mn and no discrete Mn oxyhydroxides (Gaucher et al., 2004; Landstroem and Tullborg, 1995; Lerouge et al., 2014; Zeelmaekers et al., 2015). It is worth mentioning that Mn oxyhydroxides may play a role in the case of the subsurface storage of low-activity wastes (Debure et al., 2018).

*Carbonate minerals, sulfide minerals, and phyllosilicates in pristine rock*. Fe can be found in a variety of minerals from different groups, as Fe(II), Fe(III), or in mixed Fe(II)/Fe(III) oxidation states. In most deep clay-rich formations, three main mineralogical "groups" contain Fe: sulfide minerals, carbonate minerals, and phyllosilicates. The most frequent sulfide mineral bearing Fe is pyrite ($FeS_2$), but in spite of a few reports possibly related to the difficulties associated with identifying this poorly crystalline mineral, its precursor mackinawite may play a significant role owing to its high redox reactivity (Grambow, 2016; Breynaert et al., 2010; Frohlich et al., 2012; Zeelmaekers et al., 2015; Bruggeman et al., 2007). Concerning carbonate minerals, siderite ($FeCO_3$), a pure Fe endmember, is regularly observed in clay-rich formations, but Fe-containing calcite is also common, and ankerite is regularly observed (Kars et al., 2015; Bossart et al., 2017; Zeelmaekers et al., 2015). In all carbonate minerals, Fe is present in the Fe(II) oxidation state, with a very variable concentration (Lerouge et al., 2014). Finally, several phyllosilicates are known to host iron. Among them, the most common are likely chlorite, biotite, illite (including illite layers in mixed-layered minerals), and micas (see data compilation in Lerouge et al., 2017; Finck, 2020), with distinguishing between illite and mica being almost difficult because of the close similarity in their crystal structure and because they are frequently mixed in a given sample (Grangeon et al., 2015). Thus, it is likely that the proportions of illite, illite–smectite mixed-layered minerals, and micas presented in literature studies exhibit uncertainties. In the Callovian-Oxfordian level of the deep geological laboratory of Bure, di-octahedral interlayer-deficient micas (mainly illite and illite-rich illite–smectite mixed-layered minerals) represent 36%–71% of Fe-bearing minerals, and their FeO content ranges from 1.7 to 5.7 wt%. Chlorites typically represent 2% of Fe-bearing minerals, and their FeO content is approximately 20 wt%. Finally, other phyllosilicates are present at trace concentration, but their contributions to the total Fe abundance may not be negligible. For example, although biotite is present at trace concentration, its high FeO content of 13–22 wt% means that it could contribute significantly to the total Fe content in a given sample where it would be enriched. Most of the Fe associated with phyllosilicates occurs in the Fe(II) oxidation state and is present in a phyllosilicate structure, but a minor fraction is in an exchangeable position, making the amount of exchangeable Fe in the Callovian-Oxfordian formation, at the depth of the Bure laboratory, able to reach approximately 1.2 meq/kg (Tournassat et al., 2008).

In granitic geological environments, phyllosilicates are rock-forming minerals. For example, at Aspö, biotite and chlorite are observed, with the latter possibly resulting from hydrothermal alteration (Morad et al., 2018). The presence of illite-rich illite–smectite mixed-layered minerals can also be observed as fracture-filling material, but their abundance as fracture-filling material is relatively low, typically less than 10 wt% (Stanfors et al., 1999).

*(Oxyhydr)oxides in pristine rock*. In addition to the above-mentioned minerals, Fe (oxyhydr)oxides, hereafter referred to as "Fe oxides," can also be found. In most clay-rich formations, their abundance is low; therefore, they probably have a negligible role in contributing to the whole-rock sorption capacity. However, they are of great importance for the understanding of rock geochemistry,

since they control the Fe in porewater, even if present at trace concentration. For example, in the Callovian-Oxfordian level of Bure, goethite (FeO(OH)) abundance is typically less than 0.1 wt%, a trace concentration that is, however, sufficient to control Fe in the pore water (Gailhanou et al., 2017; Kars et al., 2015).

In granitic rocks that are not subject to hydrothermal reactions, Fe oxides are commonly observed as part of the mineralogical assemblage that form fracture-filling material near the surface, but not in deep regions (Mathurin et al., 2014), coherent with their formation by the alteration of Fe-rich phyllosilicates (e.g., biotite). The typical small size of Fe oxides makes them prone to being mobilized by an advective water flow, which would be coherent with the observation of Fe-rich colloids in open fractures (Degueldre et al., 1989).

*Potential influence of construction and waste package materials on the neoformation of Fe oxides*. In many disposal concepts, construction materials remain in a repository, either because they will be used to build access structures and galleries or because they will be part of waste packages (metallic canisters and steel overpacks). Among these materials, steel in contact with either clay or cement will potentially induce the formation of Fe(II)-bearing minerals (Bildstein and Claret, 2015). In the case of the corrosion of steel in contact with clays, oxides such as magnetite, (hydroxy-)carbonates such siderite and chukanovite, Fe sulfides, and Fe-rich phyllosilicates have been observed, depending on the geochemical environment and redox conditions (Schlegel et al., 2010; El Mendili et al., 2014; Schlegel et al., 2014; Necib et al., 2016; El Hajj et al., 2013). In both freshwater and saline conditions, mixed Fe(II)/Fe(III) LDHs, termed green rusts, may form (Bach et al., 2014; Christiansen et al., 2011; Grambow et al., 1996). Contrastingly, when steel is corroded under cement pore-water conditions, $Fe(OH)_2$ and $Fe(OH)_3$ can be stabilized (Ma et al., 2019).

In addition, cement in contact with a clay-rich formation can destabilize clay minerals and lead to the precipitation of new phases that are enriched in Mg, as observed in a Cement-clay Interaction (CI) experiment in Opalinus Clay conducted at Mont Terri (Dauzères et al., 2016; Jenni et al., 2014; Lerouge et al., 2017; Mäder et al., 2018). These phases, often termed "M-S-H," are nanocrystalline defective Mg phyllosilicates that have a layer structure close to that of stevensite (Roosz et al., 2015) and that contain appreciable amounts of Fe(III) (Bonen, 1992; Lerouge et al., 2017).

The mixed Fe(II)/Fe(III) oxide magnetite is a common corrosion product under anoxic repository conditions, experimentally evidenced at the steel–clay rock interfaces of waste canisters embedded in clay backfill (Schlegel et al., 2010; El Mendili et al., 2014; Schlegel et al., 2014; Necib et al., 2016; El Hajj et al., 2013). Magnetite, especially as a pristine nanoparticle formed under strictly anoxic conditions with near-ideal stoichiometry, rapidly reduces a suite of relevant radionuclides, including Se, Tc, U, Np, and Pu (Bender and Becker, 2019; Dumas et al., 2019; Emmanuel and Ague, 2009; Emmanuel et al., 2010; Kirsch et al., 2011; Kobayashi et al., 2013; Um et al., 2011; Yalçıntaş et al., 2016; Scheinost and Charlet, 2008; Scheinost et al., 2008; Christiansen et al., 2011; Wylie et al., 2016; O'Loughlin et al., 2003; O'Loughlin et al., 2010; Huber et al., 2012; Pidchenko et al., 2017; Roberts et al., 2017; Börsig et al., 2018). The mechanisms of reduction follow a complex multi-step process, which is dependent on the chemical conditions of a solution (e.g., pH). For example, in the case of Se(VI), reduction is a two-steps process, starting from reduction to Se(IV) and then to trigonal Se(0). During reduction, pH oscillations may occur, leading to the formation of Fe(II) that re-adsorbs to magnetite and renews its reduction capacity (Poulain et al., 2022). This latter effect is observed at pH five and not at pH 7, highlighting the need to have a complete understanding of the chemical conditions, to be able to predict the fate of redox-sensitive elements upon interaction with magnetite.

In the case of Tc, Tc(VII) is reduced by magnetite to Tc(IV), which either forms small polymeric chains with a $TcO_2.xH_2O$-like structure sorbed onto the magnetite surface or is structurally incorporated by substituting for Fe in octahedral positions in the magnetite structure (Zachara et al., 2007; Peretyazhko et al., 2012; Kobayashi et al., 2013; McBeth et al., 2011). Incorporated Tc is better protected against reoxidation (Marshall et al., 2014; Um et al., 2017) and migration; hence, understanding the control between both processes is essential for the safety of repositories. From this perspective, numerical methods such as Density Functional Theory (DFT) can help in providing meaningful insights at the molecular-scale level by allowing elucidating the structure of nanocrystalline and cryptocrystalline phases, as exemplified with $TcO_2.nH_2O$ (Oliveira et al., 2022). Earlier work suggests that the structural incorporation of Tc might be favored under pH conditions, where magnetite is less stable, offering a more dynamic surface with frequent Fe dissolution/reprecipitation events, through which Tc(IV) with a similar ionic radius and coordination could be trapped into the magnetite structure (Yalçıntaş et al., 2016).

In the case of Pu, Pu(V) is reduced to Pu(III) and forms highly symmetric tridentate sorption complexes at the {111} faces of magnetite (Kirsch et al., 2011). In the case of neo-forming magnetite from Pu-containing solutions, Pu(III) also becomes partly trapped by magnetite but is increasingly released by Fe-enforced aging (Dumas et al., 2019). The mechanism behind this seems to be the large size of Pu(III) ions, which is largely incompatible with the magnetite structure; incorporation proceeds through the formation of pyrochlore-like islands in 2-nm magnetite nanoparticles, which are energetically less favorable than Pu(III) sorption complexes and, hence, form via kinetic entrapment rather than by being thermodynamically stable. Analogous to the Tc case, control between sorption and incorporation might be highly relevant for Pu mobility and, hence, safety.

In general, the geometry, speciation, and oxidation state of the outermost surface layer of magnetite is a function of the redox potential and pH (Katheras et al., 2024). These aspects of the magnetite surface chemistry should be considered when interpreting the sorption of radionuclides.

#### 2.3.2.2 Experimental methods to distinguish between total Fe and redox-active Fe

Fe can play an important role in the reduction and oxidation of redox-sensitive radionuclides and can, thus, influence their migration and retention. Whether electron transfer between Fe and radionuclides occurs depends on various factors: i) the form in which Fe is present (e.g., redox state, aqueous, adsorbed, structural, coordination, and mineral properties), ii) the type and redox state of the radionuclide, and iii) chemical conditions in the

solution (pH, ionic strength, etc.). Measuring total Fe, or total Fe(II) and total Fe(III), does not necessarily lead to correct estimates of the actual redox interaction between Fe and the radionuclide. Examples are the incomplete reduction of Tc(VII) by structural Fe in various clay minerals (Bishop et al., 2011), the incomplete reduction of Se(IV) by Fe(II) sorbed to clay (Charlet et al., 2007), and the absence of Se(VI) reduction by pyrite (e.g., Bruggeman and Maes, 2010; Charlet et al., 2012).

The redox properties of both sorbed Fe and structural Fe have been investigated in a variety of Fe minerals under different conditions (pH, $E_h$). Fe minerals subjected to study include Fe sulfides, siderite, magnetite, Fe associated with clay minerals, and iron (oxyhydr-)oxides. Several methods have been used to distinguish between total Fe and Fe accessible to redox reactions, and are explained in the following paragraphs.

A first method is *radionuclide-mineral batch experiments*. The extent to which the Fe in a mineral is redox-active is assessed by comparing the composition of a solution and solid state before and after the batch experiment using spectroscopic measurements such as XAS and Mössbauer spectroscopy or using (sequential) mineral dissolution methods. In these batch experiments, often small amounts of radionuclide are used; therefore, the method does not necessarily assess the total amount of redox-active Fe. However, it provides the most reliable information on whether the Fe mineral is reactive towards a specific radionuclide.

Examples of studies investigating the impact of redox-active Fe on the reduction/oxidation of radionuclides are:

- Fe associated with clay minerals and micas:
  - Tc(VII) (e.g., Bishop et al., 2011; Jaisi et al., 2009; Jaisi et al., 2005; Peretyazhko et al., 2008; Yang et al., 2012).
  - Np(V) (Schacherl et al., 2023)
  - U(VI) (e.g., Burgos, 2016; Chakraborty et al., 2010; Ilton et al., 2010; Luan et al., 2014; Tsarev et al., 2016)
  - Se(IV) (e.g., Charlet et al., 2012; Scheinost et al., 2008).
- Fe sulfides:
  - Tc(VII) (e.g., Huo et al., 2017; Liu et al., 2008)
  - U(VI) (e.g., Bruggeman and Maes, 2010; Livens et al., 2004).
  - Se (IV, VI, -II) (e.g., Bruggeman et al., 2012; Charlet et al., 2012; Curti et al., 2013; Han et al., 2011; Han et al., 2012; Kang et al., 2011; Kang et al., 2013; Naveau et al., 2007; Scheinost and Charlet, 2008)
  - Pu(VI) (e.g., Hixon et al., 2010)
- Magnetite:
  - Tc(VII) and Np(V) (e.g., Cui and Eriksen, 1996)
  - U(VI) (e.g., Grambow et al., 1996; Huber et al., 2012; Missana et al., 2003; Rovira et al., 2003)
  - Se(IV) (e.g., Scheinost and Charlet, 2008)
  - Se(VI) (Poulain et al., 2022)
  - Pu(V) (e.g., Kirsch et al., 2011; Powell et al., 2005).
- Carbonates:
  - U(VI) (e.g., Ithurbide et al., 2009; Ithurbide et al., 2010)
  - Se(IV) (e.g., Badaut et al., 2012; Chakraborty et al., 2010; Scheinost and Charlet, 2008)
  - Np(V) (e.g., Scheinost et al., 2016)
- Fe(oxyhydr)oxides:
  - Tc(VII) (Peretyazhko et al., 2012; Um et al., 2011; Yalçıntaş et al., 2016; Zachara et al., 2007)
  - Pu(V) (e.g., Powell et al., 2005)

A second method is *using probe compounds*, where the redox activity of an Fe-containing mineral is assessed using 'probe compounds.' In batch experiments, a probe compound (oxidant or reductant) reacts with an Fe mineral, and the redox activity is assessed based on both the loss of the probing compound and the quantification of Fe(II) and Fe(III) in the mineral before and after reactions. Probe compounds used to assess the redox activity of Fe are often strong oxidants and reductants. The reduction and oxidation capacities that result from these reactions can be seen as a maximum redox activity and may not be entirely representative for reactions with specific radionuclides.

Examples of relevant research are:

- Clay minerals:
  - Nitroaromatic compounds (e.g., Neumann et al., 2008; Neumann et al., 2011)
  - Dithionite and $O_2$ or $H_2O_2$ (e.g., Stucki, 2011; Gorski et al., 2012a; Qian et al., 2023).
- Fe(oxyhydr)oxides:
  - Ti-EDTA (Heron et al., 1994)
  - Ascorbate (e.g., Roden, 2003)

A third method is based on *biochemical processes (microbial reduction)*. Anaerobic microbes are often used to study the redox activity of, for example, structural Fe(III) in clay minerals. The Fe associated with a mineral is characterized before and after reduction using methods such as XAS or Mössbauer spectroscopy. These methods are limited to certain electrolyte conditions that are suitable for the microbes. Electron mediators, such as anthraquinone-2,6-disulfonate (AQDS), are often used to enhance the redox reaction occurring between a microbe and structural Fe. Many redox reactions in nature occur via microbial interaction. Therefore, these methods can give a good representation of which Fe is actually redox-active under natural conditions.

Examples of studies using microbial interaction to study redox-active Fe in minerals are:

- Clay minerals (e.g., Bishop et al., 2011; Dong et al., 2009; Dong et al., 2003; Jaisi et al., 2009; Jaisi et al., 2005; Kostka et al., 1999; Luan et al., 2014; Pentráková et al., 2013; Seabaugh et al., 2006; Stucki, 2011; Yang et al., 2012)
- Magnetite (e.g., Byrne et al., 2016; Dong et al., 2000)
- Fe(oxyhydr)oxides (e.g., Roden, 2003)

A fourth method assesses the redox activity of Fe by measuring the electron transfer (as electrical current) between an (Fe) mineral and a working electrode (possibly making use of mediators). An electric potential, reducing or oxidizing, high or low, is applied, and any resulting redox reactions with the Fe mineral are directly measured as electric current. This makes it possible to study both the extent and kinetics of a redox reaction. Measurements can be performed under well-defined conditions such as pH, ionic strength, and redox potential.

Examples of studies using this method to characterize the redox activity in Fe minerals are:

- Clay minerals (e.g., Gorski et al., 2012a; Gorski et al., 2012b; Hoving et al., 2017; Sander et al., 2015)
- Fe(oxyhydr)oxides (e.g., Aeppli et al., 2018)
- Fe sulfides (e.g., Hoving et al., 2017).

#### 2.3.2.3 Characterization of redox reactions

*Batch interaction experiments*. In a batch interaction experiment, the $K_d$ (as a distribution solid–liquid ratio) formalism is often applied. However, it is not to be seen as being strictly "sorption." The $K_d$ concept is based on reaction reversibility within a reactive transport conceptual model (see Chapter 3 on transport). When sorption is combined with a reduction reaction coupled with the oxidation of a mineral substrate (such as magnetite, pyrite, or mackinawite), the reduced RN species:

- has a much lower solubility as pure phase (e.g., U, Se, Sb, Tc, Mo); consequently, solid phases from the reduced (or oxidized) RN species can form;
- is however often present as single sorbed (e.g., U(IV), Tc(IV)) species (Chakraborty et al., 2010; Yalçıntaş et al., 2016);
- have *a priori* very limited ability to return to a solution, with the sorption reaction often being irreversible (Couture et al., 2015; Markelova, 2017).

*Spectroscopic techniques*. The determination and quantification of the redox state of elements and speciation in solution can be characterized using spectroscopic techniques by making use of special spectrochemical cells. Understanding the redox reactions of radionuclides on mineral surfaces is of importance to predict their mobility in the environment. For instance, process understanding on a molecular scale is the basis for geochemical modeling calculations that is applied in calculations for the safety assessment of nuclear waste repositories (Geckeis et al., 2013; Gorski et al., 2013). This understanding requires techniques such as XANES spectroscopy, which allow for the unambiguous identification of redox states because they are element-specific and sensitive to electronic and local structures. XAS covers almost all elements of the periodic table, but the penetration depth through water and mineral phases required for *in situ* redox speciation is given only for energies of a few keV; hence, the application of XAS is typically limited to certain elements, starting with the 3d transition metals. Since all atoms of a probed element contribute equally, and in a statistically representative way, for a measured XAS signal, this method is intrinsically suited to perform quantitative speciation analyses, without the need to account for redox-dependent absorption coefficients or the spectroscopically "silent" oxidation states of a given element. These advantages are offset by a relatively poor detection limit (approximately 1 ppm, depending on the element and matrix effects, often one or two orders of magnitude higher), and an intrinsically poor spectral resolution, especially for local structure analyses. In spite of these disadvantages, XAS is often the only spectroscopic method available for redox speciation, with the notable exception of Mössbauer spectroscopy, which is widely used for Fe redox speciation but limited to only a few other elements (Sn, Sb, Te, and possibly also I and Np).

Moreover, for actinides (An), the high-energy-resolution (HR-) XANES technique, at the An $M_{4,5}$-edge, provides a significant advantage (Vitova et al., 2013) over the widely applied conventional An $L_3$-edge XANES mode, when investigating the oxidation states and electronic structures of An elements (Bahl et al., 2017). It shows high sensitivity to minor contributions from An oxidation states in mixtures, as it directly probes the An 5f unoccupied states, which are sensitive to changes in chemical bonding. Synchrotron-based X-ray methods in combination with optical spectroscopy ultimately provide information on the structure and bonding. As an example, UV-Vis spectroscopy, as a tool for molecular speciation, is sensitive to the coordination symmetry of An complexes (Meinrath, 1997).

In sorption studies with redox-sensitive An, such as Np and Pu, it is of utmost importance to achieve well-defined redox conditions. Many studies within this topic involve strict precautions to prevent the interference of minor amounts of oxygen, for example by working under an inert gas atmosphere (Banik et al., 2016; Elo et al., 2017; Marsac et al., 2015). In addition, electrochemical methods make it possible to control and, thus, systematically vary redox conditions. The application of an electrical field *in situ* can attenuate potential artefacts resulting from the oxidation and subsequent alteration of samples during sampling, storage, and transportation prior to experimental work (Pidchenko, 2016). Moreover, a mechanistic understanding of the interfacial reactions within the first minutes up to hours of contact can be obtained.

The methods of X-ray spectroscopy, optical spectroscopy, and electrochemistry can be combined by designing a spectro-electrochemical cell (Pidchenko, 2016). Specific questions that are so far unsolved could be investigated using this setup. Such questions include how an applied redox potential influences the surface speciation of redox-sensitive radionuclides, or what surface sites facilitate electron transfer processes (Banik et al., 2016; Marsac et al., 2015).

The redox state of elements in mineral phases can be determined/quantified using synchrotron methods such as high-energy-resolution fluorescence detection XANES (HERFD-XANES).

Owing to relatively long core-hole lifetimes, elements that can be probed by their K edges (up to and including period 5) allow for XANES measurements with a resolution sufficient to discriminate different oxidation states even when several oxidation states of an element are present in the same sample. This has been demonstrated, for instance, for the four common oxidation states of Se (-II, 0, IV, and VI) (Scheinost et al., 2008; Rojo et al., 2018). Actinides, however, are typically probed at L-edges with much shorter core-hole lifetimes and a correspondingly poor resolution (>5 eV). Furthermore, the evaluation of XANES is complicated in very diverse coordination environments, such as those with uranium changing from an yl-type at oxidation states VI and V to a highly symmetric cubic coordination for U(IV) (Hennig et al., 2007; Ikeda et al., 2007). Because of this, the more exotic pentavalent oxidation state of U has been intrinsically difficult to detect and can be easily overlooked in oxidation state mixtures. Owing to the advent of secondary monochromatization with, for instance, bent analyzer crystals in Rowland geometry, the spectral resolution can be significantly improved using HERFD-XANES (Kvashnina and Scheinost, 2016). However, a substantial breakthrough in the detection and quantification of various U oxidation states in

mixtures has been obtained only after applying the HERFD-XANES technique to M edges (Butorin et al., 2017; Butorin et al., 2016a; Butorin et al., 2016b; Prieur et al., 2018; Kvashnina et al., 2018; Kvashnina et al., 2017; Leinders et al., 2020). This method has also been applied to other actinides such as Pu, Am, and Np (Kvashnina et al., 2019; Epifano et al., 2019; Prieur et al., 2018; Schacherl et al., 2022a). Detection limits depend on the element investigated, the chemical composition of a sample, and the instrumental setup (including the synchrotron source) but can reach values in the order of ppm. Such state-of-the-art detection methods benefit from additional beamline developments such as cryogenic sample environments that allow reduced beam damage (Schacherl et al., 2022b).

In addition to improving the spectral resolution of XANES by employing analyzer crystals, substantial progress has been made in the statistical treatment of spectroscopic data in order to derive reliable speciation as well as to extract the pure spectra of endmember components from spectral mixtures (Rossberg et al., 2003; Rossberg et al., 2009), a method also applied to quantitatively derive the structures of the different oxidation states of Se and Tc (Yalçıntaş et al., 2016; Rojo et al., 2018; Charlet et al., 2007). This method was further enhanced by coupling with Monte–Carlo simulations in order to derive the specific surface geometry of Pu(III) on magnetite (Rossberg and Scheinost, 2005; Kirsch et al., 2011). Finally, novel approaches can be used to directly derive a radial pair distribution function from EXAFS spectra, a method particularly well-suited for strongly disordered structures such as that of the Cm(III) aqua complex (Rossberg and Funke, 2010).

*Modeling of redox reactions*. Thermodynamic models are particularly relevant and required for a comprehensive prediction of An behavior (migration) in natural systems. Only few studies in the literature have attempted to quantitatively describe redox reactions in the presence of minerals, via mechanistic SCMs.

Soltermann (2014) described the sorption and oxidation of Fe(II) on Wyoming montmorillonite by using the 2SPN SC/CE model and considering the formation of ferric surface complexes ($\equiv S^SOFe^{2+}$) along with ferrous surface complexes ($\equiv S^SOFe^{+}$). The developed model is capable of describing the adsorption of Fe(II) on different montmorillonites; however, it does not provide a realistic mechanistic description, since it does not account for the intrinsic redox properties of a clay mineral itself.

Degueldre and Bolek (2009) discussed Pu sorption onto $Al_2O_3$, FeOOH, and $SiO_2$ colloids based on a simple $R_d$ approach. Their calculations included consideration of the effect of redox potential, which was shown to have a major impact on the calculated Pu uptake data. Schwantes and Santschi (2010) proposed an SCM involving all Pu redox states (from +III to + VI) and minerals, as well as a reversible surface-mediated Pu(V)–Pu(IV) reaction, to explain the observed kinetics of Pu uptake. Experimentally determined redox potential (pe; $E_h$), oxygen partial pressures, or redox speciation are essential for the application of SCMs to describe sorption behavior of redox-sensitive elements. However, in most studies mentioned above, such data are often not provided owing to difficulties associated with their experimental determination (Altmaier et al., 2010; Schüring, 2000).

Marsac et al. (2015) investigated the uptake of Np(V) on illite under anaerobic conditions. Partial reduction of Np(V) to Np(IV) at the mineral surface was observed under conditions where only Np(V) was expected to be stable in an aqueous solution. The results were explained using a TSM, based on measured redox potentials and the high stability of the inner-sphere surface complexes of tetravalent An (Np(IV)). The stability constants of such surface complexes can conveniently be estimated by analogy to other elements, for example to Th(IV), which is not redox-sensitive. This approach was also successful in the case of Pu adsorption on illite (Gorski et al., 2013; Banik et al., 2016). Based on such ideas, Banik et al. (2017) simulated the uptake of Np, specifically Np(IV) and Np(V), on illite even at high salt contents. The sorption behavior of pure oxidation states, which are required in the model, have been experimentally tested for Np(V) under oxidizing conditions and for Np(IV) under an inert gas atmosphere, by Nagasaki et al. (2017), Nagasaki et al. (2016). A model of Banik et al. (2017) was supported by these independent studies, while the mechanism of the redox reactions and the origin of the negative measured $E_h$-values remained unclear. To understand those findings, a SCM providing a more detailed molecular-scale description for the macroscopic quantification of the retention of redox-sensitive radionuclides under variable redox conditions should be developed. Starting from an approach by Marsac et al. (2015) and Banik et al. (2017) is possibly an appropriate option, since the modeling strategy was found to be successful for various actinides and cover a broad range of solution compositions.

*Kinetics*. Radionuclide redox kinetics in aqueous solutions depend on various parameters. These parameters include the redox potential defining the concentration of available electrons, the concentration of redox-active substances in the system under investigation, and the number of electrons that need to be transferred for a specific redox reaction. Other chemical specificities can, however, play a role. These specificities include chemical reactions as a consequence of both redox transitions (e.g., the kinetically hindered reduction of $PuO_2^+$ to Pu(IV)) and the type of binding of a redox-sensitive radionuclide to an electron acceptor or donor (e.g., inner-sphere complexation or outer-sphere interaction), and, therefore, also geochemical boundary conditions. Therefore, redox kinetics require a detailed understanding of ongoing reactions. Numerous investigations have been published (e.g., Hixon and Powell, 2018; Ma et al., 2020; Romanchuk et al., 2016).

It is also worth noting that, in natural systems, Tc(VII) reduction is found to depend strongly on the Fe(II) content of rocks (Huber et al., 2017 and references therein). Rock treatment and conditioning prior to experimental studies, such as the preservation of the rock oxidation state, is consequently of utmost importance for mimicking *in situ* conditions. Reoxidation by contacting with oxygenated groundwater, simulating oxidized melt water into a granitic fracture, seems to depend on the nature of granite-bound Tc: Surface-precipitated $TcO_2$ seems to reoxidize faster than surface-sorbed Tc(IV). The kinetics of redox reactions have been measured for Tc(VII)/Tc(IV) pairs and correlate with the redox potential measured in solution (Kobayashi et al., 2013). Relatively rapid reduction is observed when the $E_h$ is far below the Tc(VII)/Tc(IV) borderline. Experiments also revealed an acceleration of Tc(VII) reduction in the presence of Fe(II) solid phases, highlighting the possible relevance of specific surface interactions for electron transfer.

Cevirim-Papaioannou et al. (2018) found similar dependencies of U(VI) reduction to $U(IV)O_2$, in their solubility studies. Depending on the reducing agent they applied to adjust the

reducing conditions, they identified the $pe_{(exp)} - pe_{(U(VI)/U(IV))}$ difference as a driving force for reduction. This explains that, even when adding strongly reducing Sn(II) to a U(VI) solution at hyper-alkaline conditions, up to almost 2 years are required to reduce U(VI) quantitatively to U(IV)$O_2$, because the *Eh* difference is relatively low at high pH.

## 2.3.3 Solid solutions

### 2.3.3.1 Theory and current understanding

Solid solutions are mixtures of two or more components on a molecular level existing over a range of chemical compositions. Solid solutions are ubiquitous in natural and industrial systems and play a major role in the fate and transport of elements in the earth's surface environments. Solid-solution formation can lead to a retention of harmful ions in the environment and is included in the design of engineered barriers, such as for the immobilization of radionuclides or industrially generated pollutants (Prieto et al., 2016). The disordered arrangement of different atoms over the same lattice is stabilized by the entropy, providing an energetic advantage compared to that of pure, stoichiometric endmembers. The charge difference and size of substituting atoms as well as the flexibility of a host structure, such as its Young´s modulus, are important for determining the extent of solid-solution formation. The chemical composition of a solid solution can be defined in terms of fixed endmember compositions—for example, the binary solid solution $U_{1-x}Pu_xO_2$ can exist in a range of compositions specified by the mole fraction, that is, the $X_{PuO2}$ of the endmember $PuO_2$. Solid-solution formation is typically favored between isostructural endmembers, where exchangeable atoms have the same charge and similar ionic radii. In many systems, the mixing is incomplete. In general, solid-solution formation is limited at low temperatures and is favored at higher temperatures (Bosbach et al., 2020).

A special case, relevant to nuclear waste management, is the formation of solid solutions in contact with aqueous solutions. Depending on the conditions, solid solution–aqueous solution systems (SS-AS) can form via the re-crystallization of pre-existing minerals or via co-precipitation from supersaturated solutions (Klinkenberg et al., 2014). These processes can compete with classical sorption processes such as the adsorption or formation of a pure radionuclide phase. As a consequence of the uptake of radionuclides into solid solutions, these are structurally bound into a thermodynamically stable phase, sometimes leading to significantly lowered radionuclide solubility (Bosbach et al., 2020). For example, long-term laboratory experiments conducted over several years indicated that $^{226}$Ra uptake into (Ba,Ra)$SO_4$ may take place in time scales relevant to deep-geological-waste disposal (Klinkenberg et al., 2014).

**2.3.3.1.1 Solid-solution formation and radionuclide retention.** In the safety assessment of planned nuclear disposal sites, the co-precipitation of radionuclides with sulfates and carbonates is considered, as this provides more realistic aqueous concentrations of radionuclides in the pore water of the nearby fields of nuclear waste repositories (Curti, 1999; Curti et al., 2010). For instance, barite is widely studied in the field, as it is the main scavenger of $^{226}$Ra, a long-lived radionuclide (Brandt et al., 2015; Brandt et al., 2018; Klinkenberg et al., 2018). Under repository-relevant conditions, Ba and Ra released from radioactive waste will react with porewater containing sulfate, triggering the formation of (Ba,Ra)$SO_4$ (Curti et al., 2010) or even (Ba,Sr,Ra)$SO_4$ (Klinkenberg et al., 2018). In the case of $^{226}$Ra, an ideal solid solution with $BaSO_4$ irreversibly binds a contaminant in a well-defined, stable phase. Depending on the amount and the properties of the solid, the formation of solid solutions can become a very important retention mechanism and is, therefore, included in some scenarios of safety cases for deep geological repositories (NAGRA, 2002).

**2.3.3.1.2 Thermodynamic and kinetic aspects of solid-solution formation.** The most common tool used to rationalize the possible equilibrium states of a solid solution is the Lippmann diagram (Glynn, 2000; Lippmann, 1980). The Lippmann diagram is a phase diagram in which the solidus is a function of the solid-phase mole fraction, while the solutus is a function of aqueous activity fractions. The Lipmann model introduces the concept of total activity product, ($\sum$ Π). This is defined as the sum the of the partial activity products contributed by each component (endmember) of a solid solution. Considering the Lippmann diagram of a (Ba,Ra)$SO_4$ solid solution (Figure 1) as an example, the solidus is expressed ($\sum$ Π) as the total solubility product, using Equation 12, while the solutus is expressed ($\sum$ Π) in terms of the aqueous phase composition given in Equation 13.

$$\begin{aligned}\sum \Pi_{eq} &= \boldsymbol{K_{RaSO4}a_{RaSO4}} + \boldsymbol{K_{BaSO4}a_{BASO4}} \\ &= \boldsymbol{K_{RaSO4}\gamma_{RaSO4}X_{Ra}} + \boldsymbol{K_{BaSO4}\gamma_{BASO4}X_{Ra}} \end{aligned} \quad (12)$$

$$\sum \Pi_{eq} = \frac{1}{\frac{X_{Ra,aq}}{K_{RaSO4}\gamma_{RaSO4}} + \frac{X_{Ba,aq}}{K_{BaSO4}\gamma_{BASO4}}} \quad (13)$$

where $a_{Ba^{2+}}$, $a_{Ra^{2+}}$, and $a_{SO_4^{2-}}$ represent the activities in the free solution; $K_{BaSO_4}$ and $K_{RaSO_4}$, the solubility product of endmembers $BaSO_4$ and $RaSO_4$, respectively (with $K_{sp}(BaSO_4) = 10^{-9.97}$ (Hummel et al., 2002) and $K_{sp}(RaSO_4) = 10^{-10.27}$ (Langmuir and Riese, 1985)) at a temperature of 298.15 K; and $X_{Ba}$ and $X_{Ra}$, the molar fraction of $BaSO_4$ and $RaSO_4$ in the solid. $\gamma_{BaSO_4}$ and $\gamma_{RaSO_4}$ are the activity coefficients of the endmembers in the solid solution. $X_{Ra,aq}$ and $X_{Ba,aq}$ are the aqueous activity fractions.

The solid-solution composition corresponding to an equilibrium aqueous composition is determined by a horizontal line connecting the solutus and the solidus. For instance, an aqueous solution with a mole fraction of Ba in solution ($XBa^{2+}_{aq}$) equal to 0.7 (Figure 1) corresponds to a solid-phase composition with a mole fraction of $BaSO_4$ ($X_{BaSO4}$) of 0.3.

While the Lippmann diagram provides the basis for understanding the equilibrium dynamics between a solid solution and an aqueous solution, it does not consider the effect of supersaturation. The key feature of a solid-solution formation is that trace element contaminants can co-precipitate as a solid solution, even though the solution is undersaturated with respect to a pure endmember solid containing that element. The concept of supersaturation for solid solutions is extensively described in a review by Prieto (2009), and the common tools include the stoichiometric supersaturation function, ($\Omega_{st}$) (Prieto, 2009) and "δ"-functions (Astilleros et al., 2003). As an example, the supersaturation function of a hypothetical solution containing

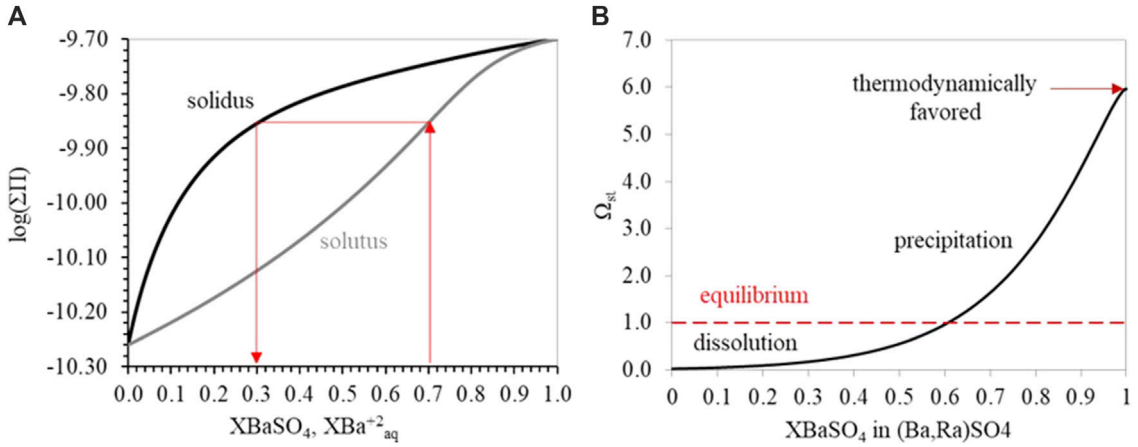


FIGURE 1
**(A)** Lippmann diagram showing the equilibrium states for (Ba,Ra)$SO_4$ for a solid solution–aqueous solution. **(B)** Supersaturation of (Ba,Ra)$SO_4$ as a function of the mole fraction of $BaSO_4$ ($XBaSO_4$). These diagrams were constructed considering a temperature of 298.15 K and a regular mixing model with an enthalpy of mixing between Ra and Ba equal to 2,947 J/mol (Vinograd et al., 2018).

$10^{-4}$ mol/L $Ba_{(aq)}$, $10^{-4}$ mol/L $SO_{4(aq)}$, and $10^{-7}$ mol/L $Ra_{(aq)}$ was computed using Equation 14 and is depicted in Figure 1B.

$$\Omega_{st}(X_{Ba}) = \frac{(a_{Ba^{2+}})^{X_{Ba}}(a_{Ra^{2+}})^{X_{Ra}}(a_{SO_4^{2-}})}{\left(K_{BaSO_4}\gamma_{BaSO_4}X_{Ba}\right)^{X_{Ba}}\cdot\left(K_{RaSO_4}\gamma_{RaSO_4}X_{Ra}\right)^{X_{Ra}}} \quad (14)$$

A supersaturation Ω equal to 1 denotes equilibrium (dashed line). Solid solutions with compositions below the dashed line are expected to dissolve, whereas solid solutions with compositions above the dashed line can precipitate with the maxima representing the thermodynamically favored solid-solution composition. The example shows that, although a solution may be undersaturated with respect to pure $RaSO_4$, radium present in trace amounts is likely to be removed from an aqueous solution through the formation of a $BaSO_4$-enriched solid solution.

Because of the complexity of sulfate mineral nucleation and precipitation kinetics, highly supersaturated solutions can lead to metastable phases (Poonoosamy et al., 2016; Prieto, 2014; Weber et al., 2017), and thermodynamic equilibrium calculations might not be sufficient for a reliable prediction of $^{226}Ra$ mobility (Curti et al., 2019). While the mathematical description of the thermodynamic equilibrium behavior of solid solutions is well-established, the implementations of kinetics still remains a challenging task (Noguera et al., 2016). The effect of the kinetics of solid solution precipitation is accounted for in various works by considering the nucleation rate of the solid solutions (Noguera et al., 2016; Pina et al., 2000).

**2.3.3.1.3 Nucleation of solid solutions in porous media.** The understanding of nucleation processes in porous media is essential for the selection and parameterization of mathematical equations implemented in numerical reactive transport tools where these processes are dominant. These equations are used to assess the geochemical long-term evolution of interfaces in deep geological nuclear waste repositories in which precipitation and co-precipitation processes are recurrent. The nucleation mechanisms of minerals are described by Kashchiev and van Rosmalen (2003). In porous media, both homogeneous and heterogeneous nucleation can occur (Poonoosamy et al., 2016; Poonoosamy et al., 2020). Homogeneous nucleation occurs in a pore solution, whereas heterogeneous nucleation occurs on the surface of existing solids that provide active centers for nucleation. It is generally acknowledged that homogeneous and heterogeneous nucleation prevail at high and low supersaturation levels, respectively (Kashchiev and van Rosmalen, 2003; Kügler et al., 2016).

The Classical Nucleation theory (CNT) is commonly applied to describe nucleation processes in porous media or confined spaces (Poonoosamy et al., 2019; Prasianakis et al., 2017). Although the applicability of CNT is highly debated (Gebauer et al., 2014), recent studies support the applicability and validity of CNT for sulfate minerals (Curti et al., 2019; Prieto, 2014) and even carbonates (Henzler et al., 2018). Although CNT is based on empirical formulations, it allows for smooth integration of experimental observations on mineral precipitation and nucleation kinetics into reactive transport simulations (Poonoosamy et al., 2019).

The nucleation rate ($J$) depends on supersaturation and can be calculated as follows

$$J = \mathrm{r}\, exp\left(-\frac{\Delta G_c}{KT}\right) \quad (15)$$

where $k$ is the Boltzmann constant, $T$ is the absolute temperature, and $r$ is a pre-exponential factor related to solubility. $\Delta G_c$ is the energy required for the formation of a nucleus of critical size and is given as:

$$\Delta G_c = \frac{\beta v_0^2 \sigma^3}{(kTln\Omega)^2} \quad (16)$$

where $v_0$ is the molecular volume in the solid phase, $\beta$ is a geometry factor that depends on the shape of the nucleus, and $\sigma$ [J/m$^2$] is the surface tension of the nucleating phase and the solution interface.

For a solid solution, the stoichiometric supersaturation ($\Omega_{st}$) is considered in Equations 15, 16. Therefore the nucleation rate for a (Ba,Ra)$SO_4$ solid solution is written as a function of the composition:

$$J\left(X_{RaSO_4}\right) = \mathrm{r}\left(X_{RaSO_4}\right) exp\left(-\frac{\Delta G_{c\,(X_{RaSO4})}}{KT}\right) \quad (17)$$

where $r(X_{RaSO4})$ and $\Delta G_c$ are functions of the solid-solution composition (Pina et al., 2000).

Nucleation in porous media is highly debated (Stack, 2015). Several authors (Prieto, 2014; Putnis and Mauthe, 2001; Stack et al., 2014) have demonstrated the dependence of nucleation kinetics on the pore size, with an inhibition of nucleation occurring in smaller pores. Unlike a free bulk solution, a porous medium divides a fluid into a large number of pores, which act as independent volumes with respect to nucleation. Because the nucleation probability is essentially proportional to the solution volume, precipitation in small pores is most likely hindered compared to that in a bulk solution. This point is illustrated by the basic equation for induction time (Kashchiev and van Rosmalen, 2003), given as:

$$t_i = \frac{1}{JV} \quad (18)$$

where $t_i$ is the induction time, $J$ is the nucleation rate (the rate of appearance of supercritical nuclei per unit solution volume), and $V$ is the volume of the fluid.

In the same line of thoughts, other authors (Emmanuel and Berkowitz, 2007) consider the solubility of minerals to be pore-size-dependent. This is commonly referred as the pore-size controlled solubility (PCS) effect. Under PCS consideration, the effective solubility of a mineral in a given pore volume, $S_e$, is related to its bulk solubility, $S_0$, as follows:

$$\frac{S_e}{S_0} = \exp\left(\frac{-V_s^c}{mRT}\frac{2\sigma\cos\theta}{r}\right) \quad (19)$$

where $V_s^c$ is the molar volume of the salt, $m$ is the number of ions per unit volume, $R$ is the gas constant, $T$ is the absolute temperature, $\sigma$ is the surface tension, $r$ is the radius of a cylindrical pore, and $\theta$ is the contact angle between the nucleating phase and the wall of the cylindrical pore. In most cases, $\theta > 90$, and $exp\left(\frac{-V_s^c}{mRT}\frac{2\sigma\cos\theta}{r}\right) > 1$, such that the effective solubility of a mineral in a given pore volume is always higher than the solubility in bulk water, that is, $S_e > S_0$. PCS, shown in Equation 20, considers that a given solution can be supersaturated in a big pore and undersaturated in a small pore, which can give rise to a heterogeneous mineral precipitation distribution with preferential mineralization in larger pores.

Although many studies found an inhibition of nucleation in small pores, according to the latest review on mineral crystallization in confinement (Meldrum and O'Shaughnessy, 2020), it is not possible to make this a generalization. Indeed, other studies have shown that nucleation occurs uniformly across all pore sizes, without size dependence (Borgia et al., 2012), or even preferentially in fine capillaries (Hedges and Whitelam, 2012). Crystallization in confinement is still an open question and requires further investigation, as it affects the pore network alteration and transport properties of host-rock.

In recent work (Poonoosamy et al., 2021), the authors tested and validated theoretical models describing the crystallization of a sulfate solid solution against microfluidic experimental datasets. The investigation showed that i) CNT extended for solid solutions can be used to determine the composition of nucleating phases, ii) nucleation kinetics can be a competitive growth mechanism, and iii) zonation phenomenon in solid-solution formation is governed by a complex interplay between the diffusion of reactants and the crystallization kinetics, as well as other factors such as surface tension and lattice mismatch.

#### 2.3.3.2 Research methods

Typically, SS-AS systems are studied in batch precipitation, solubility, or uptake experiments. Complementary to the evolution of the chemical composition of a solution via wet chemical and radiochemical methods (e.g., ICP-MS, liquid scintillation counting, or gamma spectrometry), solids are characterized in-depth to understand the details of structural uptake (Brandt et al., 2015; Klinkenberg et al., 2018). A review on the characterization of SS-AS systems is provided by Prieto et al. (2016). Classical methods for characterization are spectroscopy, such as TRLFS, X-ray absorption (EXAFS and XANES), and Raman or IR spectroscopy. Lately, methods with high spatial resolution providing chemical information, including Secondary Ion Mass Spectrometry (SIMS), Micro-X-ray Fluorescence (μ-XRF), and electron microscopy (SEM-EDX or TEM-EDX), have been applied to unravel the distribution of minor components in host materials. X-ray and neutron diffraction have been applied to assess thermodynamic quantities such as the excess mixing volume.

Complementary, theoretical methods, including DFT (Vinograd et al., 2013) and MD (Heberling et al., 2014), have also successfully been applied to SS-AS systems.

Recently a novel microscopic method for the observation of dissolution/precipitation processes in tightly confined spaces at the nano-to-micrometer scale has been developed. It consists of a combination of microfluidic experiments (lab on a chip) and pore-scale modeling (Poonoosamy et al., 2019). Micromodels enable the *in situ* live monitoring of flow and reactive transport in 2D geometries and have been used, for example, to study single and multiphase flow, including the effects of pore geometry, capillary pressure, and fluid-phase saturation (Poonoosamy et al., 2019 and references therein). Combined with spectroscopic techniques and pore-scale modeling, micromodels enable the spatiotemporal visualization of mineralogical changes and ion concentrations, resulting in supersaturation determination.

#### 2.3.3.3 Remaining uncertainties

Uncertainties remain with respect to the competition between processes in pore spaces, for example, the adsorption of $^{226}$Ra within a clay rock versus the formation of secondary phases. Some clay pore waters (e.g., Callovo-Oxfordian Clay and Opalinus Clay) contain significant amounts of Sr and sulfate, such that minor amounts of Ba and $^{226}$Ra may lead to the formation of a (Ba,Sr,Ra)$SO_4$ solid solution.

Despite the extensive studies of the thermodynamic properties of (Ba,Sr,Ra)$SO_4$ solid solutions, summarized by Vinograd et al. (2013), Vinograd et al. (2018), only a few studies (Pina et al., 2000) have been dedicated to assessing the nucleation of solid solutions or were limited to computational investigations (Noguera et al., 2016). The effect of pore size dependency on nucleation remains unknown.

## 2.4 Upscaling – "bottom-up approach"

As will be discussed in the chapter on transport, describing retention in transport mainly requires using a distribution coefficient ($K_d$), where the entire complexity of radionuclide/water/rock interactions is reduced to a single empirical value. Because of its simplicity, it is still the most used approach in transport modeling. However, sorption is a very complex process and heavily depends on the conditions. Therefore, the predictive capabilities of the transport calculations are only valid if the sorption ($K_d$) value is determined under similar (chemical/mineralogical) conditions.

For this reason, sorption models on pure clay minerals based on a mechanistic approach used to understand and quantify the processes controlling the uptake of radionuclides were developed. Recently, Baeyens and Bradbury (2017) and Bradbury and Baeyens (2017) developed so-called thermodynamic sorption databases for montmorillonite and illite, respectively. Such databases contain mineral-specific characteristics such as site types, site capacities, protolysis constants, selectivity coefficients, and surface complexation constants. These sorption models can be incorporated into reactive transport models that couple the influence of chemical interactions with the physical transport processes that take place in a water-saturated porous medium.

A commonly used approach to describe sorption in complex systems is the Component Additivity or Bottom-Up approach. This approach is based on the hypothesis that the uptake of radionuclides in complex mineral/groundwater systems can be quantitatively predicted from the knowledge and understanding of the mechanistic sorption processes on single minerals, and models developed to describe them.

The "bottom-up" approach, as studied in the EURAD WP5-FUTURE, considers three pathways (schemes) in order to address open questions: i) *from dispersed to compacted solids* (Are sorption data measured in dispersed systems applicable for compacted systems?), ii) *from single minerals to clay rocks* (Can we describe the sorption and transport behavior of radionuclides in mineral assemblages/clay host rocks by adding up effects described by a model developed for the main mineral components?), and iii) *from single radionuclide to multi-component chemical systems* (How does the presence of competing elements influence the mobility of the radionuclide under study?). In this project, bottom-up schemes were applied to three main groups of elements/radionuclides: weakly sorbing (anionic Se-species), moderately sorbing (Ra and Ba), and strongly sorbing (transition metals and lanthanides/actinides), and they were applied on a selection of clay phases (pure minerals: illite, smectites, kaolinite, and their mixtures (clay rocks), namely Opalinus Clay, Callovo-Oxfordian Clay, and Boda Claystone Formation (Maes et al., 2024).

Increasingly more literature have used the sum of major components to describe the behavior of a mineral assemblage. Some examples are given below. Bradbury and Baeyens (2011b) studied the sorption of Cs, Co, Ni, Eu, Th, and U on MX-80 bentonite and Opalinus Clay and obtained satisfactory predictions in applying the bottom-up approach. Marques Fernandes et al. (2015) tested the bottom-up approach for similar radionuclides on Opalinus Clay and Boda Claystone rocks. Montavon et al. (2022) successfully used this approach to describe uranium retention in Callovo-Oxfordian Clay.

The aspect of competition was extensively studied by Marques Fernandes and Baeyens (2020) for illite and montmorillonite. Orucoglu et al. (2022) investigated the competition between $Pb^{2+}$, $Co^{2+}$, $Zn^{2+}$, and $Mg^{2+}$ on montmorillonite edge surfaces. Sorption competition was investigated for different systems (see different contributions in (Maes et al., 2024)) and found to be a very important aspect for describing or understanding experimental observations from radionuclide sorption experiments. Often, deviations from a model find their origin in the presence of competing elements that are not taken into account in the model (insufficiently defined aqueous environment); hence, it is imperative to constrain as detailed as possible the aqueous system in a model.

Results obtained in this project provide convincing arguments that bottom-up schemes are applicable for the description of sorption processes, albeit not always straightforward, as relevant underlying mechanisms and sorption competition aspects must be taken into account rigorously. The transferability of data and models has been established from dispersed to compacted systems and from single to complex mineral assembly.

## 2.5 Sources of sorption data

This section presents an extended (but not complete) overview of available sources of sorption data, mainly $K_d$ based, relevant for clay and crystalline host rocks for safety assessment purposes.

### 2.5.1 Sorption on 2:1 clay minerals

Since 1995, the Paul Scherrer Institute has been conducting sorption studies on montmorillonite and developing a semi-quantitative mechanistic non-electrostatic sorption model for the uptake of (radio)contaminants. The studies started with detailed investigations of Ni and Zn sorption on montmorillonite (Baeyens and Bradbury, 1997; Bradbury and Baeyens, 1997b) and continued with a wide group of elements in Bradbury and Baeyens (2005b). The same basic non-electrostatic sorption model could be implemented for the clay mineral illite, and similar to montmorillonite, a number of (radio)contaminants were modeled (Bradbury and Baeyens, 2009a; Bradbury and Baeyens, 2009b). These studies formed an important basis for the development of sorption databases used in major Swiss safety assessments. Comprehensive compilations of the sorption data and modeling can be found in Baeyens and Bradbury (2017), Bradbury and Baeyens (2017), Baeyens and Marques Fernandes (2018), and Baeyens and Marques Fernandes (2018).

In the context of the European Project EURAD WP5-FUTURE ((Maes et al., 2024), final technical report), new sorption data on several 2:1 minerals have become available: Ra and Ba on illite and montmorillonite for the development of a sorption model (Klinkenberg et al., 2021; Marques Fernandes et al., 2023); Ra and Ba on illite and nontronite (sorption model, transfer batch to compacted state, contributions of Garcia-Guttierez et al. in Maes et al., 2024); Cd, Co, Zn, andNi on illite/Febex/(kaolinite)/mixtures (sorption model—additivity, transfer batch to compacted state, contribution of Missana et al. in Maes et al., 2024); Zn sorption reversibility on illite and montmorillonite (contribution of Dähn et al. in Maes et al., 2024); and $UO_2^{2+}$ on illite ($PO_4^{2-}$ competition for sorption, contribution of Del Nero et al. in Maes et al., 2024)).

## 2.5.2 Sorption on argillaceous rocks

### 2.5.2.1 Bentonite

To support the Swiss safety case, dedicated sorption studies have been performed on MX-80 bentonite. A study was specifically designed for the Swiss repository design, and the data are published in a technical report (Bradbury and Baeyens, 2011a). The bottom-up approach was also tested on selected datasets (Bradbury and Baeyens, 2011b).

A study by Grambow et al. (2006) presents sorption data for 11 different radionuclides (Cs, Ni, Pb, Eu(III), Am(III), Cm(III), Ac(III), Tc(IV), Th, Zr, and U(IV)) on MX-80 bentonite. The experimental sorption datasets were modeled, and the model uncertainty was assessed.

Comprehensive sorption studies have been carried out on FEBEX clay (a Spanish bentonite with a 98% smectite content), exhaustively characterized in the frame of the Spanish nuclear waste safety case, within homonymous projects (Huertas et al., 2000) and other international projects. Fundamental chemical parameters of FEBEX bentonite were analyzed to support geochemical modeling (Fernández et al., 2004). The radionuclides whose sorption was analyzed include anions such as selenite (Missana et al., 2009; Mayordomo et al., 2016) and cations of different valence: Cs (Missana et al., 2004; Missana et al., 2014), Ca, Co, Sr (Missana and Garcıa-Gutierrez, 2007; Missana et al., 2008b; Missana et al., 2009; Mayordomo et al., 2019), Ga (Benedicto et al., 2014a; Missana et al., 2009; Benedicto et al., 2014b), Pu (Begg et al., 2015), Np (Benedicto et al., 2014a), U (Missana et al., 2004; Missana et al., 2009), and other elements considered as actinide analogues (Galunin et al., 2009; Galunin et al., 2010). Radionuclide sorption on FEBEX smectite was mainly described based on cation exchange and surface complexation, which were interpreted considering a two-site (*weak,* $S_wOH$; *strong,* $S_sOH$) NEM. The sorption irreversibility of some radionuclides onto FEBEX bentonite was also analyzed (Missana et al., 2004; Begg et al., 2015). Recently, new sorption data on FEBEX bentonite became available for selenite, Ra, Ba, Cd, Co, Zn, and Ni. Emphasis of the sorption study was on development of sorption models, transfer of sorption data from the dispersed to compacted state, sorption reversibility, and sorption competition (see contributions of Garcia Guttierez et al. and Missana et al. in the final technical report of the project FUTURE project (Maes et al., 2024)).

### 2.5.2.2 Opalinus Clay

Similar as in the case of bentonite for the Swiss safety case, sorption measurements have been carried out on Opalinus Clay and related formations. Reports on these studies were published by Lauber et al. (2000) and Baeyens et al. (2014a). The bottom-up approach was tested on a number of datasets (Bradbury and Baeyens, 2011b; Marques Fernandes et al., 2015)).

### 2.5.2.3 Boom Clay

Within the geological disposal program in Belgium (coordinated by ONDRAF/NIRAS), sorption studies have been performed by SCK CEN to complement radionuclide migration studies. Van Laer et al. (2016) gives an overview of all the sorption experiments performed on Boom Clay and the main constituting minerals illite and montmorillonite. These emphasize the influence of natural organic matter on radionuclide sorption behavior. Boom Clay contains a considerable amount of organic matter that exhibits an important interaction (complexation and colloid formation) with a wide variety of radionuclides (transition metals, lanthanides, and actinides), changing its sorption behavior.

### 2.5.2.4 Boda Claystone

The geological disposal program in Hungary (coordinated by PURAM) considers two occurrences of the Boda Claystone Formation as potential sites (Breitner et al., 2015; Németh et al., 2016). In addition to diffusion investigations, sorption studies were performed by EK on Boda Claystone involving Cs, Sr, Co, and I (Mell et al., 2006a). Within the frame of a Swiss–Hungarian bilateral project, the bottom-up approach was tested for Cs, Co, Ni, Eu, Th, and U, in cooperation with (PSI) Paul Scherrer Institute (Marques Fernandes et al., 2015). Sorption was mostly related to illite-rich clayey matrices at the microscale (Osán et al., 2014; Kéri et al., 2016). The bottom-up approach based on illite was found to work well for Boda Claystone, despite the high hematite content due to the oxidized nature of the rock compared to the reducing properties of Opalinus Clay. Recently, new sorption data on samples of Boda Claystone became available for selenite and Ni. Sorption studies were complemented with diffusion studies, and emphasis was placed on the reversibility of sorption and competition effect (Ni vs. Co) (see contributions of Czömpöly et al. in (Maes et al., 2024)).

### 2.5.2.5 Callovo-Oxfordian argillite

Sorption studies on Callovo-Oxfordian argillite have been performed in several laboratories.

Studies for the following species have been reported: $I^-$ (Montavon et al., 2014; Bazer-Bachi et al., 2006), $SO_4^{2-}$ (Bazer-Bachi et al., 2007), Sr (Altmann et al., 2015), Cs (Chen et al., 2014b; Melkior et al., 2005), Ni (Chen et al., 2014a), Zn (Altmann et al., 2015), Pb (Orucoglu et al., 2018), Sn (Kedziorek et al., 2007; Latrille et al., 2006), Eu (Descostes et al., 2017), Pu (Latrille et al., 2006), and organic ligands and acids (EDTA, isosaccharinate (ISA), phthalate, oxalate, and polymaleic acid) (Dagnelie et al., 2018; Rasamimanana et al., 2017; Durce et al., 2014). Often, these studies were combined with migration experiments.

In Andra (2005), $K_d$ values on Callovo-Oxfordian argillite for safety relevant radionuclides are listed.

Recently, new sorption data on samples of Callovo-Oxfordian argillite became available for selenite, Ra, Ba, Eu, and U (see contributions of Garcia-Guttierrez et al., Hassan-Loni et al., and Montavon et al. in the final technical report of the FUTURE project (Maes et al., 2024)). Significant progress on the understanding of U retention in Callo-Oxfordian clay stone (Montavon et al., 2023; Montavon et al., 2022) was achieved.

## 2.5.3 Sorption on crystalline rocks and components

Compilations of sorption distribution coefficients ($K_d$) for Swedish (SKB) and Finnish (POSIVA) safety cases in crystalline bedrocks are available in Crawford (2010) and Hakanen et al. (2014). More recently, the sorption behavior of various elements has been intensively studied using rock samples provided by the Bukov Underground Research Lab (URL), Czech Republic), Onkalo (Finland), Forsmark (Sweden), and other sites with crystalline rock types potentially suitable for spent-fuel disposal.

Li et al. (2018), Li et al. (2020), and Puhakka et al. (2019) investigated the sorption behavior of Se(IV) on Grimsel granodiorite (mainly plagioclase, K-feldspar, quartz, and biotite), using artificial Grimsel groundwater and different concentrations of Se(IV). Fukushi et al. (2013) focused their study on Eu(III) sorption on granite. The distribution coefficients of Ba on Olkiluoto pegmatitic granite and veined gneiss, as well as those of Grimsel granodiorite, and their main minerals (quartz, plagioclase, K-feldspar, and biotite) were obtained using batch sorption experiments (Muuri et al., 2018; Muuri, 2019).

The sorption of Ni on fracture-filling calcite from the Bukov URL was studied and the resulting $K_d$ values at different pH levels and initial concentrations were compared. The results confirmed substantial Ni sorption, indicating its potential significance in radioactive waste repositories cf. (Parigi et al., 2022). The significant influence of pH on calcite stability and surface charge must be considered when providing $K_d$ values for performance evaluation calculations cf. (Al Mahrouqi et al., 2017).

(Fabritius et al., 2022) studied the sorption of Ra on biotite minerals and on whole rock samples using reference groundwater from the Finnish and Swedish spent nuclear fuel repositories at Olkiluoto and Forsmark, respectively. The rock types included veined gneiss, mica gneiss, diatexitic gneiss, granitic pegmatoid, granodiorite, monzogranite, and tonalite, and different water types were used, ranging from fresh to saline. The experimental and PHREEQC-interpreted distribution coefficient ($K_d$) results will be used in the safety case calculations of the Finnish and Swedish spent fuel repositories to further improve the understanding and reduce the uncertainties regarding the behavior of Ra in crystalline rocks. A multi-site SCM was developed to describe the Se sorption on biotite (Li et al., 2020).

Batch sorption experiments focused on rock-forming minerals, partially also present as fracture-filling minerals, including muscovite, orthoclase, and quartz. Various aspects of investigations comprise surface complexation modeling, TSM modeling, and data compilation for databases (e.g., Noseck et al., 2012; Noseck et al., 2018; Videnská et al., 2013; Stamberg et al., 2014; Videnska et al., 2015; Stockmann et al., 2017; Britz, 2018; Richter et al., 2016).

An application of the smart $K_d$ concept (see Section 3.1.3.3) in reactive transport calculations for porous sedimentary systems is described in detail by Noseck et al. (2012).

Newly formed sheet silicates and other precipitates in fractures, such as sulfates (e.g., baryte, celestite) or carbonates (e.g., calcite), show remarkable retention capacities for some radionuclides, such as Ra (Brandt et al., 2015; Chagneau et al., 2015; Klinkenberg et al., 2018; Curti, 1999), rare earth elements (REEs), and U(IV) (Drake et al., 2018).

A mechanistic explanation for heterogeneous sorption on nanotopographic muscovite surfaces due to the availability of energetically favorable sorption sites has been provided by Schabernack et al. (2023), who used kinetic Monte–Carlo (kMC) simulation techniques. The energetic differences of surface sorption sites available at nanotopographic structures such as steps, pits, and terraces were investigated, and the energies of adsorption and desorption reactions were obtained from DFT calculations.

### 2.5.4 Sorption databases

Publications of sorption databases ($K_d$ values) used in performance assessments are very sparse in the open literature, and they are mainly in the form of technical reports issued by waste management organizations (WMOs; e.g., ANDRA, https://www.andra.fr/sites/default/files/2018-04/dossier-options-surete-apres-fermeture_0.pdf). Examples are sorption databases on illite, bentonite, and argillaceous rocks that have been used in the Swiss safety cases for marl formations (Bradbury and Baeyens, 1997a), as well as those on bentonite (Bradbury and Baeyens, 2003b), illite (Bradbury and Baeyens, 2017), and Opalinus Clay and related formations (Bradbury and Baeyens, 2003a; Baeyens et al., 2014b).

RES³T (https://www.hzdr.de/db/res3t.login) is an acronym for the "Rossendorf Expert System for Surface and Sorption Thermodynamics" and is an open-source digitized thermodynamic sorption database comprising mineral-specific datasets for sorption modeling (e.g., SCPs, thermodynamic data, and surface complexation reactions). The database covers 145 minerals, approximately 140 sorbing ligands, 2,150 SSA measurements, 1,900 surface site datasets, and 6,700 surface complexation reactions, and it is based on literature references to ensure re-traceability and transparency.

# 3 Transport processes in host rocks

This chapter describes the current predictive models for the migration of radionuclide (RN) as dissolved species (colloid-related transport behavior and the transport of gases are not discussed here) in a fully saturated environment, the role and influence of structural properties, as well as the experimental and numerical approaches utilized for clay and crystalline host rocks. In this context, the main processes, such as diffusion, advection, and retention in clay and crystalline rocks, are characterized, including the main components and heterogeneities along the migration path and the understanding of coupled transport and retention processes.

## 3.1 Introduction to diffusion, advection, and retention processes

### 3.1.1 Basics

For a more in-depth reading, we refer to several text books (Crank, 1975; Dullien, 1991; Mitchell, 1993; Grathwohl, 1998; Cussler, 2009; Appelo and Postma, 2004).

In porous (fully saturated) media, the net flux ($J$) of a solute is equal to the sum of all the fluxes induced by the different gradients that may be present in the considered system: chemical potential, hydraulic head, electrical potential, and temperature; this is described by Onsager reciprocal relations. However, the two most dominant transport processes for radionuclide migration are:

- Diffusion (created by a gradient of chemical potential and, hence, concentration), and;
- Advection (created by a gradient of hydraulic pressure).

Diffusive flux is the net movement of dissolved species present in an aqueous solution because of a difference of chemical potential (with the concentration gradient as driving force). Fick's first law describes the relationship between a diffusive flux and a concentration gradient

$$J = -D_e \frac{\partial C}{\partial x} \tag{20}$$

where $J$ is the solute flux [mol/m$^2$s], $D_e$ is the effective diffusion coefficient [m$^2$/s] of the solute in the porous medium, and $C$ is the aqueous-phase solute concentration [mol/m$^3$].

The effective diffusion coefficient ($D_e$) of each dissolved species directly depends on the diffusion coefficient in pure water, $D_0$, its diffusion-accessible porosity in medium $\eta$ [-], and geometric factor $G$ [-] depending on the microstructure of the porous medium:

$$D_e = \eta G D_0 \tag{21}$$

The geometric factor is a lumping parameter that averages the complex morphology of a pore structure and typically consists of two terms: tortuosity $\tau$ [-] and constrictivity $\delta$ [-]. (Please note that the $G$ factor is sometimes defined as $\tau^2/\delta$ in papers cited in this report (e.g., in Appelo et al. (2010); Glaus et al. (2015a)). Tortuosity accounts for the effects of an increased path length of a molecule diffusing through the water-filled pores of a porous medium and is, therefore, larger than one. Constrictivity accounts for pore narrowing and widening but is often arbitrarily set equal to one. Both constrictivity and tortuosity cannot be measured independently. Only the lumping geometric factor $G$ can be estimated from a diffusion experiment if the porosity is known:

$$G = \frac{\delta}{\tau^2} \tag{22}$$

The molecular diffusion coefficient, $D_0$, of a dissolved species in pure water depends essentially on its chemical nature (e.g., atomic or molecular weight, hydrated radius, steric effects, and electrical charge), temperature, and the viscosity of the fluid. Typical values for the molecular diffusion coefficients of ions and molecules in water are in the range of $10^{-9}$ and $10^{-10}$ m$^2$/s (Li and Gregory, 1974).

Fick's second law describes the transient evolution of flux:

$$\frac{\partial C}{\partial t} = \frac{D_e}{\eta} \frac{\partial^2 C}{\partial x^2} \tag{23}$$

The radionuclide transport in a porous medium is influenced by retention processes at the water–rock interface (see previous chapter on retention processes). When these processes are rapid, linear, and reversible, their effect on the transport regime can be accounted for by a retardation factor, $R$ [-], which can be related to the solid–liquid distribution coefficient $K_d$ [m$^3$/kg] (often derived from sorption experiments, see Chapter 2 on retention processes):

$$R = 1 + \frac{\varrho_d K_d}{\eta} \tag{24}$$

where $\rho_d$ is the dry bulk density [kg/m$^3$].

By rewriting Fick's second law to include reversible retardation, one obtains:

$$\frac{\partial C}{\partial t} = \frac{D_e}{(\eta + \varrho_d K_d)} \frac{\partial^2 C}{\partial x^2} = \frac{D_e}{\eta R} \frac{\partial^2 C}{\partial x^2} = D_a \frac{\partial^2 C}{\partial x^2} \tag{25}$$

Other frequently used diffusion parameters (note that the correct name of each diffusion coefficient must always be clearly and explicitly stated along with its definition to avoid confusion; simply referring to a "diffusion coefficient" or to "diffusivity" is insufficient and can lead to serious errors when transferring/using data) are the pore diffusion coefficient, $D_p$, and the apparent diffusion coefficient, $D_a$, which are related to each other in following way:

$$D_a = \frac{G}{R} D_0 \text{ with } G D_0 = D_p \text{ and } D_e = \eta G D_0 = \eta D_p = \eta R D_a \tag{26}$$

The product $\eta R$ is also often referred to as the "rock capacity factor." The rock capacity factor $\alpha$, relates the concentration in a porous medium, $C_{bulk}$, to the concentration in a solution, $C$, i.e., the sum of the amount of the species in a solution and in a solid normalized to the solution and solid volumes (Tournassat and Steefel, 2015). Hence the term refers to a "storage capacity" of a porous medium for a certain species.

$$C_{bulk} = \alpha C = \eta R C = (\eta + \varrho_d K_d) C \tag{27}$$

The transport of dissolved species by advection is the result of the movement of pore water under the effect of a hydraulic pressure gradient. The hydraulic pressure gradient causes the water to move out of a porous medium at an average velocity called the Darcy velocity, $V_{darcy}$ [m/s].

The Darcy law describes the flowrate $(Q)$ of water forced through a porous medium of cross section $S$ [m$^2$] and length $L$ [m] by a hydraulic gradient $(\Delta P/L)$:

$$Q = K S \frac{\Delta P}{L} \tag{28}$$

The Darcy velocity corresponds to the water flowrate $Q$ divided by the cross-section $S$ of the considered porous volume:

$$V_{darcy} = \frac{Q}{S} = K \frac{\Delta P}{L} \tag{29}$$

where $Q$ is the flowrate [m$^3$/s], $\Delta P$ is the hydraulic pressure difference that is exerted over the length of the porous medium (expressed in m of water column height), and $K$ is a proportionality constant called hydraulic conductivity [m/s]. While the Darcy velocity represents the velocity of water flowing out of a porous medium, the pore water velocity ($V_p$) takes into account the fact that, inside the porous medium, water flows only through the pore space. Both parameters are related via the water porosity or total porosity, $\eta$:

$$V_p = \frac{V_{darcy}}{\eta} \tag{30}$$

Of note, as soon as an advective flow is present, diffusive flow also becomes affected by mechanical and hydrodynamic dispersion and becomes a dispersion coefficient ($D_{disp}$), which is a function of the advective velocity ($a$ is the longitudinal dispersivity [m]):

$$D_{disp,p} = D_p + a V_{darcy} \tag{31}$$

Mechanical dispersion (hydrodynamic dispersion) results from ground/pore water moving at rates both greater and less than the average linear velocity (Fetter, 1992). This is caused by: 1) fluids moving faster through the center of the pores than along the edges, 2) fluids traveling shorter pathways and/or splitting or branching to the sides, and 3) fluids traveling faster through larger pores than through smaller pores.

Because solute-containing water does not travel at the same velocity everywhere, "mixing" occurs along flow paths. This mixing is called mechanical dispersion and results in a distribution of solutes at the advancing edge of flow. The dispersion coefficient in the transport equation accounts for the combined effects of mechanical dispersion and molecular diffusion, both of which cause spreading from highly concentrated areas towards less concentrated areas.

The ratio of the advective transport rate over the diffusive transport rate is known as the Péclet number, $P_e$:

$$P_e = \frac{LV}{D} \tag{32}$$

where $L$ is the characteristic length [m] (travelled length of the fluid), and $V$ and $D$ represent the water velocity and the diffusion coefficient, respectively. The Péclet number is used as an indicator of the dominant transport mechanism. Equation 32 is the general form of the equation for the Péclet number, and depending on the underlying assumptions in the solute transport equation, it can have different forms (Huysmans and Dassargues, 2004).

The advection–diffusion transport equation reads.

$$\frac{\delta C}{\delta t} = \frac{D_{disp,p}}{R}\frac{\partial^2 C}{\partial x^2} - \frac{V_{darcy}}{\eta R}\frac{\delta C}{\delta x} \tag{33}$$

Taking into account that $V_{darcy}/\eta = V_p$, and introducing the notation of "apparent" coefficients to incorporate the retardation effect, we obtain:

$$\frac{\delta C}{\delta t} = D_{disp,a}\frac{\partial^2 C}{\partial x^2} - V_a\frac{\delta C}{\delta x} \tag{34}$$

The classical diffusion-retardation equation considers the concentration of solutes to be the same over the entire pore space and accounts for linear reversible sorption processes. The latter are mainly linked to the main sorption mechanisms in clays, i.e., ion exchange and surface complexation. The equation disregards i) the presence of EDLs that has an effect on the concentration profiles of ions within pores, and ii) non-reversible retention processes (e.g., irreversible chemisorption, surface precipitation, incorporation, solid-solution formations, and precipitation).

### 3.1.2 Numerical modeling of coupled physical and chemical processes in transport

Numerical modeling of coupled physical and chemical processes of fluid flow, solute transport, and chemical reactions is vital for predicting the migration of RN in host rocks. In general, such numerical models include reactive-transport equations (Steefel and Lasaga, 1994) for both solute transport and chemical reactions, as well as the conservation of momentum for fluid flow (Steefel et al., 2005). A multitude of reactive transport codes are available, see Steefel et al. (2014) for a non-exhaustive list of reactive transport codes such as PHREEQC, PHREEQC-PHAST, HPx, HYTEC, CRUNCHFLOW, ORCHESTRA, PFLOTRAN, OpenGeoSys, TOUGHREACT, and GEM2MT.

#### 3.1.2.1 Reactive multi-species diffusion models (mainly applicable to clays)

For each species, diffusion is coupled to speciation reactions in solution, sorption reactions on mineral surfaces, as well as mineral reactions.

One-dimensional reactive multi-species diffusion in solution may be described for $i$ species in solution with concentration $C_i$ as

$$\frac{\partial C_i}{\partial t} = D_p\frac{\partial^2 C_i}{\partial x^2} - R_i - r_i, i = 1, 2, \ldots, n_{aqueous} \tag{35}$$

where $D_p$ is the pore diffusion coefficient [m$^2$/s]; $R_i$ [mol/m$^3$s] denotes a source/sink term due to equilibrium reactions between the solution and non-moving species sorbed on mineral surfaces according to

$$R_i = \sum_{j=1}^{n_{sorbed}} \nu_{i,j}\frac{1-\eta}{\eta}\rho_s\frac{\partial S_j}{\partial t}, i = 1, 2, \ldots, n_{aqueous} \tag{36}$$

where $n_{aqueous}$ and $n_{sorbed}$ [-] denote the number of species in solution and sorbed, respectively, and $\nu_{i,j}$ [-] are stoichiometric coefficients. $r_i$ [mol/m$^3$s] is a source/sink terms due to mineral reactions.

The mass action law or the assumed equilibrium chemistry in solution and between solutions and both minerals and mineral surfaces yields constraints that define the source/sink term for each species and represents the mechanistic understanding of surface and/or ion-exchange reactions of the following form

$$\equiv sc_1 + c_2 \Leftrightarrow \equiv sc_2 + c_1 \tag{37}$$

Mineral reactions can be kinetically or by chemical equilibrium controlled and have the following form

$$r_i = \sum_{m=1}^{N_m} \nu_{im} r_m, i = 1, 2, \ldots, n_{aqueous} \tag{38}$$

where $r_m$ [mol/m$^3$s] is the net rate of precipitation ($r_m > 0$) or dissolution ($r_m < 0$) of a mineral per unit volume of rock, and $\nu_{im}$ [-] is the number of moles of species $i$ per mole of mineral $m$ present in the rock.

This can be further extended by accounting for effects of electrical potentials that develop during the movement of charged species (Nernst-Planck formalisms).

#### 3.1.2.2 Reactive transport including advective fluid flow (important for crystalline rocks)

At the pore scale, crystalline rock can be considered as a binary domain consisting of a solid material and the pore space. The transport of (solute) species occurs in pore spaces and reactive processes such as the adsorption/desorption of RN, and mineral dissolution/precipitation take place at fluid–solid interfaces. The Navier–Stokes equation (NS) or the Stokes equation is employed as a momentum equation to describe fluid flow in a pore space (Li et al., 2008; Molins, 2015). Interfacial reactions are usually treated as a boundary condition at fluid–solid boundaries (Molins, 2015).

Pore-scale simulation equations.

(1) Fluid flow using NS equation:

$$\frac{\partial \boldsymbol{u}}{\partial t} + (\boldsymbol{u} \cdot \nabla)\boldsymbol{u} = -\frac{1}{\rho}\nabla \boldsymbol{p} + \nu \Delta \boldsymbol{u}, \qquad (39)$$
$$\nabla \cdot \boldsymbol{u} = 0,$$

where $u$ is a velocity vector, $p$ is pressure, $\rho$ is the fluid density, and $\nu$ is the kinematic viscosity of the fluid.

(2) Solute transport and chemical reactions; reactive transport equations:

$$\frac{\partial \boldsymbol{c_i}}{\partial t} + \nabla \cdot (\boldsymbol{u c_i} - \boldsymbol{D_i} \nabla \boldsymbol{c_i}) = \boldsymbol{R_i}, \qquad (40)$$

where $c_i$ is the molar concentration of species $i$ in solution, $D_i$ is the dispersion/diffusion coefficient, and $R_i$ is the reaction term.

(3) Surface reactions:

$$-\boldsymbol{D_i} \nabla \boldsymbol{c_i} = \boldsymbol{\xi_{im} r_m}, \qquad (41)$$

where $r_m$ denotes the surface reaction rate and $\xi_{im}$ is the stoichiometric coefficient of component $i$ in each surface reaction $m$.

At the continuum scale, a porous medium is typically conceptualized as a continuum with bulk parameters that characterize its physical and chemical properties. At this scale, mobile and immobile phases are assumed to coexist at each point in space and time. The Darcy's equation is applied as a momentum equation, while reactive transport is described by the mass balance equation of each species (Steefel and Lasaga, 1994). Reactive transport in fractured porous media can be simulated using the coupled Stokes–Brinkman equation and reactive-transport equations (Yuan et al., 2016; Yuan and Zhang, 2019), which allows for efficiently modeling the alterations of rock properties caused by chemical reactions:

$$\boldsymbol{\mu K_{perm}^{-1} u} + \nabla \boldsymbol{p} - \boldsymbol{\mu^* \Delta u} = 0 \qquad (42)$$
$$\nabla \cdot \boldsymbol{u} = 0,$$

where $K_{perm}^{-1}$ is a permeability tensor, $u$ represents the physical velocity of the fluid in the fractures and the Darcy velocity in porous media, $\mu$ is the dynamic viscosity of the fluid, and $\mu^*$ is the effective dynamic viscosity.

### 3.1.3 Accounting for retention processes in transport: Empirical and thermodynamic approaches

There are different approaches for describing sorption and desorption processes at water–rock interfaces:

a) Empirical relationships, such as e.g., Langmuir, Freundlich, or linear sorption isotherms (Kd), and
b) Conceptual TSMs that describe ion-surface associations based on mechanistic approaches to characterize coordinative properties of surface complexes using, for example, the DDLM or more sophisticated model theories (Ochs et al., 2012).

Approaches from Langmuir and Freundlich, as well as TSMs, assume a thermodynamic equilibrium between a solid and surrounding electrolytes. However, compared to empirical approaches, mechanistic TSMs are based on the law of mass action.

#### 3.1.3.1 Empirical – constant $K_d$ approach

In performance and safety assessment (PA/SA) calculations, sorption is usually described using linear distribution coefficients (also see Section 2.1) constant in space and time, i.e., simple $K_d$ values (NAGRA, 2002; POSIVA, 2012b; SKB, 2011), and applied in the classical advection–diffusion equation as a retardation factor, $R$.

Since the sorption of many elements and radionuclides strongly depends on the geochemical properties of the surrounding solution and sediments, the approach of constant $K_d$ values is justified only for constant hydrogeological and geochemical conditions expected in various parts of a GDS.

For transport simulations for PA/SA purposes, typically, databases with experimental $K_d$ values (and uncertainty ranges) are compiled, and the databases are often extended for different conditions, geological strata, and other factors.

Within large time frames or in dynamic systems close to an engineered barrier system, a variability of geochemical conditions can be expected due to spatial heterogeneities and environmental variations. Therefore, it may be desirable to describe the transport and/or sorption of potential contaminants as a function of important environmental parameters such as pH or ionic strength.

#### 3.1.3.2 Process understanding–Thermodynamic approaches

Reactive transport simulations typically rely on transport codes coupled with a geochemical code, capable of using TSMs based on mass action law equations:

$$\equiv \boldsymbol{s c_1} + \boldsymbol{c_2} \Leftrightarrow \equiv \boldsymbol{s c_2} + \boldsymbol{c_1} \qquad (43)$$

These coupled models are useful for acquiring process and system understanding, as they are able to account for different chemical conditions, in contrast to the constant $K_d$ approach.

Different TSMs have been elaborated on to describe the mineral–fluid interface during sorption processes (Ochs et al., 2012) (also see Section 2.2.2). TSMs that are used to calculate defined surface complexation processes of, for example, metal cations (Me) are called SCMs. All TSMs are based on the law of mass action and mole balance equations (Davis and Kent, 1990a), but they involve different descriptions of EDLs, i.e., electrostatic interaction term (Davis and Kent, 1990a; Westall and Hohl, 1980). In non-EDL models (noEDLMs) electrostatic interaction is not considered; thus, a DDL is neglected. Each TSM (except noEDLMs) considers different electrostatic planes that can contribute to sorption processes.

For use in PA/SA, when it comes to simulating the impact of changing geochemical conditions over very long time frames and/or under variability in composition over larger distances, a fully coupled reactive transport approach may result in unfeasible computation times owing to the complexity of mechanistic model approaches (Noseck et al., 2014). However, it enables the complementing of sorption databases by underpinning a selected

value range, as well as the binding of sorption values for current/changing conditions or alternative scenarios.

For application in safety assessment (Noseck et al., 2012; Noseck et al., 2018), the "smart $K_d$ concept" (http://www.smartkd-concept.de/) has been proposed and developed, and it has been implemented in transport modeling. It combines state-of-the-art mechanistic TSM theories with the traditional empirical, constant, linear, and reversible $K_d$ approach and presents a computation-time-efficient approach to simulate long-term contaminant transport over large areas and long distances.

It allows for the interpolation of distribution coefficients (referred to as smart $K_d$ values) for any observed (or hypothetic) combination of environmental boundary conditions, treating complex systems in a more rigorous way. This approach is based on SCMs and considers further ion exchange, solid-phase equilibria, and complexation in aqueous solutions (Stockmann et al., 2017).

An application of the smart $K_d$ concept in reactive transport calculations for porous sedimentary systems is described in detail by Noseck et al. (2012).

## 3.2 Transport in clays

### 3.2.1 Structural aspects of clays

Argillaceous sediments are deposited in various marine (Opalinus, Callovo-Oxfordian, and Boom Clay) and lacustrine (Boda Claystone) environments. Because of water–rock interactions and microbial activity, physico-chemical changes occur in clay sediments after their deposition, and the sediments undergo diagenesis by being progressively transformed in clay rocks. The diagenesis of clay sediments depends on many factors, such as the depositional environment, types of clay minerals, amount of organic matter, pore water chemistry, geothermal gradient, and burial history. Increasing burial depth leads to sediment compaction and chemical diagenesis, which results in a systematic decrease of porosity, water expulsion, and progressive transformation reaction of smectite to illite (Velde and Meunier, 2008; Weaver, 1989).

The principal minerals in argillaceous sediments are clay minerals, with additional quartz, feldspars, and calcite, small amounts of pyrite, Fe-carbonates, and apatite. In addition, solid or immobile organic matter in the form of more or less evolved kerogen may be present. When argillaceous sediments are sufficiently compacted, such that they are no longer soft or plastic but still not fissile (i.e., not cleavable along weak planes as shales or metamorphic slates), they are called clay rock or mudstone. Depending on its mineralogy (smectite content), a clay sediment may exhibit swelling properties in the presence of water; this is important in applications for nuclear waste disposal, as it provides self-sealing properties. Argillaceous sediments contain variable amounts of water present both in the clay mineral structures and in the nanometer pore spaces. High water contents (>20 vol%) result in soft and plastic clay (e.g., Boom Clay), whereas clay rocks/mudstones (Opalinus Clay, Callovo-Oxfordian Clay, and Boda Claystone) are drier (<20 vol% pore water) and stiffer. Further compaction and water expulsion from the pores result in further alignment of clay mineral grains such that the rocks become fissile, forming shales and, eventually, slates.

Clay minerals are phyllosilicates (from the Ancient Greek word φύλλον "phyllon", meaning leaf), and the principal clay minerals in argillaceous host rocks are smectite (or "swelling clay"), illite, kaolinite, and chlorite. These phyllosilicates are composed of jointed octahedral (O) layers (such as that containing $Al^{3+}$, $Mg^{2+}$, or $Fe^{2+}$) and tetrahedral (T) layers (those containing $Si^{4+}$ or $Al^{3+}$) (Figure 2). Illite and montmorillonite (main smectite) are composed of TOT layer sequences, while kaolinite is composed of TO sequences. Chlorites are TOT layer sequences with brucite-like interlayers with compositions near to $(Mg,Fe,Al)_3(OH)_6$.

Due to isomorphic substitution where a higher-valency element is replaced by a lower-valency element ($Si^{4+}$ by $Al^{3+}$ in tetrahedral layers, or $Al^{3+}$ by $Mg^{2+}$ and $Fe^{2+}$ in octahedral layers), permanent electrical charges are formed. These negative charges become charge-balanced by (hydrated) cations in the interlayers between two TOT layers. Due to the higher negative charge of illite TOT layers, cations (mainly $K^+$) are fixed strongly in interlayers without a hydration shell. In contrast, montmorillonite, which has a lower charge, has interlayer cations that maintain their hydration shells. The TO layers of kaolinite are uncharged. An excellent overview of the surface properties of clay minerals is given by Tournassat et al. (2015). For an extensive overview on the properties of clays, the reader is referred to Mitchell (1993), Velde and Meunier (2008), and Meunier and Fradin (2005).

### 3.2.2 Main processes controlling transport in clays

#### 3.2.2.1 Diffusion-dominated transport

In compact clay systems (natural host rocks, and clay-based engineered barriers) used for the geological disposal of radioactive waste, diffusion is the dominant transport mechanism owing to the very low hydraulic conductivities of these rocks ($<10^{-11}$ m/s).

Clay host rocks may experience tectonic disturbances, but due to the presence of swelling clays and water, they tend to self-seal relatively quickly (within weeks to years). The higher the amount of water and smectites, the prompter is the self-sealing response (plastic Boom Clay vs. Callovo-Oxfordian Clay and Opalinus Clay host rocks). After tectonic disturbances, the intrinsic permeability of fractured clay rock is expected to return to that of an intact non-fractured rock (OECD/NEA, 1996).

Advective transport in clays due to the presence or creation of faults and fractures (via natural processes or excavation processes) is considered negligible in terms of geological time scales because of self-sealing properties (Bernier et al., 2007; Bock et al., 2010; Li, 2013).

#### 3.2.2.2 Retention predominantly via ion exchange and surface complexation

Clay minerals such as montmorillonite and illite (including illite–smectite mixed layers) are important in the disposal of radioactive waste, since the former is the major clay mineral component of near-field bentonite (buffer and backfill) and the latter is present at significant levels in many argillaceous host rock formations under consideration.

The main sorption mechanisms of aqueous species on clay minerals are cation exchange and surface complexation (see Section 2.1 (Classical retention processes) for more details). The sorption behavior of a broad series of elements has been well investigated.

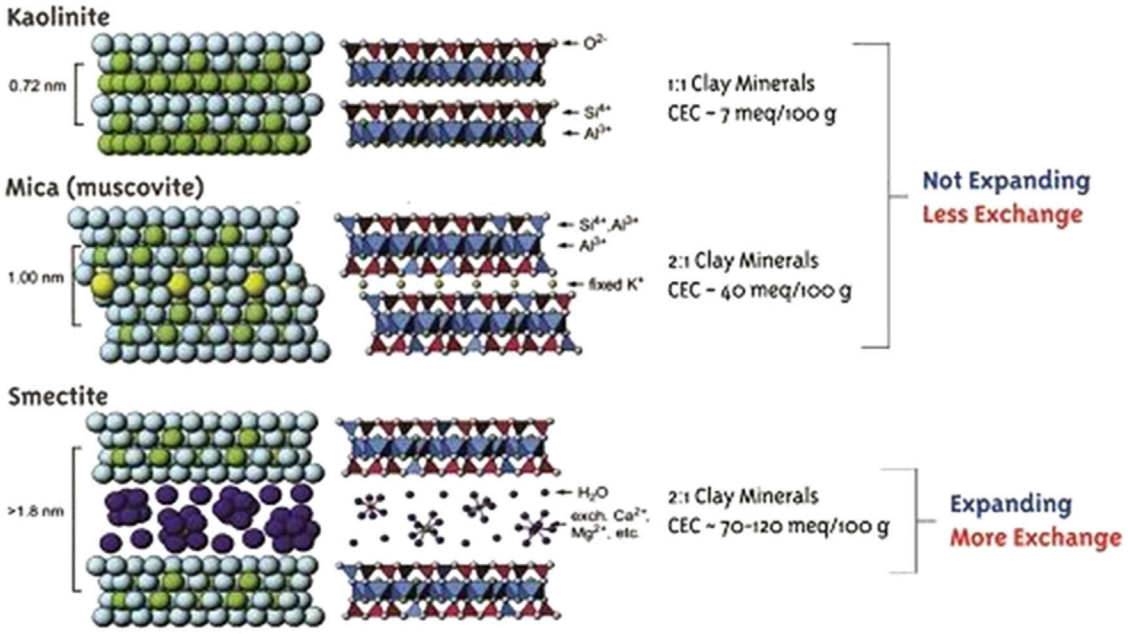


FIGURE 2
Representation of the structures of different types of clay minerals (Source, https://www.soils4teachers.org/mineralogy, with permission form SSSA).

In addition to these classical retention processes, redox-induced precipitation is also an important retention mechanism for redox-sensitive radionuclides (see Section 2.2.2 for more details).

For transition metals, another retention mechanism has been observed in clays. At higher loadings of transition metals, the surface precipitation of neo-formed phyllosilicates or the formation of LDHs may occur (also see Section 2.3.1).

The presence of carbonate and sulfate minerals in natural clays may also lead to solid-solution formation, causing strong retention for some radionuclides (e.g., Ba, Sr, and Ra) (see Section 2.3.3, Solid solutions).

### 3.2.2.3 Special effect of negatively charged clay surfaces on radionuclide transport behavior – double layer effects

Because of negatively charged clay mineral surfaces, anionic, cationic, and neutral species exhibit distinct diffusion behavior.

- Anionic species become repelled by the negatively charged surface of clay minerals, which limits their accessibility to certain pores (smallest size; access restriction by constrictivity effects) and reduces their movement to a more limited zone of bigger pores. This phenomenon is known as “anion exclusion” or “Donnan exclusion.” The higher the negative charge, the stronger is the decrease in anion-accessible porosity (see the contribution of Van Laer et al. in (Maes et al., 2024)).
- Cationic species, on the contrary, become attracted by negative clay surfaces, leading to interaction processes that enhance the sorption/uptake in host rocks. These interaction processes are generally expected to lead to a slowed down diffusive transport and are called retardation processes.
- Neutral species are hardly affected by the electrostatic forces.

Recent studies (EC CATCLAY project, Altmann et al. (2015); and EURAD WP5 FUTURE project (Maes et al., 2024) have, however, revealed that the uptake of cations in clays not only leads to an increase in the rock capacity factor (cf. Equation 26) but may also have an impact on diffusive properties by altering $D_e$ values (potential explanations for this peculiarity will be outlined in the following section). For this reason, the effect of nuclide uptake by the solid phase does not inevitably lead to retardation in all cases but is rather the result of the combined impact on $R$ and $D_e$ (cf. Equation 25).

The classical description of the diffusive processes of solutes interacting with surfaces according to Equation 25 is based on the assumption that species bound to a surface are immobile, viz. they can only change location after a desorption step (stationary and mobile phase concept borrowed from chromatography). Sorption, thus, contributes only as a “capacity factor” increasing the retardation of solutes. Once the sorption capacity is reached, or sorption sites are saturated, the amount of solute transported per unit cross section area and time, viz. the diffusive flux, is exactly the same as that for the case of an inert solute that does not interact with a clay surface. The only driving force for diffusion is the concentration gradient of dissolved species present in the bulk aqueous phase (cf. Equation 20, Fick’s first law). In such cases, $D_e$ values of different solutes would only depend on their respective $D_0$ values and on $\eta G$ factors (Equation 21). The latter factor is often assumed to be identical for all aqueous species in a given porous medium (e.g. (Aldaba et al., 2014; Jacops et al., 2017b),). However, this assumption is invalid for charged solutes in the nano-scale pore networks of negatively charged clay minerals and clay rocks (cf. Figure 3). For an overview of the literature, the reader is referred to reviews such as (Bourg et al., 2003; Miller and Wang, 2012;

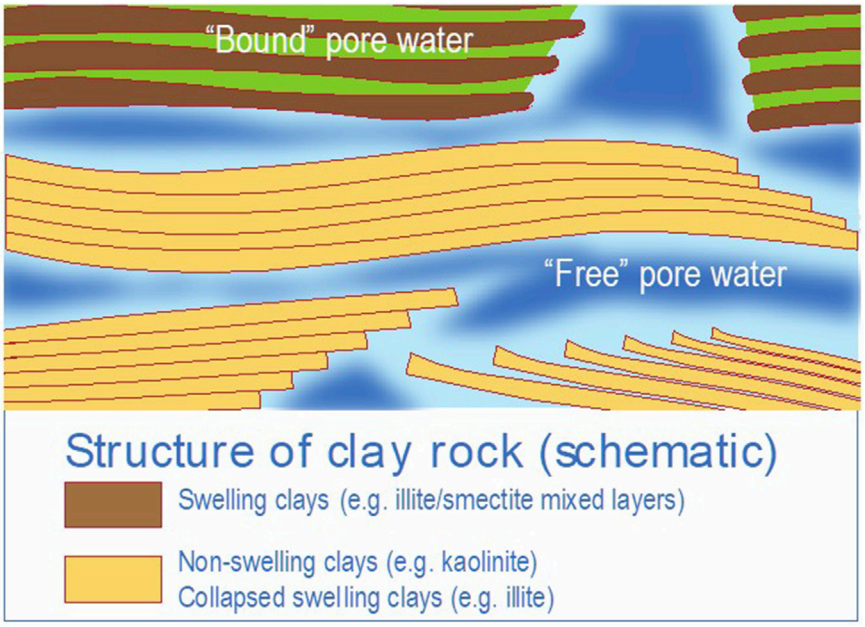


FIGURE 3
Texture of a clay rock, illustrating the various water properties and the heterogeneity of the different types of clay minerals at the nanometer scale. Dark blue colors indicate water domains with bulk water properties, light blue colors indicate water domains, which are influenced by the negatively charged surfaces of clay minerals and their electrical double layers (EDLs). Depending on the amount of fixed charges of the latter, the overall charge equivalents of positively and negatively charged solutes may vary within the different water domains. The green color represents water domains in the interlayers of swelling clays. Of note, the fractional distribution of clay and water domains does not represent the reality.

Shackelford and Moore, 2013; Altmann et al., 2015; Tinnacher et al., 2016). The $D_e$ values derived for anionic species (Equation 17) are generally lower than those of uncharged reference species such as HTO or $D_2O$, while those of cationic species are generally higher, even after normalization for individual different $D_0$ values (see Table 4). In addition, for non-charged species (dissolved gasses), unexpected phenomena, such as a functional dependence of the "geometric factor" on the molecular size, has been demonstrated (Jacops et al., 2017a; Jacops et al., 2017b).

While potential differences in geometry factors between anionic and neutral species could be a valuable explanation for the lower $D_e$ values of anionic species in the sense of a restricted accessibility of anionic species to the pore space of negatively charged clay surfaces (called "anion exclusion" (Wigger and Van Loon, 2017)), such an explanation would fail for the enhanced $D_e$ values of cationic species. It has been demonstrated (Glaus et al., 2017) for different clay materials that the diffusion-accessible porosity of uncharged species is equal to the total water porosity. If the enhanced $D_e$ values were related to geometry effects, the only reasonable explanation would be found in the reduced tortuosity factors, $\tau^2$ (cf. Equation 22). Consequently one would have to assume shorter diffusion paths (Shackelford and Moore, 2013) for cationic species compared to neutral species, which cannot be justified from a physical point of view.

In view of the conceptual difficulties in explaining the different diffusive behaviors of differently charged species by geometry effects solely, it appears to be more sensible to question the assumption of the concentration gradients of bulk aqueous species being the only driving force for diffusion. In fact, it has been demonstrated for the diffusion of cationic species in compacted smectite clay that the direction and magnitude of observed diffusive fluxes depend on the concentration gradients of cationic species bound to the cation-exchange sites present in interlayer spaces, rather than those in the aqueous phase (Glaus et al., 2013).

The process-based physical models for such phenomena are still under development and should take into account structural characteristics of clay material, aside from those of diffusing solutes. Although no direct experimental evidence exists for a Brownian type of motion of surface-associated species, it is reasonable to assume that a similar relationship exists, according to Equation 20 (Fick's first law), between the concentration gradient of these species and their respective diffusive fluxes, as for the species in the aqueous phase. Conceptually, the overall observed diffusive flux can be described as being the result of the superposition of the individual fluxes in two phases, one representing a bulk aqueous species and the second representing a mobile surface species (cf. Equation 24).

TABLE 4 Normalization of the effective diffusion coefficient ($D_{e,i}$) of an aqueous species i with the effective diffusion coefficient ($D_{e,HTO}$) of tritiated (HTO) or deuterated (HDO) water and the respective diffusion coefficients in bulk water ($D_0$). Dependence on the electrical charge of the species.

| Dissolved species | $D_{e,i}/D_{e,HTO}\cdot D_{0,HTO}/D_{0,i}$ |
|---|---|
| Anions | <1 |
| HTO or HDO | = 1 |
| Cations | >1 |

Within the scope of such a concept, Fick's first law, shown in Equation 20, can be expanded to expressions such as

$$\boldsymbol{J} = -\boldsymbol{D_e}\frac{\partial \boldsymbol{C_f}}{\partial \boldsymbol{x}} - \boldsymbol{D_s}\frac{\partial \boldsymbol{C_s}}{\partial \boldsymbol{x}} \quad (44)$$

where the subscript *f* denotes species in the bulk such as the ("free") aqueous phase, and *s* denotes the mobile surface species, with $D_s$ being the respective effective diffusion coefficient of these surface species; hence, the term "*surface diffusion*" was developed (a summary of quantitative expressions related to $D_s$ from key references can be found in (Maes et al., 2017a; Maes et al., 2017b)). Depending on the particular characteristics of a given case, it is possible to simplify Equation 24, viz. by assuming (i) that either one of the terms on the right-hand side of Equation 24 can be neglected and (ii) by replacing the concentration of the sorbed species by using well-known thermodynamic equilibrium expressions between $C_s$ and $C_f$. A few examples from the literature are mentioned in the following sections. Experimental evidence for the validity of expressions such as Equation 24 had already been found many decades ago (e.g., (van Schaik et al., 1966)).

Glaus et al. (2007) showed that the diffusion across the bulk aqueous phase of cationic species bound to a clay mineral surface via cation exchange (e.g., $Na^+$ and $Sr^{2+}$) in compacted montmorillonite was negligible, and diffusion was dominated by cationic species present in the cation-exchange sites. Cation-exchange selectivity according to the Gaines–Thomas convention was used to relate $C_s$ and $C_f$. The diffusion of cationic species across compacted montmorillonite was, thus, described using the assumption of clay porosity being represented as a single phase. The same approach was applied by Birgersson and Karnland (2009), who used an electrostatic Donnan-type distribution between the clay phase and the bulk aqueous phase to describe the chemical equilibration of differently charged species. These authors could successfully describe the diffusive behavior of negatively and positively charged species in compacted smectite minerals and bentonites.

Gimmi and Kosakowski (2011) compiled a broad collection of literature data for the diffusion of cationic species in clay minerals, clay rocks, and argillaceous soils. They used a relationship, derived from Equation 24, between observed $D_e$ values and pertinent $R_d$ (or $K_d$) values to evaluate $D_s$ values. Therefore, they could demonstrate that the resulting $D_s$ values comprised rather limited parameter ranges for the cationic species tested in their study, confirming that Equation 24 is generically applicable.

All these studies were, however, mainly related to cationic species interacting with clay surfaces via cation exchange or via electrostatic interactions. Many representatives from the transition-metal and lanthanide or actinide series were shown to form strong surface complexes via chemical bonding with surface groups present at the so-called edge surfaces of clay minerals. Owing to the presumed covalent character of this type of surface bonding, it is hardly expected that such complexes exhibit an appreciable surface mobility. Recent studies by Glaus et al. (2015a), Glaus et al. (2020), Montoya et al. (2018), and Altmann et al. (2015), who investigated the diffusion of $Co^{2+}$, $Zn^{2+}$, $Eu^{3+}$, and $Cs^+$ in compacted illite as a function of a broad variety of solution parameters, such as pH, ionic strength, or the concentration of the respective stable isotope elements, also gave evidence for surface diffusion phenomena being active in the case of these cations. Significantly larger $D_e$ values were indeed observed for these elements than could be expected from direct proportionalities with the corresponding $D_0$ values of an uncharged reference species. It was demonstrated that the characteristic parameter dependencies of the $D_e$ values were not related to the formation of surface complexes at the clay edge surfaces but rather to the species bound to planar surfaces. As an example (Glaus et al., 2015a), the diffusion depths in compacted illite of bi-valent transition metals significantly increased with decreasing ionic strength, while the total concentrations of these metals in clay at the interface between the clay and solutions were almost identical for all ionic strengths. This was a clear indication that the $D_e$ values were affected by the variation of ionic strength, rather by than sorption. It is well known that the uptake processes of cations at planar surfaces are susceptible to variations in the ionic strength, while the formation of surface complexes at edge surfaces is much less dependent on ionic strength (e.g., Bradbury and Baeyens, 2005b). It was further demonstrated that the $R_d$ values derived from diffusion experiments exhibited the same parameter dependencies as those measured in static batch sorption experiments, in which the tracer distribution between a liquid and the clay phase was measured using dilute clay suspensions.

In contrast to the very small pore sizes of smectites (order of 1 nm), the pore sizes of compacted illite may be larger by a factor of approximately 5–10 (Sanchez et al., 2008), and the planar surfaces may, thus, be in contact with bulk-type water. The distribution of charged species near such charged surfaces is frequently described using the concept of an EDL (Figure 4).

The neutralization of negative surface charges occurs via two different types of cationic species. The first type is located directly at the clay surface and is assumed to be bound as an inner-sphere complex; thus, it is considered as immobile. These surface species are frequently referred to as Stern layer species. The second type is a diffuse swarm of cations, near the surface, and assumed to be mobile. Anions, accompanied by an excess of diffuse swarm cations, may also enter the EDL domain to a reduced extent. Depending on the charge density of the solid phase and various solution parameters, cationic species are, thus, enriched in EDLs compared to their concentrations in bulk aqueous phase. If a concentration gradient parallel to planar surfaces exists, the diffusive flux of cationic species in a charged clay will, thus, be larger compared to that in uncharged clay, owing to the higher population of cations in the EDL and the resulting larger concentration gradients parallel to the clay surface. Similar to cation exchange in the interlayers of smectites, the unexpectedly large fluxes of transition metal cations can be understood as an enrichment phenomenon at the planar illite surfaces.

For quantitative purposes and for simplifying the numerical procedures for diffusion calculations, the Donnan approach has been proposed to represent the local distribution of the electrical potential near planar surfaces (Appelo et al., 2010; Appelo and Wersin, 2007; Altmann et al., 2015; Glaus et al., 2015a; Glaus et al., 2020; Gimmi and Alt-Epping, 2018). Figure 4 shows a schematic representation of the equilibrium distribution of cationic and anionic species between free pore water and EDL water for a Donnan approach using a parallel clay pore geometry.

Similarly, this concept was used for a circular pore geometry (Glaus et al., 2015a; Glaus et al., 2020). Notably, the choice of the

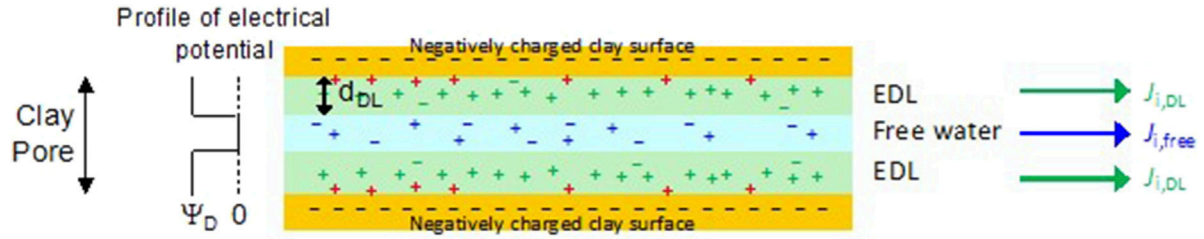


FIGURE 4
Schematic representation of the Donnan approach for an electrical double layer (EDL) at planar clay surfaces. Species in blue (ions in free water) and green (ion swarm in the Donnan volume) are assumed to be mobile, while red cationic species are present as immobile surface complexes in the Stern layer. If a concentration difference of a tracer cation species between the left and right side of a clay is present, the individual flux contributions ($J_i$) would result from the local concentration gradients parallel to the clay surface in the different domains.

model geometry is a rather arbitrary and an uncritical decision. In the Donnan approach, the extension of an EDL is finitely defined by the Donnan thickness, $d_{DL}$, exhibiting a constant potential (the Donnan potential, $\psi_D$) across the Donnan volume. The equilibrium distribution of cationic and anionic species between free pore water and water in the Donnan volume is governed by $\psi_D$, which is basically derived from the electrical potential at the surface, taking into account the shielding effect of cations in the Stern layer. $\psi_D$ and $d_{DL}$ are adjustable parameters in this model.

The total flux for each species $i$ ($J_{tot,i}$) is the sum of the fluxes in the free pore water ($J_{free,i}$) and the Donnan layer ($J_{DL,i}$) (Appelo et al., 2010; Altmann et al., 2015; Glaus et al., 2015a) (in the case of smectite-type clays with accessible interlayers, an extra flux, $J_{IL}$, is present and needs to be added to the total flux:

$J_{IL,i} = -f_{IL}\eta G_{IL}\frac{C_{IL,CEC}}{z_i}\frac{\partial\beta_i}{\partial x}D_0$, where $\beta_i$ is the molar or equivalent fraction, and $C_{IL,CEC}$ is the CEC expressed in interlayer water (mol/L), Appelo et al., 2010):

$$J_{free,i} = -f_{free}\eta G\frac{\partial C_i}{\partial x}D_0 \tag{45}$$

$$J_{DL,i} = -f_{DL}\eta G\frac{C_{DL,i}}{C_i}q_n\frac{\partial C_i}{\partial x}D_0 \tag{46}$$

$$J_{tot,i} = -\eta G\left(f_{free} + f_{DL}\frac{C_{DL,i}}{C_i}q_n\right)\frac{\partial C_i}{\partial x}D_0 = -D_{e,i}\frac{\partial C_i}{\partial x} \tag{47}$$

According to the assumed mobility of the cationic species (bulk aqueous and diffuse layer species are mobile; Stern layer species are immobile), the $D_{e,i}$ values for the situation depicted in Figure 4 were calculated as follows:

$$D_{e,i} = \eta G\left(f_{free} + f_{DL}\frac{C_{DL,i}}{C_i}q_n\right) \tag{48}$$

where $\eta$ [−] is the total water-accessible porosity, $G$ [−] is the geometry factor, $f_{free}$ [−] is the porosity fraction containing free pore water, $f_{DL}$ [−] is the fraction of the Donnan layer porosity, $D_0$ [$m^2$/s] is the diffusion coefficient in bulk water, and $q_n$ [−] is the viscosity factor. The ratio $c_{DL}/c$ represents the concentration ratio of cationic species between the diffuse layer and the bulk aqueous phase. $q_n$ reflects changes in the surface mobility compared to the mobility in the bulk pore aqueous phase. The application of expressions such as Equation 28 in transport models is limited to situations in which the various parameters are independent at concentration $c$. This can reasonably be assumed to be the case in many examples of tracer diffusion in electrolyte media.

Within the concepts of such electrostatic approaches for the description of surface uptake reactions and diffusion processes, not only the behavior of counter-ions, but also those of the co-ions (anions, in the case of negatively charged clay surfaces), are implicitly included. A valuable overview of different models used to describe the behavior of anions in charged clays can be found in Tournassat and Appelo (2011). The picture shown in Figure 4 should not be confused with the anion exclusion concept, in which an assumption is made that part of the porosity is completely inaccessible to anions (e.g., Van Loon et al., 2007). The volume fraction of free pore water in the Donnan approach is always larger than the equivalent exclusion volume in the latter approach. The results of both approaches can, however, be mutually converted for the purpose of comparison.

The description of the diffusion of charged species in charged porous argillaceous media may, thus, be based on the use of lump-defined effective diffusion coefficients, comprising the characteristic geometric properties of the porous medium and the presence of multiple chemical concentration gradients, despite the comprehension that it may actually be the result of the superposition of the diffusion of individual chemical species in multiple phases. Because the local concentration gradients of these species cannot always be measured using experimental methods, the use of thermodynamic equilibrium models for the description of lump-defined effective diffusion coefficients is indispensable for this purpose. Currently, reactive transport codes as PHREEQC (Appelo and Wersin, 2007), CRUNCHFLOW (Steefel and Tournassat, 2021), ORCHESTRA (Jenni et al., 2021), and FLOTRAN (Krejci et al., 2021) have implemented double layer effects on diffusion in their codes, using different approaches for the spatial dependence of surface potential. Evidently, the diffusion model represented in Equation 28 uses an idealized picture of the chemical species and equilibria involved. This also applies for assumptions regarding geometry. The model does not describe the effects of the orientation of clay particles with respect to the direction of diffusion. In the idealized picture, the concentration gradients responsible for tracer diffusion are assumed to be parallel to the clay surfaces, while the respective concentration gradients perpendicular to the surface determine the chemical species equilibration at those surfaces and, thus, the chemical enrichment or depletion factors.

A broad variety of influencing factors have an effect on the parenthetical expression in Equation 28. These can be roughly subdivided into factors affecting geometric aspects and those affecting the chemical effects of a model. Among the latter, the composition of an aqueous solution in equilibrium with the clay phase may have a direct influence on the ratio of concentration in the diffuse layer and in the bulk aqueous phase ($c_{DL,i}/c_i$). For example, it has been demonstrated that the electrolyte concentration, the presence of other metal cations competing with the cation of interest, or pH may directly affect this distribution ratio (Glaus et al., 2015a; Glaus et al., 2020; Glaus et al., 2021; Glaus et al., 2015b; Glaus et al., 2020; Glaus et al., 2021). A recent study within the frame of the EURAD WP 5 FUTURE work package has further shown that the cationic composition of a clay surface produces similar effects. The effective diffusivity of transition-metal cations, such as $Co^{2+}$ and $Zn^{2+}$, depends distinctly on the cation loading, in compacted illite, with the highest diffusivities being measured for Li- and Na-illite, while the K- and Cs-illite forms show lower values (contribution of Zerva et al. in (Maes et al., 2024)). This behavior can be interpreted in terms of a different shielding of the fixed negative lattice charges, which leads to different electrostatic effects related to changes in the extension of an electrical double layer.

Alternative assumptions for the equilibrium distribution of cations between the diffuse layer and the bulk aqueous phase can be made, such as a Poisson-type distribution instead of a discrete Donnan-type distribution. Such assumptions result in similar diffusion models (cf. e.g. (Ochs et al., 2001; Tachi and Yotsuji, 2014)). Furthermore, it has been suggested that Stern layer species may exhibit surface diffusion effects (Krejci et al., 2021; Krejci et al., 2023).The various ambiguities in the model assumptions can only be resolved to a limited extent by macroscopic diffusion experiments. Ambiguities remain, for instance, with respect to the individual species concentrations and their molecular mobilities. More elaborated methods, such as spectroscopic, diffractive, and microscopic techniques (e.g., Strawn and Sparks, 1999; Bostick et al., 2002; Park et al., 2008; Malikova et al., 2010; Ferrage, 2016) are required to bound critical model assumptions. This is also the case for the use of atomistic simulation methods, which can give further insights into the detailed structural characteristics and processes related to the surface reactivity of clays (Kosakowski et al., 2008; Cygan et al., 2009; Bourg et al., 2017; Bourg and Sposito, 2010; Churakov and Gimmi, 2011; Holmboe and Bourg, 2014; Tinnacher et al., 2016; Tournassat et al., 2016a; Churakov, 2013; Gimmi and Churakov, 2019).

The broad variety of model concepts for describing the dynamics of diffusive transport processes in clay minerals and clay rocks render the definition of an effective diffusion coefficient increasingly more complex. In fact, a variety of different terminologies can be found in the literature, for the exact definition of effective diffusion coefficients, which sometimes makes it difficult to compare the results of individual works. Valuable attempts to provide an overview of this situation can, however, also be found in the literature (e.g., Shackelford and Daniel, 1991; Shackelford and Moore, 2013). Despite the "unphysical" nature of such coefficients, they are frequently applied for engineering purposes, because concentration gradients in the bulk aqueous phase are the only sound basis for transport simulations. In order to attain an improved process-based understanding of the diffusion of charged species in charged porous argillaceous media, it is, however, imperative to improve the physical basis of the understanding of surface-induced diffusion phenomena.

#### 3.2.2.4 Effect of particle size and orientation on diffusion

Clay mineral particles exhibit an anisometric shape associated with a wide size range (from tens of namometers to tens of micrometers).

Regarding the influence of particle size on diffusion properties, decreasing the particle size leads to an increase in the ratio between external (basal and lateral surfaces) and internal (interlayer) surfaces (Reinholdt et al., 2013). For non-swelling clay minerals, a decrease in particle size, in turn, leads to an increase in double layer effects (cf. 3.2.2.3), which affects the diffusion properties of cationic and anionic species. For swelling low-charged clay minerals such as smectite, this effect can be enhanced by the osmotic swelling of particles and the partial or total delamination of individual smectite layers, depending on the ionic strength and interlayer cation type. In this case, low ionic strength values and monovalent interlayer cations can promote the osmotic swelling process, leading to an increase in the Donnan volumes associated with anion exclusion and an increase in the retardation process for cation diffusion (cf. 3.2.2.3). In the specific case of water diffusion, the role played by external surfaces of clay particles on the overall diffusion process is limited, in line with the limited and very local influence of the electrostatic force between clay interfaces and water molecules (Bourg and Sposito, 2011). Indeed, Tertre et al. (2018) (among others) showed similar effective diffusion coefficients for water for porous media with the same porosity and made of uncharged kaolinite or charged illite clay particles. Furthermore, these authors demonstrated the crucial role of the osmotic swelling process in the water diffusion of swelling clay materials. In the case of porous media made of highly charged swelling vermiculite particles, without osmotic swelling, the effective diffusion coefficients, $D_e$, for water were similar to those obtained for porous media made of kaolinite or illite particles at a given interparticle porosity, irrespective of the particle size fractions used (i.e., 0.1–0.2, 1–2, or 10–20 μm). In the specific case of vermiculite samples, reductions in the water molecule mobility in interlayer spaces have, thus, been considered as dead volume for overall water diffusion and confirmed using various simulation approaches (Tyagi et al., 2013; Asaad et al., 2021; Ferrage et al., 2023). Furthermore, the situation is very different in porous media made of low-charge smectite, which exhibit osmotic swelling, for which the definition of internal (interlayer) and external (surface-related) surfaces becomes rather vague. In this case, the swelling of interlayer volumes, occupying a large part or all of the pore space, coupled with a reduction in interlayer water mobilities, generally leads to an overall decrease in the effective water diffusion coefficient (Bourg and Tournassat, 2015).

Owing to the anisometric particle shapes of clay minerals (Asaad et al., 2022; Bardot et al., 1998; Reinholdt et al., 2013; Tournassat et al., 2003; Sayed Hassan et al., 2006)), their mutual arrangement in porous media is most often associated with the development of anisotropy in pore network organizations. This effect most often leads to contrasting diffusion properties between the normal and in-

plane directions of compaction in clay-rich systems such as claystones (Gimmi et al., 2014; Robinet et al., 2012; Tyagi et al., 2013; Van Loon et al., 2004a; Wenk et al., 2008), although part of this diffusion anisotropy can also be related to the presence of elongated non-clay particles (Robinet et al., 2012; Tyagi et al., 2013). The preferred orientation of particles can be quantified by the order parameter ⟨P_2 ⟩, by analyzing the intensity distribution on a 2D X-ray scattering pattern collected on a slice of hardened samples. This parameter is quite convenient, as it adopts a value of 0 for an isotropic organization, and one when all particles are perfectly oriented relative to each other. Furthermore, Dabat et al. (2019) showed that a single orientation distribution function was associated with a given ⟨P_2 ⟩ value. In the recent literature, the quantitative influence of the preferred orientation of clay particles on water diffusion has been clearly demonstrated for a large number of samples composed only of clay minerals (Dabat et al., 2020; Ferrage et al., 2023; Tyagi et al., 2013). For example, Ferrage et al. (2023) showed that a change in the preferred particle orientation from ⟨P_2 ⟩ = 0 (isotropic organization) to ⟨P_2 ⟩ = 1 (perfect anisotropic organization) had the same effect on water $D_e$ values normal to the bedding as a decrease in interparticle porosity from 0.4 to 0.15. In addition, the ratio between the effective water diffusion coefficient measured in-plane and along the normal direction to the bedding ($D_e(xy)/D_ez$) ranged between one for ⟨P_2 ⟩ = 0 and approximately five for ⟨P_2 ⟩ = 1, further evidencing the primary role played by preferred orientations of clay particles on the diffusional properties of water and, likely, cationic or anionic species.

#### 3.2.2.5 Impact of water partial saturated conditions on radionuclide transport

There are many situations in which clay-rich porous media can be partially water-saturated. The generation of hydrogen due to the corrosion of canisters may dehydrate host rocks and engineered barriers made of swelling clay materials for more than 100 000 years in deep-geological-waste disposal facilities (ANDRA, 2016; Marschall et al., 2005). Additionally, clay liners placed above the groundwater table are generally unsaturated, especially for landfills located in arid environments (Katsumi et al., 2001). Owing to the $CO_2$ intrusion into caprocks in carbon geosequestration, caprocks can also be partially water saturated (Minardi et al., 2021; Xiao et al., 2020). In these cases, understanding and parameterizing diffusion processes under partially saturated media are required to evaluate the performance of a clay system and support engineering purposes. This is a challenging task, as illustrated by the fact that only a few reports exist in the literature. For instance, Nunn et al. (2018) presented a new method of using X-ray radiography and iodide tracers for quantifying the degree of partial saturation for shale samples and measuring effective diffusion coefficients ($D_e$) for tracers under such conditions. They showed that the $D_e$ value of iodide decreased by approximately 22% when saturation decreased from 100 wt% to 93.3 wt%.

The diffusion and advective transport of gaseous species, and the effect of saturation on the diffusion of water and cations, was investigated using MD simulation. The simulations showed that surface adsorbed water films provide an important contribution for solute and water transport, even at a low partial water pressure (Owusu et al., 2023; Owusu et al., 2022; Churakov, 2013).

Savoye et al. developed a novel approach to perform diffusion experiments under partially water-saturated conditions in illite–sand mixtures (Savoye et al., 2014) and in Callovo-Oxfordian claystones, intended to host a French disposal facility for high- and intermediate-level long-lived radioactive wastes (Savoye et al., 2012c; Savoye et al., 2010; Savoye et al., 2017). An osmotic method was used to control the partially saturated conditions of the clayey samples over the duration of diffusion experiments. They observed in Callovo-Oxfordian claystones a sharp drop in the $D_e$ values for HTO, $^{125}I^-$, and $^{22}Na^+$ by factors of 6, 50, and 17, respectively, under conditions of 81% water saturation, compared to the values under full-saturation conditions. The strong decrease in $D_e$ for iodide was explained by the anion exclusion phenomenon that restricted iodide to the largest pores, where dehydration was more pronounced. Nevertheless, the distinct behavior of $D_e$ evolution for HTO and sodium remained speculative. Two different processes, for which the relative contributions require further investigation, were proposed. On the one hand, the extent of surface diffusion may be attenuated when dehydration occurs in claystones, reducing the enhanced diffusion phenomenon for cation species (Savoye et al., 2012a)). On the other hand, in addition to HTO diffusing in the liquid phase, HTO diffusing in the vapor form may contribute to the relatively high (compared to that of sodium) HTO diffusive rate, even at 81% water saturation (Savoye et al., 2017). This latter process had already been proposed by Smiles et al. (1995) and, more recently, by Maples et al. (2013), to explain the anomalously widespread distribution of HTO in layers adjacent to low-level radioactive waste burial facilities.

More recently, the same type of investigation was performed in compacted kaolinite, known to be a very weakly surface-charged clay mineral (Wang et al., 2022), in order to estimate the role played by the vapor phase in water diffusion. The results indicated that, from a degree of water saturation of 100% down to 67%, the decrease in the diffusive flux of water in kaolinite was smaller than that observed for anionic and cationic tracers (iodide and sodium) that behaved in the same manner. Based on previous results, a conceptual and numerical model was developed for describing the macroscopic diffusion of water tracers in both liquid and gas phases, in order to induce a decrease of a factor of seven from 100% down to 67% of the diffusive flux. The diffusion of water through both liquid and vapor phases explains why water tracers diffuse faster than ions that only move through the liquid phase.

However, for more complex systems made of surface-charged clay minerals, even though MD showed that surface effects can be enhanced when saturation decreases (Churakov, 2013; Le Crom et al., 2022), the understanding of the evolution of enhanced diffusion phenomena for cation species when dehydrating is still limited. This issue needs to be addressed using simpler clayey media than argillaceous rocks such as compacted illite or vermiculite.

García-Gutiérrez et al. (2023) used the Instant Planar Source method (in this report, referred to as the back-to-back method, described in Section 3.2.3.1.1) to study the diffusion of HTO, $^{36}Cl$, and $^{75}Se$ in partially saturated recompacted Callovo-Oxfordian Clay and Spanish Lutite. Upon decreasing the water saturation level from 100% to 60%, they noted a decrease in the apparent diffusion coefficient for the studied radionuclides, showing that, by lowering the saturation, transport becomes hindered.

### 3.2.3 Research methods to extract transport parameters

Several types of migration experiments are used to investigate radionuclide transport in clays. The transport parameters that are extracted from these experiments, by solving the transport equation (Section 3.1) analytically or numerically for the correct initial and boundary conditions, are $D_a$, $D_e$, and the rock capacity factor $\eta R$ (porosity times retardation factor). It is worth noting that $D_a$ and $D_e$ are related as $D_e = \eta R D_a$.

Some decades ago, pioneers in the field described experimental methods and mathematical models for deriving diffusion parameters for application in nuclear waste disposal: Crank (1975), Put et al. (1991), Shackelford (1991), and Shackelford and Daniel (1991).

More recently, some publications with comprehensive overviews became available: Aertsens (2013), Bourg and Tournassat (2015), Van Loon et al. (2012).

In this section, the focus is on classical mass transfer experiments, as these apply, in principle, to all radionuclides of interest in the context of geological disposal, and they can provide direct information on the transport behavior of these radionuclides. Detailed insights into the local mobility of ions in different pores of clay materials can also be obtained using classical and *ab initio* MD simulations. These simulations are particularly useful for understanding the ion transport in narrow pores close to the negatively charged surfaces of clay particles, viz. DDLs (see Churakov and Prasianakis (2018) and references therein). There exists techniques based on NMR, neutron scattering, and electrical conductivity (e.g., impedance spectroscopy), which also provide important information on transport in porous media, but they require sophisticated equipment and data treatment and are only applicable to a limited set of "tracers." They mainly provide qualitative information on the transport mechanism, and less quantitative data on the tracer transport parameters. Further information on key references on these methods are available in papers by Bourg and Tournassat (2015) and Van Loon et al. (2012).

Mass transfer-based methods most widely used nowadays are summarized in the present section, highlighting recent developments.

Methods used to derive migration parameters in compact clay materials can be divided in two categories:

1) Transport via diffusion only (the concentration gradient is the only driving force),
2) Transport via a combination of diffusion and an extra flux component as result of a hydraulic or electrical driving force from percolation or electromigration experiments, respectively.

The methods described here are applied for laboratory experiments performed at the cm scale for compacted and fully saturated clay systems. These methods are detailed in Table 5.

#### 3.2.3.1 Category 1 – diffusion only

**3.2.3.1.1 Back-to-back diffusion.** This is the simplest form of a diffusion experiment, in which a trace amount (below the

TABLE 5 Summary of various laboratory techniques, based on mass transfer, for diffusion measurements (adapted from Van Loon et al. (2012), with permission from Elsevier).

| Technique | Features | Diffusion parameters | Suited for | Less suited for |
|---|---|---|---|---|
| Through-diffusion | Steady-state technique<br>Time consuming<br>Porous filters may be a problem | $D_e$ $\alpha = \eta R$ | Non and weakly sorbing tracers | Strongly sorbing tracers |
| Out-diffusion | Steady-state technique<br>Time consuming<br>Porous filters may be a problem | $D_e$ $\alpha = \eta R$ | Non and weakly sorbing tracers | Strongly sorbing tracers |
| In-diffusion<br>Controlled source | Transient technique<br>Relatively fast<br>Porous filters may be a problem | $D_e$ $\alpha = \eta R$ | All kind of tracers | |
| In-diffusion<br>No control on source | Transient technique<br>Relatively fast | $D_a$ | All kind of tracers | |
| Back-to-Back diffusion (BtB) | Transient technique<br>No problem with porous filters | $D_a$ | All kind of tracers | Strongly sorbing tracers (e.g., $Cs^+$) |
| Column migration experiment – Pulse injection | Additional hydraulic gradient<br>Clay cores can be conditioned with other pore waters<br>Porous filters may be a problem | $D^i_a \sim D_a$, $\alpha = \eta R$, $K$ | Non and weakly sorbing tracers | Strongly sorbing tracers |
| Column migration experiment – BtB | Additional hydraulic gradient<br>No problem with porous filters | $D^i_a \sim D_a$, *($\alpha = \eta R$ only for weakly retarded tracers), K, (solubility information)* | All kind of tracers | Strongly sorbing tracers (e.g., $Cs^+$) |
| Electromigration | Additional electrical gradient (acceleration)<br>No problem with porous filters<br>Provides information on the chemical speciation<br>Induces chemical changes in the system | $D_a$, *(ion mobility)* | Non, weak to moderately sorbing tracers | |

solubility limit) of a diffusing species (radionuclide previously conditioned to be at chemical equilibrium with a clay in the case of redox-sensitive elements to avoid precipitation and reactive transport) is spiked (either directly on the surface or by means of a saturated thin porous disk, which does not interact with the tracer) between two clay cores in a diffusion cell that confines the system (Figure 5A). In the absence of precipitation during transport, diffusion gives rise to a typical Gaussian-shaped tracer profile in the clay core. The diffusion profile is obtained by cutting the clay core into thin slices and measuring the concentration (or radioactivity) of the diffusing species in each slice. This is a simple technique, and there is direct contact between the diffusing species and the clay material (no disturbing influences from confining porous filters, see Section 3.2.3.3). This technique provides the value of the apparent diffusion coefficient ($D_a$) only.

Back-to-back diffusion is a technique of choice for strongly sorbing radionuclides with a simple chemistry, such as cesium ($Cs^+$). However, with redox-sensitive radionuclides (e.g., Se, Tc, U, Np, and Pu), a radionuclide must first be placed at thermodynamic equilibrium with a clay prior starting the diffusion experiments. This is particularly important when reducing conditions are prevailing in the clay. If a redox-sensitive element is introduced in its oxidized state, it will be reduced during transport and may precipitate. Under such an experimental setup, it is impossible to distinguish between sorption and precipitation, and modeling will lead to erroneous overestimated retardation factors ($R$).

**3.2.3.1.2 Through-diffusion.** This is probably the most widely used method to determine diffusion parameters. A clay core is confined in a diffusion cell between two porous filter plates connected to water compartments (Figure 5B). One compartment

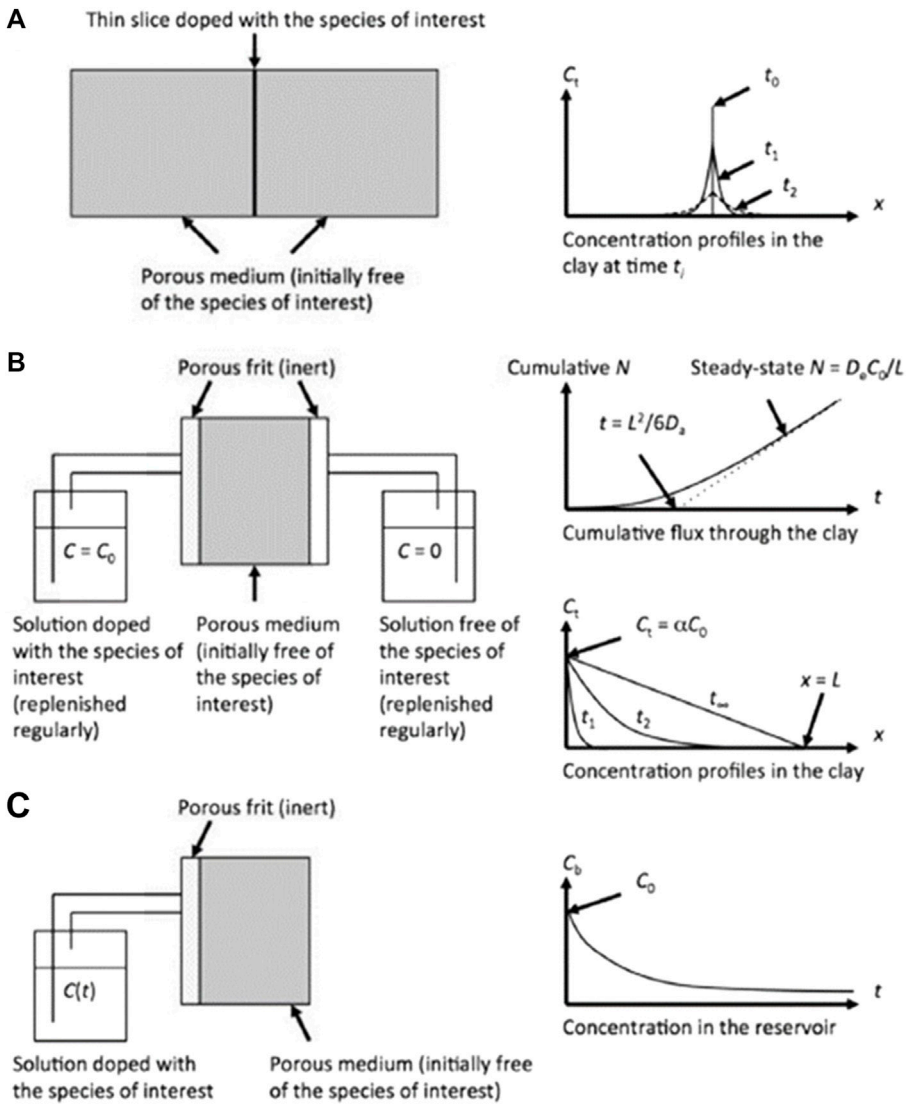


FIGURE 5
Schematic representation of different methods used to determine diffusion parameters of radionuclides in saturated porous materials where diffusion is the only transport mechanism. **(A)** Back-to-back diffusion, **(B)** through-Diffusion, **(C)** in-diffusion. Reprinted from *Bourg and Tournassat (2015)*, with permission from Elsevier.

contains diffusing species (high-concentration reservoir, upstream), whereas the other compartment is free of diffusing species (low-concentration reservoir, downstream). In these experiments, the flux arriving at the downstream compartment is monitored until a quasi steady-state flux regime has been attained. From the evolution of the flux with time, the effective diffusive coefficient ($D_e$) and the rock capacity factor (ηR, also called α) can be determined independently. As we have access to $\eta R$, these experiments can be linked to batch sorption experiments ($R$–$K_d$ relation Equation 24). In this technique, decreases in the concentration of the diffusing species in the upstream compartment can be monitored, as well as the concentration profile inside the clay (by post-mortem slicing, stated above). Related analysis of mass balance and observations of the concentrations within a clay sample can be used to crosscheck the results obtained for mass balance and internal consistency. Depending on the experimental conditions (Variable or Constant Concentrations in reservoirs), one defines different sub-types: CC-CC, VC-VC, VC-CC, and CC-VC (Takeda et al., 2008b; Takeda et al., 2008a; Aertsens et al., 2017). It is important to note that the mathematical models used to interpret measurements make use of the correct boundary conditions in line with the experiment, as this can lead to significant differences in the derived parameters. The use of porous filter materials in these experiments can play an important role in transport processes. This is not as important for non-sorbing tracers (anions or HTO), as long as the clay cores are sufficiently thick compared to the combined filter .thickness. However, porous filter materials were found to have a pronounced effect on sorbing tracers, either as an extra diffusion barrier (simple cations such as $Sr^{2+}$ or $Cs^{+}$, Glaus et al. (2015b); Aertsens et al. (2017)) or having a tendency to strongly sorb the diffusing species (transition metals, lanthanides, and actinides) (Altmann et al., 2015). Dierckx et al. (2000) demonstrated the strong sorption of $^{241}Am$ onto stainless-steel filters.

A through-diffusion (TD) experiment can be performed via out-diffusion (OD), which is a valuable technique used to crosscheck the results of the TD step. OD is measured after reaching the steady-state flux phase of a TD experiment. Both reservoirs are exchanged by solutions devoid of a diffusing species, viz. the concentration of the diffusing species is kept at an approximately zero level on both sides of a clay sample. OD can also be used to detect slow diffusion pathways. If the contributions of these pathways to the overall flux is only a small fraction (a few percents), the pathways cannot be directly revealed in a TD experiment. In an OD experiment, they will, however, become visible as two-phase flux behavior (Van Loon and Jakob, 2005). OD can also be used to reveal inconsistencies with respect to TD.

**3.2.3.1.3 In-diffusion.** The in-diffusion (ID) method can be considered a sub-type of TD experiments. The setup is similar (Figure 5C), but TD is intended to measure the flux going through an entire clay sample, while an ID experiment is not. For sorbing tracers, in particular, it may take extremely long for a tracer to diffuse. In this technique, a decrease in the tracer concentration in an upstream reservoir and the tracer profile in clay are determined, and the combination of this information provides information on the $D_e$ and ηR (Yaroshchuk and Van Loon, 2008). As with an TD experiment, the presence of a porous filter plate may have an important effect.

The ID method is also commonly applied for *in situ* tests of radionuclide transport (see Section 3.2.4); such tests include the DI, DI-A, DI-B, and DR *in situ* experiments in the Mont Terri Rock Laboratory, as well as the DIR *in situ* tests in Bure URL (overview in Van Loon et al. (2012); Gimmi et al. (2014); Leupin et al. (2017); Delay et al. (2007)). Post-mortem profile analysis is performed on a large clay core recovered by overcoring the borehole used to inject the tracer solution.

### 3.2.3.2 Category 2 – diffusion + extra driving force

In this category, an extra driving force is used to speed up the transport process. These driving forces are either a hydraulic gradient (diffusion–advection experiment) or an electric field (electromigration experiment).

**3.2.3.2.1 Column migration experiments applying a hydraulic gradient.** In these experiments, a clay core is confined in a migration cell connected at one side (inlet) with a water vessel that is at elevated pressure so that a hydraulic gradient can be applied (e.g., piston pump, HPLC pump, or pressurized water barrel). At the inlet, an HPLC injection valve is installed, from which a small pulse of tracer can be injected into the water stream in front of the clay core. This mimics a chromatographic column setup (Put et al., 1991) (Figure 6 top). At the other side of the clay core (outlet), water is collected as a function of time, and the amount of tracer flowing out is measured to obtain a breakthrough curve. Because of the presence of an additional hydraulic gradient, not an apparent diffusion coefficient but rather an apparent dispersion coefficient ($D_{disp,a} = D_a + aV_a$) can be obtained. However, as long as the advective term remains limited, the approximation of $D_{disp,a} \sim D_a$ applies. From the $V_{darcy}/V_a$ ration, information on the rock capacity factor $\alpha = \eta R$ can be derived. However, Aertsens et al. (2020) have recently shown that column migration experiments (percolation experiments or infiltration tests) do not provide a correct estimate (overestimation) of the diffusion-accessible porosity ($\eta$) of anions, compared to pure diffusive experiments (TD).

This kind of test is particularly interesting for non-sorbing (or slightly sorbing) tracers. When coupled with a manifold system, several experiments can be performed simultaneously, and successive tracer injections can be performed on the same clay core, if necessary (as no long OD is required) (Aertsens et al., 2003). This method is also useful for investigating the effect of changing chemical conditions, specifically different ionic strengths (Moors, 2005; Aertsens et al., 2009a) and the influence of an alkaline plume (ECOCLAYII, 2005; Wang et al., 2007) or a $NaNO_3$ plume (Bleyen et al., 2018), on transport in percolating water, by first analyzing the diffusion behavior pristine pore water, after which the water transforms into another type of water, followed by new tracer injections, all on the same core.

For sorbing tracers, breakthrough may not be reached even after many years, in which case the tracer profile determined on a clay core at the end of an experiment can provide information on the apparent diffusion coefficient, $D_a$, only. Similarly to the TD and ID tests, a porous filter and an injection loop may cause problems when working with strongly sorbing tracers, which often sorb onto materials (often 316 stainless steel) as well.

Again, it is necessary to emphasize the importance of the chemical speciation of redox-sensitive radionuclides at the start of a percolation experiment. If a radionuclide soluble under

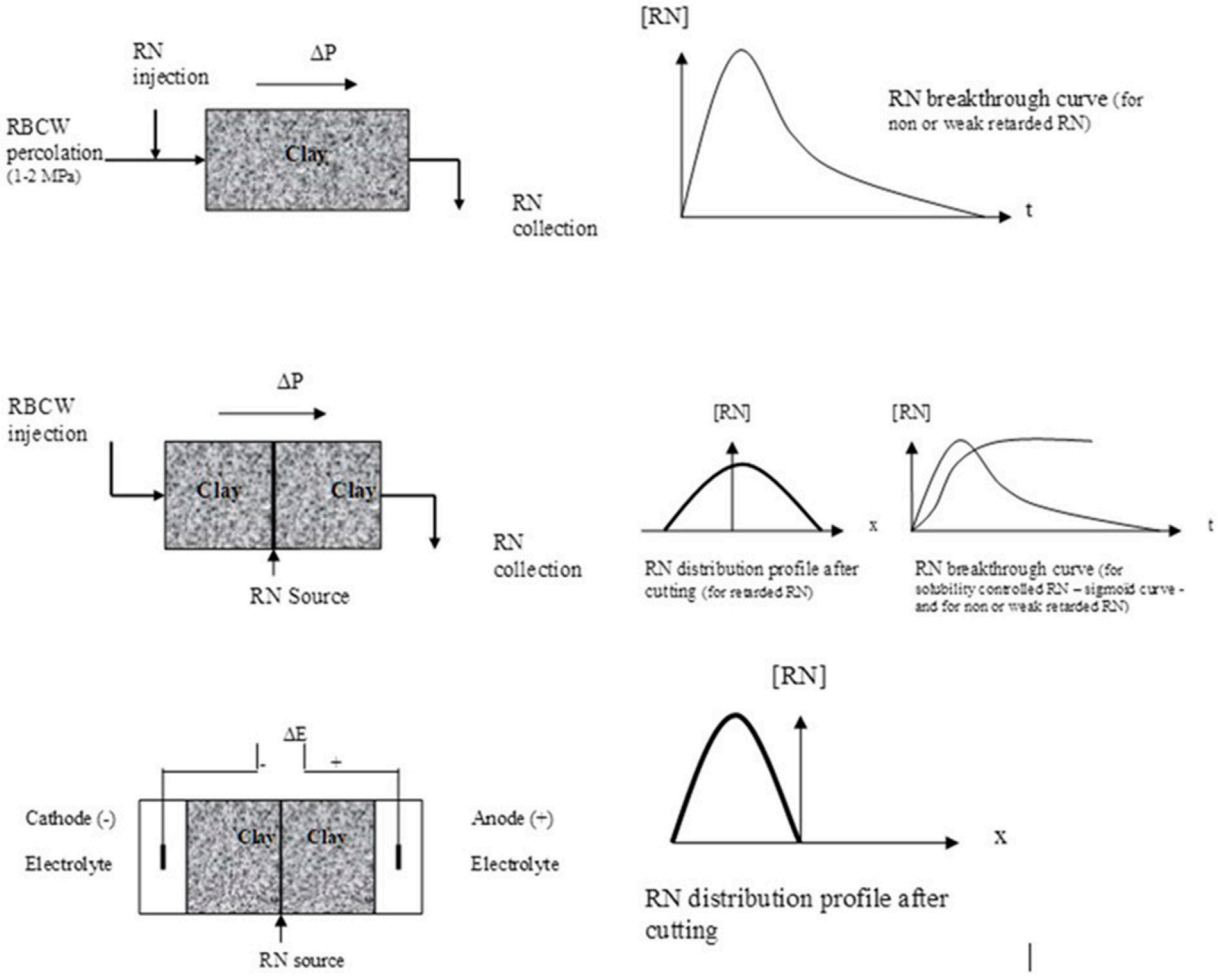


FIGURE 6
Illustration of migration experiments where an extra hydraulic or electrical gradient is applied to accelerate the transport of the radionuclide of interest. Top and middle: column migration experiments using an extra hydraulic gradient, bottom: electromigration experiment using an extra electrical gradient. Abbreviations: RN: radionuclide, RBCW: real Boom Clay water. (Figures reproduced from (Maes et al., 2004a) annex 14, with permission from SCK CEN).

oxidizing conditions (using radiotracers "as received") is progressively reduced during its transport in clay, it can precipitate if the solubility limit of its reduced species is exceeded. It is, therefore, essential to guarantee that redox-sensitive species are first at chemical equilibrium with a reducing clay before to start the experiment. Failing to properly achieve this chemical pre-equilibration step can lead to the reduction/precipitation of the redox-sensitive radionuclide during its transport, will make it difficult/impossible to derive quantitative transport parameters from it, or will cause wrong interpretation of the data.

In order to circumvent the problem of radionuclide sorption onto filters, the back-to-back configuration can be used and connected to a hydraulic gradient (Figure 6 middle). For non-sorbing or moderately sorbing tracers, a breakthrough curve can be determined. For strongly sorbing tracers, the clay core can be cut into thin slices and the radionuclide profile inside the clay can be determined to obtain $D_a$ without the problem of sorption on the filters. In these experiments one can also use a solid phase of the tracer in equilibrium with the pore water. In this case, one has a constant source (instead of a Dirac pulse) of the species controlled by the solubility.

**3.2.3.2.2 Electromigration.** By applying an external electrical field to both extremities of a cylindrical clay core confined in an appropriate cell, ions present in the clay pore water are forced to move towards the electrode of opposite charge (this phenomenon is called electromigration), which seriously accelerates their transport (Figure 6 bottom). The velocity with which a charged species moves is linearly proportional to the strength of the applied electrical field. The proportionality coefficient is the ionic mobility, which is related to the apparent diffusion coefficient ($D_a$) of the considered ion. As an effect of the moving cations, a water flow is also created, which is called electro-osmosis. The movement of water (osmosis) towards the cathode in the clay core is directly related to the movement of cations. This is because cations moving in the EDL close to the negatively charged clay surface drag the free water present in the pores and also because water in the hydration shell interacts stronger

with cations than with anions due to the smaller ionic radius of cations. Applying an electrical field to accelerate the transport is particularly interesting for strongly sorbing tracers. A method was developed by Maes et al. (1998), Maes et al. (1999), Maes et al. (2001), and Beauwens et al. (2005) to determine diffusion coefficients for radionuclides in Boom Clay. In addition to using the method in a quantitative way (determination of diffusion coefficients), it can also be used to obtain information on the speciation of the moving species (Maes et al., 2002; Maes et al., 2001) and the migration behavior (stability) of radionuclide–organic matter species/colloids (Maes et al., 2001; Maes et al., 2004b). This method was later on used and adapted for compacted clays (Higashihara et al., 2004; Tanaka et al., 2011) and for granitic rocks (Lofgren and Neretnieks (2006); Li et al. (2019b) see Section 3.3.3.2.2). Information on the apparent diffusion coefficient, $D_a$, is obtained by performing multiple experiments at varying electrical fields (E) (causing different electromigration velocities). Apparent dispersion coefficients are obtained for each electromigration velocity. To obtain $D_a$, the linear relationship of the determined dispersion coefficients as function of E is extrapolated to E =0.

Application of strong electrical fields to a clay core triggers significant heat release that may have an influence on the mobility of the diffusing species under investigation. Furthermore, it might disturb the clay core in unexpected ways, for example, electro-consolidation due to electro-osmosis.

### 3.2.3.3 Experimental challenges and technical solutions

As highlighted previously, when a compacted clay sample contacts solution reservoirs, porous filter plates are required in order to maintain the sample integrity related to the swelling behavior of clays. These porous filter plates can introduce artefacts, as they represent an additional diffusion barrier (2–3-mm thickness) specifically for TD and ID experiments, especially when thin clay slabs (5–10-mm thickness) are used (Suzuki et al., 2003; Glaus et al., 2015b; Glaus et al., 2008b; Aertsens et al., 2017). This can be accounted for in modeling, by explicitly considering the diffusion behavior of the filters. However, even when accounting for the filter behavior, there is increased uncertainty in the obtained data. Glaus et al. (2015b) designed so-called flushed filter cells in which the problem of the diffusion barrier, created by the filter, is strongly reduced. This design is based on the work of Jahnke and Radke (1989).

Furthermore, porous filter plates, typically made of fritted stainless steel (to withstand the swelling pressure developed by swelling clay) may exhibit strong sorption properties (especially for transition metals, lanthanides, and actinides at alkaline pH). In fact, any material, other than the clay, that is in contact with the tracer, such as tubing, water vessels, valves, and connectors, may exhibit sorption properties towards the diffusing species and, as such, affect the results of experiments. It is, therefore, advised to first test the sorption to the materials used. Other more "inert" materials such as PEEK, PTFE, and organic polymeric membranes may provide a solution to circumvent sorption (Glaus et al., 2015b). In some cases for clay rocks, it may be possible to avoid filters by using a very small specimen in direct contact with a tracer-containing solution (Van Loon and Muller, 2014).

Investigating the diffusion behavior of strongly sorbing tracers is further challenged by the limited travel distances, which means that experiments may need considerably long times (years) before a meaningful analysis can be performed. This entails that the chemical and physical conditions of experiments be kept stable during the entire period. Even then, the diffusion profiles that develop within clay often do not extend further than a few millimeters. Soft clays, such as Boom Clay and Ypresian Clay, and London Clay are easy to cut in slices of approximately 0.5–1 mm using a simple knife and a special cutting edge system equipped with a piston mounted on a screw to push the clay core out of the diffusion cell, and using a Palmer to precisely adapt the slice thickness. To enable a precise determination of the shorter diffusion profile in hard and brittle clays or argillites, a more sophisticated profiling technique is needed that goes into the sub-mm range. Van Loon and Eikenberg (2005) developed the abrasive peeling method. Savoye et al. (2013) have used micro-laser-induced breakdown spectroscopy to characterize concentration profiles at sub-mm scales. Rutherford backscattering spectroscopy (RBS), used by Alonso et al. (2009), is another spectroscopic technique and even considers lower scales (tens of nanometers). Moreover, laser ablation mass spectrometry (LA-MS) has been used (Wang et al., 2011; Wang et al., 2013). To study $UO_2^{2+}$ diffusion in Boda Claystone Formation, Czömpöly et al. (see contribution in (Maes et al., 2024)) used μ-XRF. A novel experimental method using TOF-SIMS was tested to investigate Pu diffusion in Opalinus Clay, by Johannes Gutenberg University (contribution of Breckheimer et al. in (Maes et al., 2024)). Glückman (2023) used accelerated mass spectroscopy (AMS) to investigate the diffusion of U(VI) and Am (III) in Opalinus Clay at ultra trace levels ($10^{-9}$ mol/m$^3$). These techniques are challenging (calibration, interpretation, sample pre-treatment, and range of application) and are not commonly available.

Linked to the limited penetration depths of diffusion profiles are the artefacts induced at the external surfaces of samples. Sample preparation (and storage) will inevitably create disturbances (physical and chemical) at external surfaces, which will be the first to contact the tracer. Furthermore, when placed in contact with water, by means of a porous filter, some swelling effects will occur, disturbing the clay surface in direct contact with the filter: clay particles may be pushed into the porous filter plates and water may locally soften the clay near the contact interface, resulting in an increased porosity and water content at the filter–clay interface. This will also change the porosity of the filter (clogging) and the properties of the first mm of the clay sample. This is very important when interpreting TD/ID experiments (Glaus et al., 2008b; Glaus et al., 2011).

In addition to experimental difficulties, there are also challenges on the modeling side. Nonetheless, the principles of diffusion are well known and accepted (Crank, 1975; Shackelford, 1991), and mathematical expressions have long been used to obtain parameters for a range of experimental conditions. It has become apparent that the number of experimental factors, which has been neglected before, has a significant effect on the derived parameters, especially for sorbing tracers. These factors include filters, the strict control of boundary conditions, and induced changes at the clay matrix at interfaces (e.g., mechanical disturbances and density and porosity changes due to clay hydration and swelling). Incorporation of all these possible influences into a consistent mathematical model has been proven to be challenging. Many TD studies (especially older studies) may provide data that were

not obtained using a correct mathematical description of the experimental conditions; as a result, the values of migration parameters are subject to large uncertainty.

Related to this is the consistency of data obtained from different types of experiments. Several studies (Aertsens et al. (2008a); Aertsens et al. (2009b); Aertsens et al. (2012) (Aertsens et al., 2020)) have indicated that different types of experiments (e.g., ID, TD, or column migration) do not always provide consistent transport parameters. Often, the derived $D_a$ is quite consistent, but not the values for the rock capacity factor $\alpha = \eta R$. This could, in part, be explained by experimental factors that have an important influence on the experimental results (filters in TD), the correct inclusion of the boundary conditions in a mathematical model, and flaws in the conceptual mathematical description of transport processes (Aertsens et al., 2020).

In support of the diffusion program for NAGRA's deep-drilling campaign in Switzerland (Van Loon et al., 2023), a cross-comparison study was setup between two labs (PSI & SCK CEN) to compare data obtained from TD experiments using HTO, $^{36}Cl^{-}$, and $^{22}Na^{+}$, based on a selection of "twin" samples taken from the Trüllikon1-1 borehole as part of confidence building in methodologies (Van Laer et al., 2023). For all three radionuclides, the variability in the effective diffusion coefficients, estimated independently by both institutes, was less than a factor two. Moreover, the parameter estimations of the capacity factor agreed well. The evaluation revealed that the minor deviations could be attributed predominantly to variations in temperature (experimental conditions) and, to a lesser extent, to minor distinctions in the modeling approach. It is important to acknowledge that local heterogeneity might have also contributed to these differences. The relatively small uncertainties within the methodological approaches provide confidence for application of diffusion parameters in radionuclide transport models.

Despite these efforts, the issue of consistency remained not fully resolved when comparing experimental data obtained from different methodologies, because there was always one important factor that could obscure the results: the nature of the samples. As these studies were performed using core material from natural clay rocks, there was the aspect of local heterogeneities that could influence the outcome. Therefore, a more dedicated study was setup by Durce et al. (2023), where different types of diffusion experiments with HTO and iodide (through diffusion, column migration, and back-to-back methods) were repeatedly performed on the same core plug (originating from Boom Clay cored at HADES URL, Mol, Belgium), hence excluding the heterogeneity aspect. A consistency study showed a good agreement in the apparent and effective diffusion coefficients and accessible porosity for HTO, which did not vary by factors of more than two and 1.6, respectively, between the three setups investigated, i.e., TD, column migration, and back-to-back experiments. On the other hand, the transport parameters obtained for iodide were shown to be more sensitive to the used experimental setup. In column migration (pulse injection, with advection) experiments, and at the scale of a few cm, the dispersion length cannot be neglected for iodide and needs to be known/assessed to extrapolate the diffusion coefficients. Column migration experiments also provide significantly higher accessible porosities than TD experiments, which confirms the findings of Aertsens et al. (2020), that this methodology is not appropriate for the determination of anion-accessible porosity. The cutting of cores and extrapolation of activity/concentration profiles in back-to-back experiments are practically more challenging, and experimental datasets display high scatter. Yet, overall, under the three experimental setups, the determined diffusion coefficients for iodide did not vary by a factor of more than three for the different samples and orientation investigated.

In experiments with redox-sensitive radionuclides (e.g., Se, Tc, U, Np, and Pu), one has to ensure that speciation is in chemical equilibrium with the reducing conditions prevailing *in situ* in the clay, before the start of migration experiments. Failing to pre-equilibrate a redox-sensitive element with clay prior to starting a diffusion test leads to considerable artefacts, making a quantitative analysis difficult/impossible.

### 3.2.4 Experimental approaches to upscaling

The mobility of ions in porous clay media depends on the electrostatic interactions in the DDL formed at the surface of negatively charged clay mineral particles and on complex coupled pore-scale transport phenomena controlled by the connectivity of pore spaces (Churakov and Prasianakis, 2018). In principle, the macroscopic mobility, such as that measured in laboratory experiments, can be obtained taking into account the local mobility of ions and the geometry of pore spaces. The local mobility of ions close to mineral surfaces has been extensively characterized using molecular simulations. Molecular simulations provide insights into the nature of the mineral–aqueous interface and allow for discriminating the effect of mean-field electrostatic interaction of ions with a surface, dynamic ion–ion correlation phenomena, and short-range steric effects at interfaces. On a larger scale, fluid transport will be mainly determined by the texture of a rock and connectivity of pore spaces. Pore-scale transport simulations are performed using stochastic methods (Random Walk and Brownian dynamics) and Lattice Boltzmann simulations techniques. One of the most critical parameters for pore-scale modeling is a realistic representation of the pore-scale geometry. While, larger sub-micrometer pores are accessible via computerized tomography (CT) measurements (Keller and Holzer, 2018), smaller nanometer-scale pores are envisaged using numerical modeling (Tyagi et al., 2013; Underwood and Bourg, 2020). Following the idea of a 'virtual rock laboratory,' several attempts have been made to merge atomistic and pore-scale simulations to explain observed experimental trends in water and ion transport as a function of compaction state, clay and pore water composition, and saturation degree. Simulation results have shown qualitative agreement with experimental observations (Churakov and Gimmi, 2011; Churakov et al., 2014a; Gimmi and Churakov, 2019).

The purpose of performing macroscopic diffusion/retention experiments is to obtain transport parameter values (and uncertainty ranges) that are relevant for the considered host formation to be used in safety assessment evaluations. This requires that the data obtained can be up-scaled with respect to time and space scales.

Laboratory diffusion experiments suffer from relatively short time scales and challenging sample preparation. Total confinement pressure release can result in decompaction and irreversible distortion of the geometric structure, which may have an impact on the transport properties. Moreover, sample preparation can

result in artefacts and alteration in the chemical environment (e.g., pyrite and clay oxidation, $CO_2$ degassing, or microbial perturbation), affecting the transport properties. Field experiments may, therefore, be seen as more realistic because tracer migration occurs, after a certain distance from a borehole, in a more or less virgin environment.

Microscopic phenomena determine the behavior of fluid dynamics in porous media. This makes the description of the pore geometry complex both at laboratory and field scales. To tackle flow and transport phenomena at relevant scales (much larger than the pore scale), mass and momentum balances at the pore scale are averaged over volumes or areas containing many pores, and they are considered as a continuum. This is related to the Representative Elementary Volume (REV).

For clays, the typical grain size of a particle measures several tens of micrometers (excluding larger inclusions such as pyrite and carbonate concretions, septaria, fossils, worm tunnels, sand lenses, and other local heterogeneities). The dimension of a REV is in the order of several millimeters. Consequently for natural clay samples, most experimental and modeling scales are larger than the dimensions of a REV. Upscaling does not require adapting hydraulic or transport parameters, as long as macroscopic heterogeneities remain limited (Marivoet et al., 2006).

Within safety evaluations, clay host formations are often considered homogeneous. However, at lower scales, heterogeneity certainly exists and may have important impact on transport parameters.

There are several ways to perform upscaling and to assess the impact of heterogeneities: large-scale tests (laboratory and *in situ*), natural tracer profiles, and laboratory diffusion/sorption tests on cores sampled over an entire stratigraphy.

Firstly, large-scale transport tests may be considered. These can be conducted in a laboratory using large blocks (up to several decimeters) or *in situ* URLs (several decimeters up to several meters). The latter experiments are an upscaling both in terms of time (tens of years) and distance (up to decimeters and even several meters). These tests mainly make use of conservative or weakly sorbing tracers in order to obtain measurable tracer profiles over sufficiently large distances still within reasonable time frames (several years to decades).

An example of a large-block experiment consists of large cylindrical drill cores where a radiotracer source is emplaced in a hole drilled at the center. After a given time, subcores are taken to determine the 3D spatial distribution of the tracers (this mimics an ID experiment where the profile in a clay is determined). These experiments provide information about the anisotropy of diffusion coefficients and can be compared to small-scale diffusion experiments. This kind of test was conducted on Opalinus Clay samples (García-Gutiérrez et al. (2006); Cormenzana et al. (2008) and Callovo-Oxfordian Clay (Cormenzana et al., 2008).

A first type of *in situ* diffusion experiment can be considered as an up-scaling of large-block experiments. In this *in situ* radial diffusion test, a borehole is drilled in a clay formation. A cylindrical filter screen is emplaced at the bottom of the borehole, enabling circulation of water that contains radiotracers. The borehole is sealed using a packer, an inflatable rubber element sealing the annular space between the down-hole equipment and the borehole wall. The radiotracers diffuse radially into the surrounding clay rock. After a given time, the experiment is ended, and the borehole is overcored. Subcoring of the part where the tracers were applied enables the determination of the 3D spatial distribution of the tracers. From the tracers' diffusion profiles in the clay rock, combined with the change in the relative concentration ($C/C_0$, where $C_0$ is the initial concentration) of the tracers in the reservoir solution as a function of time, the effective diffusion coefficient ($D_e$) and the rock capacity factor ($\alpha = \eta R$) can be calculated, accounting for anisotropy.

This type of experiment is always affected by a "skin" effect due to the excavation-disturbed zone (EDZ) that exists around the borehole (borehole-disturbed zone, BDZ). This may cause problems in the interpretation of data and is especially a problem for sorbing tracers, as their penetration depth remains limited even after several years. In general, these experimental tests still only provide information on a decimeter-scale distance limited to the overcoring dimensions. The overcoring method also represents a considerable technical challenge, and in the case of failure for unexpected reasons, all the information on the tracers' profile in the clay can be lost in a few minutes at the end of the experiment after several years of work (cf. cement water (CW) experiment at Mont Terri and two of the DIR experiments at Bure). Hence, there are intrinsic limitations related to upscaling in space and time.

This type of test has been conducted at the Mont Terri Rock laboratory on Opalinus Clay (https://www.mont-terri.ch) and includes the so-called DI and DR experiments, those at the Bure URL on Callovo-Oxfordian Clay (https://meusehautemarne.andra.fr), and the so-called DIR experiments (overview in Van Loon et al. (2012); Gimmi et al. (2014), (Van Loon et al., 2004b), Leupin et al. (2017), Delay et al. (2007), Soler et al. (2019)).

A second type of large-scale *in situ* diffusion experiment makes use of multi-filter piezometers. These tests are particularly applied in the HADES URL on Boom Clay (https://www.euridice.be), owing to its higher plasticity and porosity.

In these tests, a borehole is drilled using compressed air from an underground laboratory into the clay formation, and a stainless-steel cylindrical tube with a series of filter screens (multi-filter piezometer) at well-known distance (up to 0.5–1 m apart) is emplaced into the borehole. After convergence of the clay, the filters are in direct contact with Boom Clay because of its high plasticity, and no packer is needed to hydraulically isolate the different filter intervals. The filters are equipped with one, or sometimes two, stainless steel tubings leading to the gallery and allowing the injection/withdrawal (or recirculation in the case of two tubings) of water. In the injection filter (often the central filter), a radiotracer solution is injected/circulated, and at regular time intervals, water samples are taken from the adjacent filters. This enables the establishment of "break-through" curves for these tracers at different distances. An extension to this test is the emplacement of different multi-filters in a 3D configuration. This also enables sampling in the neighboring piezometer providing excellent 3D spatial information at a scale of several meters.

In Boom Clay, *in situ* diffusion tests do not significantly suffer from a BDZ, as the damaged clay skin around the filters is rapidly sealed by the fast convergence/creep of the plastic clay around the piezometer casing. As it is not intended to overcore, these piezometers which will remain in place, there is no time constraint, and the diffusion of conservative tracers (HTO and

$H^{14}CO_3^-$) develop over several meters without being affected by the already negligible BDZ. These tests have no end date and they continue to provide reliable data for several years/decades. Hence, these tests are very valuable with respect to upscaling to tens of years and up to several meters.

Examples of these tests in the HADES URL (Boom Clay) are the CP1, TRIBICARB, TRANCOM-R41 H/V, and MEGAS tests (Weetjens et al. (2011); Aertsens (2013); Aertsens et al. (2013); Martens et al. (2010); Weetjens et al. (2014) (Aertsens et al., 2023; Govaerts et al., 2023; Jacops et al., 2023)).

These *in situ* diffusion tests (CP1 and Tribicarb-3D) provide us with confidence that the migration of HTO and $H^{14}CO_3^-$ is correctly understood at the metric scale. Blind predictions at a large scale based on migration parameters obtained at the laboratory scale allow for the validation and verification of water flow and diffusion models. These experiments show that the applied models are consistent with our scientific understanding and adequately represent the relevant phenomena and interactions of conservative tracers at the scale of several meters (Weetjens et al. (2011); Weetjens et al. (2014) (Aertsens et al., 2023)).

At the clay-formation scale (several million years and a 100-m thickness), natural tracer profiles ($\delta^{18}O$, $\delta^2H$, He, Cl, Br, and I) provide valuable information regarding migration scenarios in natural systems and dominant transport processes. Despite the initial and boundary conditions not being well known, a careful analysis is useful to check for consistency with results and conclusions from studies at smaller scale. From natural profiles, we can better characterize the dominant transport processes (diffusion and advection) that have occurred during the burial period and may provide information on the effect of larger heterogeneities (distinct clay layers) and confirm the common up-scaling approach. Comprehensive overviews of studies on natural tracer profiles are given by Mazurek et al. (2009) and Mazurek et al. (2011) in the frame of their works performed for the ClayTrac project supported by the OECD/NEA Clay Club.

In order to evaluate the impact of heterogeneities (e.g., due to layering with regular alternation of silt and clay sediments, as observed in Boom Clay) on solute transport parameters, laboratory migration experiments can be conducted on a series of drill cores coming from boreholes drilled in the frame of site characterization campaigns. The general characteristics and microstructural features of a particular clay core can be related to experimentally determined transport parameters. In this way, the effect of heterogeneities on the general solute transport mechanisms can be evaluated. Examples of such studies for Boom Clay and Ypresian Clays include Aertsens et al. (2004), Aertsens et al. (2005a), Aertsens et al. (2005b), Aertsens et al. (2008b), Aertsens et al. (2010b), Aertsens et al. (2010a), Callovo-Oxfordian Clay by ANDRA (2018a), ANDRA (2018b), Descostes et al. (2008), Jacquier et al. (2013), Melkior et al. (2005), Robinet et al. (2012), and Van Loon et al. (2012), while studies for Opalinus Clay include Van Loon et al. (2012) and Van Loon (2014). More recently, a very extensive exploratory program by NAGRA to investigate the Mesozoic sedimentary sequence (comprising Opalinus Clay) of Northern Switzerland (nine deep boreholes (Mazurek et al., 2023)) was concluded. Part of the study comprised measuring the diffusion properties of HTO, $^{36}Cl^-$, and $^{22}Na^+$ in samples from all the different rock types across the lithostratigraphic profile of interest in order to assess the spatial distribution of the diffusion properties and to determine the degree of heterogeneity (Glaus et al., 2023; Van Laer et al., 2023; Van Loon et al., 2023). Additionally, the outcome of the study was used to identify correlations between rock properties (mineral composition and microfabric) and diffusion parameters.

The above methods are mainly applicable for conservative tracers (i.e., non-retarded) and weakly sorbing tracers. For radionuclides exhibiting strong interactions with certain mineral phases, small local variations in the clay composition (i.e., in the content of these mineral phases) may have a significant effect. Large-scale experiments for these strongly sorbing elements will not be very helpful because of their very limited diffusion distances even for very long time periods. For these elements, small-scale experiments studying the relationship between sorption and the mineralogical characteristics (variability) of clay formations will be much more relevant. Such experiments are useful for providing reliable uncertainties on the sorption distribution coefficient ($K_d$) values used in safety assessment studies (Bradbury and Baeyens, 2017). Examples of such studies are (Chen et al., 2014b) for Callovo-Oxfordian Clay, and Marques Fernandes et al. (2015) for other clay rocks.

### 3.2.5 Sources of transport data for clay host rocks

In this section, we will provide an extensive (but not complete) overview of available sources with respect to diffusion data obtained for some well-studied clay host rocks (Opalinus Clay, Callovo-Oxfordian argillite, Boom Clay, Toarcian Clay, and Boda Claystone) and single clay phases (e.g., bentonite, smectite, illite, and kaolinite).

#### 3.2.5.1 Opalinus Clay and adjacent overlying or underlying sedimentary formations

The PSI has been conducting diffusion studies on Opalinus Clay since 2000. The materials under investigation originate from different deep boreholes in Northern Switzerland, notably from the Benken borehole in the Zürcher Weinland (BE-DBH), and from the Mont Terri Rock Laboratory, where the Opalinus Clay Formation is horizontally accessible via the safety gallery of a motorway tunnel (Transjurane highway). Thus far, the diffusion of HTO, $D_2O$, $H_2{}^{18}O$, $^{36}Cl^-$, $^{125}I^-$, $^{125}IO_3^-$, $^{35}SO_4^{2-}$, $Br^-$, $^{22}Na^+$, $^{85}Sr^{2+}$, $^{134}Cs^+$, $^{60}Co^{2+}$ $^{65}Zn^{2+}$, and $^{152}Eu^{3+}$ has been investigated (Glaus et al., 2008a; Jakob et al., 2009; Leupin et al., 2017; Wu et al., 2009; Van Loon et al., 2003; Van Loon et al., 2004a; Van Loon et al., 2005a; Van Loon and Eikenberg, 2005; Van Loon et al., 2005b; Van Loon and Jakob, 2005; Van Loon, 2014; Van Loon and Mibus, 2015; Van Loon et al., 2018; Glückman, 2023; Maes et al., 2024). More recently, transport studies were reported for $^{233}U(VI)$ and $^{243}A.m.(III)$ (Glückman, 2023) and for $^{226}Ra^{2+}$ and $^{239}Pu(IV)$, as part of the EURAD WP5 FUTURE project (see respective the contributions of Brandt et al. and Breckheimer et al. in the final technical report (Maes et al., 2024)).

An extensive drilling campaign initiated by NAGRA in three study areas for the potential siting of a deep-geological repository for radioactive waste in sedimentary Mesozoic rocks of northern Switzerland (Mazurek et al., 2023) has provided a unique set of mineralogical, petrophysical, geophysical, and chemical data. Among these, the diffusion properties in terms of the effective

diffusion coefficients and rock capacity factors of HTO, $^{36}Cl^-$, and $^{22}Na^+$ were measured perpendicular to the bedding orientation in approximately 130 samples originating from a broad variety of clay-, carbonate-, and silicate-rich rock formations, including Opalinus Clay (Van Loon et al., 2023). The effective diffusion coefficients of non-charged HTO were modeled using empirical functions for porosity and geometry factors, depending on the total clay content, as the sole input variable. The chemical composition of pore water, which differed for the different study areas, had no impact on these empirical functions. In contrast, the diffusion behavior of charged tracer species depended on the pore water composition and showed the characteristic features of surface diffusion in the case of $^{22}Na^+$, and anion exclusion for $^{36}Cl^-$. The effective diffusion coefficients and rock capacity factors of these charged species were successfully modeled using an electrostatic approach realized in PhreeqC (Glaus et al., 2023), using again the total clay constant as the main input variable. Two studies (Glaus et al., 2023; Van Loon et al., 2023) were complemented by a cross-laboratory benchmark exercise (Van Laer et al., 2024; Van Laer et al., 2023) in which differences in experimental and modeling approaches were tested using five twin samples from each of the same drill cores.

Furthermore, Opalinus Clay is also used as a reference material in different international studies, such as Joseph et al. (2013), Savoye et al. (2012c), Wigger et al. (2018), Xiang et al. (2016).

#### 3.2.5.2 Boom Clay

SCK CEN has been studying diffusion in Boom Clay since 1978. The materials under investigation mainly originate from core material taken from the HADES URL in Mol (Belgium) and deep boreholes (e.g., Mol-1 borehole). Van Laer (2018) provides an overview of all long-term laboratory (Ra, Tc, Be, Ni, Zn, Pa, Zr, Am, Cm, Pu, U, Np, Pa, and NOM) and *in situ* (HTO, $HCO_3^-$, NOM, Am, and Tc) migration experiments on Boom Clay. HTO, $I^-$, and $HCO_3^-$ were used to investigate thee variability over an entire host formation using drill core samples (Aertsens et al., 2004; Aertsens et al., 2005a; Aertsens et al., 2008b; Aertsens et al., 2010b; Aertsens et al., 2010a). Transport of Dissolved Organic Matter (DOM) is of particular interest in Boom Clay (Dierckx et al., 2000; Maes et al., 2006; Maes et al., 2011; Durce et al., 2018; Maes et al., 2004b), as it may act both as a vector and a sink for radionuclides.

Moreover, the diffusion of dissolved gases ($H_2$, He, Ne, Ar, $CH_4$, and $C_2H_6$) has been extensively studied by Jacops et al. (2017b) and Jacops et al. (2017a). Dedicated compilation reports ("Topical reports") are available that describe the current phenomenological understanding of the transport behavior of so-called reference elements in Boom Clay, based on the available sorption and diffusion experiments conducted: HTO (Bruggeman et al., 2017c), I (Bruggeman et al., 2017a), $Sr^{2+}$ (Maes et al., 2017b), $Cs^+$ (Maes et al., 2017a), Se (De Canniere et al., 2010), Tc (Bruggeman et al., 2017b), $Am^{3+}$ (Bruggeman et al., 2017d), U (Salah et al., 2017), and an overview report (Bruggeman and Maes, 2017).

#### 3.2.5.3 Callovo-Oxfordian Clay

Different laboratories have performed diffusion experiments on Callovo-Oxfordian Clay and Oxfordian limestone. The following elements have been studied: HTO, $Cl^-$, $I^-$, $SO_4^{2-}$, $SeO_3^{2-}$, $Li^+$, $Na^+$, $K^+$, $Rb^+$, $Cs^+$, $Zn^{2+}$, $Eu^{3+}$, organic anions, and polymaleic acid (Bazer-Bachi et al., 2006; Melkior et al., 2007; Durce et al., 2014; Dagnelie et al., 2018; ANDRA, 2018a; ANDRA, 2018b; Bazer-Bachi et al., 2007; Descostes et al., 2008; Jacquier et al., 2013; Melkior et al., 2005; Menut et al., 2006; Savoye et al., 2012b; Savoye et al., 2013; Savoye et al., 2015).

Furthermore, for partially saturated conditions of Callovo-Oxfordian Clay, diffusion experiments were performed using HTO, $Cl^-$, $I^-$, $Na^+$, and $Cs^+$ (Savoye et al., 2010; Savoye et al., 2012a; Savoye et al., 2014; Savoye et al., 2017).

In the context of the European Project EURAD WP5-FUTURE, new data from transport studies on samples of Callovo-Oxfordian argillite became available for selenite, $Ra^{2+}$, and $Ba^{2+}$, and they were complemented with sorption data (see contributions of Garcia-Guttierrez et al. in the final technical report of the project (Maes et al., 2024)).

#### 3.2.5.4 Toarcian Clay

Diffusion experiments using HTO, $Cl^-$, and $I^-$ on the Toarcian argillite from Tournemire are reported in studies by Motellier et al. (2007), Savoye et al. (2006), and Wittebroodt et al. (2012).

#### 3.2.5.5 Boda Claystone

On Boda Claystone, a limited number of experiments using $Cs^+$, $Sr^{2+}$, $Co^{2+}$, $I^-$, $HCO_3^-$, and $TcO_4^-$ are reported by Mell et al. (2006b) and Lazar and Mathé (2012).

In the context of the European Project EURAD WP5-FUTURE, new data from transport studies on samples of Boda Claystone formation became available for selenite (Czömpöly et al., 2023) and $UO_2^{2+}$ (contribution of Czömpöly in Maes et al. (2024)).

#### 3.2.5.6 Clay minerals

Diffusion in clay minerals (e.g., bentonite, smectite, illite, and kaolinite) has been widely investigated.

Bourg and Tournassat (2015) provide a comprehensive literature overview on the diffusion studies on different types of bentonite (e.g., MX-80, Kunigel, Volclay KWK, Avonlea, and FEBEX) and smectites (e.g., Kunipia Montmorillonite, Swy-2 Montmorillonite, and Milos). These studies were mainly conducted using conservative tracers such as HTO/HDO, $I^-$/$Cl^-$,$Br^-$, and ion-exchangeable cations such as $Na^+$, $Cs^+$, $Sr^{2+}$, and ($Co^{2+}$). Glaus et al. (2017) published a detailed report on diffusion experiments using HTO, $Na^+$, $Cs^+$, $Sr^{2+}$, $Cl^-$, $SO_4^{2-}$, and $SeO_3^{2-}$ on Milos montmorillonite and Volclay KWK bentonite. They also published diffusion data for HTO, $Na^+$, and $Cl^-$ on kaolinite (Glaus et al., 2010).

In the EC project CATCLAY, the diffusion of a suite of cationic species (Sr, Co, Zn, and Eu) in illite (Illite du Puy) was intensively studied (Altmann et al., 2015; Glaus et al., 2015a; Glaus et al., 2020) in combination with dedicated sorption experiments.

In the EC project EURAD WP5 FUTURE, considerable new data from transport studies on different clay materials became available and are compiled in a final technical report (Maes et al., 2024); herewith an overview:

- Illite: Selenate and $Zn^{2+}$ (in competition with Ni) (contributions of Van Laer et al.), and $Co^{2+}$ and $Zn^{2+}$ on

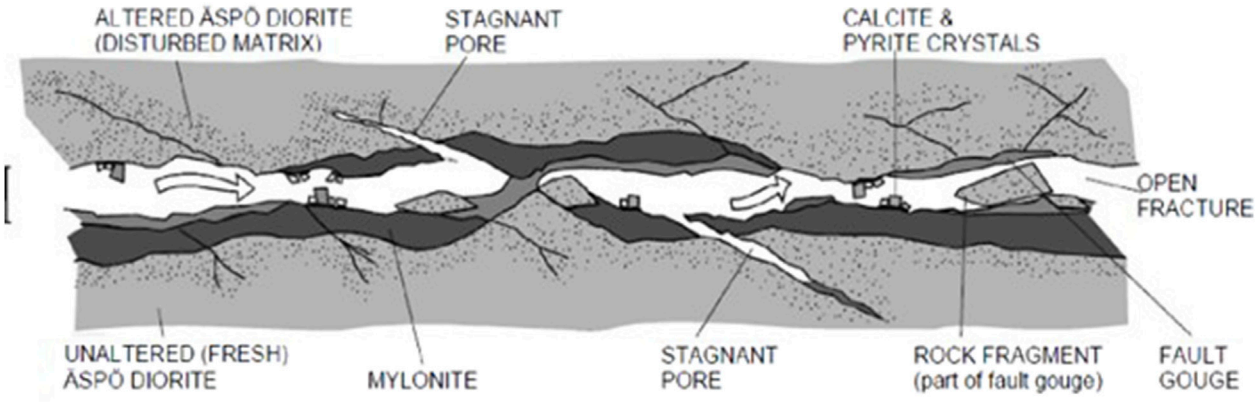


FIGURE 7
Crystalline rock features: unaltered rock, altered rock zones, fractures with and without mineralization (figure reproduced from Winberg et al., 2000, with permission from SKB).

illite preloaded with different cations (Li, Na; K, and Cs) (contribution of Zerva et al.).
- Compacted vermiculite: $Co^{2+}$ (contribution of Zerva et al.)
- FEBEX bentonite: HTO, $Cl^{-}$, $Sr^{2+}$, and $Ba^{2+}$ effect of temperature and dry density (contribution of Garcia Guttierez et al.)
- Nontronite
- Effect of water saturation on transport of HTO, $I^{-}$, and $Na^{+}$ on kaolinite, illite, and vermiculite (contribution of Savoye et al., and more information in Section 3.2.2.3)

## 3.3 Transport in crystalline rocks

### 3.3.1 Structural aspects of crystalline rocks

Crystalline formations are geological units, which consist of magmatic and/or metamorphic rocks. Metamorphic rocks have undergone changes in mineralogy, texture, and/or chemical composition as a result of increasing temperature and pressure. The original rock may have been igneous, sedimentary, or another metamorphic rock. Due to their evolution, metamorphic rocks (most frequent representative: gneiss) typically show an ordered and, therewith, anisotropic structure (foliation and schistosity). Magmatic rocks (e.g., granites) usually have a disordered and massive, more isotropic structure owing to the lack of tectonic stress during crystallization. A disordered structure is generally advantageous from the viewpoint of mechanical stability. Nevertheless, many high-grade metamorphic rocks are very mechanically stable owing to their formation and recrystallization under high-pressure and high-temperature conditions.

For the mineralogical and geochemical characterization of magmatic and metamorphic rocks, several classification schemes exist. Granite, diorite, and gneiss as important crystalline rocks mainly consist of (Na, Ca)-feldspar (plagioclase with endmembers albite $Na[AlSi_3O_8]$, anorthite $Ca[Al_2Si_2O_8]$) and (K, Na)-feldspar with endmembers orthoclase/microcline $K[AlSi_3O_8]$ and albite. Further constituents are biotite $(K(Mg,Fe^{2+},Mn^{2+})_3[(OH,F)_2|(Al,Fe^{3+},Ti^{3+})Si_3O_{10}])$, quartz ($SiO_2$), amphiboles (e.g., hornblende, $Ca_2(Mg,Fe,Al)_5(Al,Si)_8O_{22}(OH)_2$), and calcite ($Ca[CO_3]$), and pyrite ($FeS_2$). Potential alteration processes result in albitization, biotite- and hornblende-alteration, and the formation of, for example, epidote ($(Ca_2(Fe^{3+},Al)Al_2[O|OH|SiO_4|Si_2O_7])$, muscovite ($KAl_2[(OH,F)_2|AlSi_3O_{10}]$), chlorite ($((Mg,Fe)_3(Si,Al)_4O_{10}(OH)_2\cdot(Mg,Fe)_3(OH)_6$), illite ($((K,H_3O)(Al,Mg,Fe)_2(Si,Al)_4O_{10}[(OH)_2,(H_2O)]$), smectite (e. g., montmorillonite, $(Na,Ca)_{0,3}(Al,Mg)_2Si_4O_{10}(OH)_2\cdot nH_2O$), kaolinite ($Al_4[(OH)_8|Si_4O_{10}]$), calcite, stilbite ($((Ca,Na)_9[(Si,Al)_{36}O_{72}]\cdot 28H_2O$), laumontite ($Ca_4[Al_8Si_{16}O_{48}]\cdot 18H_2O$), prehnite ($Ca_2Al[(OH)_2|AlSi_3O_{10}]$), titanite (or sphene) ($CaTi[O|SiO_4]$), hematite ($Fe_2O_3$), and pyrite ($FeS_2$) (Sandström and Tullborg, 2009; Plumper and Putnis, 2009; Nishimoto and Yoshida, 2010; Stober and Bucher, 2014; Yuguchi et al., 2015; Niwa et al., 2016). Nishimoto and Yoshida (2010) considered calcite, laumontite, chlorite, epidote, and prehnite along with quartz as the most frequent fracture-filling minerals.

For the assessment of crystalline rocks as host rock for a repository for heat-generating radioactive waste, their hydrogeological properties are particularly important. In metamorphic or magmatic crystalline rocks, the permeability of pore networks plays only a minor role. However, the groundwater flow predominantly occurs through fractures. The formation of fractures is largely controlled by tectonic processes during the uplift of the rocks in depth ranges, which are suitable for radioactive waste disposal. The extent of fracture formation is mainly dependent on rock stability and regional tectonic conditions. However, due to thermodynamic disequilibrium during uplift processes, fractures are frequently mineralized by migrating hydrothermal solutions or groundwater. Thus, the permeability of fractures is significantly modified due to precipitation processes and the infiltration of fines.

To describe transport processes in crystalline rock, one has to distinguish between unaltered and altered rock matrices (Figure 7), as well as between fractures with and without mineralization.

Components of crystalline rock show a large variability in crystal size, often ranging from the millimeter-to-centimeter scale. Newly

formed minerals and alteration products in fractures may comprise much smaller crystal sizes down to the nanometer scale, and they show a large variability of pore diameter, volume, and, hence, porosity (Svensson et al., 2019).

Complex flow fields evolve due to the surface heterogeneity of fractures and complex geometric fracture features, i.e., microscale roughness, reflecting the strong impact of spatial surface variability. Fracture geometry can effectively lead to the retardation of solutes and colloidal phases solely on basis of hydrodynamic processes, without considering physico-chemical processes such as matrix diffusion, sorption, or reduction.

Fracture surfaces vary spatially, for example, due to fracture fillings or geometry variability (Moreno and Neretnieks, 1993; Moreno et al., 1997; Bodin et al., 2003). It was observed that water flows in narrow channels through fractures (Bodin et al., 2003; Moreno et al., 1997), which is referred to as the channeling effect or preferential flow paths and applies to a single fracture as well as fracture networks (Tsang, 1984; Tsang and Tsang, 1987; Tsang, 1992; Park et al., 1997; Moreno et al., 2000; Malloszewski and Zuber, 1992; Shahkarami et al., 2016). Channeling can arise due to: 1) a variable aperture, 2) intersecting fractures, and 3) the offset displacements of fractures (Löfgren et al., 2007) and, among others, affect the hydraulic properties of crystalline rock. It also influences the fracture retention capacity, since matrix diffusion processes can be affected.

### 3.3.2 Main processes controlling transport in crystalline rocks

Reactive transport in fractured crystalline rocks is controlled by the physical and chemical properties of fractures, namely fracture walls and fracture-filling materials.

#### 3.3.2.1 Advection in fractures is the dominant transport process

A mechanistic understanding, quantitative description, and prediction of advective transport in fractured porous media are still challenging. The surface building-block size on fracture walls covers a large range of the length scale, from the molecular dimension up to the characteristic extension of fractures in the field scale (Berkowitz, 2002; Pyrak-Nolte and Nolte, 2016). The fracture geometry causes heterogeneity, such as channeling of the flow path, which is also coupled to the adjacent porous and/or microfractured matrix material. Characterization of the fracture flow, its interplay with the pore space, and upscaling to the field scale relevant for performance assessment is a continuing issue (Wersin, 2017). The fractal nature and partial self-similarity of rough fracture surfaces have been studied for their effects on the geometric constraints of transport models (Cardona et al., 2021; Wang et al., 2022). This topic has recently been discussed in a general review on transport mechanisms (Gao et al., 2023a) and with a focus on RN transport (Zhang et al., 2022)). The complexity increases further when fracture infills (infiltration of fines) and mineralization are considered (Antonellini et al., 2017; Soler, 2016). Fracture-filling materials modify the transport conditions owing to multiple processes of precipitation/crystallization and/or particle aggregation and filtration. As a result, a large diversity of pore shapes, pore size distributions, pore network geometries, and accessible internal surface areas is reported (James et al., 2018; Jones and Detwiler, 2016; Nollet et al., 2009; Zhang et al., 2015).

Apart from advection through fractures with apertures larger than 100 µm, additional 2D tight flow pathways exist along microfractures and grain boundaries. Consequently, length-scale-depending variability of permeability has been observed and compared to multi-scale porosity and pore network data using multiple methods, such as mercury intrusion porosimetry (MIP) and pore network tomography (e.g., µCT, FIB-SEM, or BIB-SEM) (David et al., 2018).

#### 3.3.2.2 Matrix diffusion

A simplified description of fluid transport in fractured crystalline rock is based on the dual-porosity model (e.g., Smith et al., 1991). In the dual-porosity model, diffusion into the rock material adjacent to fractures is included via matrix diffusion. The matrix-controlled transport is determined by the sorption on solid surfaces as well as parameters controlling the diffusion process, particularly the diffusion coefficient and the matrix porosity.

The concept of anion exclusion explains, similarly as in a clay environment (see Section 3.2.2), charge-depending modifications of the mobility of ions. The electrostatic interactions modifying ion mobility are dominant for pore sizes in the nanometer range. While this effect has been often observed in and described for argillaceous rocks, anion exclusion can be significant in crystalline rock matrices as well. Consequently, diffusion coefficients determined in diffusion experiments in crystalline rock matrices using anions tend to be smaller compared to cations or water (Smellie et al., 2014; Tachi et al., 2015; Voutilainen et al., 2019; Kuva et al., 2018).

#### 3.3.2.3 Role of sorption and surface-induced processes

Retention processes, which have a common physical background for both clay and crystalline rock environments, are described in Section 2. Some specific issues, specifically focused on crystalline fractured environments, are tackled here.

**3.3.2.3.1 Sorption on fracture surfaces, including fracture-filling materials.** In Hakanen et al. (2014), the evaluation of data for rock materials is based on the laboratory-derived $K_d$ values of crushed rocks. Based on the results of the mineral-specific sorption of radionuclides in diffusion experiments and results of sorption to rock surfaces, these distribution coefficients were converted to $K_d$ values for intact rock. From this evaluation, it was suggested that mica minerals and other minerals with high CECs or high surface areas dominate sorption in intact rock.

Nevertheless, such minerals are not restricted to the rock matrix; they are also found in fractures, where they play a critical role in immobilizing contaminants during advective transport. In addition, carbonate minerals such as calcite are commonly found as hydrothermally formed fracture fills and may contribute to contaminant retention in fractured rock as well. While the retention properties of sheet silicates are discussed in detail in Section 3.2, for minerals such as calcite, sorption alone may not be the only process responsible for contaminant retention. Co-precipitation processes, as demonstrated by Smith et al. (2018) for Np(V) sorption on calcite, also play an important role. In addition, carbonate complexes can lead to RN migration in rock fractures without retention, as observed for Pu(IV) by Zavarin et al.

(2005). A detailed study of calcite precipitated in a borehole at the Äspö Hard Rock Laboratory showed that environment-specific partition coefficients can differ from laboratory-derived values, as seen for REEs (Drake et al., 2018).

A combination of microscopic and macroscopic investigations performed by Fukushi et al. (2013) focused on Eu(III) sorption on granite. Here, biotite was identified as the controlling factor for sorption strength. Numerical approaches considering a single-site cation-exchange reaction are able to predict the sorption behavior at pH > 4. The results suggested that sorption on a complex mineral assemblage such as granite could be modeled by using the single most relevant mineral phase (here: biotite) representative of the bulk sorption reaction in a complex mineral assemblage. Similarly, Muuri et al. (2017) and Kyllönen et al. (2008) utilized a multi-site sorption model initially introduced by Bradbury and Baeyens for Cs sorption on illite. They used this model to estimate distribution coefficients for Cs on biotite and biotite-rich rocks. Furthermore, Soderlund et al. (2019) employed the same sorption model, originally developed for Cs, to simulate the sorption of alkaline earth metals on biotite.

Li et al. (2018), Li et al. (2020), and Puhakka et al. (2019) investigated the sorption behavior of Se(IV) on Grimsel granodiorite (mainly plagioclase, K-feldspar, quartz, and biotite) using artificial Grimsel groundwater and different concentrations of Se(IV). A strong Se concentration dependence of Se sorption was observed, and the highest sorption values were found on biotite at low Se concentrations ($<10^{-7}$ mol/L). The distribution coefficients of Ba on Olkiluoto pegmatitic granite and veined gneiss, Grimsel granodiorite, and their main minerals (quartz, plagioclase, K-feldspar, and biotite) were obtained from batch sorption experiments (Muuri et al., 2018; Muuri, 2019). Highest sorption efficiencies were found on biotite and plagioclase. Recent results by Konevnik et al. (2017) suggested a strong increase in the $K_d$ values for Sr(II) and Am(III) for a temperature increase from 20°C to 90°C. Molodtsov et al. (2019) observed that, in the case of Eu(III), plagioclase was the primary mineral responsible for Eu sorption in granite, followed by intermediate sorption on biotite, and, lastly, sorption on quartz. Nevertheless, Molodtsov et al. (2021) reported that Eu(III) sorption on Bukov-magmatized gneiss showed that chlorite and amphibole exhibited the strongest Eu sorption among the complex mineral compositions present in rock.

**3.3.2.3.2 Surface-induced processes and reactivity.** The presence of specific minerals in crystalline rock can induce processes that lead to reactions, including radionuclide retention. A typical reaction is the species reduction due to the presence of either Fe minerals or Fe-bearing minerals. These processes are specified in detail in Section 2.2.2. An example of this process is the retention of I on pyrite, biotite, and magnetite (Fuhrmann et al., 1998) via the surface reduction of $IO_3^-$ to $I_2$ and oxidation of $S^{2-}$.

Similarly, selenium sorption has been studied, and results suggested that Se(IV) is more readily reduced to Se(0) or Se(-II) when a solution is exposed to metal- or Fe-containing minerals (e.g., biotite) (Videnská et al., 2013; Stamberg et al., 2014; Videnska et al., 2015; Hakanen et al., 2014). The abiotic homogeneous reduction of selenite or selenate to selenide occurs at very low rates. Thus, the reduction reaction in the environment is most likely microbe-mediated, equivalent to the reduction of sulfate to sulfide (Myneni, 1997; Hockin and Gadd, 2003; Hakanen et al., 2014). Increased Tc sorption was observed for rocks containing Cu, Fe, and Pb sulfides, and additional examples of retention of radionuclides on pyrite, galena, or chalcopyrite via reduction are provided in a review by Suter (1991).

**3.3.2.3.3 Solid solution.** Solid solutions can be formed during the precipitation of mineral phases on fracture surfaces and in pores close to the fractures (Poonoosamy et al., 2020). These are typically sulfates (e.g., baryte, celestite) or carbonates (e.g., calcite) and can become an important retention mechanism for some radionuclides, such as Ra (see Section 2.3.3 for more details). For example, the precipitation of calcite might occur in crystalline carbonate water at higher pH. Curti (1999) reported that actinides strongly partition into calcite under reducing conditions; nickel(II) incorporation is moderate, while incorporation of ions such as U(VI), Cs(I), Sr(II), and Ra(II) in calcite is weak.

## 3.3.3 Research methods to characterize fracture properties and radionuclide migration

### 3.3.3.1 Advective flow and transport properties (geoPET and PMMA)

Although methods for characterizing bulk-rock properties are highly developed, the characterization of porosity in crystalline rock still remains challenging owing to low pore spaces and a broad range of potential pore sizes (David et al., 2018). Specifically, μCT(spatial resolution in the order of 50 μm) is relevant for transport studies in large and continuous fractures with aperture widths above the instrumental resolution. Methods such as optical microscopy approaches for the quantification of surface roughness variability provide detailed insights into critical surface building blocks of fracture walls (Fischer and Luttge, 2007), but they require preparation of and accessibility to the fracture surface. Apart from the visualization of fractures on relevant scales, other challenging aspects for μCT analysis are, for example, porous fracture fillings and intergrown minerals owing to their highly porous structure that can be of negligible density in contrast to the surrounding fluid (Berg et al., 2016; Menke et al., 2018). Furthermore, the C-14 polymethylmethacrylate (PMMA) method (impregnation with C-14 labelled PMMA resin followed by autoradiography) was developed to obtain information about the spatial distribution of porosity on the core scale (Sammaljärvi et al., 2012). It has been successfully used to characterize the spatial distributions of porosity in REPRO samples from Olkiluoto and has been combined with other techniques (Ikonen et al., 2015), such as electron microscopy for mineralogical characterization (Sammaljärvi et al., 2017). Furthermore, CT tomography analysis can be combined with C-14 PMMA method-based porosity results and SEM-based mineralogical analysis to obtain a 3D structure of crystalline rock.

Radionuclide tracer propagation through rock cores with natural or artificial fractures are studied using positron emission tomography (PET) (Kulenkampff et al., 2008). PET data analysis provides spatiotemporal images of the tracer concentration during conservative transport. In contrast, reactive (sorbing) PET tracers identify reactive sites of rock surfaces during fluid–solid interactions (Kulenkampff et al., 2018). Usually, PET techniques are combined with microcomputed tomography (μCT) data for the identification

of the geometry of fractures, pores, and pore networks. Segmented μCT data yield a structural model for reactive transport modeling (Kahl et al., 2020). Flow-field interpretations based on PET data sequences are used to identify flow heterogeneities (Lippmann-Pipke et al., 2017; Zahasky and Benson, 2018). Both the parametrization and validation of numerical transport models are an important application of PET flow field and velocity data. Pulse migration experiments using the positron-emitting radionuclide F-18 have provided insights into the fluid dynamics of complex fractured crystalline materials. Both the variation of the fracture aperture and the topography of the fracture surface affect the flow field, with consequences for flow channeling and preferential flow paths. Higher flow velocities result in wider and more dispersed flow paths, while lower velocities result in more localized flow and channeling behavior (Pingel et al., 2023).

### 3.3.3.2 Matrix diffusion

**3.3.3.2.1 Through-diffusion method.** The most commonly used method to determine the effective diffusion coefficient ($D_e$) of elements in hard materials is the TD experimental method (also see Section 3.2.3.1.2 for clay materials). In this method, a sample is placed between tracer-spiked and tracer-free solutions. The sample is glued to a sample holder, equilibrated in a tracer-free solution, often with synthetic groundwater, and installed between the two reservoirs. The tracer concentration is monitored in the initially tracer-free reservoir (Voutilainen et al., 2017). The apparent and effective diffusion coefficients as well as the geometric factors (G) can be determined from the experimental results based on Fick's second law of diffusion. Another experimental approach used to determine the effective diffusion coefficient involves subjecting sorbing elements to diffusion in rock cubes. In this setup, accurate measurements of concentration decreases in solutions containing the rock cubes are critical (Muuri et al., 2018; Muuri et al., 2017). Recently, the PET technique (see Section 3.3.3.2.4) has been used to calculate spatially resolved effective diffusivities (Bollermann et al., 2022).

In addition to concentration-induced diffusion experiments using aqueous solutions, TD experiments can also be performed in the gas phase. The diffusion coefficients of helium in a nitrogen-filled sample was measured (Kuva et al., 2015). The results showed that helium gas molecules diffused more than 11 000 times faster than atoms and molecules in the water phase.

The experimental arrangement of equilibration-leaching or the OD method can also be used to determine pore diffusion coefficients (Smellie et al., 2014).

**3.3.3.2.2 Electromigration.** The through-electromigration method (André et al., 2009; Lofgren and Neretnieks, 2006; Löfgren et al., 2009), adapted from Maes et al. (1998), Maes et al. (1999), and Maes et al. (2001), combines the principle of a TD method with the electromigration method and provides the effective diffusion coefficient ($D_e$), distribution coefficient ($K_d$), and geometric factor ($G$) for an intact crystalline rock sample in a faster way than traditional block-scale diffusion experiments. It avoids the problem of rock crushing in batch sorption experiments, which can create new surfaces and significantly increase the SSA (which would lead to an overestimation of $K_d$ values). The setup is described in (Lofgren and Neretnieks, 2006). A small electric field is applied over a rock sample, which is placed between two chambers, one holding an electrolyte with a high tracer concentration (source chamber) and the other holding the same electrolyte initially free of tracers (recipient chamber). André et al. (2009) tested the migration behaviors of $I^-$ and $Cs^+$ ions in samples of intact rock.

In André et al. (2009), a device was found to have difficulties in maintaining a constant electric potential over a rock sample, making the experimental results difficult to interpret. To overcome this problem, Li et al. (2019b) upgraded this device by making use of a potentiostat instead of an ordinary power source and performed iodide ($I^-$) and selenite ($SeO_3^{2-}$) through-electromigration experiments. In addition, $NaHCO_3$ was added as buffer to the background electrolytes to stabilize the pH of the solution during the experiment. As a result, the electromigration device had the capabilities of voltage-self-controlling, continuous-current-recording, and solution-pH-stabilizing.

It should be noted that the classical theory for the interpretation of the experimental results simply applies an ideal plug-flow model that accounts only for the effect of electromigration on ionic transport but neglects contributions of electroosmosis and dispersion. To tackle this problem, an advection–dispersion model was developed by Meng et al. (2020). The model accounts for the influences of electromigration, electroosmosis, and dispersion in ion transport through rock. An analytical solution was derived in the Laplace space and described the transient tracer concentration variation in the recipient chamber.

**3.3.3.2.3 C-14 PMMA method.** As stated above (Section 3.3.3.1), the C-14 PMMA method was developed to gain information about pore networks and porosity at the core scale (Sammaljärvi et al., 2012). Relevant datasets act as a basis for the modeling of diffusion in crystalline rock (Kuva et al., 2018; Mazurier et al., 2016; Voutilainen et al., 2017; Voutilainen et al., 2019). Further refinement of image analysis in C-14 PMMA yields pore apertures from C-14 PMMA autoradiographs (Bonnet et al., 2020).

**3.3.3.2.4 Flow-field analyses: GeoPET.** Quantitative insights into flow pathway heterogeneity is provided by directly visualizing the propagation of a positron-emitting tracer, such as $^{124}I$ and $^{22}Na$, using GeoPET (Kulenkampff et al., 2016; Kulenkampff et al., 2018). This method provides a suite of quantitative tomograms of the spatial tracer distribution. This allows for the derivation of a spatially resolved tensor of molecular diffusion coefficients. A robust algorithm for reconstructing the dominant pathways and flow field ("Darcy velocity") has been developed and is being further improved. PET analysis is being increasingly used for diffusive flux analysis in argillaceous materials and can provide valuable validation of transport simulation results. This is of particular importance owing to the potential variability of pore networks in such materials, which can only be inferred using high resolution methods such as FIB-SEM based on relatively small fields of view (Bollermann et al., 2022).

**3.3.3.2.5 *In situ* vs. laboratory experiments.** Since 2004, two large-scale, long-term *in situ* diffusion (LTD) experiments have been conducted at the Grimsel Test Site, which aimed to examine *in situ* matrix diffusion and pore space visualization (Soler et al., 2015; Ikonen et al., 2016b; Ikonen et al., 2016a) (see Section 3.3.4).

Two *in situ* flow experiments have been conducted in Onkalo at the Repro site where the dominant rock type is veined gneiss. Parallel to the *in situ* experiments, the project focused on rock matrix characterization and matrix diffusion in laboratory experiments to compare conditions such as stress relaxation, which might open the pore space and increase the diffusivity of the rock (see Section 3.3.4).

#### 3.3.3.3 Sorption

Different approaches exist to characterize relevant mineral-specific sorption processes such as the acid–base behavior of surfaces and retardation, including surface complexation processes, in general. To examine sorption reactions at the solid–liquid interface, commonly applied methods are classical potentiometric titration experiments, column titration experimental setups, so-called batch experiments, and column transport experiments. These techniques are described in Section 2.2.4.

In the following section, a brief overview of titration, batch, and column experimental approaches, that are specific for crystalline rocks, is provided. Detailed information on spectroscopic methods is provided elsewhere (see Section 2.2.4.2) and not within the scope of this chapter.

**3.3.3.3.1 Titration experiments.** Potentiometric mineral titration experiments in batch are appropriate for investigating solids with large SSAs, such as clays (see Section 2.2.4). However, crystalline rock samples, in particular, can have very small surface areas. To collect trustworthy information on the acid–base behavior of samples with small SSAs, column potentiometric titration experiments may be applied (Scheidegger et al., 1994; Neumann et al., 2020). The advantage is a significantly larger solid–liquid ratio compared to that of potentiometric batch titrations. Hence, a larger surface area is exposed to a relatively small amount of titrant, making it possible to obtain trustworthy results of changes in surface charge as a function of, for example, ionic strength, pH, and ligands.

**3.3.3.3.2 Batch sorption experiments.** Batch sorption experiments can be based on the pre-equilibration of the solid phase in an electrolyte solution before adding a radionuclide, allowing it to sorb over a defined period of time, and can be used for any material, including clays. It is assumed that, after pre-equilibration of a solid, a radionuclide sorbs onto a slightly altered surface, which is expected to represent conditions that are closer to nature, compared to surfaces that have not undergone pre-treatment. Batch sorption results correlate well with data found in the literature and confirm the expected sorption trends that substantiates an approach. Unfortunately, pre-equilibration is time-consuming and may take several weeks to months, depending on the solid phase.

More time-efficient approaches are batch experiments that are carried out without pre-equilibration of a sample. A solid is briefly suspended in an acidic electrolyte that contains an element/radionuclide. Since the sorption of many relevant elements/radionuclides is pH-dependent, no significant surface reactions take place under these initially acidic conditions. Via slow adjustment of a suspension's pH to higher pH conditions, the radionuclide sorbs onto the surface of the solid systematically. To reach steady-state conditions at surface and to be able to compare the results between the two experimental setups, identical equilibration times should be used when allowing the element/radionuclide to sorb at the surface. In an ongoing research project (SMILE, funding code 02 E 11668A, German Federal Ministry of Economics and Technology), it could be shown that both experimental approaches yield comparable results for quartz and feldspar surfaces. However, the second approach bears complications when using solids that exhibit strong natural buffer capacities and that are prone to dissolution in acidic conditions: Buffer reactions of the mineral surfaces result in pH shifts when comparing initially adjusted pH values with measured pH values after equilibration of a radionuclide with a surface. Minerals that undergo unwanted dissolution processes under acidic conditions may leach silica and other cations from the crystal lattice into the solution that later on, at higher pH, might bias sorption processes and dynamics via competing surface reactions or complexation reactions in solution (formation of aqueous complexes with altered sorption tendencies).

To prevent pH shifts from buffer reactions, and, hence, to precisely control the pH values of solid-electrolyte suspensions, artificial buffers can be added that have been shown not to interfere with sorption processes (Missana et al., 2009). This technique is often used for solids that undergo pre-treatment; however, it may also be applied for batch sorption experiments without pre-equilibration of a surface.

Alonso et al. (2013) and Alonso et al. (2014) proposed combining RBS and micro particle-induced X-ray emission (μPIXE) to analyze radionuclide retention and diffusion at the mineral scale using intact crystalline rocks, thus accounting for their heterogeneity. This method has been tested using different radionuclides (or chemical analogues) and proved successful in the cases of uranium and selenium.

**3.3.3.3.3 Dynamic column transport experiments.** Different experimental setups that provide a further understanding of sorption processes at mineral–water interfaces are column experiments. While batch sorption experiments represent sorption processes under static, equilibrium conditions, with column transport experiments, it is possible to collect retardation data under dynamic conditions and/or under equilibrium conditions. In column experiments, a cylinder is homogeneously filled with crushed mineral/rock and closed. For saturated conditions, a background electrolyte with defined chemical conditions is percolated through the column. After the column is saturated and geochemical conditions are adjusted as required, an electrolyte spiked with the radionuclide/contaminant of interest can be introduced into the column. At the end of the column, fractions of the solution that percolated through the column are collected, and information on retardation factors, retention times, mineral dissolution processes, pH evolution, and ionic strength changes, among others, throughout the experiment can be obtained. Since any electrolyte may be introduced into the system, and critical parameters such as pH, ionic strength, and ligand concentrations may change, this experimental system can be used to investigate dynamic transport and retardation processes.

It should be noted that the evaluation of results collected from column experiments in general may provide transport parameters such as retardation factors and distribution coefficients ($R$ and $K_d$, respectively), the Péclet number ($P_e$), or hydrodynamic dispersion coefficients and diffusion coefficients (Stamberg et al., 2014). However, to obtain these parameters, numerical models, such as, e.g., HYDRUS, STANMOD, and 2D/3D transport models, have to be applied.

## 3.3.4 Experimental approach to upscaling

### 3.3.4.1 Advective transport processes

An extensive experimental program has been run in several underground laboratories, namely the Äspö hard rock laboratory (Sweden) and Grimsel Test Site (Switzerland). Experiments focus on RN migration/retention and fracture properties (see the overview of tracer tests in Löfgren et al. (2007) or references at https://www.grimsel.com/). A generalized view on the understanding of RN migration and retention in fractured rock was provided by projects TRUE-1 and TRUE Block Scale (Andersson et al., 2002b; Andersson et al., 2002a; Poteri et al., 2002). These projects focused on the meter scale up to the block (hundred meter) scale, similar to the Migration project (MI) and Excavation project (EP) at the Grimsel Test Site (Smith et al., 2001; Alexander et al., 2003; Alexander and Frieg, 2009). The Grimsel Test Site project CRIEPIS´s Fractured Rock Experiment (C-FSR) provided fundamental knowledge about the properties of fractures, such as aperture, dispersivity, and flow wetted surface, using tracer tests and resin injection (http://www.grimsel.com/gts-phase-vi/c-frs/). Natural fracture properties are most often determined using *in situ* tracer tests in underground laboratories (Löfgren et al., 2007). For practical reasons, the tests are generally performed in reasonably well-connected and hydraulically conductive fractures where groundwater pumping can be performed. The rock mass surrounding fractures is likely to be intersected by swarms or clusters of minor fractures that can only be described stochastically. Information concerning the accumulation of fractures, so-called deformation zones, and individual hydraulically conducting fractures in rock matrices are normally obtained by drilling boreholes and examining the boreholes geologically, hydraulically, and geophysically.

### 3.3.4.2 Diffusive transport

Since 2004, two LTD experiments were performed at the Grimsel Test Site, which aimed to examine *in situ* matrix diffusion and perform pore space visualization (Soler et al., 2015; Ikonen et al., 2016b; Ikonen et al., 2016a). Full characterization of the spatial porosity distribution in matrices, and its link to mineralogy, was performed by Voutilainen et al. (2017) based on the first LTD monopole experiment in order to better identify microstructure-derived diffusion. The heterogeneous mineral and pore structure of the studied rock, as well as the changing $K_d$ value of cesium, were taken into account for proper interpretation of the results of the *in situ* experiments.

Since 2009, *in situ* experiments have been run within the Repro cluster in the Onkalo URL (Finland) to investigate rock matrix retention properties under *in situ* conditions and to demonstrate that assumptions applied in safety cases are in line with evidence collected on site, *in situ* (Poteri et al., 2018a; Poteri et al., 2018b; Voutilainen et al., 2019). Two *in situ* flow experiments were conducted in Onkalo at the Repro site where the dominant rock type is veined gneiss. Parallel to the *in situ* experiments, the project is focused on rock matrix characterization and matrix diffusion in laboratory experiments to compare conditions such as stress relaxation, which might open pore spaces and increase the diffusivity of rock. In a study by Voutilainen et al. (2019), the transport of tritiated water (HTO), $^{36}$Cl, and $^{22}$Na was studied using laboratory and *in situ* water-phase diffusion experiments (WPDEs). The SKB Groundwater Flow and Transport of Solutes Task Force conducted WPDEs (WPDE-1 and WPDE-2) aimed at predicting tracer breakthrough curves (including those of HTO, $^{36}$Cl, $^{22}$Na, $^{85}$Sr, and $^{133}$Ba), as discussed by Soler et al. (2022). These experiments utilized simplified models to evaluate various conceptual approaches. The findings indicated that non-sorbing tracers were primarily influenced by dispersion, while sorbing tracers were impacted by diffusion and sorption parameters, as highlighted in Soler et al. (2019). This underscores the complexity of accurately predicting outcomes in well-designed field experiments, especially when extrapolating from laboratory-based geometries.

Upscaling of the results from numerical simulations at the pore scale can be used to derive key parameters for models at larger scales in crystalline host rocks. The volume-average approach has been applied as an upscaling method for the transport processes in porous media (Molins, 2015). As imaging techniques are progressively improving, "*digital rock physics*" has become a useful tool for numerically investigating reactive fluid–solid transport (Grathoff et al., 2016). Consequently, the image-based upscaling approach (Keller and Holzer, 2018; Mahrous et al., 2022) can preserve the small-scale information in large-scale simulations. However, one of the challenging aspects of upscaling is confirming whether small-scale measurements are representative of large-scale volumes.

## 3.3.5 Sources of transport data for crystalline rocks

This section presents an extensive (but not complete) overview of available data sources for understanding transport processes specific to crystalline rocks.

### 3.3.5.1 Transport and retention processes

Fracture surfaces vary spatially owing to factors such as fracture fillings or geometry variability (Moreno and Neretnieks, 1993; Moreno et al., 1997; Bodin et al., 2003). It was observed that water flows in narrow channels through fractures (Bodin et al., 2003; Moreno et al., 1997), which is referred to as the channeling effect or preferential flow paths and applies to a single fracture as well as fracture networks (Tsang, 1984; Tsang and Tsang, 1987; Tsang, 1992; Park et al., 1997; Moreno et al., 2000; Malloszewski and Zuber, 1992; Shahkarami et al., 2016). For an overview of solute transport mechanisms in fractured rock, the RETROCK Project (Nykyri, 2004) and Neretnieks (1993) are recommended. Detailed information on fracture heterogeneity and its influence on transport processes is provided by POSIVA (2012a) and Poteri et al. (2014), who describe phenomena observed at the Olkiluoto site.

An overview of tracer tests can be found in a study by Löfgren et al. (2007) or at the Grimsel Test Site publications list page at https://www.grimsel.com/

A generalized view on understanding of RN migration and retention in fractured rock was provided by the projects TRUE-1

and TRUE Block Scale (Andersson et al., 2002b; Andersson et al., 2002a; Poteri et al., 2002). These projects focused on the meter scale up to the block (hundred meter) scale, similar to the MI and Excavation EP at the Grimsel Test Site (Smith et al., 2001; Alexander et al., 2003; Alexander and Frieg, 2009).

Diffusive transport occurs at the zones adjacent to fractures, enabling radionuclides to enter a connected system of pores in a rock matrix. Recent experimental studies on potential crystalline host rocks and diffusive transport include the Grimsel LTD experiment (Havlova et al., 2013; Martin et al., 2013), investigations at the Olkiluoto site (Aromaa et al., 2019; Voutilainen et al., 2019), and Beishan granite investigations (Yang et al., 2018).

#### 3.3.5.2 Sorption processes

Many studies have focused on specific aspects of sorption in crystalline rock, generally using batch sorption experimental setups. A wide range of papers dedicated to batch sorption experiments can be found in Section 2.5.3 (sorption on crystalline rocks and components).

Detailed experimental setups of dynamic sorption column experiments can be obtained from Britz (2018), Palágyi and Vodičková (2009), Palágyi and Stamberg (2010), Palágyi et al. (2012), Videnská et al. (2013), Stamberg et al. (2014), Videnska et al. (2015), Hölttä et al. (1996), Höltä et al. (1997), Li et al. (2009), Missana et al. (2008a), Dangelmayr et al. (2017), and Porro et al. (2000).These papers present experimental data, different model approaches, advantages, as well as drawbacks compared to batch experiments.

More information on column titration as one of the methods for the determination of retention property experiments is provided by Stolze et al. (2020), García et al. (2019), and Svecova et al. (2008).

#### 3.3.5.3 Data used in safety assessment

With respect to sorption on crystalline rock material, compilations of sorption distribution coefficients ($K_d$), including uncertainties to be used in transport calculations for safety assessment, are available in Crawford (2010) and Hakanen et al. (2014). In Hakanen et al. (2014), an evaluation of data for rock material is based on laboratory-derived $K_d$ values of crushed rocks. Based on the results of the mineral-specific sorption of radionuclides in diffusion experiments and results of sorption to rock surfaces, these distribution coefficients determined on crushed rocks were converted to $K_d$ values for intact rock.

## 4 Concluding remarks on remaining research questions and needs

Research on the various topics of radionuclide migration has been conducted for more than 35 years, often co-funded by the European Commission (EC). Within the EC JOPRAD project "Towards a joint program on radioactive waste disposal" (www.joprad.eu), a consortium of WMO, technical support organization, research entity, and actor group representative organizations from European member states identified research development and demonstration (RD&D) priorities of common interest. These RD&D priorities are based on commonly defined remaining key uncertainties and research needs, and they form the basis of a Strategic Research Agenda (SRA) that is used to coordinate, plan, and conduct future research related to waste disposal in Europe, the so-called European Joint Projects (EJP). Within the SRA (JOPRAD, 2018), different sub-domains were defined by prioritizing the future research needs.

These formed the basis of the EURAD project (https://www.ejp-eurad.eu/, 2021–2024) and the objectives for further research of the different defined work packages. This manuscript, summarizing state-of-the-art knowledge in the field, is one of the main outcomes of the work package "FUTURE," which deals with several of the remaining research questions related to radionuclide retention and transport.

During the EURAD project, the JOPRAD SRA was updated to EURAD SRA 2023, accounting for additional needs identified during the on-going EC project (https://www.ejp-eurad.eu/strategic-research-agenda). This formed the basis for the different work packages proposed in the EURAD2 project to be started in October 2024.

A summary of the remaining research questions (directly copied from the SRA texts) and needs formulated based on analysis of the data and modes available in the literature, as well as new results obtained in WP-FUTURE, begins with those defined in the SRA and is further extended, or more detailed, where appropriate.

Geochemistry of host rock (intact and disturbed).

The mobility and retention of radionuclides is the result of their speciation within pore water and interaction with the solid phases of rock under intact *in situ*, or altered, conditions. It is, therefore, important to properly constrain the porewater chemistry and to adequately define reference and bounding host rock waters as well as to buffer and backfill pore waters for safety studies.

For the clay pore water chemistry, the main remaining uncertainties concern the correct measurements/determination under the undisturbed *in situ* conditions of non-preservable parameters: $pCO_2$, pH, and $E_h$. The conditions for the formation of solid solutions of carbonate and sulfate phases are also an open question.

Furthermore, the impact of "perturbations" such as pyrite oxidation, radiolysis, $CO_2$ degassing, alkaline plume, and iron/clay interactions are still poorly understood.

Chemical thermodynamics.

Assessment of the long-term performance of a disposal system relies on the understanding and quantification of the thermodynamic driving forces for the degradation of waste matrices and for the mobilization and retention of radionuclides. High-quality thermodynamic data and models can often be used beyond a given disposal configuration, and if one is able to base long-term performance assessments largely on such data, one can attain high credibility and confidence. This can be linked to the NEA-TDB approach, which provides high-quality assurance and clear identification of priorities.

There is a need to further develop transparent and quality-assured TDBs for use in performance assessment studies. This entails determining thermodynamic data for key radionuclides, principal elements of a disposal system, secondary phases, and

solid solutions; obtaining a *realistic representation of natural processes*; filling in gaps for specific environments and specific species (e.g., organic matter, humic acids, and Fe-hydroxides); and improving the treatment of uncertainties in thermodynamic data.

Another important aspect is related to the database completeness, since the absence of relevant data in any high-quality database inevitably leads to incorrect predictions.

### Sorption, site competition, speciation, and transport

Radionuclide transport in the pore water or groundwater of porous and fractured media is the main process challenging the long-term isolation and confinement of radionuclides in deep geological formations. The transport rate of species in groundwater is strongly reduced (1) by the retention of radionuclides on sorption sites present at the surfaces of minerals, engineered barrier materials, and their alteration products, and (2) in fractured media via diffusion into low-permeability rock matrices ("rock matrix diffusion"). The extent of sorption depends on the radionuclide, its speciation in solution, the geochemical boundary conditions, the heterogeneity of surface reactivity, and the permeability of solid phases. Competition for sorption sites between radionuclides and the main elements (e.g., $Ca^{2+}$, $Fe^{2+}$, and $Mn^{2+}$) naturally present in pore water and groundwater may reduce the number of sites available for radionuclides.

Sorption mechanisms (such as surface complexation) should be further characterized to improve coupled chemistry/transport models for various rock types.

Deepening our understanding of sorption via surface complexation.

- Focus on mechanistic understanding: complexation constants, spectroscopic studies, and atomistic modeling to unravel the molecular structure of surface complexes, and provide input to TDBs.
- Impact of competing elements.
- Reversibility of the sorption process (adsorption vs. incorporation).
- Transfer of data from "simple to complex" systems: from dilute to compacted systems and from single-mineral phases to polymineral host rocks.
- Integration of models into reactive transport models to account for the evolution of reactive surface areas.

Well-known heterogeneities of cement-based materials, clay rock, crystalline rocks, bentonite, and corrosion products in speciation and sorption (considering competitive effects) need to be addressed, and transport models considering the variability of barrier properties at all relevant scales need to be developed. This will elucidate the influence of 3D-rock anisotropy/heterogeneity on radionuclide migration.

Complex evaluation of the dependence of sorption process on system constituents and boundary conditions is needed in order to realistically reflect system heterogeneity.

Models that are able to take into account the behavior of radionuclides in complex systems (including the effects of organic and inorganic ligands, and redox transitions) should be further developed.

Classical transport models for porous media should be extended to include the effect of mobile surface species on the overall diffusion rates of cations and (include) the effects of anion exclusion.

- Coupling the sorption and diffusion models.
- Linking batch sorption data to transport experiments (attention to sorption competition effects) reflecting pore system heterogeneity by conventional description of diffusion process.
- Coupling physico-chemical alterations (mineral assemblage and pore structure geometry) in near- and far-field repositories to diffusive species transport.
- Appropriately using diffusion databases in safety assessment models.

### Incorporation of radionuclides in solid phases

In addition to radionuclide retention via sorption, the incorporation of radionuclides in solid phases into waste matrices and along migration paths provides a different and very powerful retention mechanism. This is because incorporated radionuclides are not necessarily released upon contact of a solid with groundwater. This leads to partially irreversible entrapment as a strong safety factor for a repository system, if colloidal transport can be excluded. Important solids in this context are spent fuel and glass, their alteration products, as well as slowly forming and dissolving mineral phases (e.g., carbonates and sulfates) in the far field.

The mechanisms for irreversible entrapment need to be further and better characterized and modeled to enable the quantification of the long-term entrapment of key radionuclides ($^{14}C$, Se, and U). There is a strong need for understanding both thermodynamics and kinetics and how to incorporate these aspects in reactive transport models.

### Redox influence on radionuclide migration

Redox conditions influence radionuclide migration. Most repository concepts are based on a reducing environment. Under these conditions, actinides and technetium are merely present in a tetravalent redox state, forming solids with very low solubility. This is the principal reason why actinides only contribute a small amount to the overall radiological risk from a geological disposal facility. Much higher solubility and mobility are expected under oxidizing conditions.

Redox conditions can, however, be influenced by waste compounds introduced to the near field (e.g., nitrates and organic matter), and in this context, micro-organisms can also play an important role.

Post-closure safety case uncertainty would be reduced by improving the understanding of:

- The temporal and spatial evolution of redox conditions in engineered barrier systems (for instance, around metallic containers and overpacks and around steel reinforcement structures in concrete).
- The effect of redox perturbations (e.g., arising from the presence of nitrates/organic matter) able to modify the expected oxidation states and the mobility of radionuclides.

- The kinetics of radionuclide reduction/oxidation. Quantification of contributions related to homogeneous and heterogeneous redox reactions.
- The effect of radiolysis on the transport of radionuclides in the near field of a disposal facility. Spatial extension and time evolution of zones affected by radiolytic processes.
- The role of redox-active system constituents (e.g., minerals) on radionuclide mobility
- The knowledge of chemical speciation in source terms.

Further research should involve:

Development of geochemical models for the identification, simulation, and spatial monitoring of local and global anoxic conditions and/or redox transitions, including the associated modeling and transfer to realistic conditions.

Characterizing the mobility of radionuclides under well controlled redox conditions and complex perturbations (e.g., $pCO_2$, pH, and nitrate levels). There is also a need for well controlled chemical preparation techniques (e.g., reducing agents, purification methods, electrochemical techniques, and the use of a potentiostat) and speciation characterization methods for chemically conditioning radionuclides and tracer sources to be used for redox-sensitive elements before starting sorption and diffusion experiments.

Improve and extend our understanding of coupled sorption and electron-transfer interface reactions governing the retention of redox-sensitive RN on Fe(II)/Fe(III)-bearing minerals, including:

- Complementing TDBs.
- Improving the capacity of sorption models with respect to redox reactions.
- Correlating mineral properties to their retention capacity and reactivity.
- Transferring data from "simple to complex" systems: from dilute to compacted systems and from single minerals to natural host rocks.
- Integrating surface-controlled redox reactions into reactive transport codes.

Transport of strongly sorbing radionuclides

Strongly sorbing radionuclides are expected to move across a very short distance over geological time periods. Typical strongly sorbing nuclides are trivalent and tetravalent actinides and tetravalent technetium. The actual migration distance is difficult to assess and requires sophisticated solid-state analytical techniques. Migration distances can increase via complexation with organic ligands originating from waste and via complexation/colloid formation with naturally present DOM, even though retention remains very strong.

Even if strongly sorbing radionuclides in a deep geologic repository constitute only a small risk to the environment, a better understanding is desirable to increase confidence, exploring, for instance, the chemical degradation of cement-based materials, the presence of organic molecules, and saline groundwaters.

Further studies are needed to determine and to better:

- Represent heterogeneous media (e.g., cement-based materials, clay rock, crystalline rocks, bentonite, and corrosion products).
- Simulate anoxic environmental conditions in experiments.
- Predict the transport of strongly sorbing nuclides, which is commonly based on the use of so-called effective diffusion coefficients ($D_e$) and sorption distribution coefficients ($R_d$). Recent experimental evidence has demonstrated that $D_e$ values may depend on various characteristics of mineral surfaces and the pertinent pore water composition, as is the case for $R_d$ values. It is, therefore, imperative to further improve the physico-chemical basis for the use of appropriate $D_e$ values in safety assessment studies.
- Characterize the retention of redox-sensitive radionuclides or toxic elements.

Retardation via isotopic exchange

This refers to the case of $H^{14}CO_3^-$ isotopic exchange with calcite and other carbonates.

The first question to answer is whether this isotopic exchange process can be treated as pure sorption/retardation (linear and reversible equilibrium, $K_d$ approach?) or is it a true incorporation in the solid phase because of precipitation/dissolution equilibrium controlling the $^{14}C$-incorporation?

Effects of microbial perturbations on radionuclide migration

Microbes and fungal activity can influence radionuclide migration via biosorption, metabolic processes, and the formation of biofilms, among other processes. By releasing organic molecules (siderophores), microbes can produce soluble radionuclide complexes. Microbial activity can also influence the chemical environment and, in particular, the redox state of radionuclides. Nitrates can influence microbial activity. In the absence of microorganisms, the transformation of sulfate to sulfide is, extremely slow, while it is fast in presence of sulfate-reducing bacteria. There is a lot of sulfate in typical repository environments, and sulfide formation may strongly influence the near-field geochemical environment. The geochemical environment and the presence of gases (e.g., $H_2$, $CH_4$, and alkanes) strongly influence microbial populations and activities.

Based on previous and ongoing work (e.g., EC MIND project), the role of microbes is typically addressed in implementers' safety cases by bounding assumptions.

Bounding conditions for predictions of microbial activity may be required for performance assessments. Quantitative information on microbe populations, energy, and carbon source availability (site-specific and waste-specific) would be beneficial in this context.

The impact of microbes on the chemical environment needs to be considered as a function of time to understand and quantify the fate and impact of microbial activity on radionuclide migration.

Assessment of the influence of gas on geochemistry and microbial activity in the near field should be performed by considering void spaces, the release of hydrogen, organic ligands, nitrates, sulfides, and methane, to assess the impact on barrier performance and radionuclide migration.

It would be beneficial to develop methods to upscale from phenomenological descriptions to mechanistic models.

### Organic–radionuclide migration

It is likely that a variety of organic substances will be part of any disposal concept, either from the waste inventory, as superplasticizers or admixture for concrete structures, or from pre-existing organic matter in geological formations. It is possible to consider a variety of substances, likely to be present and known for their stability, mobility, and radionuclide complexation in laboratory (and *in situ*) transport experiments and models. An example of a very organic-rich waste type is bituminized waste. Organic matter can influence radionuclide migration by creating soluble or colloidal complexes with radionuclides, which would otherwise be insoluble, or by blocking sorption sites. Hyperalkaline water may increase the solubility and mobility of organic matter (R–COOH and Ø–OH dissociation at high pH) along with entrained admixture compounds (such as superplasticizers) arising from cementitious systems. In compact clay rocks present at depth, only small organic molecules can be transported, whereas larger ones are filtered in clay pores.

Further research is required to enhance the understanding of the role of organics (either naturally occurring in clay formations or introduced in wastes and in engineered barrier materials) and their influence on radionuclide migration.

More specifically: (i) the nature of organic molecules generated by organic waste or admixture degradation, (ii) their stability with time, (iii) their effects on radionuclide migration (speciation, solubility, retention, and diffusion as a complex organic/radionuclide), (iv) the effect of cocktails of organic molecules, (v) the nature and release rate of organic compounds resulting from polymer radiolysis and hydrolysis, and (vi) implementation in a reactive transfer model require research.

There is also a need for acquisition of thermodynamic data on these organics for feeding into databases.

### Colloid influence on radionuclide migration

Colloids can be organic or inorganic. Their size is typically smaller than 0.5 μm; therefore, they do not settle during groundwater transport. In a repository, colloids may pre-exist in the groundwater system, or they may be generated via the interaction of groundwater with repository components. Important examples are smectite colloids formed via the interaction of glacial melt water with bentonites (peptization at low ionic strength). Clay rock and swelling clay backfills are filters against colloid transport, which is well documented (BELBaR EC project). When colloids are filtered, they do not contribute to radionuclide migration. When colloids are mobile, colloidal transport is particularly important for radionuclide migration, especially for radionuclides, which are sparingly soluble and strongly sorbed.

An improved understanding of the role of colloid generation and transport for different host rocks is required to increase confidence in post-closure safety cases, such as:

- Mechanistic descriptions of the RN–colloid interaction (e.g., kinetics of complexation, and stability).
- Colloid interaction with the solid (sorption-like).
- Colloid straining/filtering behavior: size-dependent transport.
- Reactive transport modeling of colloid migration and retention: implementation of new insights into the enhanced/inhibited particle retention on rough mineral/rock surfaces.

### Temperature influence on radionuclide migration

Elevated temperatures may change the migration behavior of radionuclides by changing the sorption constants of RN speciation, by changing diffusion coefficients in porous media, or by influencing the stabilities of minerals or organic matter. There are only a few studies on the effect of temperature increases on radionuclide migration and sorption.

There is a need to support concept optimization by studying the temperature effects on groundwater composition, solid-phase transformations, and, for some key radionuclides, the effects of elevated temperature on radionuclide speciation, solubility, sorption, and diffusion.

### Fracture filling

Most groundwater flow and, thus, radionuclide migration in higher-strength rocks take place through a network of interconnected fractures. Fractures become filled with precipitating minerals over time. How this happens depends on various factors, including temperature and reaction kinetics. This may influence the porosity, permeability, organic surface coating, microbial communities, and eventually the sorption of long-lived radionuclides on mineral surfaces.

A thorough understanding of the processes of fracture filling by precipitating minerals with a focus on precipitation kinetics is required to support the safety case of a geological disposal facility for higher-strength rock.

Moreover, fracture system characterization, including pore distribution and sorption properties, in both fracture filling and crystalline host rock is necessary in order to reflect the reality of transport pathway properties. Evaluation of system heterogeneity in connection with retention processes is inevitable.

Investigation of pore networks and the surface topography/rugosity of fractured crystalline rock samples with mineral infills:

- The impact of surface potential variability; the role of grain boundaries; the effect of water saturation, content, and chemistry (pH and ionic strength); as well as the impact of pore size variability (nanometer pore scale: mesopores/macropores).
- Analysis of the velocity field (diffusive vs. advective transport) in and close to fractures, using PET techniques.
- Derivation and quantification of parameter uncertainties to be used in transport modeling in fractured rock.

### Rock matrix diffusion

For relevant long-term safety radionuclides, it would be beneficial to gain an improved understanding of the impact of rock-matrix diffusion on travel time through the geosphere, including the anion exclusion effect, in the development of safety cases. Moreover, a realistic reflection of system heterogeneity would be desirable.

Heterogeneity

The near and far field surrounding a Geological Disposal Facility is likely to be subject to heterogeneities that are unlikely to be fully represented in models; for example, from a flow perspective, heterogeneities are either generated via the construction of a repository (e.g., voids and EDZ) or exist locally in the geological environment. Integrated modeling taking into account these heterogeneities can provide significant benefits:

- To undertake phenomenological and safety studies to take into account heterogeneities of a system (mineralogy, hydrology, water composition, permeability, porosity, and fracture networks).
- To achieve a modeling capability that can integrate available site data to account for heterogeneities in the near field.

Performance assessment tools

Modern numerical simulations are efficient tools for addressing the complexity of the flow and transport of radionuclides in porous media at large time and space scales. However, the quality of results depend on the accuracy of the input data, and the influence of each input parameter can also be difficult to quantify (sensitivity analysis and uncertainties). As a result, many mathematical methods to treat parameter sensitivity/uncertainties have been developed, which should be assessed and possibly improved in view of performance assessment calculations.

Research should aim at:

- improving mathematical methods to: (i) analyze the importance of the model input parameters of a simulation on the relevant output of the simulation (sensitivity analysis) and (ii) quantify the effect of uncertainties on these outputs (uncertainty analysis).
- developing a systematic procedure to analyze the data quality and to quantify the input data uncertainty in order to assess the confidence level of the model results.

Upscaling in support of performance assessment

Upscaling strategies (including bottom-up approaches) are developed to support and justify hypotheses, parameters, and models used in performance assessment calculations. They are based on the understanding and modeling of fundamental processes from the micro-to-macroscopic scale, taking into account spatial heterogeneity, including the multi-scale structuration of rocks/materials.

Upscaling strategy development should aim towards:

- understanding the role of physical/chemical processes at different scales and linking bottom-up and top-down approaches in performance assessments.
- extending upscaling to the materials involved in radioactive waste disposal, such as cementitious-based materials.
- developing multi-scale approaches for coupled processes (including chemical, hydraulic, and mechanical processes).
- developing multi-scale strategies to represent complex phenomena (e.g., redox processes, microbial activity, and mineral transformation).

## Author contributions

NM: Conceptualization, Writing–original draft, Writing–review and editing. SC: Writing–original draft, Writing–review and editing. MG: Writing–original draft. BB: Writing–original draft. RD: Writing–original draft. SG: Writing–original draft. LC: Writing–original draft. FB: Writing–original draft. JP: Writing–original draft. AH: Writing–original draft. VH: Writing–original draft. CF: Writing–original draft. UN: Writing–original draft. SB: Writing–original draft. MS-K: Writing–original draft. OF: Writing–original draft. TM: Writing–original draft.

## Funding

The author(s) declare that financial support was received for the research, authorship, and/or publication of this article. This document is a deliverable of the European Joint Programme on Radioactive Waste Management (EURAD). EURAD has received funding from the European Union's Horizon 2020 research and innovation programme under grant agreement No. 847593.

## Acknowledgments


## Conflict of interest

The authors declare that the research was conducted in the absence of any commercial or financial relationships that could be construed as a potential conflict of interest.

## Publisher's note

# References


Aeppli, M., Voegelin, A., Gorski, C. A., Hofstetter, T. B., and Sander, M. (2018). Mediated electrochemical reduction of iron (Oxyhydr-)Oxides under defined thermodynamic boundary conditions. *Environ. Sci. & Technol.* 52, 560–570. doi:10.1021/acs.est.7b04411

Aertsens, M. (2013). *Overview of migration experiments in the HADES underground research facility at mol SCK CEN-ER164. Mol, Belgium: SCK-CEN.*

Aertsens, M., DE Canniere, P., Lemmens, K., Maes, N., and Moors, H. (2008a). Overview and consistency of migration experiments in clay. *Phys. Chem. Earth* 33, 1019–1025. doi:10.1016/j.pce.2008.05.019

Aertsens, M., DE Cannière, P., Moors, H., and VAN Gompel, M. (2009a). "Effect of ionic strength on the transport parameters of tritiated water, iodide and $H^{14}CO_3^-$ in Boom Clay," in *Scientific basis for nuclear waste management XXXIII*. Editors B. E. BURAKOV and A. S. ALOY, 497–504.

Aertsens, M., Dierckx, A., Moors, H., DE Canniere, P., and Maes, N. (2010a). *Vertical distribution of H14CO3- transport parameters in Boom Clay in the Mol-1 borehole (Mol, Belgium) and comparison with data from independent measurements SCK CEN-ER66*. Mol, Belgium: SCK-CEN, Belgium Nuclear Research Centre.

Aertsens, M., Dierckx, A., Put, M., Moors, H., Janssen, K., VAN Ravestyn, L., et al. (2005a). *Determination of the hydraulic conductivity, the product ηR of the porosity η and the retardation factor R, and the apparent diffusion coefficient Dp on Boom Clay cores from the Mol-1 drilling SCK CEN-R3503*. Mol, Belgium: Belgian Nuclear Research Centre.

Aertsens, M., Dierckx, A., Put, M., Moors, H., Janssen, K., VAN Ravestyn, L., et al. (2005b). *Determination of the hydraulic conductivity, ηR and the apparent diffusion coefficient on Ieper Clay and Boom Clay cores from the Doel-1 and Doel-2b drillings SCK CEN-R3589*. Mol, Belgium: SCK-CEN, Belgian Nuclear Research Centre.

Aertsens, M., Govaerts, J., Maes, N., and VAN Laer, L. (2012). Consistency of the strontium transport parameters in Boom Clay obtained from different types of experiments: accounting for the filter plates. *MRS Proc.* 1475, 583–588. doi:10.1557/opl.2012.636

Aertsens, M., Maes, N., Govaerts, J., and Durce, D. (2020). Why tracer migration experiments with a pressure gradient do not always allow a correct estimation of the accessible porosity in clays. *Appl. Geochem.* 120, 104672. doi:10.1016/j.apgeochem.2020.104672

Aertsens, M., Maes, N., Labat, S., VAN Gompel, M., and Maes, T. (2010b). *Vertical distribution of HTO and 125I- transport parameters in Boom Clay in the Essen-1 borehole (Belgium) SCK CEN-ER67*. Mol, Belgium: SCK-CEN, Belgium Nuclear Research Centre.

Aertsens, M., Maes, N., and VAN Gompel, M. (2009b). "Consistency of the strontium transport parameters in Boom Clay obtained from different types of migration experiments," in *Scientific basis for nuclear waste management XXXIII*. Editors B. E. BURAKOV and A. S. ALOY, 421–428.

Aertsens, M., Maes, N., VAN Ravestyn, L., and Brassinnes, S. (2013). Overview of radionuclide migration experiments in the HADES underground research facility at mol (Belgium). *Clay Miner.* 48, 153–166. doi:10.1180/claymin.2013.048.2.01

Aertsens, M., Put, M., and Dierckx, A. (2003). An analytical model for the interpretation of pulse injection experiments performed for testing the spatial variability of clay formations. *J. Contam. Hydrology* 61, 423–436. doi:10.1016/s0169-7722(02)00118-3

Aertsens, M., VAN Gompel, M., DE Canniere, P., Maes, N., and Dierckx, A. (2008b). Vertical distribution of transport parameters in boom clay in the mol-1 borehole (mol, Belgium). *Phys. Chem. Earth* 33, S61–S66. doi:10.1016/j.pce.2008.10.060

Aertsens, M., VAN Laer, L., Maes, N., and Govaerts, J. (2017). An improved model for through-diffusion experiments: application to strontium and tritiated water (HTO) diffusion in Boom Clay and compacted illite. *Geol. Soc. Lond. Spec. Publ.* 443, 205–210. doi:10.1144/sp443.9

Aertsens, M., Weetjens, E., Govaerts, J., Maes, N., and Brassinnes, S. (2023). CP1 and Tribicarb-3D: unique long-term and large-scale *in situ* migration tests in boom clay at the HADES underground research laboratory. *Geol. Soc. Lond. Spec. Publ.* 536, 131–144. doi:10.1144/sp536-2022-41

Aertsens, M., Wemaere, I., and Wouters, L. (2004). Spatial variability of transport parameters in the Boom Clay. *Appl. Clay Sci.* 26, 37–45. doi:10.1016/j.clay.2003.09.015

Ahmed, I. A. M., and Hudson-Edwards, K. A. (2017). *Redox-reactive minerals: properties, reactions and applications in clean Technologies, mineralogical Society of great Britain and Ireland*.

Aldaba, D., Glaus, M., Leupin, O., VAN Loon, L., Vidal, M., and Rigol, A. (2014). Suitability of various materials for porous filters in diffusion experiments. *Radiochim. Acta* 102, 723–730. doi:10.1515/ract-2013-2176

Alexander, W. R., and Frieg, B. (2009). *Grimsel test site investigation Phase IV the Nagra-JAEA* in situ *study of safety relevant radionuclide retardation in fractured crystalline rock III: the RRP project final report NTB-00-07*.

Alexander, W. R., Ota, K., and Frieg, B. (2003). *The Nagra-JNC* in situ *study of safety relevant radionuclide retardation in fractured crystalline rock. II: the RRP project methodology development, field and laboratory tests*.

Alexandrov, V., and Rosso, K. M. (2013). Insights into the mechanism of Fe(II) adsorption and oxidation at Fe–clay mineral surfaces from first-principles calculations. *J. Phys. Chem. C* 117, 22880–22886. doi:10.1021/jp4073125

Allison, J. D., Brown, D. S., and Novo-Gradac, K. J. (1991). *MINTEQA2/PRODEFA2, a geochemical assessment model for environmental systems: Version 3. 0 user's manual*. Athens, GA (United States): Environmental Protection Agency.

AL Mahrouqi, D., Vinogradov, J., and Jackson, M. D. (2017). Zeta potential of artificial and natural calcite in aqueous solution. *Adv. Colloid Interface Sci.* 240, 60–76. doi:10.1016/j.cis.2016.12.006

Alonso, U., Missana, T., Garcia-Gutierrez, M., Patelli, A., Rigato, V., and Ceccato, D. (2013). "Ion beam analyses of radionuclide migration in heterogeneous rocks," in *Multidisciplinary applications of nuclear physics with ion beams*. Editors R. A. RICCI, V. RIGATO, and P. MAZZOLDI (Melville: Amer Inst Physics).

Alonso, U., Missana, T., Garcia-Gutierrez, M., Patelli, A., Siitari-Kauppi, M., and Rigato, V. (2009). Diffusion coefficient measurements in consolidated clay by RBS micro-scale profiling. *Appl. Clay Sci.* 43, 477–484. doi:10.1016/j.clay.2008.12.005

Alonso, U., Missana, T., Patelli, A., Ceccato, D., Garcia-Gutierrez, M., and Rigato, V. (2014). Se(IV) uptake by Aspo diorite: micro-scale distribution. *Appl. Geochem.* 49, 87–94. doi:10.1016/j.apgeochem.2014.06.013

Altmaier, M., Gaona, X., Fellhauer, D., and Buckau, G. (2010). *Intercomparison of redox determination methods on designed and near-natural aqueous system: FP 7 EURATOM Collaborative project "redox phenomena controlling systems"*. KIT Scientific Reports; 7572.

Altmann, S., Aertsens, M., Appelo, C. A. J., Bruggeman, C., Gaboreau, S., Glaus, M. A., et al. (2015). *Processes of cation migration in clayrocks: final scientific report of the CatClay European Project CEA-R6410*. France: CEA.

Andersson, P., Byegaard, J., Dershowitz, B., Doe, T., Hermanson, J., Meier, P., et al. (2002a). *Final report of the TRUE Block Scale project 1 Characterisation and model development SKB-TR-02-13. Sweden*.

Andersson, P., Byegaard, J., and Winberg, A. (2002b). *Final report of the TRUE Block Scale project 2 Tracer tests in the block scale SKB-TR-02-14. Sweden*.

ANDRA (2005). *Dossier 2005 Argile: safety evaluation of a geological repository*. Paris: ANDRA.

ANDRA (2016). *Dossier d'options de Sûreté partie après fermeture (DOS-AF)*. France: ANDRA.

ANDRA (2018a). *La migration des radionucléides et des toxiques chimiques dans le Callovo-Oxfordien*. France: ANDRA.

ANDRA (2018b). *Les propriétés de transfert naturel des solutés dans le Callovo-Oxforiden Fiche Bilan CG.FI.ASTR.18.0010*. France: ANDRA.

André, M., Malmström, M. E., and Neretnieks, I. (2009). Determination of sorption properties of intact rock samples: new methods based on electromigration. *J. Contam. Hydrology* 103, 71–81. doi:10.1016/j.jconhyd.2008.09.006

Antonellini, M., Mollema, P. N., and Del Sole, L. (2017). Application of analytical diffusion models to outcrop observations: implications for mass transport by fluid flow through fractures. *Water Resour. Res.* 53, 5545–5566. doi:10.1002/2016wr019864

Appelo, C. A. J., and Postma, D. (2004). *Geochemistry, groundwater and pollution*. London: CRC Press.

Appelo, C. A. J., VAN Loon, L. R., and Wersin, P. (2010). Multicomponent diffusion of a suite of tracers (HTO, Cl, Br, I, Na, Sr, Cs) in a single sample of Opalinus Clay. *Geochimica Cosmochimica Acta* 74, 1201–1219. doi:10.1016/j.gca.2009.11.013

Appelo, C. A. J., and Wersin, P. (2007). Multicomponent diffusion modeling in clay systems with application to the diffusion of tritium, iodide, and sodium in opalinus clay. *Environ. Sci. & Technol.* 41, 5002–5007. doi:10.1021/es0629256

Aqvist, J. (1990). Ion-water interaction potentials derived from free energy perturbation simulations. *J. Phys. Chem.* 94, 8021–8024. doi:10.1021/j100384a009

Arnold, T., Zorn, T., Zänker, H., Bernhard, G., and Nitsche, H. (2001). Sorption behavior of U(VI) on phyllite: experiments and modeling. *J. Contam. Hydrol.* 47, 219–231. doi:10.1016/s0169-7722(00)00151-0

Aromaa, H., Voutilainen, M., Ikonen, J., Yli-Kaila, M., Poteri, A., and Siitari-Kauppi, M. (2019). Through diffusion experiments to study the diffusion and sorption of HTO, Cl, Ba and Cs in crystalline rock. *J. Contam. Hydrology* 222, 101–111. doi:10.1016/j.jconhyd.2019.03.002

Asaad, A., Hubert, F., Dazas, B., Razafitianamaharavo, A., Brunet, J., Glaus, M. A., et al. (2022). A baseline study of mineralogical and morphological properties of different size fractions of illite du Puy. *Appl. Clay Sci.* 224, 106517. doi:10.1016/j.clay.2022.106517

Asaad, A., Hubert, F., Ferrage, E., Dabat, T., Paineau, E., Porion, P., et al. (2021). Role of interlayer porosity and particle organization in the diffusion of water in swelling clays. *Appl. Clay Sci.* 207, 106089. doi:10.1016/j.clay.2021.106089

Astilleros, J. M., Pina, C. M., Fernández-Díaz, L., and Putnis, A. (2003). Supersaturation functions in binary solid solution–aqueous solution systems. *Geochimica Cosmochimica Acta* 67, 1601–1608. doi:10.1016/s0016-7037(02)01166-3

Bach, D., Christiansen, B. C., Schild, D., and Geckeis, H. (2014). TEM study of green rust sodium sulphate ($GR_{Na,SO4}$) interacted with Neptunyl ions ($NpO_2^+$). *Radiochim. Acta* 102, 279–289. doi:10.1515/ract-2013-2105

Badaut, V., Schlegel, M. L., Descostes, M., and Moutiers, G. (2012). *In situ* time-resolved X-ray near-edge absorption spectroscopy of selenite reduction by siderite. *Environ. Sci. & Technol.* 46, 10820–10826. doi:10.1021/es301611e

Baeyens, B., and Bradbury, M. H. (1991). *A physico-chemical characterisation technique for determining the porewater chemistry in argillaceous rocks*. NAGRA NTB 90-40. Switzerland: NAGRA.

Baeyens, B., and Bradbury, M. H. (1995). "A quantitative mechanistic description of Ni, Zn and Ca sorption on Na-Montmorillonite. Part I: physico-chemical characterisation and titration measurements,". Swizerland: PSI.

Baeyens, B., and Bradbury, M. H. (1997). A mechanistic description of Ni and Zn sorption on Na-montmorillonite Part I: titration and sorption measurements. *J. Contam. Hydrology* 27, 199–222. doi:10.1016/s0169-7722(97)00008-9

Baeyens, B., and Bradbury, M. H. (2017). *The development of a thermodynamic sorption database for montmorillonite and the application to bentonite PSI Bericht 95-10/ NAGRA NTB 95-04*. Switzerland: PSI.

Baeyens, B., and Marques Fernandes, M. (2018). Adsorption of heavy metals including radionuclides. *Dev. Clay Sci.* 9, 125–172. doi:10.1016/b978-0-08-102432-4.00005-6

Baeyens, B., Marques Fernandes, M., and Bradbury, M. H. (2014a). *Comparison of sorption measurements on argillaceous rocks and bentonite with predictions using the SGT-E2 Approach to derive sorption data bases NAGRA NTB 12-05*. Switzerland: NAGRA.

Baeyens, B., Thoenen, T., Bradbury, M., and Marques Fernandes, M. (2014b). *Sorption data bases for the host rocks and lower confining units and bentonite for provisional safety analysis for SGT-E2 NAGRA NTB 12-04*. Switzerland: NAGRA.

Bahl, S., Peuge, S., Pidchenko, I., Pruessmarm, T., Rothe, J., Dardenne, K., et al. (2017). Pu coexists in three oxidation states in a Borosilicate glass: implications for Pu solubility. *Inorg. Chem.* 56, 13982–13990. doi:10.1021/acs.inorgchem.7b02118

Banik, N. L., Marsac, R., Lutzenkirchen, J., Diascorn, A., Bender, K., Marquardt, C. M., et al. (2016). Sorption and redox speciation of plutonium at the illite surface. *Environ. Sci. & Technol.* 50, 2092–2098. doi:10.1021/acs.est.5b05129

Banik, N. L., Marsac, R., Lutzenkirchen, J., Marquardt, C. M., Dardenne, K., Rothe, J., et al. (2017). Neptunium sorption and redox speciation at the illite surface under highly saline conditions. *Geochimica Cosmochimica Acta* 215, 421–431. doi:10.1016/j.gca.2017.08.008

Barbier, F., Duc, G., and Petit-Ramel, M. (2000). Adsorption of lead and cadmium ions from aqueous solution to the montmorillonite/water interface. *Colloids Surfaces A Physicochem. Eng. aspects* 166, 153–159. doi:10.1016/s0927-7757(99)00501-4

Bardot, F., Villieras, F., Michot, L. J., Francois, M., Gerard, G., and Cases, J. M. (1998). High resolution gas adsorption study on illites permuted with various cations: assessment of surface energetic properties. *J. Dispersion Sci. Technol.* 19, 739–759. doi:10.1080/01932699808913212

Batrice, R. J., Wacker, J. N., and Knope, K. E. (2016). "Speciation of actinide complexes, clusters, and Nanostructures in solution," in *Experimental and theoretical approaches to actinide chemistry* (Wiley).

Bazer-Bachi, F., Descostes, M., Tevissen, E., Meier, P., Grenut, B., Simonnot, M. O., et al. (2007). Characterization of sulphate sorption on Callovo-Oxfordian argillites by batch, column and through-diffusion experiments. *Phys. Chem. Earth* 32, 552–558. doi:10.1016/j.pce.2006.01.010

Bazer-Bachi, F., Tevissen, E., Descostes, M., Grenut, B., Meier, P., Simonnot, M. O., et al. (2006). Characterization of iodide retention on Callovo-Oxfordian argillites and its influence on iodide migration. *Phys. Chem. Earth* 31, 517–522. doi:10.1016/j.pce.2006.04.015

Beauwens, T., DE Canniere, P., Moors, H., Wang, L., and Maes, N. (2005). Studying the migration behaviour of selenate in Boom Clay by electromigration. *Eng. Geol.* 77, 285–293. doi:10.1016/j.enggeo.2004.07.019

Begg, J. D., Zavarin, M., and Kersting, A. B. (2017). Desorption of plutonium from montmorillonite: an experimental and modeling study. *Geochimica Cosmochimica Acta* 197, 278–293. doi:10.1016/j.gca.2016.10.006

Begg, J. D., Zavarin, M., Tumey, S. J., and Kersting, A. B. (2015). Plutonium sorption and desorption behavior on bentonite. *J. Environ. Radioact.* 141, 106–114. doi:10.1016/j.jenvrad.2014.12.002

Bender, W. M., and Becker, U. (2019). Quantum-mechanical investigation of the structures and energetics of uranium and plutonium incorporated into the magnetite ($Fe_3O_4$) lattice. *ACS Earth Space Chem.* 3, 637–651. doi:10.1021/acsearthspacechem.8b00167

Benedicto, A., Begg, J. D., Zhao, P., Kersting, A. B., Missana, T., and Zavarin, M. (2014a). Effect of major cation water composition on the ion exchange of Np (V) on montmorillonite: NpO2+–Na+–K+–Ca2+–Mg2+ selectivity coefficients. *Appl. Geochem.* 47, 177–185. doi:10.1016/j.apgeochem.2014.06.003

Benedicto, A., Degueldre, C., and Missana, T. (2014b). Gallium sorption on montmorillonite and illite colloids: experimental study and modelling by ionic exchange and surface complexation. *Appl. Geochem.* 40, 43–50. doi:10.1016/j.apgeochem.2013.10.015

Benedicto, A., Missana, T., and Fernández, A. M. (2014c). Interlayer collapse affects on cesium adsorption onto illite. *Environ. Sci. & Technol.* 48, 4909–4915. doi:10.1021/es5003346

Benson, L. (1982). A tabulation and evaluation of ion exchange data on smectites. *Environ. Geol.* 4, 23–29. doi:10.1007/bf02380496

Berg, S., Rücker, M., Ott, H., Georgiadis, A., VAN DER Linde, H., Enzmann, F., et al. (2016). Connected pathway relative permeability from pore-scale imaging of imbibition. *Adv. Water Resour.* 90, 24–35. doi:10.1016/j.advwatres.2016.01.010

Berkowitz, B. (2002). Characterizing flow and transport in fractured geological media: a review. *Adv. Water Resour.* 25, 861–884. doi:10.1016/s0309-1708(02)00042-8

Bernier, F., Li, X. L., Bastiaens, W., Ortiz, L., VAN Geet, M., Wouters, L., et al. (2007). *Fractures and self-healing within the excavation disturbed zone in clays (SELFRAC) EUR 22585. EC.*

Bethke, C., and Yeakel, S. (2016). *The Geochemist's Workbench: release 11*. Champain, Illinois, USA: GWB Essentials Guide.

Bildstein, O., and Claret, F. (2015). "Stability of clay barriers under chemical perturbations," in *Natural and Engineerd clay barriers*. Editors C. TOURNASSAT, C. I. STEEFEL, I. C. BOURG, and F. BERGAYA (Amsterdam: Elsevier).

Birgersson, M., and Karnland, O. (2009). Ion equilibrium between montmorillonite interlayer space and an external solution-Consequences for diffusional transport. *Geochimica Cosmochimica Acta* 73, 1908–1923. doi:10.1016/j.gca.2008.11.027

Bishop, M. E., Dong, H., Kukkadapu, R. K., Liu, C., and Edelmann, R. E. (2011). Bioreduction of Fe-bearing clay minerals and their reactivity toward pertechnetate (Tc-99). *Geochimica Cosmochimica Acta* 75, 5229–5246. doi:10.1016/j.gca.2011.06.034

Bleyen, N., Marien, A., and Valcke, E. (2018). *The geochemical perturbations of Boom Clay due to the $NaNO_3$ plume released from Eurobitumen bituminised radioactive waste: status 2013 SCK CEN-ER0221*. Mol, Belgium: SCK-CEN, Belgium Nuclear Research Centre.

Bock, H., Dehandschutter, B., Martin, C., Mazurek, M., DE Haller, A., Skoczylas, F., et al. (2010). *Self-sealing of fractures in argillaceous formations in the context of geological disposal of radioactive waste NEA report 6184*. France: OECD.

Bodin, J., Delay, F., and DE Marsily, G. (2003). Solute transport in a single fracture with negligible matrix permeability: 1. fundamental mechanisms. *Hydrogeology J.* 11, 418–433. doi:10.1007/s10040-003-0268-2

Boland, D. D., Collins, R. N., Payne, T. E., and Waite, T. D. (2011). Effect of Amorphous Fe(III) oxide transformation on the Fe(II)-Mediated reduction of U(VI). *Environ. Sci. & Technol.* 45, 1327–1333. doi:10.1021/es101848a

Bollermann, T., Yuan, T., Kulenkampff, J., Stumpf, T., and Fischer, C. (2022). Pore network and solute flux pattern analysis towards improved predictability of diffusive transport in argillaceous host rocks. *Chem. Geol.* 606, 120997. doi:10.1016/j.chemgeo.2022.120997

Bonen, D. (1992). Composition and appearance of magnesium silicate hydrate and its relation to Deterioration of cement-based materials. *J. Am. Ceram. Soc.* 75, 2904–2906. doi:10.1111/j.1151-2916.1992.tb05530.x

Bonnet, M., Sardini, P., Billon, S., Siitari-Kauppi, M., Kuva, J., Fonteneau, L., et al. (2020). Determining Crack aperture distribution in rocks using the 14 C-PMMA autoradiographic method: experiments and simulations. *J. Geophys. Res. Solid Earth* 125. doi:10.1029/2019jb018241

Borgia, A., Pruess, K., Kneafsey, T. J., Oldenburg, C. M., and Pan, L. (2012). Numerical simulation of salt precipitation in the fractures of a CO2-enhanced geothermal system. *Geothermics* 44, 13–22. doi:10.1016/j.geothermics.2012.06.002

Börsig, N., Scheinost, A. C., Shaw, S., Schild, D., and Neumann, T. (2018). Retention and multiphase transformation of selenium oxyanions during the formation of magnetite via iron(II) hydroxide and green rust. *Dalton Trans.* 47, 11002–11015. doi:10.1039/c8dt01799a

Bosbach, D., Brandt, F., Bukaemskiy, A., Deissmann, G., Kegler, P., Klinkenberg, M., et al. (2020). Research for the Safe management of nuclear waste at Forschungszentrum Jülich: materials chemistry and solid solution aspects. *Adv. Eng. Mater.* 22, 1901417. doi:10.1002/adem.201901417

Bossart, P., Bernier, F., Birkholzer, J., Bruggeman, C., Connolly, P., Dewonck, S., et al. (2017). Mont Terri rock laboratory, 20 years of research: introduction, site characteristics and overview of experiments. *Swiss J. Geosciences* 110, 3–22. doi:10.1007/978-3-319-70458-6_1

Bostick, B. C., Vairavamurthy, M. A., Karthikeyan, K. G., and Chorover, J. (2002). Cesium adsorption on clay minerals: an EXAFS spectroscopic investigation. *Environ. Sci. & Technol.* 36, 2670–2676. doi:10.1021/es0156892

Boult, K., Cowper, M., Heath, T., Sato, H., Shibutani, T., and Yui, M. (1998). Towards an understanding of the sorption of U (VI) and Se (IV) on sodium bentonite. *J. Contam. Hydrology* 35, 141–150. doi:10.1016/s0169-7722(98)00122-3

Bourg, I. C., Bourg, A. C. M., and Sposito, G. (2003). Modeling diffusion and adsorption in compacted bentonite: a critical review. *J. Contam. Hydrology* 61, 293–302. doi:10.1016/s0169-7722(02)00128-6

Bourg, I. C., Lee, S. S., Fenter, P., and Tournassat, C. (2017). Stern layer structure and energetics at mica-water interfaces. *J. Phys. Chem. C* 121, 9402–9412. doi:10.1021/acs.jpcc.7b01828

Bourg, I. C., and Sposito, G. (2010). Connecting the molecular scale to the continuum scale for diffusion processes in smectite-rich porous media. *Environ. Sci. & Technol.* 44, 2085–2091. doi:10.1021/es903645a

Bourg, I. C., and Sposito, G. (2011). Molecular dynamics simulations of the electrical double layer on smectite surfaces contacting concentrated mixed electrolyte (NaCl–CaCl2) solutions. *J. Colloid Interface Sci.* 360, 701–715. doi:10.1016/j.jcis.2011.04.063

Bourg, I. C., Sposito, G., and Bourg, A. C. (2007). Modeling the acid–base surface chemistry of montmorillonite. *J. Colloid Interface Sci.* 312, 297–310. doi:10.1016/j.jcis.2007.03.062

Bourg, I. C., and Tournassat, C. (2015). "Chapter 6 - self-diffusion of water and ions in clay barriers," in *Developments in clay science*. Editors C. TOURNASSAT, C. I. STEEFEL, I. C. BOURG, and F. BERGAYA (Elsevier).

Bradbury, M. H., and Baeyens, B. (1997a). *Far-field sorption database for performance assessment of a L/ILW repository in an undisturbed Palfris Marl host rock NAGRA NTB 96-05*. Switzerland: NAGRA.

Bradbury, M. H., and Baeyens, B. (1997b). A mechanistic description of Ni and Zn sorption on Na-montmorillonite Part II: modelling. *J. Contam. Hydrology* 27, 223–248. doi:10.1016/s0169-7722(97)00007-7

Bradbury, M. H., and Baeyens, B. (2000). A generalised sorption model for the concentration dependent uptake of caesium by argillaceous rocks. *J. Contam. Hydrology* 42, 141–163. doi:10.1016/s0169-7722(99)00094-7

Bradbury, M. H., and Baeyens, B. (2003a). *Far field sorption data bases for performance assessment of a high-level radioactive waste repository in an undisturbed Opalinus Clay host rock PSI Bericht 03-08*. Switzerland: Paul Scherrer Institut.

Bradbury, M. H., and Baeyens, B. (2003b). *Near-field sorption database for compacted MX-80 bentonite for performance assessment of a high-level radioactive waste repository in Opalinus Clay host rock NAGRA NTB 02-18*. Switzerland: NAGRA.

Bradbury, M. H., and Baeyens, B. (2005a). Modelling the sorption of Mn(II), Co(II), Ni(II), Zn(II), Cd(II), Eu(III), Am(III), Sn(IV), Th(IV), Np(V) and U(VI) on montmorillonite: linear free energy relationships and estimates of surface binding constants for some selected heavy metals and actinides. *Geochimica Cosmochimica Acta* 69, 875–892. doi:10.1016/j.gca.2004.07.020

Bradbury, M. H., and Baeyens, B. (2005b). Modelling the sorption of Mn(II), Co(II), Ni(II), Zn(II), Cd(II), Eu(III), Am(III), Sn(IV), Th(IV), Np(V) and U(VI) on montmorillonite: linear free energy relationships and estimates of surface binding constants for some selected heavy metals and actinides. *Geochimica Cosmochimica Acta* 69, 875–892. doi:10.1016/j.gca.2004.07.020

Bradbury, M. H., and Baeyens, B. (2009a). Sorption modelling on illite Part I: titration measurements and the sorption of Ni, Co, Eu and Sn. *Geochimica Cosmochimica Acta* 73, 990–1003. doi:10.1016/j.gca.2008.11.017

Bradbury, M. H., and Baeyens, B. (2009b). Sorption modelling on illite. Part II: actinide sorption and linear free energy relationships. *Geochimica Cosmochimica Acta* 73, 1004–1013. doi:10.1016/j.gca.2008.11.016

Bradbury, M. H., and Baeyens, B. (2011a). *Physico-chemical characterisation data and sorption measurements of Cs, Ni, Eu, Th, U, Cl, I and Se on MX-80 Bentonite PSI Bericht 11-05/NAGRA NTB 09-08*. Switzerland: PSI.

Bradbury, M. H., and Baeyens, B. (2011b). Predictive sorption modelling of Ni(II), Co(II), Eu(IIII), Th(IV) and U(VI) on MX-80 bentonite and Opalinus Clay: a "bottom-up" approach. *Appl. Clay Sci.* 52, 27–33. doi:10.1016/j.clay.2011.01.022

Bradbury, M., and Baeyens, B. (2017). *The development of a thermodynamic sorption data base for illite and the application to argillaceous rocks PSI Bericht 17/06/NAGRA NTB 17-14*. Switzerland: Paul Scherrer Institut.

Brandt, F., Curti, E., Klinkenberg, M., Rozov, K., and Bosbach, D. (2015). Replacement of barite by a (Ba,Ra)SO4 solid solution at close-to-equilibrium conditions: a combined experimental and theoretical study. *Geochimica Cosmochimica Acta* 155, 1–15. doi:10.1016/j.gca.2015.01.016

Brandt, F., Klinkenberg, M., Poonoosamy, J., Weber, J., and Bosbach, D. (2018). The effect of ionic strength and Sraq upon the uptake of Ra during the recrystallization of barite. *Minerals* 8, 502. doi:10.3390/min8110502

Breitner, D., Osán, J., Fábián, M., Zagyvai, P., Szabó, C., Dähn, R., et al. (2015). Characteristics of uranium uptake of Boda Claystone Formation as the candidate host rock of high level radioactive waste repository in Hungary. *Environ. Earth Sci.* 73, 209–219. doi:10.1007/s12665-014-3413-4

Breynaert, E., Bruggeman, C., and Maes, A. (2008). XANES-EXAFS analysis of se solid-phase reaction products formed upon contacting Se(IV) with FeS2 and FeS. *Environ. Sci. & Technol.* 42, 3595–3601. doi:10.1021/es071370r

Breynaert, E., Scheinost, A. C., Dom, D., Rossberg, A., Vancluysen, J., Gobechiya, E., et al. (2010). Reduction of Se(IV) in Boom Clay: XAS solid phase speciation. *Environ. Sci. & Technol.* 44, 6649–6655. doi:10.1021/es100569e

Britz, S. (2018). "Europium sorption experiments with muscovite, orthoclase, and qartz: modeling of surface complexation and reactive transport,". PhD Thesis (Germany: TUBraunschweig).

Brookshaw, D. R., Pattrick, R. A. D., Bots, P., Law, G. T. W., Lloyd, J. R., Mosselmans, J. F. W., et al. (2015). Redox interactions of Tc(VII), U(VI), and Np(V) with microbially reduced biotite and chlorite. *Environ. Sci. & Technol.* 49, 13139–13148. doi:10.1021/acs.est.5b03463

Brouwer, E., Baeyens, B., Maes, A., and Cremers, A. (1983). Cesium and rubidium ion equilibriums in illite clay. *J. Phys. Chem.* 87, 1213–1219. doi:10.1021/j100230a024

Bruggeman, C. (2006). *Assessment of the geochemical behaviour of selenium oxyanions under Boom Clay geochemical conditions*. PhD Thesis. Doctor (Belgium: KULeuven).

Bruggeman, C., Aertsens, M., Maes, N., and Salah, S. (2017a). *Iodine retention and migration behaviour in Boom Clay SCK CEN-ER0409*. Mol, Belgium: Studiecentrum voor Kernenergie.

Bruggeman, C., Maes, A., and Vancluysen, J. (2007). The identification of $FeS_2$ as a sorption sink for Tc(IV). *Phys. Chem. Earth* 32, 573–580. doi:10.1016/j.pce.2005.12.006

Bruggeman, C., and Maes, N. (2010). Uptake of uranium(VI) by pyrite under boom clay conditions: influence of dissolved organic carbon. *Environ. Sci. & Technol.* 44, 4210–4216. doi:10.1021/es100919p

Bruggeman, C., and Maes, N. (2017). *Radionuclide migration and retention in Boom clay SCK CEN-ER0345*. Mol, Belgium: Studiecentrum voor Kernenergie.

Bruggeman, C., Maes, N., Aertsens, M., Govaerts, J., Martens, E., Jacops, E., et al. (2017b). *Technetium retention and migration behaviour in Boom Clay SCK CEN-ER0403*. Mol, Belgium: Studiecentrum voor Kernenergie.

Bruggeman, C., Maes, N., Aertsens, M., and Salah, S. (2017c). *Tritiated water retention and migration behaviour in Boom Clay SCK CEN-ER0408*. Mol, Belgium: Studiecentrum voor Kernenergie.

Bruggeman, C., Maes, N., Christiansen, B. C., Stipp, S. L. S., Breynaert, E., Maes, A., et al. (2012). Redox-active phases and radionuclide equilibrium valence state in subsurface environments – new insights from 6th EC FP IP FUNMIG. *Appl. Geochem.* 27, 404–413. doi:10.1016/j.apgeochem.2011.09.010

Bruggeman, C., Salah, S., Maes, N., and Durce, D. (2017d). *Americium retention and migration behaviour in Boom Clay SCK CEN-ER0396*. Mol, Belgium: Studiecentrum voor Kernenergie.

BRUGGENWERT, M., and KAMPHORST, A. (1982). *Survey of experimental information on cation exchange in soil systems* (Elsevier).

Burgos, W. D. (2016). *Reactivity of iron-rich clays with uranium through redox transition zones*. United States: Pennsylvania State University.

Butorin, S. M., Kvashnina, K. O., Prieur, D., Rivenet, M., and Martin, P. M. (2017). Characteristics of chemical bonding of pentavalent uranium in La-doped UO2. *Chem. Commun.* 53, 115–118. doi:10.1039/c6cc07684j

Butorin, S. M., Kvashnina, K. O., Smith, A. L., Popa, K., and Martin, P. M. (2016a). Crystal-field and covalency effects in Uranates: an X-ray spectroscopic study. *Chemistry-a Eur. J.* 22, 9693–9698. doi:10.1002/chem.201505091

Butorin, S. M., Kvashnina, K. O., Vegelius, J. R., Meyer, D., and Shuh, D. K. (2016b). High-resolution X-ray absorption spectroscopy as a probe of crystal-field and covalency effects in actinide compounds. *Proc. Natl. Acad. Sci. U. S. A.* 113, 8093–8097. doi:10.1073/pnas.1601741113

Byrne, J. M., VAN DER Laan, G., Figueroa, A. I., Qafoku, O., Wang, C., Pearce, C. I., et al. (2016). Size dependent microbial oxidation and reduction of magnetite nano- and micro-particles. *Sci. Rep.* 6, 30969. doi:10.1038/srep30969

Cardona, A., Finkbeiner, T., and Santamarina, J. C. (2021). Natural rock fractures: from aperture to fluid flow. *Rock Mech. Rock Eng.* 54, 5827–5844. doi:10.1007/s00603-021-02565-1

Cevirim-Papaioannou, N., Yalcintas, E., Gaona, X., Dardenne, K., Altmaier, M., and Geckeis, H. (2018). Redox chemistry of uranium in reducing, dilute to concentrated NaCl solutions. *Appl. Geochem.* 98, 286–300. doi:10.1016/j.apgeochem.2018.07.006

Chagneau, A., Claret, F., Enzmann, F., Kersten, M., Heck, S., Madé, B., et al. (2015). Mineral precipitation-induced porosity reduction and its effect on transport parameters in diffusion-controlled porous media. *Geochem. Trans.* 16, 13. doi:10.1186/s12932-015-0027-z

Chakraborty, S., Favre, F., Banerjee, D., Scheinost, A. C., Mullet, M., Ehrhardt, J.-J., et al. (2010). U(VI) sorption and reduction by Fe(II) sorbed on montmorillonite. *Environ. Sci. & Technol.* 44, 3779–3785. doi:10.1021/es903493n

Charlet, L., Kang, M., Bardelli, F., Kirsch, R., Géhin, A., Grenèche, J.-M., et al. (2012). Nanocomposite pyrite–Greigite reactivity toward Se(IV)/Se(VI). *Environ. Sci. & Technol.* 46, 4869–4876. doi:10.1021/es204181q

Charlet, L., Scheinost, A. C., Tournassat, C., Greneche, J. M., Gehin, A., Fernandez-Martinez, A., et al. (2007). Electron transfer at the mineral/water interface: selenium reduction by ferrous iron sorbed on clay. *Geochimica Cosmochimica Acta* 71, 5731–5749. doi:10.1016/j.gca.2007.08.024

Charlet, L., and Tournassat, C. (2005). Fe (II)-Na (I)-Ca (II) cation exchange on montmorillonite in chloride medium: evidence for preferential clay adsorption of chloride–metal ion pairs in seawater. *Aquat. Geochem.* 11, 115–137. doi:10.1007/s10498-004-1166-5

Chen, Z., Montavon, G., Guo, Z., Wang, X., Razafindratsima, S., Robinet, J. C., et al. (2014a). Approaches to surface complexation modeling of Ni(II) on Callovo-Oxfordian clayrock. *Appl. Clay Sci.* 101, 369–380. doi:10.1016/j.clay.2014.07.034

Chen, Z., Montavon, G., Ribet, S., Guo, Z., Robinet, J. C., David, K., et al. (2014b). Key factors to understand *in-situ* behavior of Cs in Callovo–Oxfordian clay-rock (France). *Chem. Geol.* 387, 47–58. doi:10.1016/j.chemgeo.2014.08.008

Chisholm-Brause, C. J., Conradson, S. D., Buscher, C. T., Eller, P. G., and Morris, D. E. (1994). Speciation of uranyl sorbed at multiple binding sites on montmorillonite. *Geochimica Cosmochimica Acta* 58, 3625–3631. doi:10.1016/0016-7037(94)90154-6

Christiansen, B. C., Geckeis, H., Marquardt, C. M., Bauer, A., Römer, J., Wiss, T., et al. (2011). Neptunyl ($NpO_2^+$) interaction with green rust, $GR_{Na,SO4}$. *Geochimica Cosmochimica Acta* 75, 1216–1226. doi:10.1016/j.gca.2010.12.003

Churakov, S. V. (2006). *Ab initio* study of sorption on pyrophyllite: structure and acidity of the edge sites. *J. Phys. Chem. B* 110, 4135–4146. doi:10.1021/jp053874m

Churakov, S. V. (2007). Structure and dynamics of the water films confined between edges of pyrophyllite: a first principle study. *Geochimica Cosmochimica Acta* 71, 1130–1144. doi:10.1016/j.gca.2006.11.026

Churakov, S. V. (2013). Mobility of Na and Cs on montmorillonite surface under partially saturated conditions. *Environ. Sci. Technol.* 47, 9816–9823. doi:10.1021/es401530n

Churakov, S. V., and Daehn, R. (2012). Zinc adsorption on clays inferred from atomistic simulations and EXAFS spectroscopy. *Environ. Sci. Technol.* 46, 5713–5719.

Churakov, S. V., and Gimmi, T. (2011). Up-scaling of molecular diffusion coefficients in clays: a two-step approach. *J. Phys. Chem. C* 115, 6703–6714. doi:10.1021/jp112325n

Churakov, S. V., Gimmi, T., Unruh, T., VAN Loon, L. R., and Juranyi, F. (2014a). Resolving diffusion in clay minerals at different time scales: combination of experimental and modeling approaches. *Appl. Clay Sci.* 96, 36–44. doi:10.1016/j.clay.2014.04.030

Churakov, S. V., Hummel, W., and Fernandes, M. M. (2020). Fundamental research on Radiochemistry of geological nuclear waste disposal. *CHIMIA* 74, 1000. doi:10.2533/chimia.2020.1000

Churakov, S. V., Labbez, C., Pegado, L., and Sulpizi, M. (2014b). Intrinsic acidity of surface sites in calcium silicate hydrates and its implication to their Electrokinetic properties. *J. Phys. Chem. C* 118, 11752–11762. doi:10.1021/jp502514a

Churakov, S. V., and Liu, X. (2018). Quantum-chemical modelling of clay mineral surfaces and clay mineral–surface–adsorbate interactions. *Dev. Clay Sci.* 9, 49–87. doi:10.1016/b978-0-08-102432-4.00003-2

Churakov, S. V., and Prasianakis, N. I. (2018). Review of the current status and challenges for a holistic process-based description of mass transport and mineral reactivity in porous media. *Am. J. Sci.* 318, 921–948. doi:10.2475/09.2018.03

Cormenzana, J., Garcia-Gutierrez, M., Missana, T., and Alonso, U. (2008). Modelling large-scale laboratory HTO and strontium diffusion experiments in Mont Terri and Bure clay rocks. *Phys. Chem. Earth* 33, 949–956. doi:10.1016/j.pce.2008.05.006

Couture, R.-M., Charlet, L., Markelova, E., Madé, B. T., and Parsons, C. T. (2015). On–off mobilization of contaminants in soils during redox oscillations. *Environ. Sci. & Technol.* 49, 3015–3023. doi:10.1021/es5061879

Crank, J. (1975). *The mathematics of diffusion*. 2nd edition. United Kingdom: Oxford University Press.

Crawford, J. (2010). *Bedrock Kd data and uncertainty assessment for application in SR-Site geosphere transport calculations SKB R-10-48*. Sweden: SKB.

Cui, D., and Eriksen, T. E. (1996). *Reduction of Tc(VII) and Np(V) in solution by ferrous iron A laboratory study of homogeneous and heterogeneous redox processes SKB-TR-96-03*. Sweden: SKB.

Curti, E. (1999). Coprecipitation of radionuclides with calcite: estimation of partition coefficients based on a review of laboratory investigations and geochemical data. *Appl. Geochem.* 14, 433–445. doi:10.1016/s0883-2927(98)00065-1

Curti, E., Aimoz, L., and Kitamura, A. (2013). Selenium uptake onto natural pyrite. *J. Radioanalytical Nucl. Chem.* 295, 1655–1665. doi:10.1007/s10967-012-1966-9

Curti, E., Fujiwara, K., Iijima, K., Tits, J., Cuesta, C., Kitamura, A., et al. (2010). Radium uptake during barite recrystallization at 23±2°C as a function of solution composition: an experimental 133Ba and 226Ra tracer study. *Geochimica Cosmochimica Acta* 74, 3553–3570. doi:10.1016/j.gca.2010.03.018

Curti, E., Xto, J., Borca, C. N., Henzler, K., Huthwelker, T., and Prasianakis, N. I. (2019). Modelling Ra-bearing baryte nucleation/precipitation kinetics at the pore scale: application to radioactive waste disposal. *Eur. J. Mineralogy* 31, 247–262. doi:10.1127/ejm/2019/0031-2818

Cussler, E. L. (2009). *Diffusion: mass transfer in fluid systems*. 3rd edition. Cambridge: Cambridge University Press.

Cygan, R. T., Greathouse, J. A., Heinz, H., and Kalinichev, A. G. (2009). Molecular models and simulations of layered materials. *J. Mater. Chem.* 19, 2470–2481. doi:10.1039/b819076c

Cygan, R. T., Liang, J.-J., and Kalinichev, A. G. (2004). Molecular models of hydroxide, oxyhydroxide, and clay phases and the development of a general force field. *J. Phys. Chem. B* 108, 1255–1266. doi:10.1021/jp0363287

Czömpöly, O., Fábián, M., Korányi, T. I., Nagy, G., Horváth, Z. E., Zizak, I., et al. (2023). Adsorption and diffusion of selenite on Boda Claystone Formation. *Appl. Clay Sci.* 241, 106997. doi:10.1016/j.clay.2023.106997

Dabat, T., Hubert, F., Paineau, E., Launois, P., Laforest, C., Grégoire, B., et al. (2019). A general orientation distribution function for clay-rich media. *Nat. Commun.* 10, 5456. doi:10.1038/s41467-019-13401-0

Dabat, T., Porion, P., Hubert, F., Paineau, E., Dazas, B., Grégoire, B., et al. (2020). Influence of preferred orientation of clay particles on the diffusion of water in kaolinite porous media at constant porosity. *Appl. Clay Sci.* 184, 105354. doi:10.1016/j.clay.2019.105354

Dagnelie, R. V. H., Rasamimanana, S., Blin, V., Radwan, J., Thory, E., Robinet, J. C., et al. (2018). Diffusion of organic anions in clay-rich media: retardation and effect of anion exclusion. *Chemosphere* 213, 472–480. doi:10.1016/j.chemosphere.2018.09.064

Dähn, R., Baeyens, B., and Bradbury, M. H. (2011). Investigation of the different binding edge sites for Zn on montmorillonite using P-EXAFS – the strong/weak site concept in the 2SPNE SC/CE sorption model. *Geochimica Cosmochimica Acta* 75, 5154–5168. doi:10.1016/j.gca.2011.06.025

Dähn, R., Scheidegger, A. M., Manceau, A., Schlegel, M. L., Baeyens, B., and Bradbury, M. H. (2001). Ni clay neoformation on montmorillonite surface. *J. Synchrotron Radiat.* 8, 533–535. doi:10.1107/s0909049500017817

Dähn, R., Scheidegger, A. M., Manceau, A., Schlegel, M. L., Baeyens, B., Bradbury, M. H., et al. (2003). Structural evidence for the sorption of Ni(II) atoms on the edges of montmorillonite clay minerals. A polarized X-ray absorption fine structure study. *Geochimica Cosmochimica Acta* 67, 1–15. doi:10.1016/s0016-7037(02)01005-0

Dähn, R., Scheidegger, A. M., Manceau, A., Schlegel, M. L., Baeyens, B., Bradbury, M. H., et al. (2002). Neoformation of Ni phyllosilicate upon Ni uptake on montmorillonite: a kinetics study by powder and polarized extended X-ray absorption fine structure spectroscopy. *Geochimica Cosmochimica Acta* 66, 2335–2347. doi:10.1016/s0016-7037(02)00842-6

Dangelmayr, M. A., Reimus, P. W., Wasserman, N. L., Punsal, J. J., Johnson, R. H., Clay, J. T., et al. (2017). Laboratory column experiments and transport modeling to evaluate retardation of uranium in an aquifer downgradient of a uranium *in-situ* recovery site. *Appl. Geochem.* 80, 1–13. doi:10.1016/j.apgeochem.2017.02.018

Dauzères, A., Achiedo, G., Nied, D., Bernard, E., Alahrache, S., and Lothenbach, B. (2016). Magnesium perturbation in low-pH concretes placed in clayey environment—solid characterizations and modeling. *Cem. Concr. Res.* 79, 137–150. doi:10.1016/j.cemconres.2015.09.002

David, C., Wassermann, J., Amann, F., Klaver, J., Davy, C., Sarout, J., et al. (2018). $KG^2B$, a collaborative benchmarking exercise for estimating the permeability of the Grimsel granodiorite—Part 2: modelling, microstructures and complementary data. *Geophys. J. Int.* 215, 825–843. doi:10.1093/gji/ggy305

Davis, J. A., and Kent, D. (1990a). Surface complexation modeling in aqueous geochemistry. *Rev. Mineralogy Geochem.* 23, 177–260.

Davis, J., and Kent, D. (1990b). "Surface complexation modelling in aqueous geochemistry," in *Mineral-water interface geochemistry*. Editors M. F. Hochella and A. F. White United States: Mineralogical Society of America.

Debure, M., Tournassat, C., Lerouge, C., Madé, B., Robinet, J.-C., Fernández, A. M., et al. (2018). Retention of arsenic, chromium and boron on an outcropping clay-rich rock formation (the Tégulines Clay, eastern France). *Sci. Total Environ.* 642, 216–229. doi:10.1016/j.scitotenv.2018.06.037

DE Canniere, P., Maes, A., Wimiams, S., Bruggeman, C., Beauwens, T., Maes, N., et al. (2010). *Behaviour of selenium in Boom clay. State-of-the-art report. Mol SCK CEN-ER120*. Belgium: SCK-CEN, Belgium Nuclear Research Centre.

Degueldre, C., Baeyens, B., Goerlich, W., Riga, J., Verbist, J., and Stadelmann, P. (1989). Colloids in water from a subsurface fracture in granitic rock, Grimsel Test Site, Switzerland. *Geochimica Cosmochimica Acta* 53, 603–610. doi:10.1016/0016-7037(89)90003-3

Degueldre, C., and Bolek, M. (2009). Modelling colloid association with plutonium: the effect of pH and redox potential. *Appl. Geochem.* 24, 310–318. doi:10.1016/j.apgeochem.2008.10.008

Delay, J., Distinguin, M., and Dewonck, S. (2007). Characterization of a clay-rich rock through development and installation of specific hydrogeological and diffusion test equipment in deep boreholes. *Phys. Chem. Earth, Parts A/B/C* 32, 393–407. doi:10.1016/j.pce.2006.01.011

Delhorme, M., Labbez, C., Caillet, C., and Thomas, F. (2010). Acid-base properties of 2:1 clays. I. Modeling the role of electrostatics. *Langmuir* 26, 9240–9249. doi:10.1021/la100069g

Descostes, M., Blin, V., Bazer-Bachi, F., Meier, P., Grenut, B., Radwan, J., et al. (2008). Diffusion of anionic species in Callovo-Oxfordian argillites and Oxfordian limestones (Meuse/Haute-Marne, France). *Appl. Geochem.* 23, 655–677. doi:10.1016/j.apgeochem.2007.11.003

Descostes, M., Pointeau, I., Radwan, J., Poonoosamy, J., Lacour, J. L., Menut, D., et al. (2017). Adsorption and retarded diffusion of Eu-III-EDTA(-) through hard clay rock. *J. Hydrology* 544, 125–132. doi:10.1016/j.jhydrol.2016.11.014

Dierckx, A., Put, M., DE Cannière, P., Maes, N., Aertsens, M., Maes, A., et al. (2000) "TRANCOM-CLAY: transport of radionuclides due to complexation with organic matter in clay formations EUR19135," in *Nuclear science and technology*. Luxembourg: European Commission.

Dong, H., Fredrickson, J. K., Kennedy, D. W., Zachara, J. M., Kukkadapu, R. K., and Onstott, T. C. (2000). Mineral transformations associated with the microbial reduction of magnetite. *Chem. Geol.* 169, 299–318. doi:10.1016/s0009-2541(00)00210-2

Dong, H., Jaisi, D. P., Kim, J., and Zhang, G. (2009). Microbe-clay mineral interactions. *Am. Mineralogist* 94, 1505–1519. doi:10.2138/am.2009.3246

Dong, H., Kukkadapu, R. K., Fredrickson, J. K., Zachara, J. M., Kennedy, D. W., and Kostandarithes, H. M. (2003). Microbial reduction of structural Fe(III) in illite and goethite. *Environ. Sci. & Technol.* 37, 1268–1276. doi:10.1021/es020919d

Drake, H., Mathurin, F. A., Zack, T., Schäfer, T., Roberts, N. M. W., Whitehouse, M., et al. (2018). Incorporation of metals into calcite in a deep anoxic granite aquifer. *Environ. Sci. & Technol.* 52, 493–502. doi:10.1021/acs.est.7b05258

Duc, M., Gaboriaud, F., and Thomas, F. (2005). Sensitivity of the acid–base properties of clays to the methods of preparation and measurement: 1. Literature review. *J. colloid interface Sci.* 289, 139–147. doi:10.1016/j.jcis.2005.03.060

Dullien, F. (1991). *Fluid tansport and pore structure*. Academic Press.

Dumas, T., Fellhauer, D., Schild, D., Gaona, X., Altmaier, M., and Scheinost, A. C. (2019). Plutonium retention mechanisms by magnetite under anoxic conditions: entrapment versus sorption. *ACS Earth Space Chem.* 3, 2197–2206. doi:10.1021/acsearthspacechem.9b00147

Durce, D., Aertsens, M., Jacques, D., Maes, N., and VAN Gompel, M. (2018). Transport of dissolved organic matter in Boom Clay: size effects. *J. Contam. Hydrol.* 208, 27–34. doi:10.1016/j.jconhyd.2017.12.004

Durce, D., Aertsens, M., and VAN Gompel, M. (2023). *Revisitation of migration experiments in Boom clay - final report mol SCK CEN-ER0843*. Belgium: SCK CEN.

Durce, D., Landesman, C., Grambow, B., Ribet, S., and Giffaut, E. (2014). Adsorption and transport of polymaleic acid on Callovo-Oxfordian clay stone: batch and transport experiments. *J. Contam. Hydrol.* 164, 308–322. doi:10.1016/j.jconhyd.2014.06.015

Durrant, C. B., Begg, J. D., Kersting, A. B., and Zavarin, M. (2018). Cesium sorption reversibility and kinetics on illite, montmorillonite, and kaolinite. *Sci. Total Environ.* 610, 511–520. doi:10.1016/j.scitotenv.2017.08.122

Dzombak, D. A., and Morel, F. M. (1990). *Surface complexation modeling: hydrous ferric oxide*. John Wiley & Sons.

ECOCLAYII (2005). *Ecoclay II: effects of cement on clay barrier performance EUR21921. nuclear science and technology*. EC: Euratom.

EL Hajj, H., Abdelouas, A., EL Mendili, Y., Karakurt, G., Grambow, B., and Martin, C. (2013). Corrosion of carbon steel under sequential aerobic-anaerobic environmental conditions. *Corros. Sci.* 76, 432–440. doi:10.1016/j.corsci.2013.07.017

EL Mendili, Y., Abdelouas, A., Chaou, A. A., Bardeau, J. F., and Schlegel, M. L. (2014). Carbon steel corrosion in clay-rich environment. *Corros. Sci.* 88, 56–65. doi:10.1016/j.corsci.2014.07.020

Elo, O., Muller, K., Ikeda-Ohno, A., Bok, F., Scheinost, A. C., Holtta, P., et al. (2017). Batch sorption and spectroscopic speciation studies of neptunium uptake by montmorillonite and corundum. *Geochimica Cosmochimica Acta* 198, 168–181. doi:10.1016/j.gca.2016.10.040

Emmanuel, S., and Ague, J. J. (2009). Modeling the impact of nano-pores on mineralization in sedimentary rocks. *Water Resour. Res.* 45. doi:10.1029/2008wr007170

Emmanuel, S., Ague, J. J., and Walderhaug, O. (2010). Interfacial energy effects and the evolution of pore size distributions during quartz precipitation in sandstone. *Geochimica Cosmochimica Acta* 74, 3539–3552. doi:10.1016/j.gca.2010.03.019

Emmanuel, S., and Berkowitz, B. (2007). Effects of pore-size controlled solubility on reactive transport in heterogeneous rock. *Geophys. Res. Lett.* 34, L06404. doi:10.1029/2006gl028962

Epifano, E., Naji, M., Manara, D., Scheinost, A. C., Hennig, C., Lechelle, J., et al. (2019). Extreme multi-valence states in mixed actinide oxides. *Commun. Chem.* 2, 59–11. doi:10.1038/s42004-019-0161-0

Fabritius, O., Puhakka, E., Li, X. D., Nurminen, A., and Siitari-Kauppi, M. (2022). Radium sorption on biotite; surface complexation modeling study. *Appl. Geochem.* 140, 105289. doi:10.1016/j.apgeochem.2022.105289

Faucher, J. A., and Thomas, H. C. (1954). Adsorption studies on clay minerals. IV. The system montmorillonite-cesium-potassium. *J. Chem. Phys.* 22, 258–261. doi:10.1063/1.1740047

Fernández, A. M., Baeyens, B., Bradbury, M., and Rivas, P. (2004). Analysis of the porewater chemical composition of a Spanish compacted bentonite used in an engineered barrier. *Phys. Chem. Earth, Parts A/B/C* 29, 105–118. doi:10.1016/j.pce.2003.12.001

Ferrage, E. (2016). Investigation of the interlayer organization of water and ions in smectite from the combined use of diffraction experiments and molecular simulations. a review of methodology, applications, and perspectives. *Clays Clay Minerals* 64, 348–373. doi:10.1346/ccmn.2016.0640401

Ferrage, E., Hubert, F., Dabat, T., Asaad, A., Dazas, B., Grégoire, B., et al. (2023). Anisotropy in particle orientation controls water diffusion in clay materials. *Appl. Clay Sci.* 244, 107117. doi:10.1016/j.clay.2023.107117

Fetter, C. W. (1992). *Contaminant hydrology*. New York: Macmillan Publishing Company.

Finck, N. (2020). Iron speciation in Opalinus clay minerals. *Appl. Clay Sci.* 193, 105679. doi:10.1016/j.clay.2020.105679

Finck, N., Dardenne, K., Bosbach, D., and Geckeis, H. (2012). Selenide retention by mackinawite. *Environ. Sci. & Technol.* 46, 10004–10011. doi:10.1021/es301878y

Fischer, C., and Luttge, A. (2007). Converged surface roughness parameters A new tool to quantify rock surface morphology and reactivity alteration. *Am. J. Sci.* 307, 955–973. doi:10.2475/07.2007.01

Ford, R. G., Scheinost, A. C., and Sparks, D. L. (2001). Frontiers in metal sorption/precipitation mechanisms on soil mineral surfaces. *Avances Agron.* 74, 41–62. doi:10.1016/s0065-2113(01)74030-8

Fox, P. M., Davis, J. A., Kukkadapu, R., Singer, D. M., Bargar, J., and Williams, K. H. (2013). Abiotic U(VI) reduction by sorbed Fe(II) on natural sediments. *Geochimica Cosmochimica Acta* 117, 266–282. doi:10.1016/j.gca.2013.05.003

Frohlich, D. R., Amayri, S., Drebert, J., Grolimund, D., Huth, J., Kaplan, U., et al. (2012). Speciation of Np(V) uptake by Opalinus Clay using synchrotron microbeam techniques. *Anal. Bioanal. Chem.* 404, 2151–2162. doi:10.1007/s00216-012-6290-2

Fuhrmann, M., Bajt, S. A., and Schoonen, M. A. A. (1998). Sorption of iodine on minerals investigated by X-ray absorption near edge structure (XANES) and 125I tracer sorption experiments. *Appl. Geochem.* 13, 127–141. doi:10.1016/s0883-2927(97)00068-1

Fukushi, K., Hasegawa, Y., Maeda, K., Aoi, Y., Tamura, A., Arai, S., et al. (2013). Sorption of Eu(III) on granite: EPMA, LA–ICP–MS, batch and modeling studies. *Environ. Sci. & Technol.* 47, 12811–12818. doi:10.1021/es402676n

Fuller, A. J., Shaw, S., Ward, M. B., Haigh, S. J., Mosselmans, J. F. W., Peacock, C. L., et al. (2015). Caesium incorporation and retention in illite interlayers. *Appl. Clay Sci.* 108, 128–134. doi:10.1016/j.clay.2015.02.008

Gailhanou, H., Lerouge, C., Debure, M., Gaboreau, S., Gaucher, E. C., Grangeon, S., et al. (2017). Effects of a thermal perturbation on mineralogy and pore water composition in a clay-rock: an experimental and modeling study. *Geochimica Cosmochimica Acta* 197, 193–214. doi:10.1016/j.gca.2016.10.004

Gaines, G. L., and Thomas, H. C. (1953). Adsorption studies on clay minerals. II. A formulation of the thermodynamics of exchange adsorption. *J. Chem. Phys.* 21, 714–718. doi:10.1063/1.1698996

Gaines, G. L., and Thomas, H. C. (1955). Adsorption studies on clay minerals. V. Montmorillonite-Cesium-Strontium at several temperatures. *J. Chem. Phys.* 23, 2322–2326. doi:10.1063/1.1741873

Galunin, E., Alba, M. D., Avilés, M. A., Santos, M. J., and Vidal, M. (2009). Reversibility of La and Lu sorption onto smectites: implications for the design of engineered barriers in deep geological repositories. *J. Hazard. Mater.* 172, 1198–1205. doi:10.1016/j.jhazmat.2009.07.124

Galunin, E., Alba, M. D., Santos, M. J., Abrao, T., and Vidal, M. (2010). Lanthanide sorption on smectitic clays in presence of cement leachates. *Geochimica Cosmochimica Acta* 74, 862–875. doi:10.1016/j.gca.2009.11.003

Gao, M., Zhang, C. G., and Oh, J. (2023a). Assessments of the effects of various fracture surface morphology on single fracture flow: a review. *Int. J. Min. Sci. Technol.* 33, 1–29. doi:10.1016/j.ijmst.2022.07.005

Gao, P., Liu, X., Guo, Z., and Tournassat, C. (2023b). Acid-base properties of cis-vacant montmorillonite edge surfaces: a combined first-principles molecular dynamics and surface complexation modeling approach. *Environ. Sci. Technol.* 57, 1342–1352. doi:10.1021/acs.est.2c07171

García, D., Lützenkirchen, J., Petrov, V., Siebentritt, M., Schild, D., Lefèvre, G., et al. (2019). Sorption of Eu(III) on quartz at high salt concentrations. *Colloids Surfaces A Physicochem. Eng. Aspects* 578, 123610. doi:10.1016/j.colsurfa.2019.123610

García-Gutiérrez, M., Cormenzana, J. L., Missana, T., Mingarro, M., and Martín, P. L. (2006). Large-scale laboratory diffusion experiments in clay rocks. *Phys. Chem. Earth, Parts A/B/C* 31, 523–530. doi:10.1016/j.pce.2006.04.004

García-Gutiérrez, M., Mingarro, M., Morejón, J., Alonso, U., and Missana, T. (2023). Analysis of the role of water saturation degree in HTO, 36Cl, and 75Se diffusion in sedimentary rock. *Minerals* 13, 593. doi:10.3390/min13050593

Gaucher, E., Robelin, C., Matray, J. M., Négrel, G., Gros, Y., Heitz, J. F., et al. (2004). ANDRA underground research laboratory: interpretation of the mineralogical and geochemical data acquired in the Callovian–Oxfordian formation by investigative drilling. *Phys. Chem. Earth, Parts A/B/C* 29, 55–77. doi:10.1016/j.pce.2003.11.006

Gebauer, D., Kellermeier, M., Gale, J. D., Bergström, L., and Cölfen, H. (2014). Pre-nucleation clusters as solute precursors in crystallisation. *Chem. Soc. Rev.* 43, 2348–2371. doi:10.1039/c3cs60451a

Geckeis, H., Lützenkirchen, J., Polly, R., Rabung, T., and Schmidt, M. (2013). Mineral–water interface reactions of actinides. *Chem. Rev.* 113, 1016–1062. doi:10.1021/cr300370h

Giffaut, E., Grivé, M., Blanc, P., Vieillard, P., Colàs, E., Gailhanou, H., et al. (2014). Andra thermodynamic database for performance assessment: ThermoChimie. *Appl. Geochem.* 49, 225–236. doi:10.1016/j.apgeochem.2014.05.007

Gimmi, T., and Alt-Epping, P. (2018). Simulating Donnan equilibria based on the Nernst-Planck equation. *Geochimica Cosmochimica Acta* 232, 1–13. doi:10.1016/j.gca.2018.04.003

Gimmi, T., and Churakov, S. V. (2019). Water retention and diffusion in unsaturated clays: connecting atomistic and pore scale simulations. *Appl. Clay Sci.* 175, 169–183. doi:10.1016/j.clay.2019.03.035

Gimmi, T., and Kosakowski, G. (2011). How mobile are sorbed cations in clays and clay rocks? *Environ. Sci. & Technol.* 45, 1443–1449. doi:10.1021/es1027794

Gimmi, T., Leupin, O. X., Eikenberg, J., Glaus, M. A., VAN Loon, L. R., Waber, H. N., et al. (2014). Anisotropic diffusion at the field scale in a 4-year multi-tracer diffusion and retention experiment – I: insights from the experimental data. *Geochimica Cosmochimica Acta* 125, 373–393. doi:10.1016/j.gca.2013.10.014

Glaus, M. A., Aertsens, M., Appelo, C. A. J., Kupcik, T., Maes, N., VAN Laer, L., et al. (2015). Cation diffusion in the electrical double layer enhances the mass transfer rates for Sr2+, Co2+ and Zn2+ in compacted illite. *Geochimica Cosmochimica Acta* 165, 376–388. doi:10.1016/j.gca.2015.06.014

Glaus, M. A., Aertsens, M., Maes, N., VAN Laer, L., and VAN Loon, L. R. (2015b). Treatment of boundary conditions in through-diffusion: a case study of Sr-85(2+) diffusion in compacted illite. *J. Contam. Hydrology* 177, 239–248.

Glaus, M. A., Baeyens, B., Bradbury, M. H., Jakob, A., VAN Loon, L. R., and Yaroshchuk, A. (2007). Diffusion of $^{22}$Na and $^{85}$Sr in Montmorillonite: evidence of interlayer diffusion being the dominant pathway at high compaction. *Environ. Sci. & Technol.* 41, 478–485. doi:10.1021/es061908d

Glaus, M. A., Birgersson, M., Karnland, O., and VAN Loon, L. R. (2013). Seeming steady-state uphill diffusion of 22Na+ in compacted montmorillonite. *Environ. Sci. Technol.* 47, 11522–11527. doi:10.1021/es401968c

Glaus, M. A., Frick, S., Rosse, R., and VAN Loon, L. R. (2010). Comparative study of tracer diffusion of HTO, 22Na+ and 36Cl− in compacted kaolinite, illite and montmorillonite. *Geochimica Cosmochimica Acta* 74, 1999–2010. doi:10.1016/j.gca.2010.01.010

Glaus, M. A., Frick, S., Rosse, R., and VAN Loon, L. R. (2011). Consistent interpretation of the results of through-out-diffusion and tracer profile analysis for trace anion diffusion in compacted montmorillonite. *J. Contam. Hydrology* 123, 1–10. doi:10.1016/j.jconhyd.2010.11.009

Glaus, M. A., Frick, S., and VAN Loon, L. R. (2020). A coherent approach for cation surface diffusion in clay minerals and cation sorption models: diffusion of Cs+ and Eu3+ in compacted illite as case examples. *Geochimica Cosmochimica Acta* 274, 79–96. doi:10.1016/j.gca.2020.01.054

Glaus, M. A., Frick, S., and VAN Loon, L. R. (2021). Competitive effects of cations on the diffusion properties of strongly sorbing trace cations in compacted illite and opalinus clay. *Acs Earth Space Chem.* 5, 2621–2625. doi:10.1021/acsearthspacechem.1c00250

Glaus, M. A., Muller, W., and VAN Loon, L. R. (2008a). Diffusion of iodide and iodate through Opalinus Clay: monitoring of the redox state using an anion chromatographic technique. *Appl. Geochem.* 23, 3612–3619. doi:10.1016/j.apgeochem.2008.08.013

Glaus, M. A., Rosse, R., VAN Loon, L. R., and Yaroshchuk, A. E. (2008b). Tracer diffusion in sintered stainless steel filters: measurement of effective diffusion coefficients and implications for diffusion studies with compacted clays. *Clays Clay Minerals* 56, 677–685. doi:10.1346/ccmn.2008.0560608

Glaus, M. A., VAN Loon, L. R., and Wüst, R. A. J. (2023). Diffusion of HTO, 36Cl and 22Na in the Mesozoic rocks of northern Switzerland. II: data interpretation in terms of an electrical double layer model. *Appl. Geochem.* 162, 105842. doi:10.1016/j.apgeochem.2023.105842

Glaus, M., Frick, S., and VAN Loon, L. (2017). *Diffusion of selected cations and anions in compacted montmorillonite and bentonite PSI Bericht 17-08*. Villigen, Switzerland: PSI.

Glückman, D. (2023). "Investigation of the diffusion of U(VI) and Am(III) through Opalinus Clay down to ultra-trace levels,". PhD Thesis (Germany: Karlsruhe Institute of Technology).

Glynn, P. (2000). Solid-solution Solubilities and thermodynamics: sulfates, carbonates and Halides. *Rev. Mineralogy Geochem.* 40, 481–511. doi:10.2138/rmg.2000.40.10

Goldberg, S., and Glaubig, R. (1986). Boron adsorption and Silicon release by the clay minerals kaolinite, montmorillonite, and illite. *Soil Sci. Soc. Am. J.* 50, 1442–1448. doi:10.2136/sssaj1986.03615995005000060013x

Goldberg, S., and Glaubig, R. (1988a). Anion sorption on a calcareous, montmorillonitic soil-selenium. *Soil Sci. Soc. Am. J.* 52, 954–958. doi:10.2136/sssaj1988.03615995005200040010x

Goldberg, S., and Glaubig, R. (1988b). Anion sorption on a calcareous, montmorillonitic soil—arsenic. *Soil Sci. Soc. Am. J.* 52, 1297–1300. doi:10.2136/sssaj1988.03615995005200050015x

Goldberg, S., and Sposito, G. (1984). A chemical model of phosphate adsorption by soils: I. Reference oxide minerals. *Soil Sci. Soc. Am. J.* 48, 772–778. doi:10.2136/sssaj1984.03615995004800040015x

Gorski, C. A., Aeschbacher, M., Soltermann, D., Voegelin, A., Baeyens, B., Marques Fernandes, M., et al. (2012a). Redox properties of structural Fe in clay minerals. 1. Electrochemical quantification of electron-Donating and -accepting capacities of smectites. *Environ. Sci. & Technol.* 46, 9360–9368. doi:10.1021/es3020138

Gorski, C. A., Edwards, R., Sander, M., Hofstetter, T. B., and Stewart, S. M. (2016). Thermodynamic characterization of iron oxide–aqueous Fe2+ redox couples. *Environ. Sci. & Technol.* 50, 8538–8547. doi:10.1021/acs.est.6b02661

Gorski, C. A., Klüpfel, L. E., Voegelin, A., Sander, M., and Hofstetter, T. B. (2013). Redox properties of structural Fe in clay minerals: 3. Relationships between smectite redox and structural properties. *Environ. Sci. & Technol.* 47, 13477–13485. doi:10.1021/es403824x

Gorski, C. A., Klüpfel, L., Voegelin, A., Sander, M., and Hofstetter, T. B. (2012b). Redox properties of structural Fe in clay minerals. 2. Electrochemical and spectroscopic characterization of electron transfer irreversibility in ferruginous smectite, SWa-1. *Environ. Sci. & Technol.* 46, 9369–9377. doi:10.1021/es302014u

Govaerts, J., Maes, N., Durce, D., Aertsens, M., and Brassinnes, S. (2023). Coupled flow and transport modelling of a large-scale *in situ* migration experiment with 14C-labelled natural organic matter colloids in Boom Clay. *Geol. Soc. Lond. Spec. Publ.* 536, 145–158. doi:10.1144/sp536-2022-22

Grambow, B. (2016). Geological disposal of radioactive waste in clay. *Elements* 12, 239–245. doi:10.2113/gselements.12.4.239

Grambow, B., Fattahi, M., Montavon, G., Moisan, C., and Giffaut, E. (2006). Sorption of Cs, Ni, Pb, Eu (III), Am (III), Cm, Ac (III), Tc (IV), Th, Zr, and U (IV) on MX 80 bentonite: an experimental approach to assess model uncertainty. *Radiochim. Acta* 94, 627–636. doi:10.1524/ract.2006.94.9-11.627

Grambow, B., Smailos, E., Geckeis, H., Müller, R., and Hentschel, H. (1996). Sorption and reduction of uranium(VI) on iron corrosion products under reducing saline conditions. *Radiochim. Acta* 74, 149–154. doi:10.1524/ract.1996.74.special-issue.149

Grangeon, S., Vinsot, A., Tournassat, C., Lerouge, C., Giffaut, E., Heck, S., et al. (2015). The influence of natural trace element distribution on the mobility of radionuclides. The exemple of nickel in a clay-rock. *Appl. Geochem.* 52, 155–173. doi:10.1016/j.apgeochem.2014.11.009

Grathoff, G. H., Peltz, M., Enzmann, F., and Kaufhold, S. (2016). Porosity and permeability determination of organic-rich Posidonia shales based on 3-D analyses by FIB-SEM microscopy. *Solid earth.* 7, 1145–1156. doi:10.5194/se-7-1145-2016

Grathwohl, P. (1998). *Diffusion in natural porous media: contaminant transport, sorption,/desorption and dissolution kinetics*. Springer New York, United States: Kluwer academic publishers.

Grimm, R. E. (1953). *Clay mineralogy*. New York: McGraw-Hill.

Guillaumont, R., Fanghänel, T., Fuger, J., Grenthe, I., Neck, V., Palmer, D. A., et al. (2003). *Update on the chemical thermodynamics of uranium, Neptunium, Plutonium, Americium and technetium*. Amsterdam: Elsevier.

Guillot, B. (2002). A reappraisal of what we have learnt during three decades of computer simulations on water. *J. Mol. Liq.* 101, 219–260. doi:10.1016/s0167-7322(02)00094-6

Hadi, J., Wersin, P., Mazurek, M., Waber, H. N., Marques Fernandes, M., Baeyens, B., et al. (2019). *Intercomparison of CEC methods within the GD project*. Motn Terri Project Technical Report 2017-06.

Hakanen, M., Ervanne, H., and Puukko, E. (2014). *Safety case for the disposal of spent nuclear fuel at Olkiluoto: radionuclide migration parameters for the geosphere POSIVA report 2012-41*. Helsinki, Finland: Posiva Oy.

Han, D. S., Batchelor, B., and Abdel-Wahab, A. (2011). Sorption of selenium(IV) and selenium(VI) to mackinawite (FeS): effect of contact time, extent of removal, sorption envelopes. *J. Hazard. Mater.* 186, 451–457. doi:10.1016/j.jhazmat.2010.11.017

Han, D. S., Batchelor, B., and Abdel-Wahab, A. (2012). Sorption of selenium(IV) and selenium(VI) onto synthetic pyrite (FeS2): spectroscopic and microscopic analyses. *J. Colloid Interface Sci.* 368, 496–504. doi:10.1016/j.jcis.2011.10.065

Havlova, V., Martin, A., Landa, J., Sus, F., Siitari-Kauppi, M., Eikenberg, J., et al. (2013). *Long term diffusion experiment LTD Phase I: evaluation of results and modelling*, 188–189. Brighton, UK.

Hayes, K. F., Redden, G., Ela, W., and Leckie, J. O. (1991). Surface complexation models: an evaluation of model parameter estimation using FITEQL and oxide mineral titration data. *J. colloid interface Sci.* 142, 448–469. doi:10.1016/0021-9797(91)90075-j

Heberling, F., Vinograd, V. L., Polly, R., Gale, J. D., Heck, S., Rothe, J., et al. (2014). A thermodynamic adsorption/entrapment model for selenium(IV) coprecipitation with calcite. *Geochimica Cosmochimica Acta* 134, 16–38. doi:10.1016/j.gca.2014.02.044

Hedges, L. O., and Whitelam, S. (2012). Patterning a surface so as to speed nucleation from solution. *Soft Matter* 8, 8624. doi:10.1039/c2sm26038g

Heinz, H., Lin, T. J., Mishra, R. K., and Emami, F. S. (2013). Thermodynamically consistent force fields for the assembly of inorganic, organic, and Biological Nanostructures: the INTERFACE force field. *Langmuir* 29, 1754–1765. doi:10.1021/la3038846

Hennig, C., Schmeide, K., Brendler, V., Moll, H., Tsushima, S., and Scheinost, A. C. (2007). EXAFS investigation of U(VI), U(IV), and Th(IV) sulfato complexes in aqueous solution. *Inorg. Chem.* 46, 5882–5892. doi:10.1021/ic0619759

Henzler, K., Fetisov, E. O., Galib, M., Baer, M. D., Legg, B. A., Borca, C., et al. (2018). Supersaturated calcium carbonate solutions are classical. *Sci. Adv.* 4, 6283. doi:10.1126/sciadv.aao6283

Heron, G., Crouzet, C., Bourg, A. C. M., and Christensen, T. H. (1994). Speciation of Fe(II) and Fe(III) in contaminated aquifer sediments using chemical extraction techniques. *Environ. Sci. & Technol.* 28, 1698–1705. doi:10.1021/es00058a023

Hiemstra, T., Venema, P., and Riemsdijk, W. V. (1996). Intrinsic proton affinity of reactive surface groups of metal (hydr) oxides: the bond valence principle. *J. colloid interface Sci.* 184, 680–692. doi:10.1006/jcis.1996.0666

Higashihara, T., Kinoshita, K., Sato, S., and Kozaki, T. (2004). Electromigration of sodium ions and electro-osmotic flow in water-saturated, compacted Na-montmorillonite. *Appl. Clay Sci.* 26, 91–98. doi:10.1016/j.clay.2003.12.031

Hixon, A. E., Hu, Y.-J., Kaplan, D., Kukkadapu, R. K., Nitsche, H., Qafoku, O., et al. (2010). Influence of iron redox transformations on plutonium sorption to sediments. *Radiochim. Acta* 98, 685–692. doi:10.1524/ract.2010.1769

Hixon, A. E., and Powell, B. A. (2018). Plutonium environmental chemistry: mechanisms for the surface-mediated reduction of Pu(v/vi). *Environ. Science-Processes & Impacts* 20, 1306–1322. doi:10.1039/c7em00369b

Hockin, S. L., and Gadd, G. M. (2003). Linked redox precipitation of sulfur and selenium under anaerobic conditions by sulfate-reducing bacterial biofilms. *Appl. Environ. Microbiol.* 69, 7063–7072. doi:10.1128/aem.69.12.7063-7072.2003

Holmboe, M., and Bourg, I. C. (2014). Molecular dynamics simulations of water and sodium diffusion in smectite interlayer Nanopores as a function of pore size and temperature. *J. Phys. Chem. C* 118, 1001–1013. doi:10.1021/jp408884g

Höltä, P., Siitari-Kauppi, M., Hakanen, M., Huitti, T., Hautojärvi, A., and Lindberg, A. (1997). Radionuclide transport and retardation in rock fracture and crushed rock column experiments. *J. Contam. Hydrology* 26, 135–145. doi:10.1016/s0169-7722(96)00064-2

Hölttä, P., Hakanen, M., Hautojärvi, A., Timonen, J., and Väätäinen, K. (1996). The effects of matrix diffusion on radionuclide migration in rock column experiments. *J. Contam. Hydrology* 21, 165–173. doi:10.1016/0169-7722(95)00041-0

Hoving, A. L., Sander, M., Bruggeman, C., and Behrends, T. (2017). Redox properties of clay-rich sediments as assessed by mediated electrochemical analysis: Separating pyrite, siderite and structural Fe in clay minerals. *Chem. Geol.* 457, 149–161. doi:10.1016/j.chemgeo.2017.03.022

Huber, F. M., Totskiy, Y., Marsac, R., Schild, D., Pidchenko, I., Vitova, T., et al. (2017). Tc interaction with crystalline rock from Aspo (Sweden): effect of *in-situ* rock redox capacity. *Appl. Geochem.* 80, 90–101. doi:10.1016/j.apgeochem.2017.01.026

Huber, F., Schild, D., Vitova, T., Rothe, J., Kirsch, R., and Schafer, T. (2012). U(VI) removal kinetics in presence of synthetic magnetite nanoparticles. *Geochimica Cosmochimica Acta* 96, 154–173. doi:10.1016/j.gca.2012.07.019

Huertas, F., Fuentes-Santillana, J., Jullien, F., Rivas, P., and Linares, P. (2000). *Full scale engineered barriers experiment for a deep geological repository for high-level radioactive waste in crystalline host rock EUR19147*. EC.

Hummel, W., Berner, U., Curti, E., Pearson, F. J., and Thoenen, T. (2002). *Nagra/PSI chemical thermodynamic data base 01/01*. Nagra technical report 02-16.

Hummel, W., and Thoenen, T. (2021). *The PSI chemical thermodynamic database 2020 NTB 21-03*. Switzerland: NAGRA.

Huo, L., Xie, W., Qian, T., Guan, X., and Zhao, D. (2017). Reductive immobilization of pertechnetate in soil and groundwater using synthetic pyrite nanoparticles. *Chemosphere* 174, 456–465. doi:10.1016/j.chemosphere.2017.02.018

Huysmans, M., and Dassargues, A. (2004). Review of the use of Péclet numbers to determine the relative importance of advection and diffusion in low permeability environments. *Hydrogeology J.* 13, 895–904. doi:10.1007/s10040-004-0387-4

Ikeda, A., Hennig, C., Tsushima, S., Takao, K., Ikeda, Y., Scheinost, A. C., et al. (2007). Comparative study of uranyl(VI) and -(V) carbonato complexes in an aqueous solution. *Inorg. Chem.* 46, 4212–4219. doi:10.1021/ic070051y

Ikonen, J., Sammaljärvi, J. V. M., Kuva, J., Siitari-Kauppi, M. L. A., and Timonen, J. (2015). *Investigation of rock matrix retention properties, supporting laboratory studies I: mineralogy, porosity and pore structure*. Posiva Working Report 2014-86. Helsinki: Finland.

Ikonen, J., Sardini, P., Jokelainen, L., Siitari-Kauppi, M., Martin, A., and Eikenberg, J. (2016a). The tritiated water and iodine migration *in situ* in Grimsel granodiorite. Part I: determination of the diffusion profiles. *J. Radioanalytical Nucl. Chem.* 310, 1041–1048. doi:10.1007/s10967-016-4890-6

Ikonen, J., Sardini, P., Siitari-Kauppi, M., and Martin, A. (2016b). *In situ* migration of tritiated water and iodine in Grimsel granodiorite, part II: assessment of the diffusion coefficients by TDD modelling. *J. Radioanalytical Nucl. Chem.* 311, 339–348. doi:10.1007/s10967-016-5041-9

Ilgen, A. G., Kukkadapu, R. K., Leung, K., and Washington, R. E. (2019). "Switching on" iron in clay minerals. *Environ. Sci. Nano* 6, 1704–1715. doi:10.1039/c9en00228f

Ilton, E. S., Boily, J.-F., Buck, E. C., Skomurski, F. N., Rosso, K. M., Cahill, C. L., et al. (2010). Influence of dynamical conditions on the reduction of UVI at the Magnetite–Solution interface. *Environ. Sci. & Technol.* 44, 170–176. doi:10.1021/es9014597

Ithurbide, A., Peulon, S., Miserque, F., Beaucaire, C., and Chausse, A. (2009). Interaction between uranium(VI) and siderite (FeCO3) surfaces in carbonate solutions. *Radiochim. Acta* 97, 177–180. doi:10.1524/ract.2009.1614

Ithurbide, A., Peulon, S., Miserque, F., Beaucaire, C., and Chaussé, A. (2010). Retention and redox behaviour of uranium(VI) by siderite (FeCO3). *Radiochim. Acta* 98, 563–568. doi:10.1524/ract.2010.1754

Jacops, E., Aertsens, M., Maes, N., Bruggeman, C., Krooss, B. M., Amann-Hildenbrand, A., et al. (2017a). Interplay of molecular size and pore network geometry on the diffusion of dissolved gases and HTO in Boom Clay. *Appl. Geochem.* 76, 182–195. doi:10.1016/j.apgeochem.2016.11.022

Jacops, E., Aertsens, M., Maes, N., Bruggeman, C., Swennen, R., Krooss, B., et al. (2017b). The dependency of diffusion coefficients and geometric factor on the size of the diffusing molecule: observations for different clay-based materials. *Geofluids* 16.

Jacops, E., Yu, L., Chen, G., and Levasseur, S. (2023). Gas transport in Boom Clay: the role of the HADES URL in process understanding. *Geol. Soc. Lond. Spec. Publ.* 536, 75–92. doi:10.1144/sp536-2022-42

Jacquier, P., Hainos, D., Robinet, J. C., Herbette, M., Grenut, B., Bouchet, A., et al. (2013). The influence of mineral variability of Callovo-Oxfordian clay rocks on radionuclide transfer properties. *Appl. Clay Sci.* 83-84, 129–136. doi:10.1016/j.clay.2013.07.010

Jahnke, F. M., and Radke, C. J. (1989). A radially perfused cell for measuring diffusion in compacted, highly sorbing media. *Industrial & Eng. Chem. Res.* 28, 347–355. doi:10.1021/ie00087a015

Jaisi, D. P., Dong, H., Plymale, A. E., Fredrickson, J. K., Zachara, J. M., Heald, S., et al. (2009). Reduction and long-term immobilization of technetium by Fe(II) associated with clay mineral nontronite. *Chem. Geol.* 264, 127–138. doi:10.1016/j.chemgeo.2009.02.018

Jaisi, D. P., Kukkadapu, R. K., Eberl, D. D., and Dong, H. (2005). Control of Fe(III) site occupancy on the rate and extent of microbial reduction of Fe(III) in nontronite. *Geochimica Cosmochimica Acta* 69, 5429–5440. doi:10.1016/j.gca.2005.07.008

Jakob, A., Pfingsten, W., and VAN Loon, L. (2009). Effects of sorption competition on caesium diffusion through compacted argillaceous rock. *Geochimica Cosmochimica Acta* 73, 2441–2456. doi:10.1016/j.gca.2009.01.028

James, S. C., Wang, L., and Chrysikopoulos, C. V. (2018). Modeling colloid transport in fractures with spatially variable aperture and surface attachment. *J. Hydrology* 566, 735–742. doi:10.1016/j.jhydrol.2018.09.047

Jenni, A., Mäder, U., Lerouge, C., Gaboreau, S., and Schwyn, B. (2014). *In situ* interaction between different concretes and Opalinus Clay. *Phys. Chem. Earth Parts A/B/C* 70-71, 71–83. doi:10.1016/j.pce.2013.11.004

Jenni, A., Meeussen, J. C. L., Pakkanen, T. A., Hirvi, J. T., Akinwunmi, B., Navarro, V., et al. (2021). Coupling of chemical and hydromechanical properties in bentonite: a new reactive transport model. *Appl. Clay Sci.* 214, 106274. doi:10.1016/j.clay.2021.106274

Jeon, B.-H., Dempsey, B. A., Burgos, W. D., Barnett, M. O., and Roden, E. E. (2005). Chemical reduction of U(VI) by Fe(II) at the Solid–Water interface using natural and synthetic Fe(III) oxides. *Environ. Sci. & Technol.* 39, 5642–5649. doi:10.1021/es0487527

Joe-Wong, C., Brown, G. E., and Maher, K. (2017). Kinetics and products of chromium(VI) reduction by iron(II/III)-Bearing clay minerals. *Environ. Sci. & Technol.* 51, 9817–9825. doi:10.1021/acs.est.7b02934

Jones, A. M., Murphy, C. A., Waite, T. D., and Collins, R. N. (2017). Fe(II) interactions with smectites: temporal changes in redox reactivity and the formation of green rust. *Environ. Sci. & Technol.* 51, 12573–12582. doi:10.1021/acs.est.7b01793

Jones, T. A., and Detwiler, R. L. (2016). Fracture sealing by mineral precipitation: the role of small-scale mineral heterogeneity. *Geophys. Res. Lett.* 43, 7564–7571. doi:10.1002/2016gl069598

JOPRAD (2018). *Programme document - the scientific and technical basis for a future joint programme on radioactive waste management and disposal - deliverable 4.4*. EC.

Jorgensen, W. L., and Tirado-Rives, J. (1988). The OPLS [optimized potentials for liquid simulations] potential functions for proteins, energy minimizations for crystals of cyclic peptides and crambin. *J. Am. Chem. Soc.* 110, 1657–1666. doi:10.1021/ja00214a001

Joseph, C., VAN Loon, L. R., Jakob, A., Steudtner, R., Schmeide, K., Sachs, S., et al. (2013). Diffusion of U(VI) in opalinus clay: influence of temperature and humic acid. *Geochimica Cosmochimica Acta* 109, 74–89. doi:10.1016/j.gca.2013.01.027

Kahl, W.-A., Yuan, T., Bollermann, T., Bach, W., and Fischer, C. (2020). Crystal surface reactivity analysis using a combined approach of X-ray micro-computed tomography and vertical scanning interferometry. *Am. J. Sci.* 320, 27–52. doi:10.2475/01.2020.03

Kang, M., Chen, F., Wu, S., Yang, Y., Bruggeman, C., and Charlet, L. (2011). Effect of pH on aqueous Se(IV) reduction by pyrite. *Environ. Sci. & Technol.* 45, 2704–2710. doi:10.1021/es1033553

Kang, M., Ma, B., Bardelli, F., Chen, F., Liu, C., Zheng, Z., et al. (2013). Interaction of aqueous Se(IV)/Se(VI) with FeSe/FeSe2: Implication to Se redox process. *J. Hazard. Mater.* 248-249, 20–28. doi:10.1016/j.jhazmat.2012.12.037

Kars, M., Lerouge, C., Grangeon, S., Aubourg, C., Tournassat, C., Madé, B., et al. (2015). Identification of nanocrystalline goethite in reduced clay formations: application to the Callovian-Oxfordian formation of Bure (France). *Am. Mineralogist* 100, 1544–1553. doi:10.2138/am-2015-5096

Kashchiev, D., and VAN Rosmalen, G. M. (2003). Review: nucleation in solutions revisited. *Cryst. Res. Technol.* 38, 555–574. doi:10.1002/crat.200310070

Katheras, A. S., Karalis, K., Krack, M., Scheinost, A. C., and Churakov, S. V. (2024). Stability and speciation of hydrated magnetite {111} surfaces from *ab initio* simulations with relevance for geochemical redox processes. *Environ. Sci. & Technol.* 58, 935–946. doi:10.1021/acs.est.3c07202

Katsumi, T., Benson, C. H., Foose, G. J., and Kamon, M. (2001). Performance-based design of landfill liners. *Eng. Geol.* 60, 139–148. doi:10.1016/s0013-7952(00)00096-x

Kedziorek, M. A. M., Bourg, A. C. M., and Giffaut, E. (2007). Hydrogeochemistry of Sn(IV) in the context of radioactive waste disposal: solubility and adsorption on MX-80 bentonite and Callovo-Oxfordian argilite. *Phys. Chem. Earth* 32, 568–572. doi:10.1016/j.pce.2005.12.005

Keller, L. M., and Holzer, L. (2018). Image-based upscaling of permeability in opalinus clay. *J. Geophys. Res. Solid Earth* 123, 285–295. doi:10.1002/2017jb014717

Keri, A., Dahn, R., Marques Fernandes, M., Scheinost, A. C., Krack, M., and Churakov, S. V. (2020). Iron adsorption on clays inferred from atomistic simulations and X-ray absorption spectroscopy. *Environ. Sci. & Technol.* 54, 11886–11893. doi:10.1021/acs.est.9b07962

Kéri, A., Osán, J., Fábián, M., Dähn, R., and Török, S. (2016). Combined X-ray microanalytical study of the Nd uptake capability of argillaceous rocks. *X-Ray Spectrom.* 45, 54–62. doi:10.1002/xrs.2656

Kirsch, R., Fellhauer, D., Altmaier, M., Neck, V., Rossberg, A., Fanghänel, T., et al. (2011). Oxidation state and local structure of plutonium reacted with magnetite, mackinawite and chukanovite. *Environ. Sci. & Technol.* 45, 7267–7274. doi:10.1021/es200645a

Klinkenberg, M., Brandt, F., Baeyens, B., Bosbach, D., and Fernandes, M. M. (2021). Adsorption of barium and radium on montmorillonite: a comparative experimental and modelling study. *Appl. Geochem.* 135, 105117. doi:10.1016/j.apgeochem.2021.105117

Klinkenberg, M., Brandt, F., Breuer, U., and Bosbach, D. (2014). Uptake of Ra during the recrystallization of barite: a microscopic and time of Flight-secondary ion mass spectrometry study. *Environ. Sci. & Technol.* 48, 6620–6627. doi:10.1021/es405502e

Klinkenberg, M., Weber, J., Barthel, J., Vinograd, V., Poonoosamy, J., Kruth, M., et al. (2018). The solid solution–aqueous solution system (Sr,Ba,Ra)SO4 + H2O: a combined experimental and theoretical study of phase equilibria at Sr-rich compositions. *Chem. Geol.* 497, 1–17. doi:10.1016/j.chemgeo.2018.08.009

Kobayashi, T., Scheinost, A. C., Fellhauer, D., Gaona, X., and Altmaier, M. (2013). Redox behavior of Tc(VII)/Tc(IV) under various reducing conditions in 0.1 M NaCl solutions. *Radiochim. Acta* 101, 323–332. doi:10.1524/ract.2013.2040

Konevnik, Y. V., Zakharova, E. V., Martynov, K. V., Andryushchenko, N. D., and Proshin, I. M. (2017). Influence of temperature on the sorption properties of rocks from the Nizhnekansky massif. *Radiochemistry* 59, 313–319. doi:10.1134/s106636221703016x

Kosakowski, G., Churakov, S. V., and Thoenen, T. (2008). Diffusion of Na and Cs in montmorillonite. *Clays Clay Minerals* 56, 190–206. doi:10.1346/ccmn.2008.0560205

Kostka, J. E., Haefele, E., Viehweger, R., and Stucki, J. W. (1999). Respiration and dissolution of iron(III)-Containing clay minerals by Bacteria. *Environ. Sci. & Technol.* 33, 3127–3133. doi:10.1021/es990021x

Kowal-Fouchard, A., Drot, R., Simoni, E., and Ehrhardt, J. (2004a). Use of spectroscopic techniques for uranium (VI)/montmorillonite interaction modeling. *Environ. Sci. & Technol.* 38, 1399–1407. doi:10.1021/es0348344

Kowal-Fouchard, A., Drot, R., Simoni, E., Marmier, N., Fromage, F., and Ehrhardt, J.-J. (2004b). Structural identification of europium (III) adsorption complexes on montmorillonite. *New J. Chem.* 28, 864–869. doi:10.1039/b400306c

Kraepiel, A. M., Keller, K., and Morel, F. M. (1998). On the acid– base chemistry of permanently charged minerals. *Environ. Sci. & Technol.* 32, 2829–2838. doi:10.1021/es9802899

Kraepiel, A. M., Keller, K., and Morel, F. M. (1999). A model for metal adsorption on montmorillonite. *J. Colloid Interface Sci.* 210, 43–54. doi:10.1006/jcis.1998.5947

Krejci, P., Gimmi, T., and VAN Loon, L. R. (2021). On the concentration-dependent diffusion of sorbed cesium in Opalinus Clay. *Geochimica Cosmochimica Acta* 298, 149–166. doi:10.1016/j.gca.2021.01.012

Krejci, P., Gimmi, T., VAN Loon, L. R., and Glaus, M. (2023). Relevance of diffuse-layer, Stern-layer and interlayers for diffusion in clays: a new model and its application to Na, Sr, and Cs data in bentonite. *Appl. Clay Sci.* 244, 107086. doi:10.1016/j.clay.2023.107086

Kremleva, A., Kruger, S., and Rosch, N. (2011). Uranyl adsorption at (010) edge surfaces of kaolinite: a density functional study. *Geochimica Cosmochimica Acta* 75, 706–718. doi:10.1016/j.gca.2010.10.019

Kremleva, A., Kruger, S., and Rosch, N. (2015a). Uranyl adsorption at solvated edge surfaces of 2: 1 smectites. A density functional study. *Phys. Chem. Chem. Phys.* 17, 13757–13768. doi:10.1039/c5cp01074h

Kremleva, A., Kruger, S., and Rosch, N. (2015b). Toward a reliable energetics of adsorption at solvated mineral surfaces: a computational study of uranyl (VI) on 2: 1 clay minerals. *J. Phys. Chem. C* 120, 324–335. doi:10.1021/acs.jpcc.5b09902

Kremleva, A., Martorell, B., Kruger, S., and Rosch, N. (2012). Uranyl adsorption on solvated edge surfaces of pyrophyllite: a DFT model study. *Phys. Chem. Chem. Phys.* 14, 5815–5823. doi:10.1039/c2cp23886a

Kügler, R. T., BeißERT, K., and Kind, M. (2016). On heterogeneous nucleation during the precipitation of barium sulfate. *Chem. Eng. Res. Des.* 114, 30–38. doi:10.1016/j.cherd.2016.07.024

Kulenkampff, J., Gründig, M., Richter, M., and Enzmann, F. (2008). Evaluation of positron-emission-tomography for visualisation of migration processes in geomaterials. *Phys. Chem. Earth* 33, 937–942. doi:10.1016/j.pce.2008.05.005

Kulenkampff, J., Stoll, M., Gründig, M., Mansel, A., Lippmann-Pipke, J., and Kersten, M. (2018). Time-lapse 3D imaging by positron emission tomography of Cu mobilized in a soil column by the herbicide MCPA. *Sci. Rep.* 8, 7091. doi:10.1038/s41598-018-25413-9

Kulenkampff, J., Zakhnini, A., Gründig, M., and Lippmann-Pipke, J. (2016). Quantitative experimental monitoring of molecular diffusion in clay with positron emission tomography. *Solid earth.* 7, 1207–1215. doi:10.5194/se-7-1207-2016

Kulik, D. A., Aja, S. U., Sinitsyn, V. A., and Wood, S. A. (2000). Acid–base surface chemistry and sorption of some lanthanides on K+-saturated Marblehead illite: II. A multisite–surface complexation modeling. *Geochimica Cosmochimica Acta* 64, 195–213. doi:10.1016/s0016-7037(99)00174-x

Kulik, D. A., Wagner, T., Dmytrieva, S. V., Kosakowski, G., Hingerl, F. F., Chudnenko, K. V., et al. (2013). GEM-Selektor geochemical modeling package: revised algorithm and GEMS3K numerical kernel for coupled simulation codes. *Comput. Geosci.* 17, 1–24.

Kurganskaya, I., and Luttge, A. (2013). A comprehensive stochastic model of phyllosilicate dissolution: structure and kinematics of etch pits formed on muscovite basal face. *Geochimica Cosmochimica Acta* 120, 545–560. doi:10.1016/j.gca.2013.06.038

Kuva, J., Sammaljärvi, J., Parkkonen, J., Siitari-Kauppi, M., Lehtonen, M., Turpeinen, T., et al. (2018). Imaging connected porosity of crystalline rock by contrast agent-aided X-ray microtomography and scanning electron microscopy. *J. Microsc.* 270, 98–109. doi:10.1111/jmi.12661

Kuva, J., Voutilainen, M., Kekäläinen, P., Siitari-Kauppi, M., Timonen, J., and Koskinen, L. (2015). Gas phase measurements of porosity, diffusion coefficient, and permeability in rock samples from Olkiluoto bedrock, Finland. *Transp. Porous Media* 107, 187–204. doi:10.1007/s11242-014-0432-2

Kvashnina, K. O., Kowalski, P. M., Butorin, S. M., Leinders, G., Pakarinen, J., Bes, R., et al. (2018). Trends in the valence band electronic structures of mixed uranium oxides. *Chem. Commun. Camb. Engl.* 54, 9757–9760. doi:10.1039/c8cc05464a

Kvashnina, K. O., and Scheinost, A. C. (2016). A Johann-type X-ray emission spectrometer at the Rossendorf beamline. *J. Synchrotron Radiat.* 23, 836–841. doi:10.1107/s1600577516004483

Kvashnina, K. O., Walker, H. C., Magnani, N., Lander, G. H., and Caciuffo, R. (2017). Resonant x-ray spectroscopy of uranium intermetallics at the M-4,M-5 edges of uranium. *Phys. Rev. B* 95, 245103. doi:10.1103/physrevb.95.245103

Kvashnina, K., Romanchuk, A., Pidchenko, I., Amidani, L., Gerber, E., Trigub, A., et al. (2019). A novel meta-stable pentavalent plutonium solid phase on the pathway from aqueous Pu(VI) to $PuO_2$ nanoparticles. *Angew. Chem.* 58, 17558–17562. doi:10.1002/anie.201911637

Kyllönen, J., Hakanen, M., and Lindberg, A. (2008). Sorption of cesium on Olkiluoto mica gneiss and granodiorite in saline groundwater; retardation of cesium transport in rock fracture columns. *POSIVA*.

Lammers, L. N., Bourg, I. C., Okumura, M., Kolluri, K., Sposito, G., and Machida, M. (2017). Molecular dynamics simulations of cesium adsorption on illite nanoparticles. *J. Colloid Interface Sci.* 490, 608–620. doi:10.1016/j.jcis.2016.11.084

Landstroem, O., and Tullborg, E. L. (1995). *Interactions of trace elements with fracture filling minerals from the Äspö Hard Rock Laboratory SKB-TR-95-13*. Sweden: SKB.

Langmuir, D., and Riese, A. C. (1985). The thermodynamic properties of radium. *Geochimica Cosmochimica Acta* 49, 1593–1601. doi:10.1016/0016-7037(85)90264-9

Latrille, C., Ly, J., and Herbette, M. (2006). Retention of Sn(IV) and Pu(IV) onto four argillites from the Callovo-Oxfordian level at Bure (France) from eight equilibrated sedimentary waters. *Radiochim. Acta* 94, 421–427. doi:10.1524/ract.2006.94.8.421

Latta, D. E., Boyanov, M. I., Kemner, K. M., O'Loughlin, E. J., and Scherer, M. M. (2012). Abiotic reduction of uranium by Fe(II) in soil. *Appl. Geochem.* 27, 1512–1524. doi:10.1016/j.apgeochem.2012.03.003

Latta, D. E., Neumann, A., Premaratne, W. A. P. J., and Scherer, M. M. (2017). Fe(II)–Fe(III) electron transfer in a clay mineral with low Fe content. *ACS Earth Space Chem.* 1, 197–208. doi:10.1021/acsearthspacechem.7b00013

Lauber, M., Baeyens, B., and H, B. M. (2000). *Physico-chemical characterisation and sorption measurements of Cs, Sr, Ni, Eu, Th, Sn and Se on Opalinus clay from Mont Terri PSI Bricht 00-10/NAGRA NTB 00-11*. Switzerland: PSI.

Lazar, K., and Mathé, Z. (2012). "Claystone as a potential host rock for nuclear waste storage," in *Clay minerals in nature - their characterization, modification and application - chapter 10*.

Le Crom, S., Tournassat, C., Robinet, J.-C., and Marry, V. (2022). Influence of water saturation Llevel on electrical double layer properties in a clay mineral mesopore: a molecular dynamics study. *J. Phys. Chem. C* 126, 647–654. doi:10.1021/acs.jpcc.1c08637

Lee, S., Anderson, P. R., Bunker, B. A., and Karanfil, C. (2004). EXAFS study of Zn sorption mechanisms on montmorillonite. *Environ. Sci. & Technol.* 38, 5426–5432. doi:10.1021/es0350076

Leinders, G., Bes, R., Kvashnina, K., and Verwerft, M. (2020). Local structure in U(IV) and U(V) environments: the case of $U_3O_7$. *Inorg. Chem.* 59, 4576–4587. doi:10.1021/acs.inorgchem.9b03702

Lerouge, C., Gaboreau, S., Grangeon, S., Claret, F., Warmont, F., Jenni, A., et al. (2017). *In situ* interactions between opalinus clay and low alkali concrete. *Phys. Chem. Earth, Parts A/B/C* 99, 3–21. doi:10.1016/j.pce.2017.01.005

Lerouge, C., Grangeon, S., Claret, F., Gaucher, E., Blanc, P., Guerrot, C., et al. (2014). Mineralogical and isotopic record of diagenesis from the opalinus Clay Formation at Benken, Switzerland: implications for the modeling of pore-water chemistry in a Clay Formation. *Clays Clay Minerals* 62, 286–312. doi:10.1346/ccmn.2014.0620404

Leupin, O. X., VAN Loon, L. R., Gimmi, T., Wersin, P., and Soler, J. M. (2017). Exploring diffusion and sorption processes at the Mont Terri rock laboratory (Switzerland): lessons learned from 20 years of field research. *Swiss J. Geosciences* 110, 391–403. doi:10.1007/s00015-016-0254-z

Li, X. L. (2013). TIMODAZ: a successful international cooperation project to investigate the thermal impact on the EDZ around a radioactive waste disposal in clay host rocks. *J. rock Mech. geotechnical Eng.* 8, 231–242. doi:10.1016/j.jrmge.2013.05.003

Li, Y. H., and Gregory, S. (1974). Diffusion of ions in Sea-water and in deep-Sea sediments. *Geochimica Cosmochimica Acta* 38, 703–714. doi:10.1016/0016-7037(74)90145-8

Li, L., Steefel, C. I., and Yang, L. (2008). Scale dependence of mineral dissolution rates within single pores and fractures. *Geochimica Cosmochimica Acta* 72, 360–377. doi:10.1016/j.gca.2007.10.027

Li, M.-H., Wang, T.-H., and Teng, S.-P. (2009). Experimental and numerical investigations of effect of column length on retardation factor determination: a case study of cesium transport in crushed granite. *J. Hazard. Mater.* 162, 530–535. doi:10.1016/j.jhazmat.2008.05.076

Liger, E., Charlet, L., and VAN Cappellen, P. (1999). Surface catalysis of uranium(VI) reduction by iron(II). *Geochimica Cosmochimica Acta* 63, 2939–2955. doi:10.1016/s0016-7037(99)00265-3

Lippmann, F. (1980). Phase diagrams depicting the aqeous solubility of binary mineral systems. *N. Jahrb. Mineral. Abh* 139, 1–25.

Lippmann-Pipke, J., Gerasch, R., Schikora, J., and Kulenkampff, J. (2017). Benchmarking PET for geoscientific applications: 3D quantitative diffusion coefficient determination in clay rock. *Comput. Geosciences* 101, 21–27. doi:10.1016/j.cageo.2017.01.002

Li, X., Liu, L., Wu, Y., and Liu, T. (2019a). Determination of the redox potentials of solution and solid surface of Fe(II) associated with iron oxyhydroxides. *ACS Earth Space Chem.* 3, 711–717. doi:10.1021/acsearthspacechem.9b00001

Li, X., Meng, S., Puhakka, E., Ikonen, J., Liu, L., and Siitari-Kauppi, M. (2019b). A modification of the electromigration device and modelling methods for diffusion and sorption studies of radionuclides in intact crystalline rocks. *J. Contam. Hydrol.* 103585.

Li, X., Puhakka, E., Ikonen, J., Söderlund, M., Lindberg, A., Holgersson, S., et al. (2018). Sorption of Se species on mineral surfaces, part I: batch sorption and multi-site modelling. *Appl. Geochem.* 95, 147–157. doi:10.1016/j.apgeochem.2018.05.024

Li, X., Puhakka, E., Liu, L., Zhang, W., Ikonen, J., Lindberg, A., et al. (2020). Multi-site surface complexation modelling of Se(IV) sorption on biotite. *Chem. Geol.* 533, 119433. doi:10.1016/j.chemgeo.2019.119433

Liu, X. D., Tournassat, C., Grangeon, S., Kalinichev, A. G., Takahashi, Y., and Fernandes, M. M. (2022). Molecular-level understanding of metal ion retention in clay-rich materials. *Nat. Rev. Earth & Environ.* 3, 461–476. doi:10.1038/s43017-022-00301-z

Liu, X., Cheng, J., Sprik, M., Lu, X., and Wang, R. (2015a). Interfacial structures and acidity of edge surfaces of ferruginous smectites. *Geochimica Cosmochimica Acta* 168, 293–301. doi:10.1016/j.gca.2015.07.015

Liu, X., Cheng, J., Sprik, M., Lu, X., and Wang, R. (2014). Surface acidity of 2:1-type dioctahedral clay minerals from first principles molecular dynamics simulations. *Geochimica Cosmochimica Acta* 140, 410–417. doi:10.1016/j.gca.2014.05.044

Liu, X., Fattahi, M., Montavon, G., and Grambow, B. (2008). Selenide retention onto pyrite under reducing conditions. *Radiochim. Acta* 96, 473–479. doi:10.1524/ract.2008.1514

Liu, X., Jan Meijer, E., Lu, X., and Wang, R. (2012a). First-principles molecular dynamics insight into Fe2+ complexes adsorbed on edge surfaces of clay minerals. *Clays clay minerals* 60, 341–347. doi:10.1346/ccmn.2012.0600401

Liu, X., Lu, X., Cheng, J., Sprik, M., and Wang, R. (2015b). Temperature dependence of interfacial structures and acidity of clay edge surfaces. *Geochimica Cosmochimica Acta* 160, 91–99. doi:10.1016/j.gca.2015.04.005

Liu, X., Lu, X., Meijer, E. J., Wang, R., and Zhou, H. (2012b). Atomic-scale structures of interfaces between phyllosilicate edges and water. *Geochimica Cosmochimica Acta* 81, 56–68. doi:10.1016/j.gca.2011.12.009

Liu, X., Lu, X., Sprik, M., Cheng, J., Meijer, E. J., and Wang, R. (2013). Acidity of edge surface sites of montmorillonite and kaolinite. *Geochimica Cosmochimica Acta* 117, 180–190. doi:10.1016/j.gca.2013.04.008

Liu, X., Lu, X., Wang, R., Meijer, E. J., and Zhou, H. (2011). Acidities of confined water in interlayer space of clay minerals. *Geochimica Cosmochimica Acta* 75, 4978–4986. doi:10.1016/j.gca.2011.06.011

Livens, F. R., Jones, M. J., Hynes, A. J., Charnock, J. M., Mosselmans, J. F. W., Hennig, C., et al. (2004). X-ray absorption spectroscopy studies of reactions of technetium, uranium and neptunium with mackinawite. *J. Environ. Radioact.* 74, 211–219. doi:10.1016/j.jenvrad.2004.01.012

Llorens, I., Fattahi, M., and Grambow, B. (2007). "New synthesis route and characterization of siderite (FeCO3) and coprecipitation of 99Tc," in *Scientific basis for nuclear waste management Xxx*. Editors D. DUNN, C. POINSSOT, and B. BEGG Cambridge University Press.

Löfgren, M., Crawford, J., and Elert, M. (2007). *Tracer tests - possibilities and limitations. Experience from SKB fieldwork: 1977-2007*. SKB report P-07-39. Stockholm, Sweden: SKB.

Lofgren, M., and Neretnieks, I. (2006). Through-electromigration: a new method of investigating pore connectivity and obtaining formation factors. *J. Contam. Hydrol.* 87, 237–252. doi:10.1016/j.jconhyd.2006.05.006

Löfgren, M., Vecernik, P., and Havlova, V. (2009). *Studying the influence of pore water electrical conductivity on the formation factor, as estimated based on electrical methods SKB-R-09-57*. Sweden: SKB.

Luan, F., Gorski, C. A., and Burgos, W. D. (2014). Thermodynamic controls on the microbial reduction of iron-bearing nontronite and uranium. *Environ. Sci. & Technol.* 48, 2750–2758. doi:10.1021/es404885e

Lützenkirchen, J., Preočanin, T., Bauer, A., Metz, V., and Sjöberg, S. (2012a). Net surface proton excess of smectites obtained from a combination of potentiometric acid–base, mass and electrolyte titrations. *Colloids Surf. A: Physicochem. Eng. Asp.* 412, 11–19. doi:10.5562/cca2062

Lützenkirchen, J., Preočanin, T., Kovačević, D., Tomišić, V., Lövgren, L., and Kallay, N. (2012b). Potentiometric titrations as a tool for surface charge determination. *Croat. Chem. Acta.* 85, 391–417. doi:10.1016/j.colsurfa.2012.06.024

Ma, B., Charlet, L., Fernandez-Martinez, A., Kang, M., and Madé, B. (2019). A review of the retention mechanisms of redox-sensitive radionuclides in multi-barrier systems. *Appl. Geochem.* 100, 414–431. doi:10.1016/j.apgeochem.2018.12.001

Ma, B., Fernandez-Martinez, A., Wang, K. F., Made, B., Henocq, P., Tisserand, D., et al. (2020). Selenite sorption on hydrated CEM-V/A cement in the presence of steel corrosion products: redox vs Nonredox sorption. *Environ. Sci. & Technol.* 54, 2344–2352. doi:10.1021/acs.est.9b06876

Mäder, U., Jenni, A., Lerouge, C., Gaboreau, S., Miyoshi, S., Kimura, Y., et al. (2018). "5-year chemico-physical evolution of concrete-claystone interfaces, Mont Terri rock laboratory (Switzerland)," in *Mont Terri rock laboratory, 20 years* (Switzerland: Birkhäuser).

Maes, A., Peigneur, P., and Cremers, A. (1975). Thermodynamics of transition metal ion exchange in montmorillonite. *Proc. Int. Clay Conf.*, 319–333.

Maes, N., Bruggeman, C., Govaerts, J., Martens, E., Salah, S., and VAN Gompel, M. (2011). A consistent phenomenological model for natural organic matter linked migration of Tc (IV), Cm (III), Np (IV), Pu (III/IV) and Pa (V) in the Boom Clay. *Phys. Chem. Earth* 36, 1590–1599. doi:10.1016/j.pce.2011.10.003

Maes, N., Delécaut, G., Beauwens, T., VAN Geet, M., Put, M., Weetjens, E., et al. (2004a). *Migration Case Study: transport of radionuclides in a reducing Clay Sediment (TRANCOM-II) - final scientific and technical report of the EC TRANCOM-II project SCK CEN-BLG988*. Mol, Belgium: SCK CEN.

Maes, N., Glaus, M., Rainer, D., and Churakov, S. V. (2024). Final technical report on radionuclide mobility in compacted clay systems and reversibility of sorption. *Deliv. D5.4&5.6 HORIZON 2020 Proj. EURAD - WP5 FUTURE. EC grant Agreem. no*, 847593.

Maes, N., Moors, H., DE Canniere, P., Aertsens, M., and Put, M. (1998). Determination of the diffusion coefficient of ionic species in boom clay by electromigration: Feasibility study. *Radiochim. Acta* 82, 183–190. doi:10.1524/ract.1998.82.special-issue.183

Maes, N., Moors, H., Dierckx, A., Aertsens, M., Wang, L., DE Cannière, P., et al. (2001). "Studying the migration behaviour of radionuclides in Boom Clay by electromigration," in *EREM2001, 3rd symposium and status report on electrokinetic remediation, 2001 Karlsruhe*. Editors C. CZURDA, R. HAUS, C. KAPPELER, and R. ZORN (Karlsruhe: Schriftenreihe angewandte geologie Karlsruhe, Universität Karlsruhe), 35/1–21.

Maes, N., Moors, H., Dierckx, A., DE Canniere, P., and Put, M. (1999). The assessment of electromigration as a new technique to study diffusion of radionuclides in clayey soils. *J. Contam. Hydrology* 36, 231–247. doi:10.1016/s0169-7722(98)00146-6

Maes, N., Moors, H., Wang, L., Delécaut, G., DE Canniere, P., and Put, M. (2002). The use of electromigration as a qualitative technique to study the migration behaviour and speciation of uranium in the Boom Clay. *Radiochim. Acta* 90, 741–746. doi:10.1524/ract.2002.90.9-11_2002.741

Maes, N., Salah, S., Bruggeman, C., and Aertsens, M. (2017a). *Caesium retention and migration behaviour in Boom Clay SCK CEN-0387*. Mol, Belgium: Studiecentrum voor Kernenergie.

Maes, N., Salah, S., Bruggeman, C., Aertsens, M., Martens, E., and VAN Laer, L. (2017b). Strontium retention and migration behaviour in Boom Clay. *Mol SCK CEN-ER0394, Belg. Stud. Kernenerg.*

Maes, N., Wang, L., Delécaut, G., Beauwens, T., VAN Geet, M., Put, M., et al. (2004b) "Migration case study: transport of radionuclides in a reducing clay sediment (Trancom-II) EUR 21022," in *Nuclear science and technology*. Luxembourg: EC.

Maes, N., Wang, L., Hicks, T., Bennett, D., Warwick, P., Hall, T., et al. (2006). The role of natural organic matter in the migration behaviour of americium in the Boom Clay - Part I: migration experiments. *Phys. Chem. Earth* 31, 541–547. doi:10.1016/j.pce.2006.04.006

Mahrous, M., Curti, E., Churakov, S. V., and Prasianakis, N. I. (2022). Petrophysical initialization of core-scale reactive transport simulations on Indiana limestones: pore-scale characterization, spatial autocorrelations, and representative elementary volume analysis. *J. Petroleum Sci. Eng.* 213, 110389. doi:10.1016/j.petrol.2022.110389

Malikova, N., Dubois, E., Marry, V., Rotenberg, B., and Turq, P. (2010). Dynamics in clays - combining neutron scattering and microscopic simulation. *Zeitschrift Fur Physikalische Chemie-International J. Res. Phys. Chem. & Chem. Phys.* 224, 153–181. doi:10.1524/zpch.2010.6097

Malloszewski, P., and Zuber, A. (1992). On the calibration and validation of mathematical models for the interpretation of tracer experiments in groundwater. *Adv. Water Resour.* 15, 47–62. doi:10.1016/0309-1708(92)90031-v

Manceau, A., Chateigner, D., and Gates, W. P. (1998). Polarized EXAFS, distance-valence least-squares modeling (DVLS), and quantitative texture analysis approaches to the structural refinement of Garfield nontronite. *Phys. Chem. Minerals* 25, 347–365. doi:10.1007/s002690050125

Manceau, A., Drits, V. A., Silvester, E., Bartoli, C., and Lanson, B. (1997). Structural mechanism of $Co^{2+}$ oxidation by the phyllomanganate buserite. *Am. Mineralogist* 82, 1150–1175. doi:10.2138/am-1997-11-1213

Manceau, A., Lanson, B., Schlegel, M. L., Hargé, J. C., Musso, M., Eybert-Bérard, L., et al. (2000). Quantitative Zn speciation in smelter-contaminated soils by EXAFS spectroscopy. *Am. J. Sci.* 300, 289–343. doi:10.2475/ajs.300.4.289

Manceau, A., Schlegel, M. L., Nagy, K. L., and Charlet, L. (1999). Evidence for the formation of trioctahedral clay upon sorption of Co2+ on quartz. *J. Colloid Interface Sci.* 220, 181–197. doi:10.1006/jcis.1999.6547

Manning, B. A., and Goldberg, S. (1996). Modeling arsenate competitive adsorption on kaolinite, montmorillonite and illite. *Clays clay minerals* 44, 609–623. doi:10.1346/ccmn.1996.0440504

Maples, S. R., Andraski, B. J., Stonestrom, D. A., Cooper, C. A., Pohll, G., and Michel, R. L. (2013). Tritium plume dynamics in the Shallow unsaturated zone in an arid environment. *Vadose Zone J.* 12, 1–15. doi:10.2136/vzj2013.05.0080

Marivoet, J., Jacques, D., VAN Geet, M., Bastiaens, W., and Wemaere, I. (2006). *Considerations on up-scaling of hydraulid and transport parameters for clay formations. IP-FUNMIG Project Internal Deliverable PID3.4.4.* Mol SCK CEN report06/JMa/P-13. Belgium.

Markelova, E. (2017). Interpretation of redox potential and assessment of oxyanion (As, Sb, Cr) mobility during oxic-anoxic oscillations. *UWSpace*.

Marques Fernandes, M., and Baeyens, B. (2020). *Competitive adsorption on illite and montmorillonite: experimental and modelling investigations NAGRA NTB 19-05*. Switzerland: NAGRA.

Marques Fernandes, M., Klinkenberg, M., Baeyens, B., Bosbach, D., and Brandt, F. (2023). Adsorption of Ba and 226Ra on illite: a comparative experimental and modelling study. *Appl. Geochem.* 159, 105815. doi:10.1016/j.apgeochem.2023.105815

Marques Fernandes, M., Ver, N., and Baeyens, B. (2015). Predicting the uptake of Cs, Co, Ni, Eu, Th and U on argillaceous rocks using sorption models for illite. *Appl. Geochem.* 59, 189–199. doi:10.1016/j.apgeochem.2015.05.006

Marsac, R., Banik, N. L., Lutzenkirchen, J., Marquardt, C. M., Dardenne, K., Schild, D., et al. (2015). Neptunium redox speciation at the illite surface. *Geochimica Cosmochimica Acta* 152, 39–51. doi:10.1016/j.gca.2014.12.021

Marschall, P., Horseman, S., and Gimmi, T. (2005). Characterisation of gas transport properties of the opalinus clay, a potential host rock formation for radioactive waste disposal. *Oil & Gas Sci. Technol. - Rev. IFP* 60, 121–139. doi:10.2516/ogst:2005008

Marshall, T. A., Morris, K., Law, G. T. W., Mosselmans, J. F. W., Bots, P., Parry, S. A., et al. (2014). Incorporation and retention of 99-Tc(IV) in magnetite under high pH conditions. *Environ. Sci. & Technol.* 48, 11853–11862. doi:10.1021/es503438e

Martens, E., Maes, N., Weetjens, E., VAN Gompel, M., and VAN Ravestyn, L. (2010). Modelling of a large-scale*in-situ*migration experiment with$^{14}$C-labelled natural organic matter in Boom Clay. *Radiochim. Acta* 98, 695–701. doi:10.1524/ract.2010.1770

Martin, A., Siitari-Kauppi, M., Havlova, V., Tachi, Y., and Miksova, J. (2013). "An overview of the long-term diffusion test, Grimsel Test Site, Switzerland," in *Migration conference 2013*, 313–314. 2013 2013 Brighton, UK.

Mathurin, F. A., Drake, H., Tullborg, E.-L., Berger, T., Peltola, P., Kalinowski, B. E., et al. (2014). High cesium concentrations in groundwater in the upper 1.2km of fractured crystalline rock – influence of groundwater origin and secondary minerals. *Geochimica Cosmochimica Acta* 132, 187–213. doi:10.1016/j.gca.2014.02.001

Mayordomo, N., Alonso, U., and Missana, T. (2016). Analysis of the improvement of selenite retention in smectite by adding alumina nanoparticles. *Sci. Total Environ.* 572, 1025–1032. doi:10.1016/j.scitotenv.2016.08.008

Mayordomo, N., Alonso, U., and Missana, T. (2019). Effects of γ-alumina nanoparticles on strontium sorption in smectite: Additive model approach. *Appl. Geochem.* 100, 121–130. doi:10.1016/j.apgeochem.2018.11.012

Mazurek, M., Alt-Epping, P., Bath, A., Gimmi, T., Waber, H. N., Buschaert, S., et al. (2011). Natural tracer profiles across argillaceous formations. *Appl. Geochem.* 26, 1035–1064. doi:10.1016/j.apgeochem.2011.03.124

Mazurek, M., Alt-Epping, P., Gimi, T., Niklaus Waber, H., Bath, A., and Gimmi, T. (2009). *Natural tracer profiles across argillaceous formations: the Claytrac project, Nuclear Energy Agency of the OECD (NEA)*. France: Organisation for Economic Co-Operation and Development Nuclear Energy Agency.

Mazurek, M., Gimmi, T., Zwahlen, C., Aschwanden, L., Gaucher, E. C., Kiczka, M., et al. (2023). Swiss deep drilling campaign 2019–2022: geological overview and rock properties with focus on porosity and pore-space architecture. *Appl. Geochem.* 159, 105839. doi:10.1016/j.apgeochem.2023.105839

Mazurier, A., Sardini, P., Rossi, A. M., Graham, R. C., Hellmuth, K.-H., Parneix, J.-C., et al. (2016). Development of a fracture network in crystalline rocks during weathering: study of Bishop Creek chronosequence using X-ray computed tomography and14C-PMMA impregnation method. *Geol. Soc. Am. Bull.* 128, 1423–1438. doi:10.1130/b31336.1

Mcbeth, J. M., Lloyd, J. R., Law, G. T. W., Livens, F. R., Burke, I. T., and Morris, K. (2011). Redox interactions of technetium with iron-bearing minerals. *Mineral. Mag.* 75, 2419–2430. doi:10.1180/minmag.2011.075.4.2419

Mckinley, J. P., Zachara, J. M., Smith, S. C., and Turner, G. D. (1995). The influence of uranyl hydrolysis and multiple site-binding reactions on adsorption of U (VI) to montmorillonite. *Clays clay minerals* 43, 586–598. doi:10.1346/ccmn.1995.0430508

Means, J. L., Crerar, D. A., Borcsik, M. P., and Duguid, J. O. (1978). Radionuclide adsorption by manganese oxides and implications for radioactive waste disposal. *Nature* 274, 44–47. doi:10.1038/274044a0

Meena, A. H., and Arai, Y. (2017). Environmental geochemistry of technetium. *Environ. Chem. Lett.* 15, 241–263. doi:10.1007/s10311-017-0605-7

Meier, L. P., and Kahr, G. (1999). Determination of the cation exchange capacity (CEC) of clay minerals using the complexes of copper(II) ion with triethylenetetramine and tetraethylenepentamine. *Clays & Clay Minerals* 47, 386–388. doi:10.1346/ccmn.1999.0470315

Meinrath, G. (1997). Uranium(VI) speciation by spectroscopy. *J. Radioanalytical Nucl. Chem.* 224, 119–126. doi:10.1007/bf02034623

Meldrum, F. C., and O'Shaughnessy, C. (2020). Crystallization in confinement. *Adv. Mater.* 32, 2001068. Crystallization in Confinement. doi:10.1002/adma.202001068

Melkior, T., Yahiaoui, S., Motellier, S., Thoby, D., and Tevissen, E. (2005). Cesium sorption and diffusion in Bure mudrock samples. *Appl. Clay Sci.* 29, 172–186. doi:10.1016/j.clay.2004.12.008

Melkior, T., Yahiaoui, S., Thoby, D., Motellier, S., and Barthes, V. (2007). Diffusion coefficients of alkaline cations in Bure mudrock. *Phys. Chem. Earth* 32, 453–462. doi:10.1016/j.pce.2006.04.035

Mell, P., Megyeri, J., Riess, L., Máthé, Z., Csicsák, J., and Lázár, K. (2006a). Sorption of Co, Cs, Sr and I onto argillaceous rock as studied by radiotracers</p> </p>. *J. radioanalytical Nucl. Chem.* 268, 405–410. doi:10.1556/jrnc.268.2006.2.31

Mell, P., Megyeri, J., Riess, L., Máthé, Z., Hámos, G., and Lázár, K. (2006b). Diffusion of Sr, Cs, Co and I in argillaceous rock as studied by radiotracers</p> </p>. *J. Radioanalytical Nucl. Chem.* 268, 411–417. doi:10.1007/s10967-006-0178-6

Meng, S., Li, X., Siitari-Kauppi, M., and Liu, L. (2020). Development and application of an advection-dispersion model for data analysis of electromigration experiments with intact rock cores. *J. Contam. Hydrology* 231, 103618. doi:10.1016/j.jconhyd.2020.103618

Menke, H. P., Reynolds, C. A., Andrew, M. G., Pereira Nunes, J. P., Bijeljic, B., and Blunt, M. J. (2018). 4D multi-scale imaging of reactive flow in carbonates: assessing the impact of heterogeneity on dissolution regimes using streamlines at multiple length scales. *Chem. Geol.* 481, 27–37. doi:10.1016/j.chemgeo.2018.01.016

Menut, D., Descostes, M., Meier, P., Radwan, J., Mauchien, P., and Poinssot, C. (2006). "Europium migration in argilaceous rocks: on the use of micro laser-induced breakdown spectroscopy (micro LIBS) as a microanalysis tool," in *Scientific basis for nuclear waste management Xxix*. Editor P. VANISEGHEM Materials Research Society.

Meunier, A., and Fradin, N. (2005). *Clays*. Springer.

Miller, A. W., and Wang, Y. (2012). Radionuclide interaction with clays in dilute and heavily compacted systems: a critical review. *Environ. Sci. Technol.* 46, 1981–1994. doi:10.1021/es203025q

Minardi, A., Giger, S. B., Ewy, R. T., Stankovic, R., Stenebråten, J., Soldal, M., et al. (2021). Benchmark study of undrained triaxial testing of Opalinus Clay shale: results and implications for robust testing. *Geomechanics Energy Environ.* 25, 100210. doi:10.1016/j.gete.2020.100210

Missana, T., Alonso, U., and García-Gutiérrez, M. (2009). Experimental study and modelling of selenite sorption onto illite and smectite clays. *J. Colloid Interface Sci.* 334, 132–138. doi:10.1016/j.jcis.2009.02.059

Missana, T., Alonso, Ú., García-Gutiérrez, M., and Mingarro, M. (2008a). Role of bentonite colloids on europium and plutonium migration in a granite fracture. *Appl. Geochem.* 23, 1484–1497. doi:10.1016/j.apgeochem.2008.01.008

Missana, T., Benedicto, A., García-Gutiérrez, M., and Alonso, U. (2014). Modeling cesium retention onto Na-K-and Ca-smectite: effects of ionic strength, exchange and

competing cations on the determination of selectivity coefficients. *Geochimica Cosmochimica Acta* 128, 266–277. doi:10.1016/j.gca.2013.10.007

Missana, T., and GarcıA-Gutierrez, M. (2007). Adsorption of bivalent ions (Ca (II), Sr (II) and Co (II)) onto FEBEX bentonite. *Phys. Chem. Earth, Parts A/B/C* 32, 559–567. doi:10.1016/j.pce.2006.02.052

Missana, T., GarcıA-Gutiérrez, M., and Alonso, U. (2004). Kinetics and irreversibility of cesium and uranium sorption onto bentonite colloids in a deep granitic environment. *Appl. clay Sci.* 26, 137–150. doi:10.1016/j.clay.2003.09.008

Missana, T., Garcia-Gutierrez, M., and Alonso, U. (2008b). Sorption of strontium onto illite/smectite mixed clays. *Phys. Chem. Earth, Parts A/B/C* 33, S156–S162. doi:10.1016/j.pce.2008.10.020

Missana, T., Maffiotte, C., and GarcıA-Gutiérrez, M. (2003). Surface reactions kinetics between nanocrystalline magnetite and uranyl. *J. Colloid Interface Sci.* 261, 154–160. doi:10.1016/s0021-9797(02)00227-8

Mitchell, J. K. (1993). *Fundamentals of soil behavior*. Wiley.

Molins, S. (2015). Reactive interfaces in direct numerical simulation of pore-scale processes. *Rev. Mineralogy Geochem.* 80, 461–481. doi:10.2138/rmg.2015.80.14

Molodtsov, K., Demnitz, M., Schymura, S., Jankovský, F., Zuna, M., Havlová, V., et al. (2021). Molecular-level speciation of Eu(III) adsorbed on a Migmatized gneiss as determined using μTRLFS. *Environ. Sci. & Technol.* 55, 4871–4879. doi:10.1021/acs.est.0c07998

Molodtsov, K., Schymura, S., Rothe, J., Dardenne, K., and Schmidt, M. (2019). Sorption of Eu(III) on Eibenstock granite studied by μTRLFS: a novel spatially-resolved luminescence-spectroscopic technique. *Sci. Rep.* 9, 6287. doi:10.1038/s41598-019-42664-2

Montavon, G., Ribet, S., Bailly, C., Loni, Y. H., Made, B., and Grambow, B. (2023). U(VI) retention in compact Callovo-Oxfordian clay stone at temperature (20-80 °C); what is the applicability of adsorption models? *Appl. Clay Sci.* 244, 107093. doi:10.1016/j.clay.2023.107093

Montavon, G., Ribet, S., Loni, Y. H., Maia, F., Bailly, C., David, K., et al. (2022). Uranium retention in a Callovo-Oxfordian clay rock formation: from laboratory-based models to in natura conditions. *Chemosphere* 299, 134307. doi:10.1016/j.chemosphere.2022.134307

Montavon, G., Sabatie-Gogova, A., Ribet, S., Bailly, C., Bessaguet, N., Durce, D., et al. (2014). Retention of iodide by the Callovo-Oxfordian formation: an experimental study. *Appl. Clay Sci.* 87, 142–149. doi:10.1016/j.clay.2013.10.023

Montoya, V., Baeyens, B., Glaus, M. A., Kupcik, T., Fernandes, M. M., VAN Laer, L., et al. (2018). Sorption of Sr, Co and Zn on illite: batch experiments and modelling including Co in-diffusion measurements on compacted samples. *Geochimica Cosmochimica Acta* 223, 1–20. doi:10.1016/j.gca.2017.11.027

Moors, H. (2005). *Topical report on the effect of the ionic strength on the diffusion accessible porosity of Boom Clay SCK CEN-ER02*. Mol, Belgium: SCK-CEN, Belgian Nuclear Research Centre.

Morad, S., Sirat, M., EL-Ghali, M. A. K., and Mansurbeg, H. (2018). Chloritization in Proterozoic granite from the Äspö Laboratory, southeastern Sweden: record of hydrothermal alterations and implications for nuclear waste storage. *Clay Miner.* 46, 495–513. doi:10.1180/claymin.2011.046.3.495

Moreno, L., Gylling, B., and Neretnieks, I. (1997). Solute transport in fractured media — the important mechanisms for performance assessment. *J. Contam. Hydrology* 25, 283–298. doi:10.1016/s0169-7722(96)00037-x

Moreno, L., and Neretnieks, I. (1993). Fluid flow and solute transport in a network of channels. *J. Contam. Hydrology* 14, 163–192. doi:10.1016/0169-7722(93)90023-l

Moreno, L., Svensson, E., and Neretnieks, I. (2000). Determination of the flow-wetted surface in fractured media. *MRS Proc.* 663, 869. doi:10.1557/proc-663-869

Morton, J. D., Semrau, J. D., and Hayes, K. F. (2001). An X-ray absorption spectroscopy study of the structure and reversibility of copper adsorbed to montmorillonite clay. *Geochimica Cosmochimica Acta* 65, 2709–2722. doi:10.1016/s0016-7037(01)00633-0

Motellier, S., Devol-Brown, I., Savoye, S., Thoby, D., and Alberto, J. C. (2007). Evaluation of tritiated water diffusion through the Toarcian clayey formation of the Tournemire experimental site (France). *J. Contam. Hydrology* 94, 99–108. doi:10.1016/j.jconhyd.2007.05.012

Motta, M. M., and Miranda, C. (1989). Molybdate adsorption on kaolinite, montmorillonite, and illite: constant capacitance modeling. *Soil Sci. Soc. Am. J.* 53, 380–385. doi:10.2136/sssaj1989.03615995005300020011x

Moyes, L. N., Jones, M. J., Reed, W. A., Livens, F. R., Charnock, J. M., Mosselmans, J. F. W., et al. (2002). An X-ray absorption spectroscopy study of neptunium(V) reactions with mackinawite (FeS). *Environ. Sci. & Technol.* 36, 179–183. doi:10.1021/es0100928

Muller, F., Besson, G., Manceau, A., and Drits, V. A. (1997). Distribution of isomorphous cations within octahedral sheets in montmorillonite from Camp-Bertaux. *Phys. Chem. Minerals* 24, 159–166. doi:10.1007/s002690050029

Muuri, E. (2019). *Migration of barium in crystalline rock: interpretation of* in situ *experiments*. PhD Thesis (Finland: University of Helsinki).

Muuri, E., Matara-Aho, M., Puhakka, E., Ikonen, J., Martin, A., Koskinen, L., et al. (2018). The sorption and diffusion of 133Ba in crushed and intact granitic rocks from the Olkiluoto and Grimsel *in-situ* test sites. *Appl. Geochem.* 89, 138–149. doi:10.1016/j.apgeochem.2017.12.004

Muuri, E., Siitari-Kauppi, M., Matara-Aho, M., Ikonen, J., Lindberg, A., Qian, L., et al. (2017). Cesium sorption and diffusion on crystalline rock: Olkiluoto case study. *J. Radioanalytical Nucl. Chem.* 311, 439–446. doi:10.1007/s10967-016-5087-8

Nagasaki, S., Riddoch, J., Saito, T., Goguen, J., Walker, A., and Yang, T. T. (2017). Sorption behaviour of Np(IV) on illite, shale and MX-80 in high ionic strength solutions. *J. Radioanalytical Nucl. Chem.* 313, 1–11. doi:10.1007/s10967-017-5290-2

Nagasaki, S., Saito, T., and Yang, T. T. (2016). Sorption behavior of Np(V) on illite, shale and MX-80 in high ionic strength solutions. *J. Radioanalytical Nucl. Chem.* 308, 143–153. doi:10.1007/s10967-015-4332-x

NAGRA (2002). *Project Opalinus Clay – Safety report – Demonstration of disposal feasibility for spent fuel, vitrified high-level waste and long-lived intermediate-level waste (Entsorgungsnachweis) NAGRA NTB 02-05*. Wettingen, Switzerland: National Cooperative for the Disposal of Radioactive Waste.

Naveau, A., Monteil-Rivera, F., Guillon, E., and Dumonceau, J. (2007). Interactions of aqueous selenium (–II) and (IV) with metallic sulfide surfaces. *Environ. Sci. & Technol.* 41, 5376–5382. doi:10.1021/es0704481

Necib, S., Linard, Y., Crusset, D., Michau, N., Daumas, S., Burger, E., et al. (2016). Corrosion at the carbon steel□clay borehole water and gas interfaces at 85 °C under anoxic and transient acidic conditions. *Corros. Sci.* 111, 242–258. doi:10.1016/j.corsci.2016.04.039

Németh, T., Máthé, Z., Pekker, P., Dódony, I., Kovács-Kis, V., Sipos, P., et al. (2016). Clay mineralogy of the Boda Claystone Formation (Mecsek Mts., SW Hungary). *Open Geosci.* 8, 259–274. doi:10.1515/geo-2016-0024

Neretnieks, I. (1993). *Solute transport in fractured rock — applications to radionuclide waste repositories*. Elsevier.

Neumann, A., Hofstetter, T. B., Lüssi, M., Cirpka, O. A., Petit, S., and Schwarzenbach, R. P. (2008). Assessing the redox reactivity of structural iron in smectites using Nitroaromatic compounds as kinetic probes. *Environ. Sci. & Technol.* 42, 8381–8387. doi:10.1021/es801840x

Neumann, A., Sander, M., and Hofstetter, T. B. (2011). "Redox properties of structural Fe in smectite clay minerals," in *Aquatic redox chemistry* (American Chemical Society).

Neumann, J., Brinkmann, H., Britz, S., Lützenkirchen, J., Bok, F., Stockmann, M., et al. (2020). A comprehensive study of the sorption mechanism and thermodynamics of f-element sorption onto K-feldspar. *J. Colloid Interface Sci.* 591, 490–499. under review. doi:10.1016/j.jcis.2020.11.041

Nilsson, N., Persson, P., Lövgren, L., and Sjöberg, S. (1996). Competitive surface complexation of o-phthalate and phosphate on goethite (α-FeOOH) particles. *Geochimica cosmochimica acta* 60, 4385–4395. doi:10.1016/s0016-7037(96)00258-x

Nishimoto, S., and Yoshida, H. (2010). Hydrothermal alteration of deep fractured granite: effects of dissolution and precipitation. *Lithos* 115, 153–162. doi:10.1016/j.lithos.2009.11.015

Niwa, M., Shimada, K., Tamura, H., Shibata, K., Sueoka, S., Yasue, K.-I., et al. (2016). Thermal constraints on clay growth in fault Gouge and their relationship with Fault-zone evolution and hydrothermal alteration: case study of Gouges in the Kojaku granite, Central Japan. *Clays Clay Minerals* 64, 86–107. doi:10.1346/ccmn.2016.0640202

Noguera, C., Fritz, B., and Clément, A. (2016). Kinetics of precipitation of non-ideal solid-solutions in a liquid environment. *Chem. Geol.* 431, 20–35. doi:10.1016/j.chemgeo.2016.03.009

Noh, J. S., and Schwarz, J. A. (1989). Estimation of the point of zero charge of simple oxides by mass titration. *J. Colloid Interface Sci.* 130, 157–164. doi:10.1016/0021-9797(89)90086-6

Nollet, S., Koerner, T., Kramm, U., and Hilgers, C. (2009). Precipitation of fracture fillings and cements in the Buntsandstein (NW Germany). *Geofluids* 9, 373–385. doi:10.1111/j.1468-8123.2009.00261.x

Noseck, U., Brendler, V., Britz, S., Stockmann, M., Fricke, J., Richter, C., et al. (2018). *Smart Kd-concept for long-term safety assessments - extension towards more complex applications*. Braunschweig, Gremany. GRS Series, GRS-500.

Noseck, U., Britz, S., Flügge, J., and Mönig, J. B. V. S. M. (2014). *New methodology for realistic integration of sorption processes in safety assessments*. Arizona, USA. 2014 2014 Phoenix.

Noseck, U., Fluegge, J., Britz, S., Schneider, A., Brendler, V., Stockmann, M., et al. (2012). *Realistic integration of sorption processes in transport codes for long-term safety assessments GRS-297*. Germany.

Nunn, J. A., Xiang, Y., and AL, T. A. (2018). Investigation of partial water saturation effects on diffusion in shale. *Appl. Geochem.* 97, 93–101. doi:10.1016/j.apgeochem.2018.08.004

Nykyri, M. (2004). *RETROCK Project Treatment of geosphere retention phenomena in safety assessments Scientific basis of retention processes and their implementation in safety assessment models (WP2) Work Package 2 report of the RETROCK Concerted Action*. Sweden.

Ochs, M., Lothenbach, B., Wanner, H., Sato, H., and Yui, M. (2001). An integrated sorption-diffusion model for the calculation of consistent distribution and diffusion coefficients in compacted bentonite. *J. Contam. Hydrology* 47, 283–296. doi:10.1016/s0169-7722(00)00157-1

Ochs, M., Payne, T. E., and Brendler, V. (2012). "NEA sorption project," in *Phase III: thermodynamic sorption modelling in support of radioactive waste disposal safety cases* (France: NEA OECD publication). No. 6914.

OECD/NEA (1996). "Fluid Flow through faults and fractures in argillaceous formations," in *Joint NEA/EC workshop on fluid flow through faults and fractures in argillaceous formations, 1996 Berne* (Paris: OECD/NEA).

Okumura, M., Sassi, M., Rosso, K. M., and Machida, M. (2017). Origin of 6-fold coordinated aluminum at (010)-type pyrophyllite edges. *Aip Adv.* 7, 055211. doi:10.1063/1.4983213

Olin, A., Nolang, B., Osadchii, E. G., Ohman, L.-O., and Rosén, E. (2005). *Chemical thermodynamics of selenium*. Amsterdam; London: Elsevier.

Oliveira, A. F., Kuc, A., Heine, T., Abram, U., and Scheinost, A. C. (2022). Shedding light on the Enigmatic TcO2 · xH2O structure with density functional theory and EXAFS spectroscopy. *Chem. – A Eur. J.* 28, e202202235. doi:10.1002/chem.202202235

O'Loughlin, E. J., Kelly, S. D., Cook, R. E., Csencsits, R., and Kemner, K. M. (2003). Reduction of uranium(VI) by mixed iron(II)/Iron(III) hydroxide (green rust): formation of UO2 nanoparticles. *Environ. Sci. & Technol.* 37, 721–727. doi:10.1021/es0208409

O'Loughlin, E. J., Kelly, S. D., and Kemner, K. M. (2010). XAFS investigation of the interactions of U-VI with secondary mineralization products from the bioreduction of Fe-III oxides. *Environ. Sci. & Technol.* 44, 1656–1661. doi:10.1021/es9027953

ONDRAF/NIRAS (2001). *Safir 2: safety assessment and feasibility Interim report 2 NIROND 2001-05*. Brussels, Belgium.

ONDRAF/NIRAS (2013). *ONDRAF/NIRAS Research, Development and Demonstration (RD&D) Plan for the geological disposal of high-level and/or long-lived radioactive waste including irradiated fuel if considered as waste NIROND-TR 2013-12*. Brussels, Belgium: ONDRAF/NIRAS.

Orucoglu, E., Grangeon, S., Gloter, A., Robinet, J.-C., Madé, B., and Tournassat, C. (2022). Competitive adsorption processes at clay mineral surfaces: a coupled experimental and modeling approach. *ACS Earth Space Chem.* 6, 144–159. doi:10.1021/acsearthspacechem.1c00323

Orucoglu, E., Tournassat, C., Robinet, J. C., Made, B., and Lundy, M. (2018). From experimental variability to the sorption related retention parameters necessary for performance assessment models for nuclear waste disposal systems: the example of Pb adsorption on clay minerals. *Appl. Clay Sci.* 163, 20–32. doi:10.1016/j.clay.2018.07.003

Osán, J., Kéri, A., Breitner, D., Fábián, M., Dähn, R., Simon, R., et al. (2014). Microscale analysis of metal uptake by argillaceous rocks using positive matrix factorization of microscopic X-ray fluorescence elemental maps. *Spectrochim. Acta Part B At. Spectrosc.* 91, 12–23. doi:10.1016/j.sab.2013.11.002

Owusu, J. P., Karalis, K., Prasianakis, N. I., and Churakov, S. V. (2022). Mobility of dissolved gases in smectites under saturated conditions: effects of pore size, gas types, temperature, and surface interaction. *J. Phys. Chem. C* 126, 17441–17455. doi:10.1021/acs.jpcc.2c05678

Owusu, J. P., Karalis, K., Prasianakis, N. I., and Churakov, S. V. (2023). Diffusion and gas flow dynamics in partially saturated smectites. *J. Phys. Chem. C* 127, 14425–14438. doi:10.1021/acs.jpcc.3c02264

Pabalan, R. T., and Turner, D. R. (1996). Uranium (6+) sorption on montmorillonite: experimental and surface complexation modeling study. *Aquat. Geochem.* 2, 203–226. doi:10.1007/bf00119855

Palágyi, S., and Stamberg, K. (2010). Modeling of transport of radionuclides in beds of crushed crystalline rocks under equilibrium non-linear sorption isotherm conditions. *Radiochim. Acta* 98, 359–365. doi:10.1524/ract.2010.1729

Palágyi, Š., Štamberg, K., Havlova, V., and Vodičková, H. (2012). Effect of grain size on the 85Sr2+ sorption and desorption in columns of crushed granite and infill materials from granitic water under dynamic conditions. *J. Radioanalytical Nucl. Chem.* 297, 33–39. doi:10.1007/s10967-012-2311-z

Palágyi, Š., and Vodičková, H. (2009). Sorption and desorption of 125I-137Cs+, 85Sr2+ and 152,154Eu3+ on disturbed soils under dynamic flow and static batch conditions. *J. Radioanalytical Nucl. Chem.* 280, 3–14. doi:10.1007/s10967-008-7436-8

Parigi, R., Chen, N., Liu, P., Ptacek, C. J., and Blowes, D. W. (2022). Mechanisms of Ni removal from contaminated groundwater by calcite using X-ray absorption spectroscopy and Ni isotope measurements. *J. Hazard. Mater.* 440, 129679. doi:10.1016/j.jhazmat.2022.129679

Park, C.-K., Vandergraaf, T. T., Drew, D. J., and Hahn, P.-S. (1997). Analysis of the migration of nonsorbing tracers in a natural fracture in granite using a variable aperture channel model. *J. Contam. Hydrology* 26, 97–108. doi:10.1016/s0169-7722(96)00061-7

Park, C., Fenter, P. A., Sturchio, N. C., and Nagy, K. L. (2008). Thermodynamics, interfacial structure, and pH hysteresis of Rb+ and Sr2+ adsorption at the muscovite (001)-solution interface. *Langmuir* 24, 13993–14004. doi:10.1021/la802446m

Parkhurst, D. L., and Appelo, C. A. J. (2013). "Description of input and examples for PHREEQC version 3: a computer program for speciation, batch-reaction, one-dimensional transport, and inverse geochemical calculations," in *Techniques and methods* (Reston, VA: USGS).

Parkhurst, D. L., Thorstenson, D. C., and Plummer, N. (1980). *Phreeqe: a computer program for geochemical calculations*. Water-Resources Investigations Report.

Pearce, C. I., Icenhower, J. P., Asmussen, R. M., Tratnyek, P. G., Rosso, K. M., Lukens, W. W., et al. (2018). Technetium Stabilization in low-solubility sulfide phases: a review. *Acs Earth Space Chem.* 2, 532–547. doi:10.1021/acsearthspacechem.8b00015

Pearce, C. I., Moore, R. C., Morad, J. W., Asmussen, R. M., Chatterjee, S., Lawter, A. R., et al. (2020). Technetium immobilization by materials through sorption and redox-driven processes: a literature review. *Sci. Total Environ.* 716, 132849. doi:10.1016/j.scitotenv.2019.06.195

Pearce, C. I., Rosso, K. M., Pattrick, R. A. D., Felmy, A. R., Ahmed, I. A. M., and Hudson-Edwards, K. A. (2017). "Impact of iron redox chemistry on nuclear waste disposal," in *Redox-reactive minerals: properties, reactions and applications in clean Technologies* (Mineralogical Society of Great Britain and Ireland).

Pentráková, L., Su, K., Pentrák, M., and Stucki, J. W. (2013). A review of microbial redox interactions with structural Fe in clay minerals. *Clay Miner.* 48, 543–560. doi:10.1180/claymin.2013.048.3.10

Peretyazhko, T. S., Zachara, J. M., Kukkadapu, R. K., Heald, S. M., Kutnyakov, I. V., Resch, C. T., et al. (2012). Pertechnetate (TcO4−) reduction by reactive ferrous iron forms in naturally anoxic, redox transition zone sediments from the Hanford Site, USA. *Geochimica Cosmochimica Acta* 92, 48–66. doi:10.1016/j.gca.2012.05.041

Peretyazhko, T., Zachara, J. M., Heald, S. M., Jeon, B. H., Kukkadapu, R. K., Liu, C., et al. (2008). Heterogeneous reduction of Tc(VII) by Fe(II) at the solid–water interface. *Geochimica Cosmochimica Acta* 72, 1521–1539. doi:10.1016/j.gca.2008.01.004

Pidchenko, I. (2016). Characterization of structural properties of U and Pu in model systems by advanced synchrotron based X-ray spectroscopy. Available at: http://inis.iaea.org/search/search.aspx?orig_q=RN:48037780.

Pidchenko, I., Kvashnina, K. O., Yokosawa, T., Finck, N., Bahl, S., Schild, D., et al. (2017). Uranium redox transformations after U(VI) coprecipitation with magnetite nanoparticles. *Environ. Sci. & Technol.* 51, 2217–2225. doi:10.1021/acs.est.6b04035

Pina, C. M., Enders, M., and Putnis, A. (2000). The composition of solid solutions crystallising from aqueous solutions: the influence of supersaturation and growth mechanisms. *Chem. Geol.* 168, 195–210. doi:10.1016/s0009-2541(00)00227-8

Pingel, J. L., Kulenkampff, J., Jara-Heredia, D., Stoll, M., Zhou, W. Y., Fischer, C., et al. (2023). *In-situ* flow visualization with Geo-Positron-Emission-Tomography in a granite fracture from Soultz-sous-Fore?ts, France. *Geothermics* 111, 102705. doi:10.1016/j.geothermics.2023.102705

Plumper, O., and Putnis, A. (2009). The complex hydrothermal history of granitic rocks: multiple feldspar Replacement reactions under Subsolidus conditions. *J. Petrology* 50, 967–987. doi:10.1093/petrology/egp028

Poinssot, C., Baeyens, B., and Bradbury, M. H. (1999). Experimental and modelling studies of caesium sorption on illite. *Geochim. Cosmochim. Acta* 63, 3217–3227. doi:10.1016/s0016-7037(99)00246-x

Poonoosamy, J., Curti, E., Kosakowski, G., Grolimund, D., VAN Loon, L. R., and Mäder, U. (2016). Barite precipitation following celestite dissolution in a porous medium: a SEM/BSE and μ-XRD/XRF study. *Geochimica Cosmochimica Acta* 182, 131–144. doi:10.1016/j.gca.2016.03.011

Poonoosamy, J., Klinkenberg, M., Deissmann, G., Brandt, F., Bosbach, D., Mäder, U., et al. (2020). Effects of solution supersaturation on barite precipitation in porous media and consequences on permeability: experiments and modelling. *Geochimica Cosmochimica Acta* 270, 43–60. doi:10.1016/j.gca.2019.11.018

Poonoosamy, J., Mahrous, M., Curti, E., Bosbach, D., Deissmann, G., Churakov, S. V., et al. (2021). A lab-on-a-chip approach integrating *in-situ* characterization and reactive transport modelling diagnostics to unravel (Ba,Sr)SO4 oscillatory zoning. *Sci. Rep.* 11, 23678. doi:10.1038/s41598-021-02840-9

Poonoosamy, J., Westerwalbesloh, C., Deissmann, G., Mahrous, M., Curti, E., Churakov, S. V., et al. (2019). A microfluidic experiment and pore scale modelling diagnostics for assessing mineral precipitation and dissolution in confined spaces. *Chem. Geol.* 528, 119264. doi:10.1016/j.chemgeo.2019.07.039

Porro, I., Newman, M. E., and Dunnivant, F. M. (2000). Comparison of batch and column methods for determining strontium distribution coefficients for unsaturated transport in basalt. *Environ. Sci. & Technol.* 34, 1679–1686. doi:10.1021/es9901361

POSIVA (2012a). *Olkiluoto site description 2011 POSIVA-11-02*. Finland, Helsinki: Posiva Oy.

POSIVA (2012b). *Safety case for the disposal of spent nuclear fuel at Olkiluoto Description of the disposal system 2012 POSIVA-12-5*. Finland: Posiva Oy.

Poteri, A., Andersson, P., Nilsson, K., Byegård, J., Skålberg, M., Siitari-Kauppi, M. K., et al. (2018a). *The second matrix diffusion experiment in the water phase of the Repro project: WPDE 2 POSIVA working report 2017-24*. Finland.

Poteri, A., Andersson, P., Nilsson, K., Johan, B., Skålberg, M., Siitari-Kauppi, M. K., et al. (2018b). *The first matrix diffusion experiment in the water phase of the REPRO project: WPDE 1 POSIVA working report 2017-23*. Finland.

Poteri, A., Billaux, D., Dershowitz, W., Gomez-Hernandez, J., Cvetkovic, V., Hautojaervi, A., et al. (2002). *Final report of the TRUE Block Scale project 3 Modelling of flow and transport SKB-TR-02-15*. Sweden.

Poteri, A., Nordman, H., Pulkkanen, V. M., and Smith, P. (2014). *Radionuclide transport in the repository near-field and far-field POSIVA-14-02*. Finland.

Poulain, A., Fernandez-Martinez, A., Greneche, J.-M., Prieur, D., Scheinost, A. C., Menguy, N., et al. (2022). Selenium Nanowire formation by reacting selenate with magnetite. *Environ. Sci. & Technol.* 56, 14817–14827. doi:10.1021/acs.est.1c08377

Powell, B. A., Fjeld, R. A., Kaplan, D. I., Coates, J. T., and Serkiz, S. M. (2005). Pu(V) O2+ adsorption and reduction by synthetic hematite and goethite. *Environ. Sci. & Technol.* 39, 2107–2114. doi:10.1021/es0487168

Prasianakis, N. I., Curti, E., Kosakowski, G., Poonoosamy, J., and Churakov, S. V. (2017). Deciphering pore-level precipitation mechanisms. *Sci. Rep.* 7, 13765. doi:10.1038/s41598-017-14142-0

Preocanin, T., and Kallay, N. (1998). Application of mass titration to determination of surface charge of metal oxides. *Croat. Chem. Acta* 71, 1117–1125. doi:10.1021/acs.jpcc.1c08637

Prieto, M. (2009). Thermodynamics of solid solution-aqueous solution systems. *Rev. Mineralogy Geochem.* 70, 47–85. doi:10.2138/rmg.2009.70.2

Prieto, M. (2014). Nucleation and supersaturation in porous media (revisited). *Mineral. Mag.* 78, 1437–1447. doi:10.1180/minmag.2014.078.6.11

Prieto, M., Heberling, F., Rodríguez-Galán, R. M., and Brandt, F. (2016). Crystallization behavior of solid solutions from aqueous solutions: an environmental perspective. *Prog. Cryst. Growth Charact. Mater.* 62, 29–68. doi:10.1016/j.pcrysgrow.2016.05.001

Prieur, D., Martel, L., Vigier, J.-F., Scheinost, A. C., Kvashnina, K. O., Somers, J., et al. (2018). Aliovalent cation substitution in $UO_2$: electronic and local structures of $U_{1-y}La_yO_{2\pm x}$ solid solutions. *Inorg. Chem.* 57, 1535–1544. doi:10.1021/acs.inorgchem.7b02839

Puhakka, E., Li, X., Ikonen, J., and Siitari-Kauppi, M. (2019). Sorption of selenium species onto phlogopite and calcite surfaces: DFT studies. *J. Contam. Hydrology* 227, 103553. doi:10.1016/j.jconhyd.2019.103553

Put, M., Monsecour, M., Foneyne, A., and Yoshida, H. (1991). Estimation of the migration parameters for the Boom Clay formation by percolation experiments on undisturbed clay cores. *Mater. Res. Soc. symposium Proc.* 212, 823–829.

Putnis, A., and Mauthe, G. (2001). The effect of pore size on cementation in porous rocks. *Geofluids* 1, 37–41. doi:10.1046/j.1468-8123.2001.11001.x

Pyrak-Nolte, L. J., and Nolte, D. D. (2016). Approaching a universal scaling relationship between fracture stiffness and fluid flow. *Nat. Commun.* 7, 10663. doi:10.1038/ncomms10663

Qian, Y. T., Scheinost, A. C., Grangeon, S., Greneche, J. M., Hoving, A., Bourhis, E., et al. (2023). Oxidation state and structure of Fe in nontronite: from oxidizing to reducing conditions. *Acs Earth Space Chem.* 7, 1868–1881. doi:10.1021/acsearthspacechem.3c00136

Rasamimanana, S., Lefevre, G., and Dagnelie, R. V. H. (2017). Various causes behind the desorption hysteresis of carboxylic acids on mudstones. *Chemosphere* 168, 559–567. doi:10.1016/j.chemosphere.2016.11.025

Reinholdt, M. X., Hubert, F., Faurel, M., Tertre, E., Razafitianamaharavo, A., Francius, G., et al. (2013). Morphological properties of vermiculite particles in size-selected fractions obtained by sonication. *Appl. Clay Sci.* 77-78, 18–32. doi:10.1016/j.clay.2013.03.013

Remy, J. C., and Orsini, L. (1976). Utilisation du chlorure de cobaltihéxamine pour la détermination simultanée de la capacité d'échange et des bases échangeables dans les sols. *Sci. Du. Sol.* 4, 269–275.

Richter, C., Müller, K., Drobot, B., Steudtner, R., GroßMANN, K., Stockmann, M., et al. (2016). Macroscopic and spectroscopic characterization of uranium(VI) sorption onto orthoclase and muscovite and the influence of competing Ca2+. *Geochimica Cosmochimica Acta* 189, 143–157. doi:10.1016/j.gca.2016.05.045

Roberts, H. E., Morris, K., Law, G. T. W., Mosselmans, J. F. W., Bots, P., Kvashnina, K., et al. (2017). Uranium(V) incorporation mechanisms and stability in Fe(II)/Fe(III) (oxyhydr)Oxides. *Environ. Sci. & Technol. Lett.* 4, 421–426. doi:10.1021/acs.estlett.7b00348

Roberts, H. E., Morris, K., Mosselmans, J. F. W., Law, G. T. W., and Shaw, S. (2019). Neptunium reactivity during Co-precipitation and oxidation of Fe(II)/Fe(III) (Oxyhydr)oxides. *Geosciences* 9, 27. doi:10.3390/geosciences9010027

Robinet, J. C., Sardini, P., Coelho, D., Parneix, J. C., Pret, D., Sammartino, S., et al. (2012). Effects of mineral distribution at mesoscopic scale on solute diffusion in a clay-rich rock: example of the Callovo-Oxfordian mudstone (Bure, France). *Water Resour. Res.* 48, 17. doi:10.1029/2011wr011352

Roden, E. E. (2003). Fe(III) oxide reactivity toward Biological versus chemical reduction. *Environ. Sci. & Technol.* 37, 1319–1324. doi:10.1021/es026038o

Rodriguez, D. M., Mayordomo, N., Scheinost, A. C., Schild, D., Brendler, V., Müller, K., et al. (2020). New insights into 99Tc(VII) removal by pyrite: a spectroscopic approach. *Environ. Sci. & Technol.* 54, 2678–2687. doi:10.1021/acs.est.9b05341

Rojo, H., Scheinost, A. C., Lothenbach, B., Laube, A., Wieland, E., and Tits, J. (2018). Retention of selenium by calcium aluminate hydrate (AFm) phases under strongly reducing radioactive waste repository conditions. *Dalton Trans.* 47, 4209–4218. doi:10.1039/c7dt04824f

Romanchuk, A. Y., Kalmykov, S. N., Kersting, A. B., and Zavarin, M. (2016). Behavior of plutonium in the environment. *Russ. Chem. Rev.* 85, 995–1010. doi:10.1070/rcr4602

Roosz, C., Grangeon, S., Blanc, P., Montouillout, V., Lothenbach, B., Henocq, P., et al. (2015). Crystal structure of magnesium silicate hydrates (M-S-H): the relation with 2:1 Mg–Si phyllosilicates. *Cem. Concr. Res.* 73, 228–237. doi:10.1016/j.cemconres.2015.03.014

Rossberg, A., and Funke, H. (2010). Determining the radial pair distribution function from X-ray absorption spectra by use of the Landweber iteration method. *J. Synchrotron Radiat.* 17, 280–288. doi:10.1107/s0909049509052200

Rossberg, A., Reich, T., and Bernhard, G. (2003). Complexation of uranium(VI) with protocatechuic acid - application of iterative transformation factor analysis to EXAFS spectroscopy. *Anal. Bioanal. Chem.* 376, 631–638. doi:10.1007/s00216-003-1963-5

Rossberg, A., and Scheinost, A. C. (2005). Three-dimensional modeling of EXAFS spectral mixtures by combining Monte Carlo simulations and target transformation factor analysis. *Anal. Bioanal. Chem.* 383, 56–66. doi:10.1007/s00216-005-3369-z

Rossberg, A., Ulrich, K.-U., Weiss, S., Tsushima, S., Hiemstra, T., and Scheinost, A. C. (2009). Identification of uranyl surface complexes on ferrihydrite: advanced EXAFS data analysis and CD-MUSIC modeling. *Environ. Sci. & Technol.* 43, 1400–1406. doi:10.1021/es801727w

Rotenberg, B., Morel, J.-P., Marry, V., Turq, P., and Morel-Desrosiers, N. (2009). On the driving force of cation exchange in clays: insights from combined microcalorimetry experiments and molecular simulation. *Geochimica Cosmochimica Acta* 73, 4034–4044. doi:10.1016/j.gca.2009.04.012

Rovira, M., DE Pablo, J., EL Amrani, S., Duro, L., Grivé, M., and Bruno, J. (2003). *Study of the role of magnetite in the immobilisation of U(VI) by reduction to U(IV) under the presence of H2(g) in hydrogen carbonate medium SKB-TR-03-04*. Sweden.

Salah, S., Bruggeman, C., and Maes, N. (2017). *Uranium retention and migration behaviour in Boom Clay SCK CEN-ER0410*. Mol, Belgium: Studiecentrum voor Kernenergie.

Sammaljärvi, J., Jokelainen, L., Ikonen, J., and Siitari-Kauppi, M. (2012). Free radical polymerisation of MMA with thermal initiator in brick and Grimsel granodiorite. *Eng. Geol.* 135-136, 52–59. doi:10.1016/j.enggeo.2012.03.005

Sammaljärvi, J., Lindberg, A., Voutilainen, M., Ikonen, J., Siitari-Kauppi, M., Pitkänen, P., et al. (2017). Multi-scale study of the mineral porosity of veined gneiss and pegmatitic granite from Olkiluoto, Western Finland. *J. Radioanalytical Nucl. Chem.* 314, 1557–1575. doi:10.1007/s10967-017-5530-5

Sanchez, F. G., VAN Loon, L. R., Gimmi, T., Jakob, A., Glaus, M. A., and Diamond, L. W. (2008). Self-diffusion of water and its dependence on temperature and ionic strength in highly compacted montmorillonite, illite and kaolinite. *Appl. Geochem.* 23, 3840–3851. doi:10.1016/j.apgeochem.2008.08.008

Sander, M., Hofstetter, T. B., and Gorski, C. A. (2015). Electrochemical analyses of redox-active iron minerals: a review of Nonmediated and mediated approaches. *Environ. Sci. & Technol.* 49, 5862–5878. doi:10.1021/acs.est.5b00006

Sandström, B., and Tullborg, E.-L. (2009). Episodic fluid migration in the Fennoscandian Shield recorded by stable isotopes, rare earth elements and fluid inclusions in fracture minerals at Forsmark, Sweden. *Chem. Geol.* 266, 126–142. doi:10.1016/j.chemgeo.2009.04.019

Savoye, S., Beaucaire, C., Fayette, A., Herbette, M., and Coelho, D. (2012a). Mobility of cesium through the Callovo-Oxfordian claystones under partially saturated conditions. *Environ. Sci. & Technol.* 46, 2633–2641. doi:10.1021/es2037433

Savoye, S., Beaucaire, C., Grenut, B., and Fayette, A. (2015). Impact of the solution ionic strength on strontium diffusion through the Callovo-Oxfordian clayrocks: an experimental and modeling study. *Appl. Geochem.* 61, 41–52. doi:10.1016/j.apgeochem.2015.05.011

Savoye, S., Frasca, B., Grenut, B., and Fayette, A. (2012b). How mobile is iodide in the Callovo-Oxfordian claystones under experimental conditions close to the *in situ* ones? *J. Contam. Hydrol.* 142-143, 82–92. doi:10.1016/j.jconhyd.2012.10.003

Savoye, S., Imbert, C., Fayette, A., and Coelho, D. (2014). "Experimental study on diffusion of tritiated water and anions under variable water-saturation and clay mineral content: comparison with the Callovo-Oxfordian claystones," in *Clays in natural and engineered barriers for radioactive waste confinement*. Editors S. NORRIS, J. BRUNO, M. CATHELINEAU, P. DELAGE, C. FAIRHURST, E. C. GAUCHER, et al. (Bath: Geological Soc Publishing House).

Savoye, S., Lacour, J. L., Fayette, A., and Beaucaire, C. (2013). Mobility of zinc in the Callovo-Oxfordian claystone. *Procedia Earth Planet. Sci.* 7, 774–777. doi:10.1016/j.proeps.2013.03.080

Savoye, S., Lefevre, S., Fayette, A., and Robinet, J.-C. (2017). Effect of water saturation on the diffusion/adsorption of 22Na and cesium onto the Callovo-Oxfordian claystones. *Geofluids* 2017, 1–17. doi:10.1155/2017/1683979

Savoye, S., Michelot, J. L., Matray, J. M., Wittebroodt, C., and Mifsud, A. (2012c). A laboratory experiment for determining both the hydraulic and diffusive properties and the initial pore-water composition of an argillaceous rock sample: a test with the

Opalinus clay (Mont Terri, Switzerland). *J. Contam. Hydrology* 128, 47–57. doi:10.1016/j.jconhyd.2011.09.011

Savoye, S., Michelot, J. L., and Wittebroodt, C. (2006). Evaluation of the reversibility of iodide uptake by argillaceous rocks by the radial diffusion method. *Radiochim. Acta* 94, 699–704. doi:10.1524/ract.2006.94.9-11.699

Savoye, S., Page, J., Puente, C., Imbert, C., and Coelho, D. (2010). New experimental approach for studying diffusion through an intact and unsaturated medium: a case study with Callovo-Oxfordian argillite. *Environ. Sci. & Technol.* 44, 3698–3704. doi:10.1021/es903738t

Sayed Hassan, M., Villieras, F., Gaboriaud, F., and Razafitianamaharavo, A. (2006). AFM and low-pressure argon adsorption analysis of geometrical properties of phyllosilicates. *J. Colloid Interface Sci.* 296, 614–623. doi:10.1016/j.jcis.2005.09.028

Schabernack, J., Oliveira, A. F., Heine, T., and Fischer, C. (2023). Variability of radionuclide sorption efficiency on muscovite cleavage planes. *Adv. Theory Simul.* 6 (12). doi:10.1002/adts.202300406

Schacherl, B., Joseph, C., Beck, A., Lavrova, P., Schnurr, A., Dardenne, K., et al. (2023). Np(V) Retention at the Illite du Puy Surface. *Environ. Sci. & Technol.* 57, 11185–11194. doi:10.1021/acs.est.2c09356

Schacherl, B., Joseph, C., Lavrova, P., Beck, A., Reitz, C., Pruessmann, T., et al. (2022a). Paving the way for examination of coupled redox/solid-liquid interface reactions: 1 ppm Np adsorbed on clay studied by Np M5-edge HR-XANES spectroscopy. *Anal. Chim. Acta* 1202, 339636. doi:10.1016/j.aca.2022.339636

Schacherl, B., Prussmann, T., Dardenne, K., Hardock, K., Krepper, V., Rothe, J., et al. (2022b). Implementation of cryogenic tender X-ray HR-XANES spectroscopy at the ACT station of the CAT-ACT beamline at the KIT Light Source. *J. Synchrotron Radiat.* 29, 80–88. doi:10.1107/s1600577521012650

Schaefer, M. V., Gorski, C. A., and Scherer, M. M. (2011). Spectroscopic evidence for interfacial Fe(II)-Fe(III) electron transfer in a clay mineral. *Environ. Sci. & Technol.* 45, 540–545. doi:10.1021/es102560m

Schecher, W. D., and Mcavoy, D. C. (1992). MINEQL+: a software environment for chemical equilibrium modeling. *Comput. Environ. Urban Syst.* 16, 65–76. doi:10.1016/0198-9715(92)90053-t

Scheidegger, A. C. S. B., Borkovec, M., Sticher, H., Meeussen, J. C. L., and VAN Riemsdijk, W. (1994). Convective transport of acids and bases in porous media. *water Resour. Res.* 30, 2937–2944. doi:10.1029/94wr01785

Scheidegger, A. M., Lamble, G. M., and Sparks, D. L. (1997). Spectroscopic evidence for the formation of mixed-cation hydroxide phases upon metal sorption on clays and aluminum oxides. *J. Colloid Interface Sci.* 186, 118–128. doi:10.1006/jcis.1996.4624

Scheidegger, A. M., Strawn, D. G., Lamble, G. M., and Sparks, D. L. (1998). The kinetics of mixed Ni-Al hydroxide formation on clay and aluminum oxide minerals: a time-resolved XAFS study. *Geochimica Cosmochimica Acta* 62, 2233–2245. doi:10.1016/s0016-7037(98)00136-7

Scheinost, A. C., and Charlet, L. (2008). Selenite reduction by mackinawite, magnetite and siderite: XAS characterization of nanosized redox products. *Environ. Sci. & Technol.* 42, 1984–1989. doi:10.1021/es071573f

Scheinost, A. C., Kirsch, R., Banerjee, D., Fernandez-Martinez, A., Zaenker, H., Funke, H., et al. (2008). X-ray absorption and photoelectron spectroscopy investigation of selenite reduction by Fe-II-bearing minerals. *J. Contam. Hydrology* 102, 228–245. doi:10.1016/j.jconhyd.2008.09.018

Scheinost, A. C., Steudtner, R., Hubner, R., Weiss, S., and Bok, F. (2016). Neptunium$^{V}$ retention by siderite under anoxic conditions: precipitation of $NpO_2$–like nanoparticles and of $Np^{IV}$ pentacarbonate. *Environ. Sci. & Technol.* 50, 10413–10420. doi:10.1021/acs.est.6b02399

Schlegel, M. L., Bataillon, C., Blanc, C., Pret, D., and Foy, E. (2010). Anodic Activation of iron corrosion in clay media under water-saturated conditions at 90 °C: characterization of the corrosion interface. *Environ. Sci. & Technol.* 44, 1503–1508. doi:10.1021/es9021987

Schlegel, M. L., Bataillon, C., Brucker, F., Blanc, C., Pret, D., Foy, E., et al. (2014). Corrosion of metal iron in contact with anoxic clay at 90 °C: characterization of the corrosion products after two years of interaction. *Appl. Geochem.* 51, 1–14. doi:10.1016/j.apgeochem.2014.09.002

Schlegel, M. L., Manceau, A., Charlet, L., Chateigner, D., and Hazemann, J. L. (2001a). Sorption of metal ions on clay minerals. III. Nucleation and epitaxial growth of Zn phyllosilicate on the edges of hectorite. *Geochimica Cosmochimica Acta* 65, 4155–4170. doi:10.1016/s0016-7037(01)00700-1

Schlegel, M. L., Manceau, A., Charlet, L., and Hazemann, J. L. (2001b). Adsorption mechanisms of Zn on hectorite as a function of time, pH, and ionic strength. *Am. J. Sci.* 301, 798–830. doi:10.2475/ajs.301.9.798

Schliemann, R., and Churakov, S. V. (2021a). Atomic scale mechanism of clay minerals dissolution revealed by *ab initio* simulations. *Geochimica Cosmochimica Acta* 293, 438–460. doi:10.1016/j.gca.2020.10.026

Schliemann, R., and Churakov, S. V. (2021b). Pyrophyllite dissolution at elevated pressure conditions: an *ab initio* study. *Geochimica Cosmochimica Acta* 307, 42–55. doi:10.1016/j.gca.2021.05.017

Schulthess, C., and Sparks, D. (1986). Backtitration technique for proton isotherm modeling of oxide surfaces. *Soil Sci. Soc. Am. J.* 50, 1406–1411. doi:10.2136/sssaj1986.03615995005000060007x

Schüring, J. (2000). *Redox: fundamentals, processes, and applications*. Berlin: Springer.

Schwantes, J. M., and Santschi, P. H. (2010). Mechanisms of plutonium sorption to mineral oxide surfaces: new insights with implications for colloid-enhanced migration. *Radiochim. Acta* 98, 737–742. doi:10.1524/ract.2010.1775

Schwarz, J. A., Driscoll, C. T., and Bhanot, A. K. (1984). The zero point of charge of silica—alumina oxide suspensions. *J. Colloid Interface Sci.* 97, 55–61. doi:10.1016/0021-9797(84)90274-1

Seabaugh, J. L., Dong, H., Kukkadapu, R. K., Eberl, D. D., Morton, J. P., and Kim, J. (2006). Microbial reduction of Fe(III) in the Fithian and Muloorina illites: contrasting extents and rates of bioreduction. *Clays Clay Minerals* 54, 67–79. doi:10.1346/ccmn.2006.0540109

Shackelford, C. D. (1991). Laboratory diffusion testing for waste disposal - a review. *J. Contam. Hydrology* 7, 177–217. doi:10.1016/0169-7722(91)90028-y

Shackelford, C. D., and Daniel, D. E. (1991). Diffusion in saturated soil. I: background. *J. Geotechnical Engineering-Asce* 117, 467–484. doi:10.1061/(asce)0733-9410(1991)117:3(467)

Shackelford, C. D., and Moore, S. M. (2013). Fickian diffusion of radionuclides for engineered containment barriers: diffusion coefficients, porosities, and complicating issues. *Eng. Geol.* 152, 133–147. doi:10.1016/j.enggeo.2012.10.014

Shahkarami, P., Liu, L., Moreno, L., and Neretnieks, I. (2016). The effect of stagnant water zones on retarding radionuclide transport in fractured rocks: an extension to the Channel Network Model. *J. Hydrology* 540, 1122–1135. doi:10.1016/j.jhydrol.2016.07.031

Singhal, J., and Kumar, D. (1975). *Thermodynamics of ion exchange equilibria involving Fe2+ ion on Na+-montmorillonite*.

Sinitsyn, V., Aja, S., Kulik, D., and Wood, S. (2000). Acid–base surface chemistry and sorption of some lanthanides on K+-saturated Marblehead illite: I. Results of an experimental investigation. *Geochimica Cosmochimica Acta* 64, 185–194. doi:10.1016/s0016-7037(99)00175-1

SKB (2011). *Long-term safety for the final repository for spent nuclear fuel at Forsmark Main report of the SR-Site project SKB-TR-11-01. Sweden: Swedish Nuclear*. Stockholm: FuelWaste Management Co.

Smellie, J., Pitkänene, P., Koskinen, L., Aaltonen, I., Eichinger, F., Waber, N., et al. (2014). *Evolution of Olkiluoto site: Paleohydrogeochemical considerations POSIVA working report 2014-17*. Finland.

Smiles, D. E., Gardner, W. R., and Schulz, R. K. (1995). Diffusion of tritium in arid disposal sites. *Water Resour. Res.* 31, 1483–1488. doi:10.1029/94wr02013

Smith, K. F., Bryan, N. D., Law, G. T. W., Hibberd, R., Shaw, S., Livens, F. R., et al. (2018). Np(V) sorption and solubility in high pH calcite systems. *Chem. Geol.* 493, 396–404. doi:10.1016/j.chemgeo.2018.06.016

Smith, P. A., Alexander, W. R., Heer, W., Fierz, T., Meier, P. M., Bayerns, B., et al. (2001). *Grimsel Test Site – investigation Phase IV (1994-1996): the Nagra-JAEA* in situ *study of safety relevant radionuclide retardation in fractured crystalline rock I: radionuclide migration experiment – overview 1990 – 1996*. Wettingen, Switzerland. NAGRA Technical Report NTB 00-09.

Smith, P., Hadermann, J., and Bischoff, K. (1991). Dual-porosity modelling of infiltration experiments on fractured granite. *Saf. Assess. Radioact. Waste Repos.*

Soderlund, M., Ervanne, H., Muuri, E., and Lehto, J. (2019). The sorption of alkaline earth metals on biotite. *Geochem. J.* 53, 223–234. doi:10.2343/geochemj.2.0561

Soler, J. M. (2016). Two-dimensional reactive transport modeling of the alteration of a fractured limestone by hyperalkaline solutions at Maqarin (Jordan). *Appl. Geochem.* 66, 162–173. doi:10.1016/j.apgeochem.2015.12.012

Soler, J. M., Landa, J., Havlova, V., Tachi, Y., Ebina, T., Sardini, P., et al. (2015). Comparative modeling of an *in situ* diffusion experiment in granite at the Grimsel Test Site. *J. Contam. Hydrology* 179, 89–101. doi:10.1016/j.jconhyd.2015.06.002

Soler, J. M., Neretnieks, I., Moreno, L., Liu, L., Meng, S., Svensson, U., et al. (2022). Predictive modeling of a simple field matrix diffusion experiment addressing radionuclide transport in fractured rock. Is it so straightforward? *Nucl. Technol.* 208, 1059–1073. doi:10.1080/00295450.2021.1988822

Soler, J. M., Steefel, C. I., Gimmi, T., Leupin, O. X., and Cloet, V. (2019). Modeling the ionic strength effect on diffusion in clay. The DR-A experiment at Mont Terri. *ACS Earth Space Chem.* 3, 442–451. doi:10.1021/acsearthspacechem.8b00192

Soltermann, D. (2014). "Ferrous iron uptake mechanisms at the montmorillonite-water interface under anoxic and electrochemically reduced conditions,". PhD thesis. Switzerland: ETH-Zürich.

Soltermann, D., Baeyens, B., Bradbury, M. H., and Fernandes, M. M. (2014a). Fe(II) uptake on natural montmorillonites. II. Surface complexation modeling. *Environ. Sci. & Technol.* 48, 8698–8705. doi:10.1021/es501902f

Soltermann, D., Fernandes, M. M., Baeyens, B., Dähn, R., Miehé-Brendlé, J., Wehrli, B., et al. (2013a). Fe(II) sorption on a synthetic montmorillonite. A combined

macroscopic and spectroscopic study. *Environ. Sci. & Technol.* 47, 6978–6986. doi:10.1021/es304270c

Soltermann, D., Marques, M. F., Baeyens, B., Brendlé, J. M., and Dähn, R. (2014b). Competitive Fe(II)–Zn(II) uptake on a synthetic montmorillonite. *Environ. Sci. & Technol.* 48, 190–198. doi:10.1021/es402783r

Soltermann, D., Marques, M. F., Baeyens, B., Dähn, R., Brendlé, J. M., Wehrli, B., et al. (2013b). Fe(II) sorption on a synthetic clay mineral without structural Fe. A wet chemistry and spectroscopic study. *Environ. Sci. & Technol.* 47, 6978–6986.

Soltermann, D., Marques, M. F., Baeyens, B., Dähn, R., Joshi, P. A., Scheinost, A. C., et al. (2014c). Fe(II) uptake on natural montmorillonites. I. Macroscopic and spectroscopic characterization. *Environ. Sci. & Technol.* 48, 8688–8697. doi:10.1021/es501887q

Sparks, D. L. (2003). *Environmental soil chemistry*. Elsevier.

Sposito, G. (1984). *The surface chemistry of soils*. New York: Oxford University Press.

Stack, A. G. (2015). Precipitation in pores: a geochemical Frontier. *Rev. Mineralogy Geochem.* 80, 165–190. doi:10.2138/rmg.2015.80.05

Stack, A. G., Fernandez-Martinez, A., Allard, L. F., Bañuelos, J. L., Rother, G., Anovitz, L. M., et al. (2014). Pore-size-dependent calcium carbonate precipitation controlled by surface chemistry. *Environ. Sci. & Technol.* 48, 6177–6183. doi:10.1021/es405574a

Stamberg, K., Palagyi, S., Videnska, K., and Havlova, V. (2014). Interaction of 3H+ (as HTO) and 36Cl– (as Na36Cl) with crushed granite and corresponding fracture infill material investigated in column experiments. *J. Radioanalytical Nucl. Chem.* 299, 1625–1633. doi:10.1007/s10967-013-2870-7

Stanfors, R., Rhén, I., Tullborg, E.-L., and Wikberg, P. (1999). Overview of geological and hydrogeological conditions of the Äspö hard rock laboratory site. *Appl. Geochem.* 14, 819–834. doi:10.1016/s0883-2927(99)00022-0

Steefel, C. I., Appelo, C. A. J., Arora, B., Jacques, D., Kalbacher, T., Kolditz, O., et al. (2014). Reactive transport codes for subsurface environmental simulation. *Comput. Geosci.* 19, 445–478. doi:10.1007/s10596-014-9443-x

Steefel, C. I., and Lasaga, A. C. (1994). A coupled model for transport of multiple chemical species and kinetic precipitation/dissolution reactions with application to reactive flow in single phase hydrothermal systems. *Am. J. Sci.* 294, 529–592. doi:10.2475/ajs.294.5.529

Steefel, C. I., and Tournassat, C. (2021). A model for discrete fracture-clay rock interaction incorporating electrostatic effects on transport. *Comput. Geosci.* 25, 395–410. doi:10.1007/s10596-020-10012-3

Steefel, C., Depaolo, D., and Lichtner, P. (2005). Reactive transport modeling: an essential tool and a new research approach for the Earth sciences. *Earth Planet. Sci. Lett.* 240, 539–558. doi:10.1016/j.epsl.2005.09.017

Stober, I., and Bucher, K. (2014). Hydraulic conductivity of fractured upper crust: insights from hydraulic tests in boreholes and fluid-rock interaction in crystalline basement rocks. *Geofluids* 15, 161–178. doi:10.1111/gfl.12104

Stockmann, M., Schikora, J., Becker, D. A., Flügge, J., Noseck, U., and Brendler, V. (2017). Smart Kd-values, their uncertainties and sensitivities - applying a new approach for realistic distribution coefficients in geochemical modeling of complex systems. *Chemosphere* 187, 277–285. doi:10.1016/j.chemosphere.2017.08.115

Stolze, L., Wagner, J. B., Damsgaard, C. D., and Rolle, M. (2020). Impact of surface complexation and electrostatic interactions on pH front propagation in silica porous media. *Geochimica Cosmochimica Acta* 277, 132–149. doi:10.1016/j.gca.2020.03.016

Strawn, D. G., and Sparks, D. L. (1999). The use of XAFS to distinguish between inner- and outer-sphere lead adsorption complexes on montmorillonite. *J. Colloid Interface Sci.* 216, 257–269. doi:10.1006/jcis.1999.6330

Stucki, J. W. (2011). A review of the effects of iron redox cycles on smectite properties. *Comptes Rendus Geosci.* 343, 199–209. doi:10.1016/j.crte.2010.10.008

Stumm, W., and Sulzberger, B. (1992). The cycling of iron in natural environments: Considerations based on laboratory studies of heterogeneous redox processes. *Geochimica Cosmochimica Acta* 56, 3233–3257. doi:10.1016/0016-7037(92)90301-x

Suter, D. (1991). *Chemistry of the redox sensitive elements Literature review NAGRA NTB-91-32*. Switzerland: NAGRA.

Suzuki, S., Sato, H., and Tachi, Y. (2003). A technical problem in the through-diffusion experiments for compacted bentonite. *J. Nucl. Sci. Technol.* 40, 698–701. doi:10.1080/18811248.2003.9715409

Svecova, L., Cremel, S., Sirguey, C., Simonnot, M.-O., Sardin, M., Dossot, M., et al. (2008). Comparison between batch and column experiments to determine the surface charge properties of rutile TiO2 powder. *J. Colloid Interface Sci.* 325, 363–370. doi:10.1016/j.jcis.2008.05.067

Svensson, U., Voutilainen, M., Muuri, E., Ferry, M., and Gylling, B. (2019). Modelling transport of reactive tracers in a heterogeneous crystalline rock matrix. *J. Contam. Hydrol.* 227, 103552. doi:10.1016/j.jconhyd.2019.103552

Tachi, Y., Ebina, T., Takeda, C., Saito, T., Takahashi, H., Ohuchi, Y., et al. (2015). Matrix diffusion and sorption of Cs+, Na+, I– and HTO in granodiorite: laboratory-scale results and their extrapolation to the *in situ* condition. *J. Contam. Hydrology* 179, 10–24. doi:10.1016/j.jconhyd.2015.05.003

Tachi, Y., and Yotsuji, K. (2014). Diffusion and sorption of Cs+, Na+, I– and HTO in compacted sodium montmorillonite as a function of porewater salinity: integrated sorption and diffusion model. *Geochimica Cosmochimica Acta* 132, 75–93. doi:10.1016/j.gca.2014.02.004

Takeda, M., Nakajima, H., Zhang, M., and Hiratsuka, T. (2008a). Laboratory longitudinal diffusion tests: 1. Dimensionless formulations and validity of simplified solutions. *J. Contam. Hydrol.* 97, 117–134. doi:10.1016/j.jconhyd.2008.01.004

Takeda, M., Zhang, M., Nakajima, H., and Hiratsuka, T. (2008b). Laboratory longitudinal diffusion tests: 2. Parameter estimation by inverse analysis. *J. Contam. Hydrol.* 97, 100–116. doi:10.1016/j.jconhyd.2008.01.003

Tanaka, S., Noda, N., Sato, S., Kozaki, T., Sato, H., and Hatanaka, K. (2011). Electrokinetic study of migration of anions, cations, and water in water-saturated compacted sodium montmorillonite. *J. Nucl. Sci. Technol.* 48, 454–462. doi:10.1080/18811248.2011.9711719

Tazi, S., Rotenberg, B., Salanne, M., Sprik, M., and Sulpizi, M. (2012). Absolute acidity of clay edge sites from ab-initio simulations. *Geochimica Cosmochimica Acta* 94, 1–11. doi:10.1016/j.gca.2012.07.010

Tertre, E., Savoye, S., Hubert, F., Prêt, D., Dabat, T., and Ferraget, E. (2018). Diffusion of water through the dual-porosity swelling clay mineral vermiculite. *Environ. Sci. & Technol.* 52, 1899–1907. doi:10.1021/acs.est.7b05343

Tesson, S., Salanne, M., Rotenberg, B., Tazi, S., and Marry, V. (2016). Classical polarizable force field for clays: pyrophyllite and Talc. *J. Phys. Chem. C* 120, 3749–3758. doi:10.1021/acs.jpcc.5b10181

Thompson, H. A., Parks, G. A., and Brown, G. E., JR (1999a). Ambient-temperature synthesis, evolution, and characterization of cobalt-aluminum hydrotalcite-like solids. *Clays Clay Minerals* 47, 425–438. doi:10.1346/ccmn.1999.0470405

Thompson, H. A., Parks, G. A., and Brown, G. E., JR (1999b). Dynamic interactions of dissolution, surface adsorption, and precipitation in an aging cobalt(II)-clay-water system. *Geochimica Cosmochimica Acta* 63, 1767–1779. doi:10.1016/s0016-7037(99)00125-8

Tinnacher, R. M., Holmboe, M., Tournassat, C., Bourg, I. C., and Davis, J. A. (2016). Ion adsorption and diffusion in smectite: molecular, pore, and continuum scale views. *Geochimica Cosmochimica Acta* 177, 130–149. doi:10.1016/j.gca.2015.12.010

Tournassat, C., and Appelo, C. A. J. (2011). Modelling approaches for anion-exclusion in compacted Na-bentonite. *Geochimica Cosmochimica Acta* 75, 3698–3710. doi:10.1016/j.gca.2011.04.001

Tournassat, C., Bizi, M., Braibant, G., and Crouzet, C. (2011). Influence of montmorillonite tactoid size on Na–Ca cation exchange reactions. *J. Colloid Interface Sci.* 364, 443–454. doi:10.1016/j.jcis.2011.07.039

Tournassat, C., Bourg, I. C., Holmboe, M., Sposito, G., and Steefel, C. I. (2016a). MOLECULAR DYNAMICS SIMULATIONS OF ANION EXCLUSION IN CLAY INTERLAYER NANOPORES. *Clays Clay Minerals* 64, 374–388. doi:10.1346/ccmn.2016.0640403

Tournassat, C., Bourg, I. C., Steefel, C. I., and Bergaya, F. (2015). "Chapter 1 - surface properties of clay minerals," in *Developments in clay science*. Editors C. TOURNASSAT, C. I. STEEFEL, I. C. BOURG, and F. BERGAYA (Elsevier).

Tournassat, C., Ferrage, E., Poinsignon, C., and Charlet, L. (2004a). The titration of clay minerals: II. Structure-based model and implications for clay reactivity. *J. Colloid Interface Sci.* 273, 234–246. doi:10.1016/j.jcis.2003.11.022

Tournassat, C., Gailhanou, H., Crouzet, C., Braibant, G., Gautier, A., and Gaucher, E. C. (2009). Cation exchange selectivity coefficient values on smectite and mixed-layer illite/smectite minerals. *Soil Sci. Soc. Am. J.* 73, 928–942. doi:10.2136/sssaj2008.0285

Tournassat, C., Gailhanou, H., Crouzet, C., Braibant, G., Gautier, A., Lassin, A., et al. (2007). Two cation exchange models for direct and inverse modelling of solution major cation composition in equilibrium with illite surfaces. *Geochimica Cosmochimica Acta* 71, 1098–1114. doi:10.1016/j.gca.2006.11.018

Tournassat, C., Greneche, J.-M., Tisserand, D., and Charlet, L. (2004b). The titration of clay minerals: I. Discontinuous backtitration technique combined with CEC measurements. *J. colloid interface Sci.* 273, 224–233. doi:10.1016/j.jcis.2003.11.021

Tournassat, C., Lerouge, C., Blanc, P., Brendlé, J., Greneche, J.-M., Touzelet, S., et al. (2008). Cation exchanged Fe (II) and Sr compared to other divalent cations (Ca, Mg) in the bure Callovian–Oxfordian formation: implications for porewater composition modelling. *Appl. Geochem.* 23, 641–654. doi:10.1016/j.apgeochem.2007.11.002

Tournassat, C., Neaman, A., Villiéras, F., Bosbach, D., and Charlet, L. (2003). Nanomorphology of montmorillonite particles:: estimation of the clay edge sorption site density by low-pressure gas adsorption and AFM observations. *Am. Mineralogist* 88, 1989–1995. doi:10.2138/am-2003-11-1243

Tournassat, C., and Steefel, C. I. (2015). Ionic transport in nano-porous clays with consideration of electrostatic effects. *Rev. Mineralogy Geochem.* 80, 287–329. doi:10.2138/rmg.2015.80.09

Tournassat, C., Tinnacher, R. M., Grangeon, S., and Davis, J. A. (2018). Modeling uranium (VI) adsorption onto montmorillonite under varying carbonate concentrations: a surface complexation model accounting for the spillover effect on surface potential. *Geochimica Cosmochimica Acta* 220, 291–308. doi:10.1016/j.gca.2017.09.049

Towle, S. N., Bargar, J. R., Brown, G. E., JR, and Parks, G. A. (1997). Surface precipitations of Co(II) on $Al_2O_3$. *J. Colloid Interface Sci.* 187, 62–82. doi:10.1006/jcis.1996.4539

Tsang, Y. W. (1984). The effect of tortuosity on fluid flow through a single fracture. *Water Resour. Res.* 20, 1209–1215. doi:10.1029/wr020i009p01209

Tsang, Y. W. (1992). Usage of "Equivalent apertures" for rock fractures as derived from hydraulic and tracer tests. *Water Resour. Res.* 28, 1451–1455. doi:10.1029/92wr00361

Tsang, Y. W., and Tsang, C. F. (1987). Channel model of flow through fractured media. *Water Resour. Res.* 23, 467–479. doi:10.1029/wr023i003p00467

Tsarev, S., Waite, T. D., and Collins, R. N. (2016). Uranium reduction by Fe(II) in the presence of montmorillonite and nontronite. *Environ. Sci. & Technol.* 50, 8223–8230. doi:10.1021/acs.est.6b02000

Turner, D. R., Pabalan, R. T., and Bertetti, F. P. (1998). Neptunium (V) sorption on montmorillonite: an experimental and surface complexation modeling study. *Clays Clay Minerals* 46, 256–269. doi:10.1346/ccmn.1998.0460305

Tyagi, M., Gimmi, T., and Churakov, S. V. (2013). Multi-scale micro-structure generation strategy for up-scaling transport in clays. *Adv. Water Resour.* 59, 181–195. doi:10.1016/j.advwatres.2013.06.002

Um, W., Chang, H. S., Icenhower, J. P., Lukens, W. W., Serne, R. J., Qafoku, N. P., et al. (2011). Immobilization of 99-technetium (VII) by Fe(II)-goethite and limited reoxidation. *Environ. Sci. & Technol.* 45, 4904–4913. doi:10.1021/es104343p

Um, W., Luksic, S. A., Wang, G. H., Saslow, S., Kim, D. S., Schweiger, M. J., et al. (2017). Enhanced 99Tc retention in glass waste form using Tc(IV)-incorporated Fe minerals. *J. Nucl. Mater.* 495, 455–462. doi:10.1016/j.jnucmat.2017.09.007

Underwood, T. R., and Bourg, I. C. (2020). Large-scale molecular dynamics simulation of the dehydration of a suspension of smectite clay nanoparticles. *J. Phys. Chem. C* 124, 3702–3714. doi:10.1021/acs.jpcc.9b11197

VAN DER Lee, J., and DE Windt, L. (2002). CHESS Tutorial and Cookbook. Update for version 3. User manual. *Fontainebleu, Fr*.

VAN Laer, L. (2018). *Long-term laboratory and* in-situ *migration experiments in Boom Clay - status 2017 SCK CEN-ER0390*. Mol, Belgium.

VAN Laer, L., Aertsens, M., Maes, N., VAN Loon, L. R., Glaus, M. A., and Wüst, R. A. J. (2023). Diffusion of HTO, $^{36}Cl$ and $^{22}Na$ in the Mesozoic rocks of northern Switzerland: III. Cross-lab comparison of diffusion measurements on argillaceous twin sample. *Appl. Geochem.* 160, 105840. doi:10.1016/j.apgeochem.2023.105840

VAN Laer, L., Durce, D., Salah, S., and Maes, N. (2016). *Sorption studies on Boom clay and clay minerals - status 2016 SCK CEN-ER0346*. Mol, Belgium: SCK CEN.

VAN Loon, L. R., Baeyens, B., and Bradbury, M. H. (2005a). Diffusion and retention of sodium and strontium in Opalinus clay: comparison of sorption data from diffusion and batch sorption measurements, and geochemical calculations. *Appl. Geochem.* 20, 2351–2363. doi:10.1016/j.apgeochem.2005.08.008

VAN Loon, L. R., Bunic, P., Frick, S., Glaus, M. A., and Wüst, R. A. J. (2023). Diffusion of HTO, 36Cl and 22Na in the Mesozoic rocks of Northern Switzerland: I. Effective diffusion coefficients and capacity factors across the heterogeneous sediment sequences. *Appl. Geochem.* 159, 105843. doi:10.1016/j.apgeochem.2023.105843

VAN Loon, L. R., and Eikenberg, J. (2005). A high-resolution abrasive method for determining diffusion profiles of sorbing radionuclides in dense argillaceous rocks. *Appl. Radiat. Isot.* 63, 11–21. doi:10.1016/j.apradiso.2005.02.001

VAN Loon, L. R., Glaus, M. A., and Muller, W. (2007). Anion exclusion effects in compacted bentonites: towards a better understanding of anion diffusion. *Appl. Geochem.* 22, 2536–2552. doi:10.1016/j.apgeochem.2007.07.008

VAN Loon, L. R., and Jakob, A. (2005). Evidence for a second transport porosity for the diffusion of tritiated water (HTO) in a sedimentary rock (Opalinus clay-OPA): application of through- and out-diffusion techniques. *Transp. Porous Media* 61, 193–214. doi:10.1007/s11242-004-7464-y

VAN Loon, L. R., Leupin, O. X., and Cloet, V. (2018). The diffusion of SO42− in Opalinus Clay: measurements of effective diffusion coefficients and evaluation of their importance in view of microbial mediated reactions in the near field of radioactive waste repositories. *Appl. Geochem.* 95, 19–24. doi:10.1016/j.apgeochem.2018.05.009

VAN Loon, L. R., and Mibus, J. (2015). A modified version of Archie's law to estimate effective diffusion coefficients of radionuclides in argillaceous rocks and its application in safety analysis studies. *Appl. Geochem.* 59, 85–94. doi:10.1016/j.apgeochem.2015.04.002

VAN Loon, L. R., and Muller, W. (2014). A modified version of the combined in-diffusion/abrasive peeling technique for measuring diffusion of strongly sorbing radionuclides in argillaceous rocks: a test study on the diffusion of caesium in Opalinus Clay. *Appl. Radiat. Isot.* 90, 197–202. doi:10.1016/j.apradiso.2014.04.009

VAN Loon, L. R., Muller, W., and Iijima, K. (2005b). Activation energies of the self-diffusion of HTO, 22Na+ and 36Cl− in a highly compacted argillaceous rock (Opalinus Clay). *Appl. Geochem.* 20, 961–972. doi:10.1016/j.apgeochem.2004.10.007

VAN Loon, L. R., Soler, J. M., Jakob, A., and Bradbury, M. H. (2003). Effect of confining pressure on the diffusion of HTO, 36Cl− and 125I− in a layered argillaceous rock (Opalinus Clay): diffusion perpendicular to the fabric. *Appl. Geochem.* 18, 1653–1662. doi:10.1016/s0883-2927(03)00047-7

VAN Loon, L. R., Soler, J. M., Muller, W., and Bradbury, M. H. (2004a). Anisotropic diffusion in layered argillaceous rocks: a case study with opalinus clay. *Environ. Sci. & Technol.* 38, 5721–5728. doi:10.1021/es049937g

VAN Loon, L. R., Wersin, P., Soler, J. M., Eikenberg, J., Gimmi, T., Hernan, P., et al. (2004b). *In-situ* diffusion of HTO, $^{22}Na^+$, $Cs^+$ and $I^-$ in Opalinus Clay at the Mont Terri underground rock laboratory. *Radiochim. Acta* 92, 757–763. doi:10.1524/ract.92.9.757.54988

VAN Loon, L. (2014). *Effective diffusion coefficients and porosity values for argillacous rocks and bentonite: measured and estimated values for the provisional safety analysis for SGT-02*. Switzerland: NAGRA.

VAN Loon, L., Glaus, M., Ferry, C., and Latrille, C. (2012). Studying radionuclide migration on different scales: the complementary roles of laboratory and *in situ* experiments. *Radionucl. Behav. Nat. Environ.*, 446–483. doi:10.1533/9780857097194.2.446

VAN Olphen, H. (1963). *An introduction to clay colloid chemistry*. New York-London: Interscience.

VAN Schaik, J. C., Kemper, W. D., and Olsen, S. R. (1966). Contribution of adsorbed cations to diffusion in clay-water systems. *Soil Sci. Soc. Am.* 30, 17–22. doi:10.2136/sssaj1966.03615995003000010013x

Vanselow, A. P. (1932). Equilibria of the base-exchange reactions of bentonites, permutites, soil colloids, and zeolites. *Soil Sci.* 33, 95–114. doi:10.1097/00010694-193202000-00002

Velde, B. B., and Meunier, A. (2008). *The origin of clay minerals in soils and weathered rocks*. Springer Berlin Heidelberg.

Vespa, M., Manceau, A., and Lanson, M. (2010). Natural attenuation of zinc pollution in smelter-affected soil. *Environ. Sci. & Technol.* 44, 7814–7820. doi:10.1021/es101567u

Videnska, K., Gondolli, J., Stamberg, K., and Havlova, V. (2015). Retention of selenium and caesium on crystalline rock: the effect of redox conditions and mineralogical composition. *J. Radioanalytical Nucl. Chem.* 304, 417–423. doi:10.1007/s10967-014-3885-4

Videnská, K., Palágyi, Š., Štamberg, K., Vodičková, H., and Havlova, V. (2013). Effect of grain size on the sorption and desorption of SeO4 2− and SeO3 2− in columns of crushed granite and fracture infill from granitic water under dynamic conditions. *J. Radioanalytical Nucl. Chem.* 298, 547–554. doi:10.1007/s10967-013-2429-7

Vinograd, V. L., Brandt, F., Rozov, K., Klinkenberg, M., Refson, K., Winkler, B., et al. (2013). Solid-aqueous equilibrium in the BaSO4-RaSO4-H2O system: first-principles calculations and a thermodynamic assessment. *Geochimica Cosmochimica Acta* 122, 398–417. doi:10.1016/j.gca.2013.08.028

Vinograd, V. L., Kulik, D. A., Brandt, F., Klinkenberg, M., Weber, J., Winkler, B., et al. (2018). Thermodynamics of the solid solution - aqueous solution system (Ba,Sr,Ra)SO4 + H2O: I. The effect of strontium content on radium uptake by barite. *Appl. Geochem.* 89, 59–74. doi:10.1016/j.apgeochem.2017.11.009

Vitova, T., Denecke, M. A., Gottlicher, J., Jorissen, K., Kas, J. J., Kvashnina, K., et al. (2013). "Actinide and lanthanide speciation with high-energy resolution X-ray techniques," in 15th International Conference on X-Ray Absorption Fine Structure (Xafs15), 430.

Voigt, W., Brendler, V., Marsh, K., Rarey, R., Wanner, H., Gaune-Escard, M., et al. (2007). Quality assurance in thermodynamic databases for performance assessment studies in waste disposal. *Pure Appl. Chem.* 79, 883–894. doi:10.1351/pac200779050883

Voutilainen, M., Kekäläinen, P., Poteri, A., Siitari-Kauppi, M., Helariutta, K., Andersson, P., et al. (2019). Comparison of water phase diffusion experiments in laboratory and *in situ* conditions. *J. Hydrology* 575, 716–729. doi:10.1016/j.jhydrol.2019.05.069

Voutilainen, M., Kekäläinen, P., Siitari-Kauppi, M., Sardini, P., Muuri, E., Timonen, J., et al. (2017). Modeling transport of cesium in Grimsel granodiorite with micrometer scale heterogeneities and dynamic update of *d. Water Resour. Res.* 53, 9245–9265. doi:10.1002/2017wr020695

Wang, H. A. O., Grolimund, D., Giesen, C., Borca, C. N., Shaw-Stewart, J. R. H., Bodenmiller, B., et al. (2013). Fast chemical imaging at high spatial resolution by laser ablation Inductively coupled Plasma mass spectrometry. *Anal. Chem.* 85, 10107–10116. doi:10.1021/ac400996x

Wang, H. A. O., Grolimund, D., VAN Loon, L. R., Barmettler, K., Borca, C. N., Aeschimann, B., et al. (2011). Quantitative chemical imaging of element diffusion into heterogeneous media using laser ablation Inductively coupled Plasma mass spectrometry, synchrotron micro-X-ray fluorescence, and extended X-ray absorption fine structure spectroscopy. *Anal. Chem.* 83, 6259–6266. doi:10.1021/ac200899x

Wang, Z. Z., Bao, Y. Y., Pereira, J. M., Sauret, E., and Gan, Y. X. (2022). Influence of multiscale surface roughness on permeability in fractures. *Phys. Rev. Fluids* 7, 024101. doi:10.1103/physrevfluids.7.024101

Wang, L., Jacques, D., and DE Canniere, P. (2007). *Effects of an alkaline plume on the Boom Clay as a otential host formation for geological disposal of radioactive waste. First full draft - v1.0 SCK CEN-ER28*. Mol, Belgium: SCK-CEN, Belgium Nuclear Research Centre.

Wang, L., Salah, S., and DE Soete, H. (2020a). *MOLDATA: a thermochemical data base for phenomenological and safety assessment studies for disposal of radioactive waste in Belgium – data Compilation Strateg SCK CEN-820*. Mol, Belgium: SCK-CEN.

Wang, L., Salah, S., and DE Soete, H. (2020b). *MOLDATA: a thermochemical data base for phenomenological and safety assessment studies for disposal of radioactive waste in Belgium – selected data and argumentations Release 2.0 SCK CEN-ER813*. Mol, Belgium: SCK-CEN.

Wanner, H., Albinsson, Y., Karnland, O., Wieland, E., Charlet, L., and Wersin, P. (1994). The acid/base chemistry of montmorillonite. *Radiochim. Acta* 66, 157–162. doi:10.1524/ract.1994.6667.special-issue.157

Weaver, C. E. (1989). *Clays, Muds, and shales*. Elsevier Science.

Weber, J., Barthel, J., Klinkenberg, M., Bosbach, D., Kruth, M., and Brandt, F. (2017). Retention of 226Ra by barite: the role of internal porosity. *Chem. Geol.* 466, 722–732. doi:10.1016/j.chemgeo.2017.07.021

Weetjens, E., Govaerts, J., and Aertsens, M. (2011). "Model and parameter validation based on *in situ* experiments in Boom Clay," in *Mol SCK CEN-ER171* (Belgium: SCK-CEN).

Weetjens, E., Maes, N., and VAN Ravestyn, L. (2014). *Model validation based on* in situ *radionuclide migration tests in Boom Clay: status of a large-scale migration experiment, 24 years after injection*. London: Geological Society, 613–623. Special Publications, 400.

Wenk, H. R., Voltolini, M., Mazurek, M., VAN Loon, L. R., and Vinsot, A. (2008). Preferred orientations and anisotropy in shales: Callovo-Oxfordian shale (France) and opalinus clay (Switzerland). *Clays Clay Minerals* 56, 285–306. doi:10.1346/ccmn.2008.0560301

Wersin, P. (2017). *Topics and processes dealt with in the IP FUNMIG and their treatment in the Safety Case of geologic repositories for radioactive waste*. Wettingen, Switzerland. NAGRA Technical Report NTB 09-01.

Westall, J. C., Zachary, J. L., Morel, F., Massachusetts Institute Of, T., Department Of Civil, E., Ralph, M. P. L. F. W. R., et al. (1976). "MINEQL: a computer program for the calculation of chemical equilibrium composition of aqueous systems, Cambridge, Mass., Water Quality Laboratory," in *Laboratory for water resources and environmental engineering [sic], Dept. Of Civil engineering*. Editor R. M. Parsons (United States: Massachusetts Institute of Technology).

Westall, J., and Hohl, H. (1980). A comparison of electrostatic models for the oxide/solution interface. *Adv. Colloid Interface Sci.* 12, 265–294. doi:10.1016/0001-8686(80)80012-1

Wharton, M. J., Atkins, B., Charnock, J. M., Livens, F. R., Pattrick, R. A. D., and Collison, D. (2000). An X-ray absorption spectroscopy study of the coprecipitation of Tc and Re with mackinawite (FeS). *Appl. Geochem.* 15, 347–354. doi:10.1016/s0883-2927(99)00045-1

Wick, S., Baeyens, B., Fernandes, M. M., and Voegelin, A. (2018). Thallium adsorption onto illite. *Environ. Sci. & Technol.* 52, 571–580. doi:10.1021/acs.est.7b04485

Wigger, C., Kennell-Morrison, L., Jensen, M., Glaus, M., and VAN Loon, L. (2018). A comparative anion diffusion study on different argillaceous, low permeability sedimentary rocks with various pore waters. *Appl. Geochem.* 92, 157–165. doi:10.1016/j.apgeochem.2018.02.009

Wigger, C., and VAN Loon, L. R. (2017). Importance of interlayer equivalent pores for anion diffusion in clay-rich sedimentary rocks. *Environ. Sci. Technol.* 51, 1998–2006. doi:10.1021/acs.est.6b03781

Winberg, A., Andersson, P., Hermanson, J., Byegard, J., Cvetcovik, V., and Birgersson, V. (2000). *Äspö Hard Rock Laboratory, finial report of the first stage of the tracer retention understanding experiments*. SKB Technical Report TR-00-07. Stockholm, Sweden.

Winkel, L. H. E., Johnson, C. A., Lenz, M., Grundl, T., Leupin, O. X., Amini, M., et al. (2012). Environmental selenium research: from microscopic processes to global understanding. *Environ. Sci. & Technol.* 46, 571–579. doi:10.1021/es203434d

Wittebroodt, C., Savoye, S., Frasca, B., Gouze, P., and Michelot, J. L. (2012). Diffusion of HTO, 36Cl– and 125I– in Upper Toarcian argillite samples from Tournemire: effects of initial iodide concentration and ionic strength. *Appl. Geochem.* 27, 1432–1441. doi:10.1016/j.apgeochem.2011.12.017

Wolery, T. J., and Daveler, S. A. (1992). *EQ6, a computer program for reaction path modeling of aqueous geochemical systems: theoretical manual, user`s guide, and related documentation (Version 7.0)*. Part 4. United States.

Wu, T., Amayri, S., Drebert, J., VAN Loon, L. R., and Reich, T. (2009). Neptunium (V) sorption and diffusion in opalinus clay. *Environ. Sci. & Technol.* 43, 6567–6571. doi:10.1021/es9008568

Wylie, E. M., Olive, D. T., and Powell, B. A. (2016). Effects of Titanium Doping in Titanomagnetite on neptunium sorption and speciation. *Environ. Sci. & Technol.* 50, 1853–1858. doi:10.1021/acs.est.5b05339

Xiang, Y., AL, T., and Mazurek, M. (2016). Effect of confining pressure on diffusion coefficients in clay-rich, low-permeability sedimentary rocks. *J. Contam. Hydrology* 195, 1–10. doi:10.1016/j.jconhyd.2016.10.004

Xiao, T., Xu, H., Moodie, N., Esser, R., Jia, W., Zheng, L. G., et al. (2020). Chemical-mechanical impacts of $CO_2$ intrusion into heterogeneous caprock. *Water Resour. Res.* 56. doi:10.1029/2020wr027193

YalçıNTAŞ, E., Scheinost, A. C., Gaona, X., and Altmaier, M. (2016). Systematic XAS study on the reduction and uptake of Tc by magnetite and mackinawite. *Dalton Trans.* 45, 17874–17885. doi:10.1039/c6dt02872a

Yang, G., Prasianakis, N. I., and S, V. C. (2020). Comparative modeling of ions and solvent properties in Ca-Na montmorillonite by atomistic simulations and fluid density functional theory. *Clays Clay Minerals* 68, 100–114. doi:10.1007/s42860-019-00058-5

Yang, J., Kukkadapu, R. K., Dong, H., Shelobolina, E. S., Zhang, J., and Kim, J. (2012). Effects of redox cycling of iron in nontronite on reduction of technetium. *Chem. Geol.* 291, 206–216. doi:10.1016/j.chemgeo.2011.10.013

Yang, X., Ge, X., He, J., Wang, C., Qi, L., Wang, X., et al. (2018). Effects of mineral compositions on matrix diffusion and sorption of 75Se(IV) in granite. *Environ. Sci. & Technol.* 52, 1320–1329. doi:10.1021/acs.est.7b05795

Yaroshchuk, A. E., and VAN Loon, L. R. (2008). Improved interpretation of in-diffusion measurements with confined swelling clays. *J. Contam. Hydrology* 97, 67–74. doi:10.1016/j.jconhyd.2007.12.003

Yuan, T., Ning, Y., and Qin, G. (2016). Numerical modeling and simulation of coupled processes of mineral dissolution and fluid flow in fractured carbonate formations. *Transp. Porous Media* 114, 747–775. doi:10.1007/s11242-016-0742-7

Yuguchi, T., Sasao, E., Ishibashi, M., and Nishiyama, T. (2015). Hydrothermal chloritization processes from biotite in the Toki granite, Central Japan: temporal variations of of the compositions of hydrothermal fluids associated with chloritization. *Am. Mineralogist* 100, 1134–1152. doi:10.2138/am-2015-5126

Zachara, J. M., Heald, S. M., Jeon, B.-H., Kukkadapu, R. K., Liu, C., Mckinley, J. P., et al. (2007). Reduction of pertechnetate [Tc(VII)] by aqueous Fe(II) and the nature of solid phase redox products. *Geochimica Cosmochimica Acta* 71, 2137–2157. doi:10.1016/j.gca.2006.10.025

Zahasky, C., and Benson, S. (2018). Micro-positron emission tomography for measuring sub-core scale single and multiphase transport parameters in porous media. *Adv. Water Resour.* 115, 1–16. doi:10.1016/j.advwatres.2018.03.002

Zavarin, M., Roberts, S. K., Hakem, N., Sawvel, A. M., and Kersting, A. B. (2005). Eu(III), Sm(III), Np(V), Pu(V), and Pu(IV) sorption to calcite. *Radiochim. Acta* 93, 93–102. doi:10.1524/ract.93.2.93.59413

Zeelmaekers, E., Honty, M., Derkowski, A., Srodon, J., DE Craen, M., Vandenberghe, N., et al. (2015). Qualitative and quantitative mineralogical composition of the Rupelian boom clay in Belgium. *Clay Miner.* 50, 249–272. doi:10.1180/claymin.2015.050.2.08

Zhang, X. Y., Ma, F. N., Dai, Z. X., Wang, J., Chen, L., Ling, H., et al. (2022). Radionuclide transport in multi-scale fractured rocks: a review. *J. Hazard. Mater.* 424, 127550. doi:10.1016/j.jhazmat.2021.127550

Zhang, C., Liu, X. D., Lu, X. C., He, M. J., Meijer, E. J., and Wang, R. C. (2017). Surface complexation of heavy metal cations on clay edges: insights from first principles molecular dynamics simulation of Ni(II). *Geochimica Cosmochimica Acta* 203, 54–68. doi:10.1016/j.gca.2017.01.014

Zhang, C., Liu, X., Lu, X., Meijer, E. J., Wang, K., He, M., et al. (2016). Cadmium(ii) complexes adsorbed on clay edge surfaces: insight from first principles molecular dynamics simulation. *Clays Clay Minerals* 64, 337–347. doi:10.1346/ccmn.2016.0640402

Zhang, W., Tang, X.-Y., Weisbrod, N., Zhao, P., and Reid, B. J. (2015). A coupled field study of subsurface fracture flow and colloid transport. *J. Hydrology* 524, 476–488. doi:10.1016/j.jhydrol.2015.03.001

Zhu, Y., and Elzinga, E. J. (2014). Formation of layered Fe(II)-Hydroxides during Fe(II) sorption onto clay and metal-oxide substrates. *Environ. Sci. & Technol.* 48, 4937–4945. doi:10.1021/es500579p